THE JOURNAL
OF
CHEMICAL PHYSICS

VOLUME 17, NUMBER 5 MAY, 1949

The C—C Bond Energy in Ethylbenzene*

M. SZWARC
Department of Chemistry, University of Manchester, Manchester 13, England
(Received September 13, 1948)

The pyrolysis of ethylbenzene in the presence of excess of toluene has been shown to be a unimolecular process, the rate-determining step being

$$C_6H_5\cdot CH_2\cdot CH_3 \rightarrow C_6H_5\cdot CH_2\cdot + CH_3\cdot.$$

The methyl radicals were removed by a reaction with toluene, yielding CH_4 and benzyl radicals, and the quantity of methane obtained was a measure of the extent of the decomposition of ethylbenzene. The energy of activation and the frequency factor were estimated experimentally at 63.2 kcal./mole and $1.0\cdot10^{13}$ sec.$^{-1}$, respectively. Taking the $D(C-C)_{C_6H_5\cdot C_2H_5}$ at 63.2 kcal./mole and using this value in conjunction with the value reported previously for $D(C-H)_{C_6H_5\cdot CH_3}$ and the relevant thermochemical data, we calculated the $D(C-H)_{CH_4}$ at 102.9 kcal./mole.

The results of the thermal decomposition of ethylbenzene in the absence of toluene have been investigated, but it has been found unsuitable for kinetics studies because of a complicating chain process.

A short discussion on the frequency factors of these unimolecular reactions is given.

THERE is little doubt that the weakest bond in ethylbenzene is the aliphatic C—C bond, and it is probable, therefore, that the first step in the pyrolysis of $C_6H_5\cdot CH_2\cdot CH_3$ will be the splitting of this molecule into a benzyl and a methyl radical

$$C_6H_5\cdot CH_2\cdot CH_3 \rightarrow C_6H_5\cdot CH_2\cdot + CH_3\cdot. \quad (1)$$

In consequence, one could expect that the quantity of CH_4, produced in the pyrolysis of ethylbenzene, would provide a measure for the initial decomposition of this compound. However, a number of pyrolytical experiments in which the thermal decomposition of ethylbenzene was investigated by the same technique as that previously used for toluene[1] showed that the actual process is rather complicated and unsuitable for an exact kinetics study. We shall give, therefore, only a brief account of the results obtained by this method and then, after discussing the reasons for its failure, we shall outline the features of a new technique, which enabled us to carry out successfully the present work.

EXPERIMENTAL

The first series of experiments was carried out in the apparatus previously described,[1] the ethylbenzene flowed under pressure of a few mm of Hg, with a time of contact of about 0.3 sec., and the temperatures ranged from 550°C up to 700°C. The main gaseous products were: H_2, CH_4, in quantities only 10–20 percent of those of H_2, and a high proportion of C_2 hydrocarbons (amounting to about 1/3 of the quantity of H_2). The reproducibility of the reaction was not very good; both the rate of formation of the gaseous products and the composition of the mixture varied, the rate occasionally varying by as much as a factor of 3. In addition to gaseous products we observed the formation of dibenzyl and styrene. The molar quantities of dibenzyl were definitely smaller than those of CH_4, and styrene was the main non-gaseous product. (The exact determination of its quantity was prevented, however, by the formation of polystyrene, which was deposited on the wall of the tube leading from the furnace.) The repeated pyrolysis of samples of ethylbenzene pyrolyzed in previous experiments (i.e., purified by pyrolysis) gave the same results as those obtained with unpyrolyzed material, thus showing that the observed processes were not due to the presence of some impurities in the original ethylbenzene.

All these observations can be accounted for on the basis of a chain process initiated by a reaction between a CH_3 radical and a molecule of undecom-

* The expression "bond energy" is used here, as in previous papers, in the sense of the dissociation energy of the bond.

[1] M. Szwarc, J. Chem. Phys. **16**, 128 (1948).

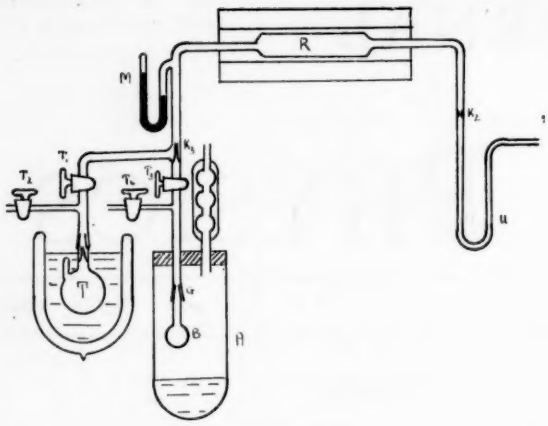

FIG. 1. Apparatus diagram.

posed $C_6H_5\cdot CH_2\cdot CH_3$,

$$CH_3\cdot + C_6H_5\cdot CH_2\cdot CH_3 \rightarrow CH_4 + C_6H_5\dot{C}H\cdot CH_3, \quad (2)$$
$$(\text{or } C_6H_5\cdot CH_2\cdot \dot{C}H_2)$$

followed by the rapid decomposition of the so produced $C_6H_5\cdot C_2H_4\cdot$ radical into a molecule of styrene and an H atom:

$$C_6H_5\cdot C_2H_4\cdot \rightarrow C_6H_5\cdot CH{:}CH_2 + H. \quad (3)$$

The hydrogen atoms may attack the undecomposed ethylbenzene in several ways:

$$C_6H_5\cdot C_2H_5 + H \rightarrow C_6H_5\cdot C_2H_4\cdot + H_2, \quad (4a)$$

$$C_6H_5\cdot C_2H_5 + H \rightarrow C_6H_6 + C_2H_5\cdot, \quad (4b)$$

$$C_6H_5\cdot C_2H_5 + H \rightarrow C_6H_5\cdot CH_2\cdot + CH_4. \quad (4c)$$

The reactions (3) and (4a) represent the chain propagation in which H_2 is produced, and the reactions (3) and (4b) in conjunction with reaction (5),

$$C_6H_5\cdot C_2H_5 + C_2H_5\cdot \rightarrow C_6H_5\cdot C_2H_4\cdot + C_2H_6, \quad (5)$$

represent the chain propagation in which C_2H_6 is produced. The reaction (4c) represents one of the possible chain terminations,** and is responsible for an additional production of CH_4.

TABLE I.

Run	T°C	$P_{C_6H_5\cdot C_2H_5}$ mm Hg	$P_{C_6H_5\cdot CH_3}$ mm Hg	Time of contact/ sec.	Percent decomp.	$K\cdot 10^2$ sec.$^{-1}$
18	614	0.16	8.0	0.420	0.14	0.34
21	619	0.17	8.3	0.340	0.11	0.32
20	619	0.17	8.3	0.345	0.14	0.41
19	633	0.15	8.2	0.420	0.25	0.60
22	639	0.17	8.3	0.330	0.26	0.78
25	642	0.15	7.6	0.295	0.28	0.93
26	655	0.14	7.4	0.290	0.38	1.31
1	674	0.35	7.5	0.315	0.69	2.19
2	674	0.35	7.6	0.315	0.61	1.93
16	673	0.15	8.6	0.385	1.00	2.60
12	675	0.35	13.7	1.15	2.50	2.20
13	674	0.16	13.5	0.410	1.00	2.45
15	674	0.18	8.9	1.05	2.36	2.26
14	682	0.24	8.0	0.340	1.26	3.7
24	696	0.10	7.5	0.320	1.95	6.1
17	702	0.13	8.6	0.375	3.13	8.5
27	710	0.15	7.4	0.270	2.70	10.0
4	732	0.35	7.5	0.290	4.98	17.5
3	735	0.34	7.5	0.285	5.22	18.5
5	735	0.35	7.25	0.300	5.12	17.4
6	736	0.11	7.2	0.292	5.2	18.1
10	735	0.13	8.0	1.05	17.6	18.5
11	735	0.14	16.0	0.95	15.5	18.0
9	738	0.30	15.6	1.06	21.0	22.2
7	745	0.12	8.0	0.270	6.75	25.9
8	745	0.15	7.0	0.270	6.80	26.1

This suggested mechanism does not pretend to be complete but it probably represents all the main reactions which participate in the thermal decomposition of ethylbenzene, and it accounts for the observed products.*** Subsequent work has provided us with data to calculate the rate of reaction (1). On the basis of the suggested scheme, this rate is equal to the rate of formation of CH_4 produced in reactions (1) and (2), and to the rate of chain initiation. The actually observed rate of formation of CH_4 is higher than the calculated rate by about 50–100 percent, and we assume that this increase is due to the participation of reaction (4c) in the over-all process. Assuming this to be the case and knowing the relative abundance of H_2, CH_4, and C_2 hydrocarbons in the products, we are able to calculate the chain length as about 15–25, and the relative probabilities of reactions (4a), (4b), and (4c) as 100:30–40:10–5.****

The difficulties arising from the occurrence of a chain reaction can be avoided by choosing experimental conditions under which reaction (2) is suppressed. This has been achieved by using toluene as a carrier gas, since under these circumstances the methyl radicals produced by the decomposition of ethylbenzene react mainly with toluene, the concentration of which is much higher than that of ethylbenzene, yielding eventually CH_4 and benzyl radicals, as has been demonstrated by Taylor and Smith.[2] The reaction (6),

$$C_6H_5\cdot CH_3 + CH_3\cdot \rightarrow C_6H_5\cdot CH_2\cdot + CH_4, \quad (6)$$

is very rapid, so that in our experiments the rate of formation of CH_4 should be equal to the rate of dissociation of the ethylbenzene molecule into a CH_3 and a benzyl radical.

The second series of experiments, using this newly developed technique with toluene as a carrier gas, was performed in an apparatus represented in Fig. 1. The vapor of toluene was introduced into

** There are a number of possible chain termination processes, e.g. $C_6H_5\cdot CH_2\cdot + H \rightarrow C_6H_5\cdot CH_3$, $2C_2H_5\cdot \rightarrow C_2H_4 + C_2H_6$, $H + H + \text{wall} \rightarrow H_2$, and so on. It is, however, beyond the scope of this work to discuss which of them participate, and to what extent, in the actual process.

*** The direct split of ethylbenzene into styrene and H_2 seems to be of a minor importance. The reason for this conclusion will be given later in the discussion.

**** The reaction (4b) proceeds probably via complex

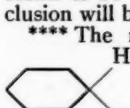

[2] H. S. Taylor and J. O. Smith, J. Chem. Phys. **8**, 543 (1940).

the system from a vessel, T, which was immersed in a large Dewar containing water at a constant temperature. By changing the temperature of this water bath we were able to vary the pressure of toluene in the reaction vessel R. The vapor of ethylbenzene was introduced into the system through a very fine capillary, K_3. The ethylbenzene was kept in a small flask, B, heated by vapor from a liquid boiling in a wide boiling tube, A, surrounding the flask B. By changing the liquid (alcohol, water, or toluene), we were able to change the partial pressure of ethylbenzene in the reaction vessel. To avoid any condensation of $C_6H_5 \cdot C_2H_5$ vapor, the tube leading from the flask B to the capillary K_3 (including the capillary, the tap T_3, and the side tube to the tap T_4) was wound with Nichrome wire and electrically heated to a temperature of about 150°C. The ground joint G and both taps T_3 and T_4 were greased by Dow Corning's high vacuum grease, and special tests proved that no leakage occurred even if the tap was maintained at 180°C. The tap, however, required cleaning and regreasing every second day. By sealing suitable capillary K_2 into the tube leading from the reaction vessel, it was possible to adjust the time of contact as desired. Otherwise, the apparatus was the same as described previously.[1]

The runs were started by opening tap T_1, followed almost immediately by opening tap T_3. The high pressure of the vapor of ethylbenzene flowing into capillary K_3 (several hundred mm of Hg) prevented any back diffusion of toluene, and, therefore, the quantity of pyrolyzed ethylbenzene could be determined by weighing flask B before and after each run. The pressure in the reaction vessel was measured on the manometer, M, and from it and the rates of vaporization of toluene and ethylbenzene we could calculate the time of contact. The runs were terminated by removing the boiling tube, A, and immersing flask B in a solid CO_2—acetone bath. One minute later taps T_3 and T_1 were closed. The quantities and composition of the collected gases were determined by the methods described in the previous paper.[1]

The toluene used for this work was of a "sulfur-free" grade. It was purified by pyrolysis at 810–820°C, followed by a careful distillation through an efficient column. The commercially pure ethylbenzene was distilled, then pyrolyzed at 690°–700°C, and finally fractionated twice.

The pyrolysis was carried out at temperatures ranging from 615°C up to 745°C. The ratio of toluene/ethylbenzene was usually kept between 20:1 and 50:1. Blank runs proved that the decomposition of toluene below 710°C was immeasurably small. With temperatures above 710°C, correction for decomposition of toluene was introduced. This correction was never greater than a few percent.

The results obtained are summarized in Table I.

TABLE II.

Run	Dibenzyl collected		Dibenzyl calculated (1:1 ratio)
	Amount	Melting point	
3	90 mg	50°C–51°C	110 mg
4	85 mg	50°C–51°C	115 mg
6, 7, 8	160 mg	49°C–51°C	165 mg
9	85 mg	48°C–51°C	95 mg

The following points should be emphasized:

(i) The collected gas was mainly methane. The amount of H_2 was between 15–25 percent, while that of C_2 hydrocarbons was below 2 percent (in most cases less than one percent).

(ii) In addition to gaseous products pure dibenzyl was collected in quantities corresponding nearly to one mole of dibenzyl for one mole of CH_4. This is illustrated in Table II.

(iii) The reproducibility of the results was very good. The rate of formation of CH_4 was shown to obey a first-order law by changing the partial pressure of ethylbenzene by a factor of 3.5 (from 0.10 mm of Hg up to 0.35 mm of Hg), and the time of contact by a factor of 3 (from 0.3 sec. up to 1 sec.). The rate of formation of CH_4 was independent of the partial pressure of toluene. (Compare runs 1, 2, 16, 12, 13, 15 and 4, 3, 5, 6, 10, 11.)

(iv) The plot of $\log k_u$ for CH_4 formation against $1/T$ (represented in Fig. 2) gives a straight line which corresponds to an energy of activation of 63.2±1.5 kcal./mole and a frequency factor of $1.0 \cdot 10^{13}$ sec.$^{-1}$

DISCUSSION

The above results are in accordance with the suggested mechanism, namely,

$$C_6H_5 \cdot CH_2 \cdot CH_3 \rightarrow C_6H_5 \cdot CH_2 \cdot + CH_3 \cdot, \quad (1)$$

$$C_6H_5 \cdot CH_3 + CH_3 \cdot \rightarrow C_6H_5 \cdot CH_2 \cdot + CH_4. \quad (6)$$

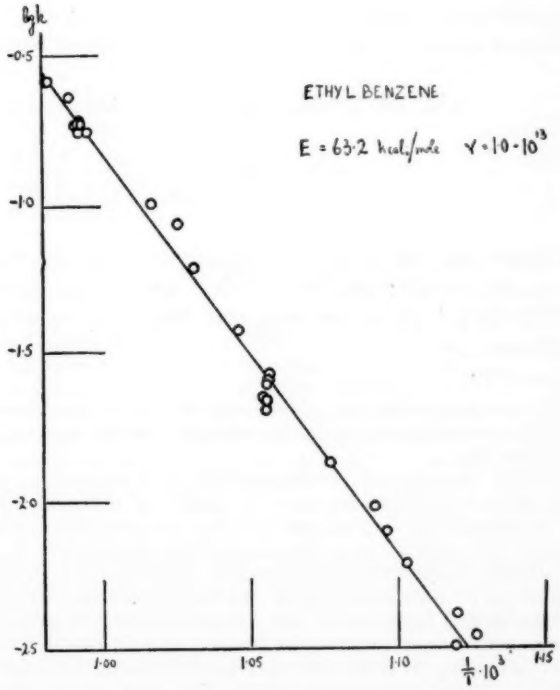

FIG. 2. Plot of $\log K$ against $1/T$.

The benzyl radicals eventually dimerize, and the molar ratio 1:1 of dibenzyl and CH_4 strongly favors the above mechanism.

The rate-determining step in the formation of CH_4 is reaction (1), and, therefore, we interpret the observed energy of activation as equal to the C−C bond energy in ethylbenzene.†

Part of the observed H_2 can be accounted for by reaction (2) followed by (3). With a toluene/ethylbenzene ratio of 20:1, the methyl radicals have a probability of about 0.05 for reaction with ethylbenzene molecules. The H atoms formed as a result of reaction (3) react mainly with toluene molecules, and from the investigation of the pyrolysis of toluene we know that the products of this reaction contain 60 percent H_2. Thus on the basis of reaction (2), only about three percent H_2 would be expected to be present in the pyrolysis products. To account for the remainder (about 15–20 percent), we suggest reaction (7),

$$C_6H_5\cdot CH_2\cdot CH_3 \rightarrow C_6H_5\cdot CH{:}CH_2 + H_2. \quad (7)$$

Judging from the analysis of the gas obtained at various temperatures it seems that the energy of activation of reaction (7) is slightly lower than that of reaction (1), while the temperature independent factor of (7) is considerably lower than that of (1). It is probable that reaction (7) is mainly a wall reaction,†† but the results are not sufficiently accurate to allow any further quantitative conclusions.

Nevertheless, reaction (7) cannot account for the production of H_2 and styrene in the first series of experiments, when ethylbenzene was pyrolyzed without addition of toluene. In these experiments the rate of formation of H_2 was about 50–100 times higher than would be expected in the pyrolysis of ethylbenzene (at the same partial pressure) mixed with twenty-fold excess of toluene, and this can only be accounted for by the suggested chain process.

The small quantities of C_2 hydrocarbons obtained can be accounted for by reaction (8),

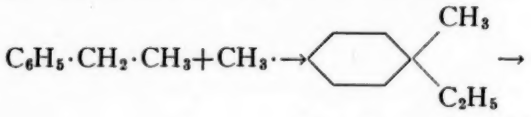

followed by (9),

$$C_6H_5\cdot CH_3 + C_2H_5\cdot \rightarrow C_6H_5\cdot CH_2\cdot + C_2H_6. \quad (9)$$

It should be noted that the suggested mechanism for the pyrolysis of ethylbenzene in excess of toluene leads to the conclusion that the thermal decomposition of toluene is not a chain reaction, as was suggested by Dewar during the discussion on "the labile molecule."††† The observation that the decomposition of ethylbenzene does not induce any chain decomposition of toluene, although each CH_3 radical decomposes one molecule of toluene into a benzyl radical, is a strong argument against the assumption of any chain mechanism in the pyrolysis of toluene.

THE CALCULATION OF D(C−H) IN METHANE

A knowledge of the C−C bond energy in ethylbenzene enables us to calculate the C−H bond energy in methane from the following thermochemical equations:

$$\Delta H_f(C_6H_5\cdot CH_2\cdot CH_3) = \Delta H_f(C_6H_5\cdot CH_2\cdot) + \Delta H_f(CH_3\cdot) - D(C-C)_{C_6H_5\cdot C_2H_5}$$
$$\Delta H_f(H_2) = 2\Delta H_f(H) - D(H-H)_{H_2}$$
$$\Delta H_f(C_6H_5\cdot CH_3) = \Delta H_f(C_6H_5\cdot CH_2\cdot) + \Delta H_f(H) - D(C-H)_{C_6H_5\cdot CH_3}$$
$$\Delta H_f(CH_4) = \Delta H_f(CH_3\cdot) + \Delta H_f(H) - D(C-H)_{CH_4}.$$

Subtracting the last two equations from the first two, one obtains the D(C−H) in methane in terms of the D(C−H) in toluene and D(C−C) in ethylbenzene, i.e.,

$$D(C-H)_{CH_4} = \Delta H_f(C_6H_5\cdot C_2H_5) + \Delta H_f(H_2) - \Delta H_f(C_6H_5\cdot CH_3) - \Delta H_f(CH_4) + D(C-C)_{C_6H_5\cdot C_2H_5} + D(H-H)_{H_2} - D(C-H)_{C_6H_5\cdot CH_3}.$$

The D(C−H) in toluene was estimated previously at 77.5±1.3 kcal./mole by the investigation of the pyrolysis of toluene,[1] and thus, using the recent thermochemical data,[3] we obtain the D(C−H) in methane at 102.9±2.8 kcal./mole.

In the course of the last fifteen years the C−H

† It is assumed that the recombination of benzyl and methyl radicals to ethylbenzene molecules does not involve any energy of activation.

†† The heterogenous decomposition of ethylbenzene into styrene and hydrogen has been the subject of a great number of investigations. If a suitable catalyst is used, the reaction occurs at temperatures as low as 420°C to 480°C. [See S. R. Sergienko, Comptes Rendus U.S.S.R. **20**, 69 (1940) or A. G. Oblad, R. F. Marschner, and W. Heard, J. Am. Chem. Soc. **62**, 2066 (1940).] However, as the temperature of the pyrolysis rises, increasing quantities of toluene appear in the products, and, according to Sergienko's interpretation, the breaking of the C−C bond starts to take place. [See also S. R. Sergienko, Comptes Rendus U.S.S.R. **29**, 36 (1940).]

††† See Trans. Faraday Soc. **2**, 69 and 71 (1947).

[3] $\Delta H_f(CH_4) = -17.9$ kcal./mole, $\Delta H_f(C_6H_5\cdot CH_3) = +11.95$ kcal./mole, $\Delta H_f(C_6H_5\cdot C_2H_5) = +7.1$ kcal./mole. Heat of dissociation of $H_2 = 104.18$ kcal./mole. Taken from: *Selected Data of Properties of Hydrocarbons*, American Petroleum Institute Research Project 44 (1948).

bond energy in methane has been estimated by several investigators.[4] The values obtained ranged from 100 kcal./mole to 103 kcal./mole, and particularly precise data were obtained by Kistiakowsky and his collaborators.[5] The agreement between Kistiakowsky's D(C−H) in CH_4 (102 kcal./mole) and that reported in the present paper (102.9±2.8 kcal./mole) provides, therefore, a powerful argument in favor of our values of the D(C−C) in ethylbenzene and D(C−H) in toluene.

THE FREQUENCY FACTOR OF THE UNIMOLECULAR REACTION

It was found experimentally that the frequency factor of the unimolecular decomposition of toluene and the xylenes is $2\cdot10^{13}$–$2.5\cdot10^{13}$ sec.$^{-1}$ for each methyl group,[1] i.e., about 0.7–$0.8\cdot10^{13}$ for one C−H bond of the methyl group (less by the symmetry factor of 3). The present investigation shows that the frequency factor of the unimolecular decomposition of ethylbenzene is $1.0\cdot10^{13}$ sec.$^{-1}$. The uncertainty of these estimations is roughly within a factor of 2 (due to the experimental errors of 1.3 kcal. and 1.5 kcal., respectively, in the estimations of the activation energy of the corresponding reactions). The estimation of the ratio $\gamma_{C-C}/\gamma_{C-H}$, the ratio of the frequency factors for the breaking of one C−C and one C−H bond of the corresponding molecules, is uncertain, therefore, within the factor of 4. We can obtain, however, a more accurate estimation of the $\gamma_{C-C}/\gamma_{C-H}$ ratio by direct comparison of the rates of the decomposition of ethylbenzene and toluene at the same temperature, say 1000°K,

$$\log(k_{C_6H_5\cdot C_2H_5}/k_{C_6H_5\cdot CH_3}) = \log(\gamma_{C-C}/3\gamma_{C-H})+(\Delta E/4.6).$$

ΔE is the difference of the C−H bond energy in toluene and the C−C bond energy in ethylbenzene, which can be calculated directly using the thermochemical data and Kistiakowsky's value for the D(C−H) in methane. Such an estimation gives $\Delta E=15.2$ kcal. with a probable error of ±0.5 kcal. The average values of $k_{C_6H_5\cdot C_2H_5}$ and $k_{C_6H_5\cdot CH_3}$ at 1000°K are $15.0\cdot10^{-2}$ sec.$^{-1}$ and $0.0325\cdot10^{-2}$ sec.$^{-1}$, respectively, the experimental errors being about ten percent. Using this data we obtain

$$\gamma_{C-C}/\gamma_{C-H}=0.69,$$

a value which is uncertain within a factor of 1.5.

We feel that further discussion should be postponed until more experimental data are available. Nevertheless, it should be emphasized that this trend in γ is what one expects from the change in the reduced mass of the system.

I am pleased to express my gratitude to Professor M. Polanyi for his continuous encouragement and to the Manchester University for the I.C.I. fellowship.

[4] F. O. Rice and M. D. Dooley, J. Am. Chem. Soc. **56**, 2747 (1934); E. C. Baughan and M. Polanyi, Nature **146**, 685 (1940); D. P. Stevenson J. Chem. Phys. **10**, 291 (1942).
[5] G. B. Kistiakowsky and E. R. Van Artsdalen, J. Chem. Phys. **12**, 479 (1944).

THE JOURNAL OF CHEMICAL PHYSICS VOLUME 17, NUMBER 5 MAY, 1949

Some Magnetic Properties of Manganese-Activated Luminescent Solids*

PETER D. JOHNSON AND FERD E. WILLIAMS
Chemistry Department, University of North Carolina, Chapel Hill, North Carolina
(Received November 5, 1948)

The specific susceptibilities of a series of manganese-activated zinc fluoride phosphors and their components have been measured. The unexcited manganese was found to be in the divalent ^6S state. There is evidence for exchange demagnetization of adjacent paramagnetic activator ions.

The change in paramagnetic susceptibility with excitation, predicted by Williams and Eyring [F. E. Williams and H. Eyring, J. Chem. Phys. **15**, 289 (1947)] to explain the long non-temperature-dependent lifetimes of the emitting states of luminescent solids containing paramagnetic activators, has been measured for manganese-activated zinc fluoride. Radiation from a high voltage discharge lamp was used to excite the phosphor in a vacuum magnetic balance having a sensitivity of 10^{-6} dyne per mm scale deflection. The observed change in susceptibility corresponds to a decrease of the order of magnitude of one Bohr magneton per excited activator ion.

I. INTRODUCTION

MAGNETIC susceptibility changes accompanying excitation have been reported by Rupp[1] and Sibaiya and Venkataramiah[2] for sulfide phosphors. In such materials the apparent long-life of the excited state results from the trapping of

* Supported by the Office of Naval Research under Contract N7onr-284, Task Order I. Presented at the American Physical Society Meeting in Washington on May 1, 1948.

[1] E. Rupp, Ann. d. Physik **78**, 505 (1925).
[2] L. Sibaiya and H. S. Venkataramiah, Curr. Sci. **9**, 224 (1940).

TABLE I.

Substance	Specific susceptibility	Equivalent susceptibility of MnF_2
ZnF_2	-0.40×10^{-6}	
ZnF_2:0.0055 Mn	0.40×10^{-6}	162×10^{-6}
ZnF_2:0.0400 Mn	5.1×10^{-6}	153×10^{-6}
MnF_2*		108×10^{-6}
MnF_2 (theoretical)		162×10^{-6}
MnF_2 (0.09-mole percent H_2O solution)**		162×10^{-6}

* H. Bizette and B. Tsai, Comptes Rendus **209**, 205 (1939).
** O. Liebknecht and A. Wills, Ann. d. Physik **1** (4), 178 (1900).

electrons; therefore, the susceptibility change is a property of the difference in magnetic character of the unexcited and the trapped electrons. Jensen[3] has measured the paramagnetic susceptibility of trapped electrons in alkali halides. Lewis[4] and co-workers have shown that multiplicity changes are active in the luminescence of organic phosphors.

The phosphorescence of manganese-activated inorganic luminescent solids is characterized by an initial non-temperature-dependent exponential afterglow followed by a slowly decaying temperature-dependent afterglow. The initial stage depends on the transition probability of the emission process, whereas the later stage depends on the electron trapping phenomena. To explain the low transition probability of the initial afterglow and the low frequency factor of the specific rate constant for the electron trap contribution to phosphorescence, Williams and Eyring[5] have proposed that the three states involved have different multiplicities.

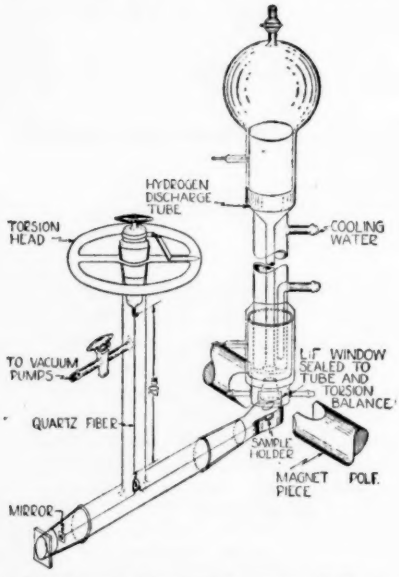

FIG. 1. Change of magnetic susceptibility with excitation apparatus.

[3] P. Jensen, Ann de Physik **34**, 161 (1939).
[4] G. N. Lewis *et al.*, J. Am. Chem. Soc. **63**, 3005 (1941); **64**, 1774 (1942); **66**, 2100 (1944); **67**, 1232 (1945).
[5] F. E. Williams and H. Eyring, J. Chem. Phys. **15**, 289 (1947).
[6] F. E. Williams, J. Opt. Soc. Am. **36**, 353 (1946).

The present work was undertaken to determine whether the actual emission process for manganese-activated zinc fluoride involves a change in multiplicity by attempting to detect the predicted change in magnetic susceptibility with excitation. For the proposed measurement ZnF_2:Mn has the following particularly desirable properties: (a) it exhibits the longest non-temperature-dependent afterglow of any known inorganic luminescent solid;[6] (b) electron trapping is negligible at room temperature,[7] and (c) the phosphor consists of a substitutional paramagnetic activator in a simple ionic diamagnetic lattice.

Preliminary to the change in susceptibility determination, specific susceptibility measurements were made to determine the unexcited state of the activator.

II. MEASUREMENTS OF SPECIFIC MAGNETIC SUSCEPTIBILITIES

The apparatus used for the measurement of specific susceptibilities was similar in principle to the Cheneveau modification[8] of the Faraday method. Calibration with different substances of known susceptibilities: $CuSO_4\cdot5H_2O$,[9] $\chi=5.90\times10^{-6}$ and Pt,[10] $\chi=1.10\times10^{-6}$ agreed within one percent. All reported values are an average of at least ten separate determinations. An accurate mapping of the magnetic field was unnecessary because the sample was always returned to the same position in the field by adjustment of a torsion head.

The activator concentrations were checked by oxidizing the manganese with periodate and determining the permanganate colorimetrically in a Coleman spectrophotometer. The analytical procedure was standardized using mechanical mixtures of ZnF_2 and MnF_2.

In Table I are presented for some ZnF_2:Mn phosphors crystallized at 1125°K and their components the measured specific susceptibilities and the effective specific susceptibilities of the MnF_2. In addition, the theoretical "spin only" value for Mn^{++} at infinite dilution and pertinent published data are shown. All values are for 18°C.

Both for the "magnetically dilute" phosphor and the water solution the contributions of the manganese to the susceptibilities correspond precisely to divalent manganese in the ^6S state. The lower equivalent susceptibility of the activator in the 4.0-mole percent phosphor, as well as of the manganese in solid MnF_2, may be ascribed to exchange demagnetization of adjacent activator ions. A preliminary analysis of the data indicates that there exists an appreciable departure from a random distribution of

[7] J. S. Johnson and F. E. Williams, unpublished data.
[8] C. Cheneveau, Phil. Mag. **20**, 357 (1910).
[9] E. Feytis, Comptes Rendus **153**, 668 (1912).
[10] K. Honda, Ann. d. Physik **32** (4), 1027 (1910).

activator ions over lattice sites. Measurements of specific susceptibilities of manganese-activated phosphors of diverse activator content prepared under various conditions and a theoretical analysis of the effect of the exchange demagnetization on the luminescent properties are in progress.

III MEASUREMENT OF THE CHANGE OF MAGNETIC SUSCEPTIBILITY WITH EXCITATION

The apparatus used for the measurement of the change in magnetic susceptibility with excitation is shown diagrammatically in Fig. 1.** The components are: (a) a hydrogen discharge lamp operated at 2.3 kv and 1.2 amp.; (b) a torsion balance, enclosed in a Pyrex vacuum chamber, consisting of a quartz fiber about 0.5μ in diameter and 18 cm long, and a torsion beam 20 cm long with the sample at one end on a Pyrex paddle and a mirror on the other end; and (c) an electromagnet producing an inhomogeneous magnetic field perpendicular to both the axis of the torsion fiber and the axis of the torsion beam with a useful field of 5000 gauss and a field gradient of 3000 gauss per cm. By determining the period of oscillation of a torsion arm of known moment of inertia it was found that a force of 10^{-6} dyne gave a 1-mm deflection of a light beam on a scale one meter from the mirror. The hydrogen lamp was sealed to the balance enclosure vertically to eliminate the superposition of a component of the radiation pressure on the magnetic effect being measured. Only a 1-mm thick LiF window separated the discharge from the phosphor.

The experimental procedure was as follows: Sufficient phosphor to balance as nearly as possible the diamagnetic susceptibility of the support was deposited on the Pyrex paddle. The system was assembled and evacuated, the magnet switched on, and the torsion head adjusted to place the sample in the part of the field, as determined by previous mapping, with maximum $H(dH/dx)$. After the field was applied, the torsion arm oscillated with a period of 10 sec., and when the amplitude of the oscillations attenuated to less than 5 mm on the scale, the hydrogen source was turned on at the extreme of an oscillation. After several minutes, the source was turned off at the extreme of an oscillation. By plotting midpoints between successive readings of the extremes of oscillation as a function of time, a plot such as shown in Fig. 2 is obtained. Because the times the source was turned on and off are known, the change in susceptibility can be followed as a function of excitation. However, because the period of the balance is greater than the average lifetime (0.1 sec.) of the excited state of the phosphor, it is impossible with the apparatus to follow in detail susceptibility changes occurring in periods as short as the lifetime of the emitting state. The slope of the curve obtained immediately after turning the source on or off is almost exactly the same as that obtained by suddenly changing the magnetic field by switching a resistance in or out of the circuit carrying the current for the magnetizing coils.

IV. INTERPRETATION OF THE SUSCEPTIBILITY CHANGES WITH EXCITATION

The specific susceptibility measurements on the ZnF_2:Mn phosphor indicated that the unexcited Mn^{++} is in the state of maximum multiplicity with five unpaired electron spins in the *3d* shell. From energy considerations it is unlikely that electrons in the more deeply lying shells are responsible for the luminescent properties; therefore, if the long lifetime of the emitting state arises from a difference in multiplicity compared to the ground state of the activator, it is clear that a decrease in paramagnetic susceptibility must accompany excitation. Unfortunately, any heating of the phosphor during excitation also produces a decrease in susceptibility, as shown by the following expression[11] for the paramagnetism of a solid with S unpaired electron spins and weak spin interaction:

$$X_M=(N\beta^2/3k(T+\Delta))[4S(S+1)].$$

Because ZnF_2:Mn is excited throughout the region of strong absorption below 2300A and because there is negligible infra-red from the hydrogen

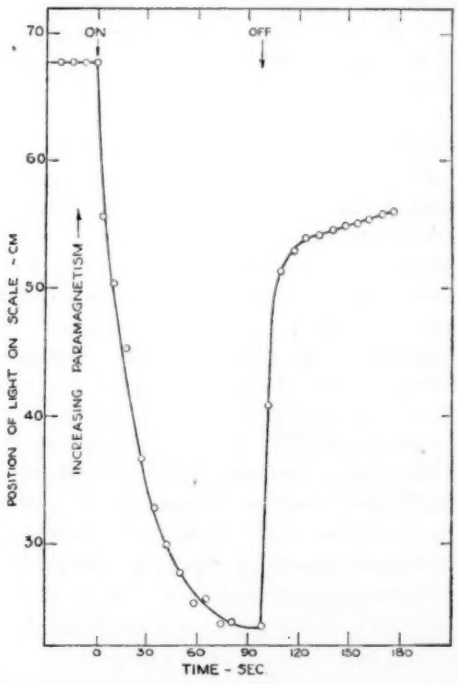

FIG. 2. Change of susceptibility with excitation.

** We are indebted to S. H. Patten for the preparation of the drawings in this paper.

[11] J. H. Van Vleck, *Electric and Magnetic Susceptibilities* (Oxford University Press, New York, 1932).

source, the principle contributions to heating of the phosphor are the atomic rearrangements occurring during luminescence and resulting in the large difference between excitation and emission energies. From the rearrangement energy and the heat capacity of the sample and support, the temperature rise during the period of excitation was calculated using the maximum conceivable number and the most probable number of activators excited simultaneously. 5°C and 0.3°C were obtained, respectively. A temperature rise less than 0.3°C was measured during the period of excitation by a thermocouple fused in a sample. To confirm that the thermocouple reading is both a true measurement of the temperature of the fused phosphor and a measure of the heating of the powdered sample used in the change of susceptibility determination, both materials were heated, but not excited, with a 500-watt tungsten projection lamp with a filter passing only radiation longer than 6000A; the temperatures were measured by the change in susceptibility and checked by the thermocouple reading for the fused sample. In four minutes the temperature of the fused sample increased 14°C, whereas the temperature of the powdered sample increased 12°C. It is concluded, therefore, that the increase in temperature of the powdered phosphor by the hydrogen source during the change in susceptibility with excitation measurement is less than 1°C. Because the decrease in paramagnetic susceptibility observed and shown in Fig. 2 can be explained by heating alone only if at least a 25°C increase in temperature accompanies excitation, it is concluded that a change in multiplicity accompanies excitation. The long-time components of the change in susceptibility on excitation can be attributed to the small heating effect plus a small contribution from the difference in multiplicity of trapped electrons. The latter effect is eliminated as the principal short-time component of the multiplicity change by the previously mentioned observation that electron trapping in ZnF_2:Mn is insufficient at room temperature to account for the observed susceptibility change, by the fact[7] that the time constant of the electron trap contribution to phosphorescence is large compared to the time interval of the susceptibility change, and by preliminary measurements of the temperature-dependence of the change of susceptibility with excitation which indicated that the temperature coefficient is less than would be expected for electron trap release. It is concluded, therefore, that the observed change in magnetic susceptibility with excitation is primarily a result of the difference in multiplicities of the emitting and ground states of Mn^{++}.

To determine the change in multiplicity per excited activator, in addition to the total change in susceptibility, it is obviously necessary to know the number of activators excited simultaneously, n. The latter was estimated by three methods: (a) The thickest sample that could be excited to saturation by the hydrogen source was found to contain 2×10^{16} Mn^{++}. (b) The number of exciting quanta from the hydrogen source incident on the sample during the lifetime of the emitting state was estimated at 3×10^{15}. (c) By measuring the luminance of the excited sample and knowing the transition probability for the emission process, a value of 5×10^{14} activators excited simultaneously was obtained. The geometric mean of the three estimations gave a value of 3×10^{15} activators excited simultaneously and is believed to be correct well within an order of magnitude.

The strength and gradient of the magnetic field for the region occupied by the sample were, respectively, 3000 gauss and 2000 gauss per cm. For a change in specific susceptibility corresponding to a change in multiplicity from 6 to 5 for 3×10^{15} activators, the change in force on the sample is:[12]

$$\Delta f=(n/N)\Delta X\cdot M\cdot H(dH/dx)\cong6\times10^{-5}\text{ dyne.}$$

From the sensitivity of the balance, this should produce a scale deflection of 6 cm. The observed deflection as shown in Fig. 2 is 4 cm. It can, therefore, be stated that the observed change in susceptibility corresponds to approximately a change of multiplicity of one per activator.

Zn_2SiO_4:Mn was found to exhibit a small decrease in paramagnetic susceptibility on excitation, indicating that the initial spontaneous afterglow of manganese-activated phosphor, in general, is probably due to a difference in multiplicity of the emitting state compared to the normal state.

The results of preliminary measurements on pure MnF_2 suggest that the mechanism of absorption, at least at the long wave-length edge of the absorption band, of non-luminescent as well as luminescent paramagnetic salts is often excitation to a state of different multiplicity and that the excited state has a long lifetime. Experiments are under way to confirm the measurements on MnF_2.

V. CONCLUSIONS

The unexcited manganese in ZnF_2:Mn is in the divalent ^6S state.

The long non-temperature dependent afterglow of manganese-activated luminescent solids results from a difference in multiplicities of the emitting and the ground states of Mn^{++}.

[12] P. W. Selwood, *Magnetochemistry* (Interscience Publishers, Inc., New York 1943).

An Asymptotic Expression for the Energy Levels of the Asymmetric Rotor. III. Approximation for the Essentially Degenerate Levels of the Rigid Rotor*

S. GOLDEN** AND J. K. BRAGG***
Mallinckrodt Chemical Laboratory, Harvard University, Cambridge, Massachusetts
(Received November 15, 1948)

Formulas are given for an approximation to the energy values of the levels of the asymmetric rotor when the latter are essentially twofold degenerate. The method of arriving at these formulas follows that described recently, in which the energy matrix is examined under conditions where $J\to\infty$. In contrast to the latter method, however, the present approximation considers those levels for which (in the limiting symmetric cases) $|K|$ is very nearly equal to J. With these restrictions, the energy matrix of the asymmetric rotor assumes a form that can be related to that which may be obtained from a perturbed harmonic oscillator.

INTRODUCTION

THE recent application of the correspondence principle[1] to the problem of the rigid asymmetric rotor has simplified considerably the labor involved in approximating the energy values for the higher levels corresponding to large values of J. The correspondence principle gives results which may be expected to give good energy values for those asymmetric rotor levels which are essentially twofold degenerate.

In order to simplify further the computational work which is involved in the correspondence principle method, the energy matrix of the asymmetric rotor, evaluated in terms of a basis of symmetric rotor wave functions, has been examined under conditions where J is increased indefinitely. A similar method has been described recently for those levels which correspond to small values of $|K|$ (in the limiting symmetric cases), in which it was found that the energy matrix assumed an asymptotic form ($J\to\infty$) similar to that which may be obtained from Mathieu's equation.[2] In contrast, the present paper is concerned with those levels for which $|K|$ assumes values very nearly equal to J. For this condition, the energy matrix assumes an asymptotic form ($J\to\infty$) which is similar to that which may be realized from the characteristic value problem of a perturbed harmonic oscillator.[2a]

As a consequence, it has been found possible to obtain an expression for the energy values of those rigid asymmetric rotor levels for which $|K|$ is very nearly equal to J. The most significant portion of the expression involves the asymmetry parameter of the rotor in a closed form; some higher order corrections are given explicitly. An inherent shortcoming of the present method is its inability to reveal the removal with increasing asymmetry of the twofold degeneracy in $|K|(K\neq 0)$. Thus, as in the correspondence principle treatment, the present results must be restricted to those asymmetric rotor levels which are essentially twofold degenerate.

ASYMPTOTIC FORM OF THE ENERGY MATRIX

For the sake of brevity, use will be made of the results of (I). The problem then reduces to finding the diagonal elements of $\mathbf{E}'(\kappa)$ (cf. Eq. (5) of (I)). The elements of the latter, evaluated in terms of a basis of symmetric rotor wave functions, are given by Eqs. (6) and (7) of (I), *viz.*,

$$E'_{K;K}=K^2, \tag{1}$$

and

$$E'_{K;K+2}=E'_{K+2;K}=(H/G-F)[f(J,K+1)]^{\frac{1}{2}}, \tag{2}$$

where

$$f(J,n)=\tfrac{1}{4}[J(J+1)-n(n+1)][J(J+1)-n(n-1)].$$

For $|K|$ nearly equal to J, the off-diagonal elements of $\mathbf{E}'(\kappa)$ may be put into a form suitable for expansion. To this end let[3]

$$K=-J+m, \tag{3}$$

where m is a positive integer or zero. On substituting Eq. (3) into the expression for $[f(J,K+1)]^{\frac{1}{2}}$, there results

$$\begin{aligned}[f(J,K+1)]^{\frac{1}{2}}&=\tfrac{1}{2}[(m+1)(m+2)(2J-m)\\&\qquad\times(2J-m-1)]^{\frac{1}{2}} \qquad (4)\\&=J[(m+1)(m+2)]^{\frac{1}{2}}(1-(m/2J))\\&\qquad\times(1-(1/2J-m))^{\frac{1}{2}}.\end{aligned}$$

* The support given by the Navy Department is gratefully acknowledged for some of the computational work reported here. It was carried out under Task Order V of Contract N5ori-76, Office of Naval Research, by Mrs. Grace C. Ek.
** National Research Council Predoctoral Fellow. Present address: Hydrocarbon Research, Inc., 115 Broadway, New York City.
*** Present address: Department of Chemistry, Cornell University, Ithaca, New York.
[1] G. W. King, J. Chem. Phys. 15, 820 (1947).
[2] S. Golden, J. Chem. Phys. 16, 78 (1948), hereinafter referred to as (I).
[2a] Professor J. H. Van Vleck has kindly pointed out that the method employed here is similar to that employed by Luttinger and Kittel, "Note on the quantum theory of ferromagnetic resonance," to be published.
[3] The results for $K=J-m$ are identical with those derived from Eq. (3). The present choice is essentially a matter of convenience in notation.

For $m/2J \ll 1 \ll 2J$, the following expansion may be obtained:

$$[f(J,K+1)]^{\frac{1}{2}} = J[(m+1)(m+2)]^{\frac{1}{2}}\{1+1/2J-1/32J^2 +1/64J^3+\cdots-((m+3/2)/2J) \times(1+1/32J^2+\cdots)+O(m^2/128J^4)\}. \quad (5)$$

Hence the off-diagonal elements of $\mathbf{E}'(\kappa)$ may be written

$$E'_{K;K+2}=E'_{m;m+2} \cong J(H/G-F)(1+1/2J-1/32J^2 +1/64J^3)[(m+1)(m+2)]^{\frac{1}{2}} -\tfrac{1}{2}(H/G-F)(1+1/32J^2) \times(m+3/2)[(m+1)(m+2)]^{\frac{1}{2}}. \quad (6)$$

The diagonal elements are

$$E'_{K;K}=E'_{m;m}=J^2-2Jm+m^2. \quad (7)$$

Now, the diagonal term J^2 may be subtracted from $\mathbf{E}'(\kappa)$, and the resulting matrix may be divided by $(-2J)$, so that

$$\mathbf{E}'(\kappa)=J^2\mathbf{I}-2J\mathbf{E}''(\kappa), \quad (8)$$

where $\mathbf{E}''(\kappa)$ has the following non-vanishing elements.

$$E''_{m;m}=m-m^2/2J, \quad (9)$$

and

$$E''_{m;m+2} \cong -\beta[(m+1)(m+2)]^{\frac{1}{2}} +(\beta'/2J)(m+3/2) \times[(m+1)(m+2)]^{\frac{1}{2}}, \quad (10)$$

with

$$\beta=\tfrac{1}{2}(H/G-F)(1+1/2J-1/32J^2+1/64J^3),$$
$$\beta'=\tfrac{1}{2}(H/G-F)(1+1/32J^2).$$

If terms $O(m^2/J)$ are neglected in comparison with terms $O(m)$, as $J\to\infty$,

$$E''_{m;m}\to m,$$
$$E''_{m;m+2}\to -\beta[(m+1)(m+2)]^{\frac{1}{2}}. \quad (11)$$

The matrix constructed from the elements of Eq. (11) may be recognized as involving the square of the momentum and the square of the displacement of a linear harmonic oscillator in the Heisenberg matrix representation. This suggests the use of a complete set of normalized Hermite orthogonal functions (i.e., harmonic oscillator wave functions) as a basis to develop the matrix defined by Eqs. (9) and (10). The operators required to accomplish this will be developed in the following section.

TABLE I. Operators and non-vanishing matrix elements used with the harmonic oscillator representation.

Operator	Definition	Matrix elements
$\mathcal{P}_1$	$-\frac{d^2}{dx^2}+x^2$	$\mathcal{P}_1(m;m)=2m+1$
$\mathcal{P}_2$	$\frac{d^2}{dx^2}+x^2$	$\mathcal{P}_2(m;m+2)=[(m+1)(m+2)]^{\frac{1}{2}}$
$\mathcal{P}_3$	$-\frac{d^4}{dx^4}+x^4$	$\mathcal{P}_3(m;m+2)=(2m+3)[(m+1)(m+2)]^{\frac{1}{2}}$
$\mathcal{P}_4$	$\frac{d^4}{dx^4}+x^4$	$\mathcal{P}_4(m;m)=3(m^2+m+\frac{1}{2})$
		$\mathcal{P}_4(m;m+4)=[(m+1)(m+2)(m+3)(m+4)]^{\frac{1}{2}}$

OPERATORS FOR THE HARMONIC OSCILLATOR REPRESENTATION

In terms of a basis of Hermite orthogonal functions,[4]

$$y_m(x)=(2^m m!\pi^{\frac{1}{2}})^{-\frac{1}{2}}H_m\exp(-\tfrac{1}{2}x^2), \quad m=0,1,\cdots, \quad (12)$$

the operator

$$\mathfrak{L}=\tfrac{1}{2}(1+1/2J)\mathcal{P}_1-(1/8J)\mathcal{P}_1^2-\tfrac{1}{2}(1+1/4J) -\beta\mathcal{P}_2+(\beta'/4J)\mathcal{P}_3 \quad (13)$$

gives rise to the matrix $\mathbf{E}''(\kappa)$. The various operators are defined in Table I, which gives also their non-vanishing matrix elements. The table may be verified readily from the properties of the Hermite orthogonal functions.[5]

The approximate characteristic values of the matrix $\mathbf{E}''(\kappa)$ are now given by the characteristic values of the differential equation

$$\mathfrak{L}y=\lambda y, \quad (14)$$

where $\mathfrak{L}$ is given by Eq. (13). When β and β' vanish, the functions y_m of Eq. (12) are the solutions of Eq. (14).

APPROXIMATE SOLUTION OF THE DIFFERENTIAL EQUATION

In Eq. (14) let

$$\alpha=\lambda+\tfrac{1}{2}(1+1/4J). \quad (15)$$

The equation to be solved is

$$\{\tfrac{1}{2}(1+1/2J)\mathcal{P}_1-(1/8J)\mathcal{P}_1^2 -\beta\mathcal{P}_2+(\beta'/4J)\mathcal{P}_3\}y=\alpha y. \quad (16)$$

The operator $\mathcal{P}_2$ gives rise to off-diagonal elements of order β. These may be eliminated by the change of variable

$$x=\xi[(1+1/2J+2\beta)/(1+1/2J-2\beta)]^{\frac{1}{4}}.$$

Substitution of this expression into Eq. (16) gives, after some algebraic manipulation,

$$\mathfrak{L}'y=\{\tfrac{1}{2}\mathcal{P}_1'-(1/8Jw)\mathcal{P}_1'^2 -A\mathcal{P}_3'-B\mathcal{P}_4'\}y=\alpha' y, \quad (17)$$

[4] For a discussion of these functions see, for example, L. Pauling and E. B. Wilson, Jr., *Introduction to Quantum Mechanics* (McGraw-Hill Book Company, Inc., New York, 1935), p. 77.

[5] See, for example, V. Rojansky, *Introductory Quantum Mechanics* (Prentice-Hall, Inc., New York, 1946), pp. 26 and 41.

where the $\mathcal{P}'$ are the operators listed in Table I with ξ as the variable instead of x. Here

$$w=[(1+1/2J)^2-4\beta^2]^{\frac{1}{2}},$$
$$A=(1/4Jw^3)[2\beta(1+1/2J-4\beta\beta')-\beta'w^2],$$
$$B=(\beta/Jw^3)[\beta-\beta'(1+1/2J)],$$
$$\alpha'=\alpha/w. \tag{18}$$

The first two terms of Eq. (17) are diagonal in a new harmonic oscillator representation. The off-diagonal elements in this new representation are now of order (β/J). Even for moderately large values of J, therefore, a rapid convergence of the usual perturbation series may be expected.

Before giving this series, it is convenient to consider the coefficient B. Since the quantity

$$[\beta-\beta'(1+1/2J)]\sim-(1/32J^2)(H/G-F),$$

and for $\kappa=0$, $|(H/G-F)|=1/3$, a representative value for B is $(1/128J^3)$. An examination of the matrix elements of $\mathcal{P}_4'$ shows that with this value of B second-order terms may safely be neglected.

Combination of the above results gives the conventional perturbation series, correct to and including second-order terms:

$$\alpha=\alpha^{(0)}+\alpha^{(1)}+\alpha^{(2)}, \tag{19}$$

where

$$\alpha^{(0)}=(m+\tfrac{1}{2})w-(1/2J)(m+\tfrac{1}{2})^2,$$
$$\alpha^{(1)}=-3Bw(m^2+m+\tfrac{1}{2}),$$
$$\alpha^{(2)}=-(4A^2w)[(m+1)(m+2)\times(m+3/2)^2/(2-(2m+3)/Jw)-m(m-1)(m-\tfrac{1}{2})^2/(2-(2m-1)/Jw)]. \tag{20}$$

PERTURBATION TECHNIQUE

The perturbation technique utilized in (I) may be employed here to account for the disparity in the magnitudes of the order of the asymmetric rotor matrix and the order of the matrix developed from Eq. (14). Formally, one augments the former by adding suitably to it rows and columns of zeros. A remainder matrix **R** is added to the latter to adjust for such inequalities that remain between the elements of the latter and the former. By construction, the remainder matrix will give no appreciable contribution in the region being considered. From the practical viewpoint, therefore, its influence on the characteristic values being approximated here may be neglected.

When it is necessary to consider the influence of **R**, it will be necessary to determine the transformation matrix that diagonalizes the matrix obtained from Eq. (14). Since the characteristic values of the latter may be determined approximately from Eq. (20), the transformation matrix is, in principle, readily evaluated. The transformed **R** matrix may then be regarded as a perturbation to be added to the diagonal matrix obtained from Eq. (14). Its effect may be evaluated by using the conventional series-perturbation procedure.

When **R** may be safely neglected, the reduced energy values of the asymmetric rotor are given approximately by combining Eqs. (8), (15), and (20):

$$E'_\tau{}^J(\kappa)=(J+\tfrac{1}{2})^2-2J(m+\tfrac{1}{2})w+(m+\tfrac{1}{2})^2-2J(\alpha^{(1)}+\alpha^{(2)}), \tag{21}$$

where

$$\tau=K_{-1}-K_{+1},$$
$$m=J-K_{-1} \text{ for type } I \text{ representation},$$
$$=J-K_{+1} \text{ for type } III \text{ representation}.$$

For comparison with the values tabulated by King, Hainer, and Cross,[6] use is made of the relation

$$E_\tau{}^J(\kappa)=FJ(J+1)+(G-F)E'_\tau{}^J(\kappa). \tag{22}$$

Such a comparison is given in Table II.

TABLE II. Computation of the energy values of essentially degenerate levels of the asymmetric rotor.

Level,* $J_{K-1,K+1}$	Harmonic oscillator approximation	Tables of reference 6
	$\kappa=-0.8$	
$10_{10,0-1}$	91.02780	91.02780
$10_{9,1-2}$	54.98445	54.98444
$10_{8,2-3}$	22.74492	22.74489
$10_{7,3-4}$	−5.68590	−5.68593
$10_{6,4}$	−30.29838	−30.29839
$10_{6,5}$	−30.29838	−30.29846
	$\kappa=-0.6$	
$10_{10,0-1}$	92.11766	92.11765
$10_{9,1-2}$	58.15739	58.15739
$10_{8,2-3}$	27.81338	27.81341
$10_{7,3}$	1.10654	1.10694
$10_{7,4}$	1.10654	1.10677
	$\kappa=-0.4$	
$10_{10,0-1}$	93.28164	93.28164
$10_{9,1}$	61.55563	61.55565
$10_{9,2}$	61.55563	61.55564
$10_{8,2}$	33.26898	33.26924
$10_{8,3}$	33.26898	33.26914
	$\kappa=-0.2$	
$10_{10,0-1}$	94.53635	94.53636
$10_{9,1}$	65.22976	65.22987
$10_{9,2}$	65.22976	65.22984
	$\kappa=0.0$	
$10_{10,0-1}$	95.90572	95.90573

* The convention of reference (6) is used for the labeling of the energy levels.

ACKNOWLEDGMENT

We wish to express our appreciation for the encouragement given us by Professor E. Bright Wilson, Jr.

[6] G. W. King, R. M. Hainer, and P. C. Cross, J. Chem. Phys. 11, 27 (1943). See also, R. M. Hainer, P. C. Cross, and G. W. King, "The Asymmetric Rotor. VII", J. Chem. Phys. (to be published) where a careful comparison is made of several methods of approximating the energy values for J = 12.

The Rotatory Diffusion Constants of Flexible Molecules

JACOB RISEMAN AND JOHN G. KIRKWOOD
Institute of Polymer Research, Polytechnic Institute of Brooklyn, Brooklyn, New York and Gates and Crellin Laboratories, California Institute of Technology, Pasadena California

(Received September 20, 1948)

Using the model and methods of a previous paper, the average components of the rotary diffusion tensor of a flexible molecule are calculated. The results obtained are found to be related to both the intrinsic viscosity and to the translational diffusion constant. In particular the rotatory diffusion constant of the molecule as a whole is shown to be a simple function of the intrinsic viscosity. The theory developed, in conjunction with the theory of intrinsic viscosity and translational diffusion coordinates the result of the various hydrodynamical physical methods used in high polymer research.

I. INTRODUCTION

IF a system of molecules is aligned by an external force so that a particular direction in each molecule is made to coincide with an arbitrary reference axis, the removal of this force results in a gradual rotatory Brownian motion towards a uniform distribution of directions. The rate with which such diffusion occurs, when the constraining field is removed, is related to the molecular structure of the molecule through the rotatory diffusion constant. In the same way, a molecule having many internal degrees of rotatory freedom, can by internal rotatory Brownian motion take up a large number of configurations corresponding to different sets of possible coordinates of the diffusing segments. This latter consideration applies especially to the so-called flexible macromolecules, represented, for example, by the linear high polymers. Recognition of these facts has led to the statistical description of many of the properties of high polymers both in bulk and in the solution phase.

The concepts of both macro and micro Brownian motion has been of great importance in connection with a variety of different types of physical problems. Mention might be made of the phenomena of dielectric loss, mechanical properties, flow birefringence, and non-Newtonian flow.[1] In all of these problems a parameter, the rotatory diffusion constant, appears, related to the structure of the molecule under consideration. For rigid molecules, expressions for the rotatory diffusion constant have been obtained, utilizing the Einstein relationship between that quantity and the resistance constant. Thus, for spherical particles, the rotary diffusion constant is given by the expression

$$D=(kT/8\pi\eta a^3).$$

For ellipsoidal particles, Burgers[2] gives values for the rotational resistance, from which the rotational diffusion constant can be obtained.

In the case of flexible macromolecules Kirkwood[1] derives expressions for the components of the diffusion tensor, treating the macromolecule as made up of hydrodynamically independent elements. Actually, as has been discussed in an earlier paper, hydrodynamic interaction of the elements of the chain exist so that the over-all influence of the macromolecule on the fluid flow cannot be taken as merely a linear superposition of independent segment effects. To describe the fluid flow through the chain and calculate the components of the rotatory diffusion tensor, we shall use the model and methods described in our previous paper, to which the reader is referred.[3]

II. THE INTERNAL ROTATORY DIFFUSION CONSTANT

We consider a polymer molecule, immersed in a fluid, the segments of which are considered to move with average velocity U_l relative to the solvent. This segmental velocity is derived from the angular motion of the individual elements about the various bonds joining the elements, in addition to the angular motion of the molecule as a whole.

$$\begin{aligned} U_l &= \sum_{k=-n}^{l-1} (\Omega_k \times R_{lk}) + (\Omega_0 \times R_{0l}), \\ \Omega_k &= \dot{\phi}_k b_k, \\ \Omega_0 &= -i(\sin\phi)\dot{\theta} + j(\cos\phi)\dot{\theta} + k\dot{\phi}. \end{aligned} \tag{1}$$

Ω_k is the angular velocity associated with the rotation about bond b_k and Ω_0 the angular velocity associated with the rotation of the molecule as a whole. θ and ϕ describe the orientations of a fixed direction, which we can take to be the bond joining elements 0 and 1, with a fixed rectangular coordinate system. The component of the torque T_j about the bond b_j can then be expressed by

$$T_j = \sum_{k=-n}^{n} \dot{\phi}_k \rho_{jk} \tag{2}$$

which defines the components of the rotational re-

[1] Kirkwood and Fuoss, J. Chem. Phys. 7, 911 (1939).
[2] J. M. Burgers, Chapter III; *Second Report on Viscosity and Plasticity of the Amsterdam Academy of Sciences* (Nordemann, New York, 1938).
[3] J. G. Kirkwood and J. Riseman, J. Chem. Phys. 16, 565 (1948).

sistance tensor around bond b_j. The rotational diffusion tensor can be obtained by means of the Einstein relation

$$D=kT\rho^{-1}, \qquad \rho_{sk}^{-1}=(\Delta_{sk}/|\rho_{sk}|), \tag{3}$$

where $|\rho_{sk}|$ is the determinant of the resistance tensor and Δ_{sk} the co-factor of the corresponding element in the determinant. In particular, if the rotational resistance tensor contains only diagonal elements then

$$D_{ss}=(kT/\rho_{ss}). \tag{4}$$

Therefore to calculate the rotatory diffusion constants it is necessary to compute the torques about the various bonds. We shall here calculate the average torques and consequently the average diffusion constants, since physically it is these average quantities over all configurations of the molecule that one encounters experimentally.

The notation used in this paper is similar to that in our previous paper.[3] For convenience, however, we review the definitions of the terms being used.

k = Boltzmann's constant,
T = the absolute temperature,
R_{lj} = the position of an element j of the chain, relative to an element 1,
b_j = the unit vector directed from chain element $j-1$ to j,
ζ = the friction constant associated with the elements of the chain,
v_{0l} = the unperturbed fluid flow at the location of element l, if that element were absent,
u_l = the velocity of element l,
η_0 = the coefficient of viscosity of the solvent,
Z = the degree of polymerization equal to M/M_0 where M and M_0 are, respectively, the molecular weights of the polymer and monomer units, CHX.

The net torque about an arbitrary element j, caused by the forces acting on elements l is

$$T_j=-\sum_{l=j+1}^{n}(R_{lj}\times F_l)+\sum_{l=-n}^{j-1}(R_{lj}\times F_l), \tag{5}$$

where $-F_l$ is the force acting on element l.[3] The component of this net torque about bond b_j, is associated with the rotatory motion about b_j as an axis.

$$T_j=T_j\cdot b_j=-\sum_{l=j+1}^{n} b_j\cdot(R_{lj}\times F_l) + \sum_{l=-n}^{j-1} b_j\cdot(R_{lj}\times F_l). \tag{6}$$

The average of T_j over-all configurations of the molecule is

$$\langle T_j\rangle_{Av}=-\sum_{l=j+1}^{n}\langle b_j\cdot(R_{lj}\times F_l)\rangle_{Av} + \sum_{l=-n}^{j-1}\langle b_j\cdot(R_{lj}\times F_l)\rangle_{Av},$$

$$\langle T_j\rangle_{Av}=\sum_{k=-n}^{n}\phi_k\langle\rho_{jk}\rangle_{Av}. \tag{7}$$

The quantities $\langle b_j\cdot(R_{lj}\times F_l)\rangle_{Av}$ are now evaluated using the Oseen equation

$$F_l=-\zeta(v_{0l}-u_l)-\zeta\sum_{\substack{s=-n\\ s\neq l}}^{n} T_{ls}\cdot F_s. \tag{8}$$

Setting $(v_{0l}-u_l)$ in (8) equal to U_l,[1] multiplying vectorially by the quantity $(b_j\cdot R_{lj}\times)$ and averaging, we obtain

$$\langle b_j\cdot R_{lj}\times F_l\rangle_{Av}=-\zeta\langle b_j\cdot R_{lj}\times U_l\rangle_{Av} -\zeta\sum_{\substack{s=-n\\ s\neq l}}^{n}\langle b_j\cdot R_{lj}\times T_{ls}\cdot F_s\rangle_{Av},$$

$$\langle b_j\cdot R_{lj}\times U_l\rangle_{Av}=\tfrac{2}{3}b^2(l-j)\phi_j\delta_{jk} \quad l>j$$
$$=0, \quad l<j$$

$$\langle b_j\cdot R_{lj}\times T_{ls}\cdot F_s\rangle_{Av}=\langle b_j\cdot R_{lj}\times\langle T_{ls}\rangle_{Av}\cdot F_s\rangle_{Av} +\langle b_j\cdot R_{lj}\times(T_{ls}-\langle T_{ls}\rangle_{Av})\cdot F_s\rangle_{Av},$$

$$\langle T_{ls}\rangle_{Av}=\frac{1}{(6\pi^3)^{\frac{1}{2}}\eta_0 b|l-s|^{\frac{1}{2}}},$$

$$\delta_{jk}=0 \quad j\neq k$$
$$=1 \quad j=k. \tag{9}$$

Equation (8) therefore becomes

$$\phi_l=f_l-\frac{\lambda}{n^{\frac{1}{2}}}\sum_{\substack{s=-n\\ s\neq l}}^{n}\frac{\phi_s}{(|l-s|)^{\frac{1}{2}}} \quad j<l,$$

$$\phi_l=-\frac{\lambda}{n^{\frac{1}{2}}}\sum_{\substack{s=-n\\ s\neq l}}^{n}\frac{\phi_s}{(|l-s|)^{\frac{1}{2}}} \quad j>l,$$

$$\phi_s=\langle b_j\cdot R_{lj}\times F_s\rangle_{Av},$$

$$f_l=-\tfrac{3}{2}\zeta b^2(l-j)\phi_j,$$

$$\lambda=\frac{\zeta}{(12\pi^3)^{\frac{1}{2}}\eta_0 b}\left(\frac{M}{M_0}\right)^{\frac{1}{2}}. \tag{10}$$

The Eqs. (10) are a set of linear equations in the variables ϕ_k, which for large n can be asymptotically

approximated by the integral equations

$$\phi(x)=f(x)-\lambda\int_{-1}^{1}\frac{\phi(t)}{(|l-t|)^{\frac{1}{2}}}dt \quad j<nx,$$

$$\phi(x)=-\lambda\int_{-1}^{1}\frac{\phi(t)}{(|l-t|)^{\frac{1}{2}}}dt \quad j>nx,$$

$$f(x)=-\tfrac{2}{3}\zeta b^2\dot{\phi}_j(nx-j),$$

$$x=l/n, \quad t=s/n. \tag{11}$$

For $j<nx$, the integral equation is of the form encountered in the viscosity theory, and using those results we can write

$$\phi(x)=\phi_0+\sum_{\substack{m=-\infty\\ m\neq 0}}^{\infty}\phi_m e^{im\pi x},$$

$$\phi_0=\frac{f_0}{1+\frac{8}{3}\sqrt{2}\lambda},$$

$$\phi_m=\frac{f_m-u_m f_0}{1+\lambda(2/|m|)^{\frac{1}{2}}},$$

$$u_m=\frac{\lambda(-1)^{m+1}}{(m\pi)^{\frac{1}{2}}}I_m\int_0^{2\pi m}\frac{e^{iu}}{u^{\frac{1}{2}}}du,^*$$

$$f_0=\tfrac{2}{3}b^2\zeta\dot{\phi}_j j,$$

$$f_m=\frac{\frac{2}{3}b^2\zeta n\dot{\phi}_j i(-1)^{m+1}}{m\pi}, \quad i=\sqrt{-1}. \tag{12}$$

For $j>nx$ we have a linear, homogenous, integral equation. Solutions other than the trivial one $\phi(x)=0$ are obtained only for particular values of λ.[4] Such values of λ are the eigenvalues of the kernel $1/(|x-s|)^{\frac{1}{2}}$. Insofar as λ, in this case, is an experimental constant, the probability of such values of λ arising would be very small. If necessary, should a λ occur which is an eigenvalue, then we could always change the numerical value of λ by one in the last decimal place, destroy its eigenvalue character and in no way change the physical results.

In terms of the variables $\phi(x)$, Eq. (7) for the average component of the torque about bond b_j becomes

$$\langle T_j\rangle_{Av}=\sum_{l=j+1}^{n}\phi(l/n). \tag{13}$$

It is obvious from symmetry considerations, that the methods that have been applied above to evaluate the component of the torque about the bond j could have been applied to obtain the torque about bond $-j$. That is, the elements of either half of the chain could have been designated by positive integers. Then for the lower half of the chain, remembering that a change of direction occurs

$$\Omega_k=-\phi_k' b_k,$$
$$T_k=-T_k\cdot b_k. \tag{14}$$

It is therefore unnecessary to repeat the above calculations.

If the sums, defining $\langle T_j\rangle_{Av}$ both for positive and negative j, are approximated by integrals, we finally obtain

$$\langle T_j\rangle_{Av}=\langle\rho_{jj}\rangle_{Av}\dot{\phi}_j,$$

$$\langle\rho_{jj}\rangle_{Av}=-\tfrac{2}{3}\zeta b^2\Big\{|j|\Big(|j|-\frac{Z}{2}\Big)+F(\lambda)+G(j,\lambda)-H(j,\lambda)\Big\},$$

$$F(\lambda)=\frac{Z^2}{2\pi^2}\sum_{m=1}^{\infty}\frac{1}{m^2[1+\lambda(2/m)^{\frac{1}{2}}]},$$

$$G(j,\lambda)=\frac{Z^2}{2\pi^2}\sum_{m=1}^{\infty}\frac{(-1)^{m+1}\cos 2m\pi\Big(\frac{|j|+1}{Z}\Big)}{[m^2(1+\lambda(2/m)^{\frac{1}{2}})]},$$

$$H(j,\lambda)=\frac{|j|Z}{1+\frac{8}{3}\sqrt{2}\lambda}\sum_{m=1}^{\infty}\frac{u_m\sin 2m\pi\Big(\frac{|j|}{Z}+\frac{1}{Z}\Big)}{m\pi[1+\lambda(2/m)^{\frac{1}{2}}]},$$

$$Z=\frac{M}{M_0},$$

$$\langle D_{jj}\rangle_{Av}=\frac{kT}{\langle\rho_{jj}\rangle_{Av}}. \tag{15}$$

In the limit of small λ, corresponding to negligible hydrodynamic interaction we obtain from (15)

$$\langle\rho_{jj}\rangle_{Av}=\tfrac{1}{3}\zeta b^2(n-|j|)^2$$

which is the result obtained for this case by Kirkwood.[1]

III. THE ROTATIONAL DIFFUSION CONSTANT

This calculation proceeds in a manner analagous to the calculation of the internal rotatory diffusion constants. The total torque about the center of mass is

$$T=\sum_{l=-n}^{n}T_l,$$

$$T_l=-R_{0l}\times F_l. \tag{16}$$

* See E. Jahnke and F. Emde, *Funktiontafeln* (Dover Publications, New York, 1943).

[4] R. Courant and D. Hilbert, *Methoden Der Mathematischen Physik* (Verlag. Julius Springer, Berlin 1931).

Defining quantities

$$\langle R_{0l'}\times F_l\rangle_{Av}=-(4/9)\zeta b^2 n\phi_{l,l'},$$

$$\langle T\rangle_{Av}=(4/9)\zeta b^2 n^2\int_{-1}^{1}\phi(x,x)dx,$$

$$x=l/n,\quad y=l'/n, \tag{17}$$

we obtain from the Oseen Eq. (8) after multiplying by $(R_{0l'}\times)$ and averaging over-all internal configurations of the chain,

$$\phi_{l,l'}=f_{l,l'}+\frac{9}{4b^2 n}\sum_{\substack{s=-n\\ s\neq l}}^{n}\langle R_{0l'}\times T_{ls}\cdot F_s\rangle_{Av}$$

$$-n\leqslant l\leqslant +n$$

$$-n\leqslant l'+n$$

$$f_{l,l'}=\frac{1}{8n^2}[3(l^2+l'^2)-6n|l-l'|+2n^2]\Omega_0. \tag{18}$$

Here as in the other cases we assume the fluctuation

$$\langle R_{0l'}\times(T_{ls}-\langle T_{ls}\rangle_{Av})\cdot F_s\rangle_{Av}$$

can be neglected and therefore introduce the approximation

$$\langle R_{0l'}\times T_{ls}\cdot F_s\rangle_{Av}=\langle R_{0l'}\times\langle T_{ls}\rangle_{Av}\cdot F_s\rangle_{Av}. \tag{19}$$

Equation (18) therefore reduces to the following set of linear equations in the variables $\phi_{j,l}$

$$\phi_{l,l'}=f_{l,l'}-\frac{\lambda}{n^{\frac{1}{2}}}\sum_{\substack{s=-n\\ s\neq l}}^{n}\frac{\phi_{l',s}}{(|l-s|)^{\frac{1}{2}}}. \tag{20}$$

We again replace (20) by the asymptotic integral equation

$$\phi(x,y)=f(x,y)-\lambda\int_{-1}^{1}\frac{\phi(t,y)}{(|x-t|)^{\frac{1}{2}}}dt. \tag{21}$$

We recognize (21) to be identical with the integral equation encountered in the viscosity theory so that[3]

$$\phi(x,y)=\sum_{\substack{m=-\infty\\ m\neq 0}}^{\infty}\frac{f_m(y)e^{im\pi x}}{1+\lambda(2/m)^{\frac{1}{2}}},$$

$$f_m(y)=\left(\frac{3}{4\pi^2 m^2}e^{-im\pi y}+\frac{(-1)^m 3iy}{4\pi|m|}\right)\Omega, \tag{22}$$

and from (17)

$$\langle T\rangle_{Av}=(4/9)\zeta b^2 n^2 F(\lambda)I\cdot\Omega_0,$$

$$F(\lambda)=\frac{6}{\pi^2}\sum_{m=1}^{\infty}\frac{1}{[m^2(1+\lambda(2/m)^{\frac{1}{2}}]},$$

$$\langle T\rangle_{Av}=\langle\rho_{00}\rangle_{Av}\cdot\Omega_0. \tag{23}$$

We have, therefore, obtained the average of the over-all rotational resistance tensor

$$\langle\rho_{00}\rangle_{Av}=(4/9)b^2 n^2\zeta F(\lambda)I,$$

$$\langle\rho_{\theta\theta}\rangle_{Av}=\langle\rho_{\phi\phi}\rangle_{Av}=\tfrac{1}{2}\langle\rho_{00}\rangle_{Av},$$

$$\langle D_{\theta\theta}\rangle_{Av}=\langle D_{\phi\phi}\rangle_{Av}=2\langle D_{00}\rangle_{Av}=\frac{9kT}{2b^2 n^2\zeta F(\lambda)}. \tag{24}$$

For small λ, $\langle\rho_{00}\rangle_{Av}$ reduces to Kirkwood's expression

$$(4/9)b^2 n^2\zeta I.^1$$

IV. DISCUSSION

It is interesting to point out here that in terms of the parameters ξ and b which have been discussed in the previous paper,[3] we have been able to correlate the hydrodynamic behavior of long chain molecules with regard to the various tools used in high polymer research. Thus evaluating ξ and b from viscosity data, for example, allows one to predict the behavior of the long chain molecule in a centrifugal field or in a diffusion cell or in a streaming birefringence experiment. In the latter case notice must be taken of the fact that the averages over all internal configurations are performed with the understanding that they pertain to an equilibrium distribution, not affected by the fluid flow. This means that the values as given pertain to small rates of shearing strain. At high rates of shearing strain, some stretching of the molecule will occur so that, in such a field, a different distribution of internal configurations will result. Therefore, the rotatory diffusion constants obtained experimentally from streaming birefringence measurements should be extrapolated to small shear rates in order to compare with our theory.

On the other hand, values of b can be obtained by comparing this theory with the experimental determination, by means of streaming birefringence, of rotatory diffusion constants. In this case one might expect b the effective hydrodynamic distance between chain elements to increase with increase in velocity gradient and therefore rate of shearing strain. One could, therefore, follow this change of molecular length with velocity gradient.

For purposes of calculation the quantities $F(\lambda)$, $G(j,\lambda)$ and $H(j,\lambda)$ are readily evaluated. $F(\lambda)$ is tabulated in our viscosity paper,[3] and the latter two quantities converge sufficiently rapidly so that one may take the first 10 terms to obtain a result good to 10 percent. The value of λ necessary for the evaluation of the sums are easily obtained from intrinsic viscosity data.

It was mentioned above that Eq. (21) was similar in form to the integral equation of the intrinsic viscosity theory. If we write for the intrinsic

TABLE I.

Molecular weight	Benzene $[\eta]$	Benzene $\langle D_{\phi\phi}\rangle_{Av}\times10^{-3}$	Methyl ethyl ketone $[\eta]$	Methyl ethyl ketone $\langle D_{\phi\phi}\rangle_{Av}\times10^{-3}$
1,540,000	4.00	2.08	1.54	12.22
1,070,000	3.06	3.93	1.24	21.88
650,000	2.11	9.39	0.976	45.80
400,000	1.49	21.50	0.734	98.60
265,000	1.10	44.06	0.535	204.2
162,000	0.765	103.7	0.409	437.2
116,000	0.593	186.8	0.342	728.6
75,000	0.432	396.4	0.246	1573
45,000	0.294	991.8	0.188	3412
23,000	0.179	3110	0.127	9922

viscosity

$$[\eta]=\frac{N\zeta b^2}{3600\eta_0 M_0}ZF(\lambda)$$

and compare with (24), we see that

$$\langle\rho_{\phi\phi}\rangle_{Av}=200\frac{M}{N}\eta_0[\eta],$$

$$\langle D_{\phi\phi}\rangle_{Av}=\frac{NkT}{200M\eta_0[\eta]}.$$

This yields an interesting relationship between the intrinsic viscosity and the component of the rotatory diffusion constant of the molecule as a whole. This result is not unexpected as can be seen by comparing the rotational diffusion constant for a spherical particle with the Einstein intrinsic viscosity formula.[5] In Table I, we present values of $\langle D_{\phi\phi}\rangle_{Av}$ of polystyrene calculated from the intrinsic viscosity data of our previous paper.[3] In the poorer solvent, in which the root mean square end to end length of the molecule is smaller than in the good solvent benzene, the values of the rotatory diffusion constant are larger, as is to be expected. The ratio in the poor and good solvents decreases from a value of 6 at the high molecular weight range to about 3 at 23,000, where the effect resulting from the differences in hydrodynamic shielding because of the more compact configuration in the poor solvent would be decreased. One might expect that the influence of a high velocity gradient upon such a compact configuration would be more marked than in the case of the more extended one in a good solvent, leading to a more noticeable increase of measured rotatory diffusion constant with increase in velocity gradient.

Some preliminary streaming birefringence experiments on polystyrene in toluene, carried out at the Brooklyn Polytechnic Institute, gave for a fraction having intrinsic viscosity about 10 and molecular weight about 4×10^6 a diffusion constant of about 800. This experimental value compares favorably as to order of magnitude with our theoretical calculations. The present difficulty in the theoretical interpretation of streaming birefringence data does not allow us to do more than compare orders of magnitude.

We are very grateful to Mr. Melvin Schoenberg of the Brooklyn Polytechnic Institute for making available to us his preliminary flow birefringence data on polystyrene.

[5] Simha in a personal communication mentions the fact that the form of the relationship between the diffusion constant and the intrinsic viscosity is general, with the specific nature of the model affecting only the numerical factor. Consequently, for a flexible molecule one would expect a variation of this factor with molecular weight.

TABLE II. Experimental and calculated values of the translational diffusion constant of polystyrene in butanone.

M. W. (ultracentrifuge)	$(D\times10^7)$ exp.	$(D\times10^7)$ calc.
96,900	9.22	9.60
244,000	4.95	5.89
584,000	3.16	3.91
933,000	2.44	2.95
982,000	2.43	2.87

APPENDIX

Comparison of Experimental and Theoretical Diffusion Constants of Polystyrene in Butanone

In a recent publication,[3] the first of this series, the following result for the translational diffusion constant of a flexible molecule was obtained.

$$D=[1+(8\lambda_0/3)Z^{\frac{1}{2}}]\frac{kT}{Z\zeta}.$$

Because of the absence of reliable data no comparison of this theoretically derived result with experimental data was possible. Recently,** diffusion constant measurements of fractionated polystyrene in butanone were made. In making a comparison of this data with our theoretical results, shown in Table II, we have used for the values of the hydrodynamic parameters b and ζ the results mentioned in our previous paper.[3] It would have been preferable in making such comparison to have calculated these parameters from viscosity measurements on polystyrene fractions identical with those on which the diffusion constant measurements were made. The absence of such concurrent experimental data therefore compels us to use the results from the viscosity measurements on polystyrene fractions in one laboratory to calculate diffusion constants for comparison with those obtained in another laboratory.

The agreement between experiment and theory is about as good as one could expect for high polymeric systems.

** The diffusion data presented here is from the doctoral thesis of A. Schick, Polytechnic Institute of Brooklyn, 1948.

Quasi-Chemical Theory of Order for the Copper Gold Alloy System

YIN-YUAN LI
Department of Physics, University of Washington, Seattle, Washington
(Received August 4, 1948)

Yang's general quasi-chemical theory of superstructure is further generalized in terms of the atomic distribution on sublattices of any number and of any geometrical arrangement. The possibility of the formation of different types of long-distance order due to the different recombinations of sublattices is discussed. By making use of this theory the behavior of the general Cu-Au system at very low temperatures and its phase diagram are shown. The critical temperature, latent heat, curve of long-distance order and energy *vs.* temperature for the CuAu tetragonal crystal are obtained. Our results are found to be quite different from those of Shockley's theory. All the experimental findings that are available to the author have been used for comparison with our results; so far no qualitative disagreement can be shown.

I. INTRODUCTION

AFTER the accumulation in the 20's of knowledge of the order-disorder transformation in alloys and allied changes of physical quantities, physicists have developed the theory of superstructure with some success.[1] There was, and still is, some difficulty in specifying quantitatively the so-called degree of order which should describe the configuration of the system in a statistical way. Bragg and Williams[2] simplified the consideration of long-distance order by introducing an assignment of right and wrong positions to the atoms of two different kinds, A and B atoms. All atoms occupy their right positions in an alloy of perfect order, as can be realized by a process of annealing and cooling down to very low temperatures. A certain fraction of atoms in an imperfectly ordered alloy are missing from their right positions. The right positions for A atoms are designated as α-sites and those for B atoms as β-sites. A similar classification of sites is used in more recent methods of Bethe[3] and of Yang. The principal improvements which have been made in the newer theories are the use of better statistical methods and introduction of forces acting between nearest atoms.

The variable S, generally called the long-distance order, has been defined as

$$S=\theta_\alpha-\theta_\beta, \tag{1}$$

where θ_α (or θ_β) is the fraction of α- (or β-) sites occupied by A atoms. For an alloy of a given composition only one of θ_α and θ_β is an independent variable; therefore, at a given temperature the free energy of the system is a function of S, θ_α, or θ_β. Suppose we now divide the class of α-sites into sub-sets of α_1-, α_2-, $\cdots$, α_m-sites and also the β-sites into sub-sets of β_1-, β_2-, $\cdots$, $\beta_{m'}$-sites. When the number of sites in each set is large enough such that the variables $\theta_{\alpha_1}, \theta_{\alpha_2}, \cdots, \theta_{\alpha_m}, \theta_{\beta_1}, \cdots, \theta_{\beta_{m'}}$ defined in a similar way as θ_α and θ_β may be roughly regarded as continuous variables, the free energy may be written as a function of $m+m'-1$ variables of the $m+m'\theta$'s. On the $(m+m'-1)$-dimensional surface $F(\theta_{\alpha_1}, \cdots, \theta_{\beta_1}, \cdots)$, a curve satisfying the condition $\theta_{\alpha_1}=\theta_{\alpha_2}=\cdots=\theta_{\alpha_m}$, $\theta_{\beta_1}=\theta_{\beta_2}=\cdots=\theta_{\beta_{m'}}$ gives $F(\theta_\alpha)$ which is the free energy curve by the old α- and β-assignment. Equilibrium states of the system are going to be determined by the minima of the free energy. We see that all the minima other than those lying on the curve $F(\theta_\alpha)$ must be missing in a theory using the α- and β-assignment. The way in which this division of lattice sites into more than two sets is to be made must be determined in each particular instance. In some cases only two sets will be required, but we no longer assume the sufficiency of two sets without further investigation. In general we will find that the curve $F(\theta_\alpha)$ does not contain all of the minima. Experimental facts will have to be relied upon in each instance to determine the manner of division of lattice sites into suitable sets. The criterion must be that the resulting free energy function successfully describes the system.

Some binary alloys have more than one ordered phase.† For example, the Cu-Au†† system appears in a face-centered cubic superlattice ($\alpha\beta_3$ type), when its atomic ratio is around 1:3, and in a face-centered tetragonal superlattice ($\alpha\beta$ type), when its atomic ratio is around 1:1. For the purpose of dealing with the different phases at the same time and of detecting the possibility of order which cannot be described by a single variable of long-distance order, Shockley[4] divided the face-centered lattice into four simple cubic sublattices in his paper

[1] F. C. Nix and W. Shockley, Rev. Mod. Phys. **10**, 2 (1938).
[2] W. L. Bragg and E. J. Williams, Proc. Roy. Soc. **A145**, 699 (1934).
[3] H. A. Bethe, Proc. Roy. Soc. **A150**, 552 (1935).

† Here and later we will conveniently call the different kinds of order "phases."
†† From now on we use A–B to indicate an alloy of A and B atoms of any atomic ratio, AB when it contains equal number of A and B atoms, AB_3 when the ratio of the numbers of A and B atoms is 1:3, etc. Use $\alpha\beta$ when α- and β-sites are of equal statistical weights, $\alpha\beta_3$ when β-sites are given 3 times the weight of α-sites, etc.
[4] W. Shockley, J. Chem. Phys. **6**, 130 (1938).

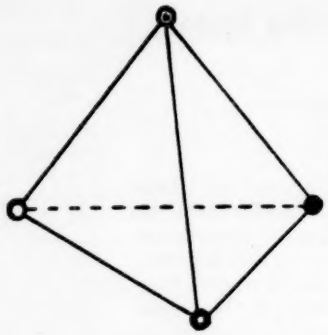

FIG. 1. The tetrahedron group. The interactions between atoms are indicated by lines. Sites of different sublattices are shown by different symbols.

on the theory of the Cu-Au system. Later in the present paper, any (regular) set of lattice sites will be called a sublattice.

Yang,[5] and later Yang and the present author,[6] generalized the quasi-chemical method, originally introduced into the theory of superlattices by Fowler and Guggenheim,[7] to the case of a binary alloy with any atomic ratio and to the free choice of a local group of any shape and size. If we compare the work and results of Yang and Li in the problem of the Cu-Au alloy in face-centered cubic superlattice with those of Peierls[8] using Bethe's method, the practical advantage of Yang's method in choosing a smaller local group rather than a Bethe group, containing a central site and its next shell or shells, becomes evident. Yang and Li also obtained the curve of the critical temperature of the above mentioned alloy against its atomic ratio and for the first time furnished a theoretical verification of the experimental facts found by Haughton and Payne,[9] and by Borelius,[10] that, for Cu-Au and Cu-Pd in cubic crystal form, the maximum of the critical temperature occurs at the atomic ratio of 1:3.

A theoretical discussion of the Cu-Au system including the transformation between phases has been worked out by Shockley using Bethe's nearest neighbor assumption, and the Bragg-Williams method, which is a method of "zeroth approximation."[11] A comparison between the curve of the critical temperature against the atomic ratio obtained by the Bragg-Williams method (shown as a dotted line in the region marked by $\xi+\eta$ in Fig. 26 of 1*) and the corresponding curve obtained by Yang's method (Fig. 4 of 6) evidently shows vital disagreements. The present author will develop a general theory of order in terms of sublattices with Yang's method, and then apply it to the case of the Cu-Au system. Finally conclusions will be drawn by comparing his findings with Shockley's theory as well as experimental data. In this paper the consideration of interactions among atoms continues to be restricted to Bethe's nearest neighbor assumption.

[5] C. N. Yang, J. Chem. Phys. **13**, 66 (1945).
[6] C. N. Yang and Y.-Y. Li, Chinese J. Phys. **7**, 59 (1947).
[7] R. H. Fowler and E. A. Guggenheim, Proc. Roy. Soc. **A174**, 189 (1940).
[8] R. Peierls, Proc. Roy. Soc. **A175**, 213 (1936).
[9] Haughton and Payne, J. Inst. Metals **46**, 547 (1931).
[10] Borelius, Ann. d. Physik **86**, 291 (1928).
[11] R. H. Fowler and E. A. Guggenheim, *Statistical Thermodynamics* (Cambridge University Press, London, 1939), Chap. 13.
* Here and later in this paper, references will be cited by 1, 2, ··· as numbered in the footnotes, and equations, by (1), (2), ··· as numbered in the textual part.

II. QUASI-CHEMICAL METHOD

The present theory is devised in a general form for any desired number of sublattices, $L_1, L_2, \cdots, L_m$. Its usefulness may be proved through the applications to alloys with rather complicated superlattices. Consider an A–B alloy system with altogether N atoms, $N\theta$ of them being A atoms, and $N(1-\theta)$ B atoms. N is also the total number of the lattice sites. Let the number of sites on L_h be $Nr_h (h=1, 2, \cdots, m)$. θ_h is used to denote the order parameter of L_h. In a given distribution of atoms among the lattice sites, the number of A atoms in the sites of L_h is $Nr_h\theta_h$. Evidently, the order parameters satisfy the condition:

$$\sum_{h=1}^{m} r_h\theta_h = \theta. \tag{2}$$

In the quasi-chemical method, the whole crystal is conceived as being a superposition of groups, each consisting of a connected set of sites and all of identical shape. The sites of each group may be labeled by 1, 2, ···, n, in one and the same way. However it may happen that the ith site ($i=1, 2, \cdots, n$) is on L_1 in one group but on L_2 in another group. And so the M groups taken into consideration may fall into l different types with Mc_λ groups of the type $\lambda(\lambda=1, 2, \cdots, l)$. The difference between the present treatment and that given in 6 is only that, instead of two sublattices (α- and β-sites), we have now m sublattices with m unspecified. Fortunately, it can be verified that the quasi-chemical argument, statistical method, and mathematical evaluation are mainly unchanged, when we replace θ_α and θ_β, and r and $1-r$ of 6, respectively, by summing over $\theta_1, \theta_2, \cdots, \theta_m$, and $r_1, r_2, \cdots, r_m$. We will not write the details here. All the counterparts of Eqs. (3)–(15) of 6 hold for the present theory. So we have the *average energy* of the alloy at a given distribution, $\theta_1, \theta_2, \cdots, \theta_m$, given by

$$E=(Nz/2p)kT^2 \sum_\lambda c_\lambda[(\partial/\partial T)\ln\varphi_\lambda]_{\mu's} \tag{3}$$

with z, the number of nearest neighbors of a site; p, the number of pairs of nearest sites in each group; T, the absolute temperature; k, Boltzmann's constant; and

$$\varphi_\lambda = \sum_{q's} \mu_{\lambda 1}^{q_1} \cdots \mu_{\lambda n}^{q_n} \exp\{-\chi(q_1, \cdots, q_n)/kT\}. \tag{4}$$

$q_i=1$, or 0, according to whether the ith site of the group is occupied by an A or a B atom. $\chi(q_1, q_2, \cdots,$

q_n) is the interaction energy of the group with the distribution of atoms as indicated by $(q_1, q_2, \cdots, q_n)$. $\mu_{\lambda i}$'s are uniquely determined by

$$\mu_{\lambda i}(\partial \ln\varphi_\lambda/\partial\mu_{\lambda i}) = \theta_{\lambda i}, \tag{5}$$

where $\theta_{\lambda i}$ is θ_h if the ith site of the group of the type λ is on L_h. The free energy function is

$$F(\theta_1, \theta_2, \cdots, \theta_m, T) = -\frac{Nz}{2p}kT\{\sum_\lambda c_\lambda(\ln\varphi_\lambda - \sum_i \theta_{\lambda i}\ln\mu_{\lambda i}) + D\sum_h r_h[\theta_h\ln\theta_h + (1-\theta_h)\ln(1-\theta_h)]\} \tag{6}$$

with

$$D = n - (2p/z). \tag{7}$$

Now we can minimize the free energy function to determine the equilibrium distribution $(\theta_1, \theta_2, \cdots, \theta_m)$. Taking the relation (2), we find a necessary condition of equilibrium:

$$\sum_\lambda c_\lambda \sum_{(h)} \ln\mu_{\lambda i} - r_h[D\ln(\theta_h/1-\theta_h) - C] = 0, \tag{8}$$

where C is a Lagrange multiplier. $\sum_{(h)}$ indicates that the summation is taken over all the variables $\mu_{\lambda i}$ in the group of type λ and belonging to L_h-sites. The disordered distribution is always a solution of (8), since the only solution of (5) is $\mu_{\lambda i} = \mu$ for all λ and i, when $\theta_1 = \theta_2 = \cdots = \theta$. Remembering (7) and the relation

$$\sum_{\lambda, i} c_\lambda f(\theta_{\lambda i}) = n\sum_h r_h f(\theta_h), \tag{9}$$

we see that the *only* solution of (8) at $T = \infty$ is $\theta_h = \theta$ for $h = 1, 2, \cdots, m$. When the temperature is below a certain value, there will be one or more sets of solutions other than the distribution $\theta_1 = \theta_2 = \cdots = \theta$. The multiplier C may have different values for different sets of solutions.

If it happens that a solution gives $\theta_1 = \theta_2 = \cdots \theta_k \neq \theta_{k+1} = \cdots = \theta_m$, we may then regard $L_1, \cdots, L_k$ together as a single sublattice and $L_{k+1}, \cdots, L_m$ as another. Different recombinations of sublattices might result in different crystal forms, since A and B are different atoms.

In a statistical theory we are interested only in the state of equilibrium; therefore we do not need to draw the hypersurface F or any section of it. What we have to consider is the values of F at equilibrium states. The absolute minimum of F at given temperature and atomic composition determines the phase of the stable equilibrium. The other minima of F give the metastable states. The unstable equilibrium states given by maxima of F are also included in the solutions of (8). In the neighborhood of the intersection point between two branches (of the minimum F *vs.* θ curve) belonging to equilibrium states of different types, a common tangent can be drawn. For compositions between the points of tangency the most stable state of the alloy should be a mixture of two phases having compositions, respectively, corresponding to the points of tangency. However, the intersection points themselves give the critical temperatures for alloys of homogeneous composition, when the condition is, as usually, not favorable for the formation of two phases with different compositions (cf. 4).

In our theory A and B atoms are symmetric. There would be no difference if we formulated the theory by paying attention to B atoms instead of A atoms. Therefore, to an equilibrium state $(\theta_1, \theta_2, \cdots, \theta_m)$ at θ, correspondingly $(1-\theta_1, 1-\theta_2, \cdots, 1-\theta_m)$ is also an equilibrium state at $1-\theta$. Similarly,

$$F(\theta_1, \theta_2, \cdots, \theta_m, T) = F(1-\theta_1, 1-\theta_2, \cdots, 1-\theta_m, T) \tag{10}$$

and similar relations for other physical quantities. Consequently, in actual calculations we only have to work out the curve for $\theta \leqslant \frac{1}{2}$; the other half can be produced by symmetrization.

For applications of this further generalized theory, the theorem (i) and (ii) of 6 still hold and are very helpful.

III. QUASI-CHEMICAL THEORY OF THE CU-AU SUPERSTRUCTURE

Besides serving to illustrate the preceding general theory, this part will provide new theoretical findings on the Cu-Au system. Following Shockley we divide the lattice sites of a face-centered cubic lattice into four simple cubic lattices (cf. 4). As in 5 and 6 a tetrahedron of four nearest sites is chosen as the local group; each of the sites belongs to one of the four different sublattices (Fig. 1). In this case,

$$m=4, \quad l=1, \quad z=12, \quad n=4, \quad p=6, \quad D=3, \quad r_h=\tfrac{1}{4}. \tag{11}$$

It is justifiable that the variation of the interaction between two neighboring atoms may be ignored when the ratio of the lattice constants changes only slightly from unity. X-ray investigation shows a/c of the highly ordered tetragonal phase being less than 1.08.[12] (The sides of the unit cell are a, a, c.) This change is only a secondary effect of ordering. The inaccuracy introduced by neglecting it could not be more serious than that due to the nearest neighbor assumption.

The four sites of each group are geometrically symmetric. Let the four variables be μ_h, $h = 1, 2, 3, 4$, respectively belonging to the sites on L_1, L_2, L_3 and

[12] W. Gorsky, Zeits. f. physik. **50**, 64 (1928).

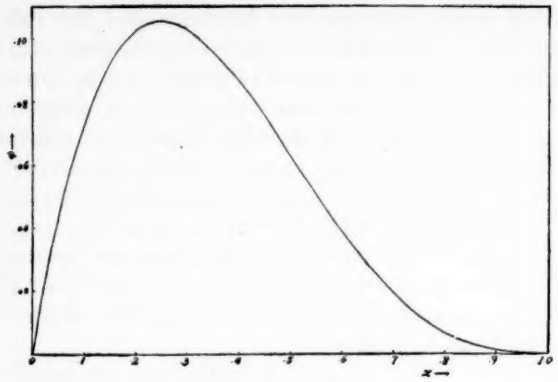

FIG. 2. The function: $\phi = x(1-x)^3$.

L_4. Explicitly φ is given by

$$\varphi = 1+(\mu_1+\mu_2+\mu_3+\mu_4) +(\mu_1\mu_2+\mu_2\mu_3+\mu_3\mu_4+\mu_4\mu_1+\mu_2\mu_4+\mu_1\mu_3)X +(\mu_1\mu_2\mu_3+\mu_2\mu_3\mu_4+\mu_3\mu_4\mu_1+\mu_4\mu_1\mu_2)X^3 +\mu_1\mu_2\mu_3\mu_4X^6, \quad (12)$$

where

$$X=\exp\{-(v_{AA}+v_{BB}-2v_{AB})/kT\} =\exp(-2v/kT), \quad (13)$$

$$v=\tfrac{1}{2}(v_{AA}+v_{BB}-2v_{AB}). \quad (14)$$

Theorem $(i-b)$ of 6 has been used, and v_{AA}, v_{BB} and v_{AB} are the interactions between the nearest pairs of atoms $A-A$, $B-B$ and $A-B$, respectively. It is interesting to note that each term of (12) contains an elementary symmetric function (called the $\sum$-polynominals) of μ_1, μ_2, μ_3, and μ_4. (5), (6), and (8) reduce to

$$\mu_h\frac{\partial\varphi}{\partial\mu_h}=\theta_h\varphi,$$

$$F(\theta_1,\cdots,\theta_4,T) =-NkT\{\ln\varphi-\sum_h\theta_h\ln\mu_h -\tfrac{3}{4}\sum_h[\theta_h\ln\theta_h+(1-\theta_h)\ln(1-\theta_h)]\}, \quad (16)$$

$$\mu_h=\kappa(\theta_h/1-\theta_h)^{\frac{1}{3}}, \quad (17)$$

where κ stands for $\exp(-C/4)$. From the possibility of different solutions of this equation, we may anticipate before going into detailed analysis that there might be four ordered phases as well as the disordered one: Phase ξ, with all θ_h's equal; Phase η, with only three of the four θ_h's equal; Phase ζ_2, with two different pairs of equal θ_h's; Phase ζ_1, with two and only two equal θ_h's; and Phase ϵ, with all θ_h's unequal. The symbols ξ, η, ζ_2, and ζ_1 are used in the same way as in 4. The crystal form of the ϵ-phase should be orthorhombic. The η-phase is the $\alpha\beta_3$ type cubic lattice and both the ζ_2- and the ζ_1-phase are tetragonal crystals (cf. Fig. 2 of 4).

1. Equilibrium States at Very Low Temperatures

For examining the variation of the parameters μ_h with the temperature when the latter is extremely low, let us take into consideration the equation,

$$\sum_h \mu_h(\partial\varphi/\partial\mu_h)=4\theta\varphi, \quad (18)$$

which is simply a combination of the four equations (15). By rearranging terms we have

$$4(1-\theta)X^6\sum_4+(3-4\theta)X^3\sum_3 +2(1-2\theta)X\sum_2+(1-4\theta)\sum_1-4\theta=0, \quad (19)$$

where $\sum_1$, $\sum_2$, $\sum_3$, and $\sum_4$ stand for the $\sum$-polynomials of μ_h's, respectively, of order 1, 2, 3, and 4. For simplicity, consider first the disordered case for which (19) reduces to

$$(1-\theta)\mu^4X^6+(3-4\theta)\mu^3X^3 +3(1-2\theta)\mu^2X+(1-4\theta)\mu-\theta=0. \quad (20)$$

As $X\to 0$ (i.e., $T\to 0$), μ remains either constant or approaches ∞ as some power of $X^{-\frac{1}{3}}$. This power depends on the value of θ, or more generally, on the range of values within which θ is taken to lie. A detailed analysis of (20) shows that μ approaches asymptotically

(a) $\dfrac{\theta}{1-4\theta}$, (b) $(6X)^{-\frac{1}{3}}$,

(c) $\dfrac{4\theta-1}{3(1-2\theta)}X^{-1}$, and (d) $X^{-\frac{1}{3}}$

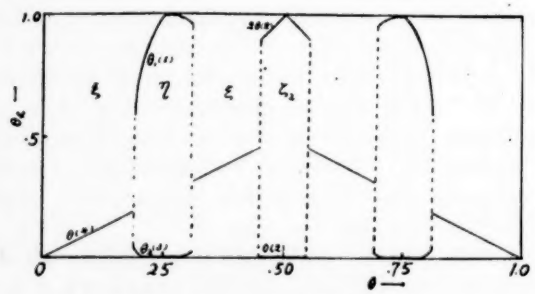

FIG. 3A. The stable equilibrium state at very low temperatures. The notation $[\theta_1(1)\theta_2(3)]$ indicates a state $(\theta_1, \theta_2, \theta_2, \theta_2)$. The upper curve is for θ_1 and the lower one for θ_2.

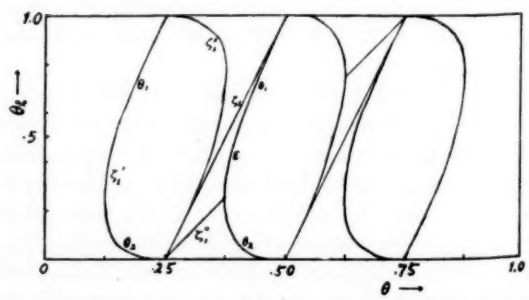

FIG. 3B. The metastable states at very low temperatures. They are $\zeta_1(1, 4\theta-1, 0, 0)$, $\zeta_1(\theta_1, \theta_2, 0, 0)$, $\zeta_1''(1, 2\theta-\frac{1}{3}, 2\theta-\frac{1}{3}, 0)$, and $\epsilon(1, \theta_1, \theta_2, 0)$.

for

(a) $0 \leqslant \theta < \frac{1}{4}$, (b) $\theta = \frac{1}{4}$,

(c) $\frac{1}{4} < \theta < \frac{1}{2}$, and (d) $\theta = \frac{1}{2}$, (21)

respectively. For the equilibrium states other than the disordered one we may consult (17) and (19). Evidently for all equilibrium states the μ_h's remain constant or approach ∞ with $X^{-\frac{1}{4}}$ as given by (21) but have different coefficients. And so we have: φ approaches asymptotically

(a) $1+\sum_1$, (b) $\sum_1$, (c) $\sum_1 + X\sum_2$, and (d) $X\sum_2$, (22)

for

(a) $0 \leqslant \theta < \frac{1}{4}$, (b) $\theta = \frac{1}{4}$, (c) $\frac{1}{4} < \theta < \frac{1}{2}$, and (d) $\theta = \frac{1}{2}$,

respectively. The other terms in each function φ are negligible because they are in higher orders of X. It follows: (a) The probability of finding a tetrahedron with two or more sites occupied by A atoms is negligible, when the system contains fewer A atoms than $\frac{1}{4}$ of the total number. (b) All the tetrahedra found in an alloy with $\theta = \frac{1}{4}$ are occupied by one A atom and three B atoms. In other words, Cu_3Au at very low temperatures is perfectly ordered in the $\alpha\beta_3$ superlattice (η-phase). (c) The probability of finding a tetrahedron occupied by other than one or two A atoms is negligible, when $\frac{1}{4} < \theta < \frac{1}{2}$. (d) The alloy with equal numbers of A and B atoms should be perfectly ordered in the $\alpha\beta$ type (ζ_2-phase).

The work for finding equilibrium states at extremely low temperatures by solving (17) with (15) is laborious in both the algebraic evaluation and the numerical calculation. In order to conserve space only the simpler case of $\theta < \frac{1}{4}$ will be given here as an example. From (15) and (22),

$$\mu_h = \theta_h(1+\sum_h \mu_h) \tag{23}$$

and so

$$\mu_h = \theta_h/1-4\theta. \tag{24}$$

Comparing with (17) we have, for θ_i, $\theta_j \neq 0$, the relation

$$\theta_i(1-\theta_i)^3 = \theta_j(1-\theta_j)^3. \tag{25}$$

Then we draw Fig. 2, with $x(1-x)^3$ plotted against $x(0 \leqslant x \leqslant 1)$. We see that corresponding to a certain value of the ordinate only two different values, θ_1 and θ_2, of the variable can be found. The combination of $\theta_1+3\theta_2$ is never less than 0.730 and so no η-solution exists for $\theta < 0.183$. There are solutions of $(2\theta, 2\theta, 0, 0)$, $(\theta_1, \theta_2, 0, 0)$, and $(\theta_1, \theta_2, \theta_2, 0)$ type for $\theta < \frac{1}{4}$. Here and later a state of equilibrium is expressed by $(\theta_1, \theta_2, \theta_3, \theta_4)$ in the order of $\theta_1 \geqslant \theta_2 \geqslant \theta_3 \geqslant \theta_4$ and written as $(\theta_1, \theta_2, \theta_2, 0)$ whenever $\theta_2 = \theta_3$ and $\theta_4 = 0$.

The stable states and metastable states at very low temperatures for the Cu-Au system are shown in Figs. 3A and 3B.

2. Free Energy and Phase Diagram

Substituting the solutions of (17) into (16) we calculate the free energy function and so obtain $F-\theta$ curves. The absolute minimum determines which of the different phases is the most stable state for different values of θ. The $F-\theta$ curves at very low temperatures are shown in Figs. 4A and

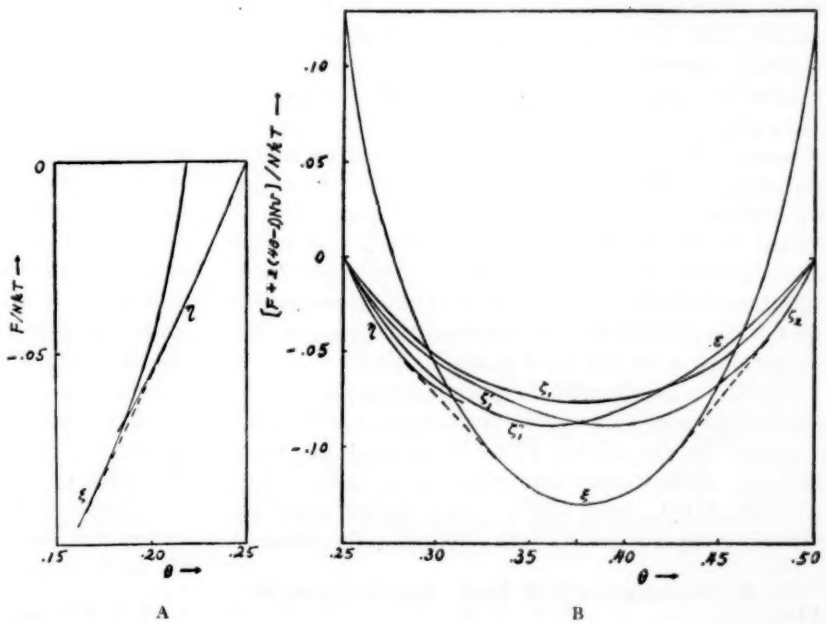

FIG. 4A. Free energy *versus* composition near $\theta = 0.20$; B. $[F+2(4\theta-1)Nv]/NkT$ is drawn against the atomic composition. Points of interaction and those of common tangency are not affected by the extra term, $2(4\theta-1)v/kT$.

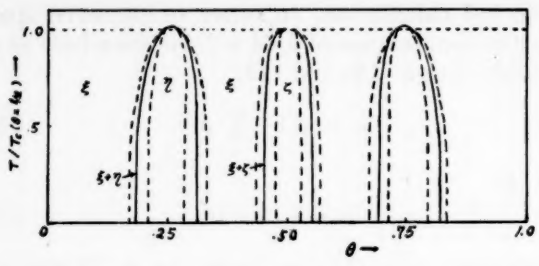

FIG. 5. Phase diagram for Cu-Au alloy system, dotted lines. Critical temperature for alloys of homogeneous composition, solid lines. $\xi+\eta$ (or $\xi+\zeta$) indicates the region in which the coexistence of $\xi-$ and $\eta-$ (or $\zeta-$) phase is possible.

4B. Only a qualitative sketch of $F-\theta$ has been made for higher temperatures. Using these results, and taking advantage of Fig. 4 of 6 and the value of $T_c(\theta=\frac{1}{2})$ found in the coming section the phase diagram was drawn as Fig. 5. We must be satisfied with this approximate curve, since in the present stage of theory of metals accurate quantitative results are beyond our reach.

Comparing our curves with both those of Shockley's theory and the experimental findings, we can reach the following interesting conclusions:

(i) At very low temperatures $(1, \theta_1, \theta_2, 0)$ offers a metastable state which exhibits a possibility of the existence of an orthorhombic phase. In Shockley's theory an ϵ-phase was absolutely impossible, because at any given value of T and θ only three different values of θ_h's for equilibrium could be found through his equations. The $(1, 4\theta-1, 0, 0)$ solution, which in his theory offered at lower temperatures a stable state for θ between 0.25 and 0.50, does not give a stable phase for any temperature and any atomic composition in the present theory. There cannot be transformations between ordered phases of different types, such as was found in his theory, but only order-disorder transformations. Shockley predicts that for Cu-Au alloys with atomic fraction $\theta<\frac{1}{2}$ but $>\frac{1}{4}$, a transition from ζ- to η-phase takes place at certain temperature and then another transition from η- to ξ-phase happens at a higher temperature; hence we may observe more than one discontinuity of specific heat. This possibility is denied by the present theory. The resolution of the face-centered cubic lattice into four simple cubic sublattices as shown is only helpful in understanding the Cu-Au system but not necessary, if we are concerned only with the *most* stable states.

(ii) An orthorhombic superstructure of Cu-Au system has been reported by Johansson and Linde.[13] It occurs for the alloys, 47 to 53 percent Au, when they are cooled after annealing at a temperature between 410°C and 420°C (i.e., higher than the critical temperature of the tetragonal phase c. 385°C) and also for alloys having between 36 and 47 or between 53 and 65 atomic percent Au which are annealed in the temperature range 400°C to 200°C (i.e., above or below the critical temperature). According to the observers, this orthorhombic phase is only different from the tetragonal phase by regular step shifts (cf. Section 16 of 1), but not an ϵ-phase. From the viewpoint of four simple cubic sublattices the mentioned step shifts would destroy all the long-distance order of a tetragonal superstructure, although apparently it still keeps a high degree of order. Whenever the step-changing orthorhombic phase should offer a stable state, a theory in terms of the four simple cubic sublattices could only show that the stable state is a disordered distribution. Compared with the mentioned experimental findings, the phase diagram (Fig. 5) is actually consistent with this conclusion. However, without any doubt, a theory of order with change-step boundaries can be approached by using our general theory with a suitable group of sites as well as some suitable assignment of sublattices other than the resolution of a face-centered cubic lattice into four simple cubic sublattices.

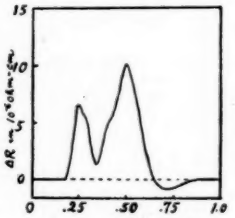

FIG. 6. Lowering of electrical resistivity due to the long-distance orderness *versus* fraction of Au atoms in Cu-Au alloys.

(iii) The present theory also shows that the disordered state is the most stable state at any temperature when the Cu-Au alloy contains A (or B) atoms fewer than 17 percent of the total number (cf. Fig. 4A). This is an expected result since cooperative phenomena should disappear, when the atoms of one kind are too scarce and consequently distributed too far apart to assert any ordering effect even at very low temperatures. This consideration remains true when we consider longer range interactions which of course decrease rapidly with the increasing of distance. However this does *not* mean that there is no order at all; the short-range order (order of neighbors) still exists and increases with the decreasing of temperature (cf. 3). A similar result for simple cubic $(z=6)$ and body-centered cubic $(z=8)$ crystals was found by Easthope[14] that a long-distance order can never exist, when A (or B) atoms are fewer than $1/z$ of the total number.

Following Bragg-Williams method Shockley assumes that for a given long-distance order the atoms on each sublattice are randomly distributed. His

[13] C. H. Johansson and J. O. Linde, Ann. d. Physik **25**, 1 (1936).

[14] E. E. Easthope, Proc. Camb. Phil. Soc. **33**, 502 (1937).

argument is only that this random distribution on each sublattice is the result of an "average process" (cf. 4). Actually there are a great many different atomic distributions with their orders of neighbors in wide difference but same long-distance order. The fluctuation of energy U among these different atomic distributions is very important in a statistical theory, because it gives different weights $\exp(-U/kT)$ to different terms of the partition function with which the statistical average should be worked out. Assume from the beginning the "average" distribution is equivalent to giving equal weight to the different atomic distributions of same long-distance order (§1314 of 11), but because of their difference in the order of neighbors they are not of equal weights. Shockley's theory is bound to the result that the disordered phase can never be the stable state at very low temperatures; since $F \simeq E$, as $T \simeq 0$ and by taking the "average" assumption, E is always less for an ordered state than for the disordered state, when $v > 0$.

(iv) It is shown in Fig. 5 that even at $T \to 0$, the coexistence of ordered and disordered phases is possible. However, in Shockley's theory it cannot happen. This disagreement between the two theories, of course, might not be settled by experimental investigations, since observations on the equilibrium state between different phases is very difficult as has been pointed out by Shockley and also by Hultgren.[15]

(v) Experimental data of electrical resistivity of Cu-Au alloys of different atomic ratios and in either ordered or disordered states have been obtained by Johannson and Linde. Taking the difference between the measured data at room temperatures from rapidly cooled Cu-Au alloys (disordered phase) and that from alloys annealed at 200°C (ordered phase), we draw Fig. 6 with the lowering of resistivity due to the long-distance order *vs.* the atomic ratio. Its largest effect occurs when θ(Au) equals 0.25 or 0.50, i.e., the two stoichiometric compositions of the η- and ζ_2-phase, and its minimum effect occurs at a certain composition between these two maxima but does not vanish. The lowering of resistivity for the alloys with 36 to 47 or 53 to 65 atomic percent Au is due to the existence of the changing-step orderness. Evidently in the range of θ(Au) not much larger than 50 percent, Fig. 6 is in fairly good agreement with our phase diagram, but the rest of Fig. 6 is not. The lack of symmetry with respect to $\theta = \frac{1}{2}$ for the physical properties of a binary alloy system is actually a difficulty of *any* statistical theory of superstructure which only inquires into the potential interaction between atoms. To provide an explanation of this asymmetry is, of course, out of the reach of the present theory.

[15] R. Hultgren, J. Chem. Phys. **7**, 203 (1939).

3. Tetragonal CuAu Alloy

We have shown that alloys with equal numbers of Cu and Au atoms form the ordered tetragonal superstructure of $\alpha\beta$-type at lower temperatures. This tetragonal alloy is of special interest for experimental investigations. Now $\theta_1 = \theta_3$, $\theta_2 = \theta_4$; and $\mu_1 = \mu_3$, $\mu_2 = \mu_4$.

$$\varphi = 1 + 2(\mu_1 + \mu_2) + (\mu_1^2 + \mu_2^2 + 4\mu_1\mu_2)X + 2\mu_1\mu_2(\mu_1 + \mu_2)X^3 + \mu_1^2\mu_2^2X^6, \quad (26)$$

$$\mu_1 \frac{\partial \varphi}{\partial \mu_1} = 2\theta_1\varphi, \quad \mu_2 \frac{\partial \varphi}{\partial \mu_2} = 2\theta_2\varphi, \quad (27)$$

and

$$\mu_1 = \kappa\sigma, \quad \mu_2 = \kappa\sigma^{-1} \quad (28)$$

with

$$\sigma = (\theta_1/1-\theta_1)^{\frac{1}{2}}. \quad (29)$$

To obtain the long-distance order $S(=\theta_1 - \theta_2)$ of equilibrium we solve the equation derived from (27) and (28):

$$c_1y^4 + c_2y^3 + 2S = 0 \quad (30)$$

where

$$c_1 = S\{(\sigma + \sigma^{-1})^2 + 2\} - (\sigma^2 - \sigma^{-2}), \quad (31)$$

$$c_2 = 2\{2S(\sigma + \sigma^{-1}) - (\sigma - \sigma^{-1})\}, \quad (32)$$

$$y = X^{-\frac{1}{4}} = \exp(v/kT), \quad (33)$$

for kT/v. The critical temperature of order-disorder transformation is the temperature T_c at which the two minima of F, $F(S \neq 0, T_c) = F(0, T_c)$. We find

$$RT_c/E_0(=kT_c/v) = 0.7306, \quad S_{eq}(T_c) = 0.983,$$

where $R = Nk$ and $E_0 = Nv$; the latter is the energy of transformation from perfect order to randomness. At higher temperatures $F(S_{eq}, T) > F(0, T)$ but still remains a minimum; the alloy might then stay as a partially ordered phase in a metastable state, until $F(S_{eq}, T)$ begins to be maximum at a certain higher temperature (Fig. 7). Its order-disorder transition occurs discontinuously.[16] With (3) $E(S_{eq}, T)$

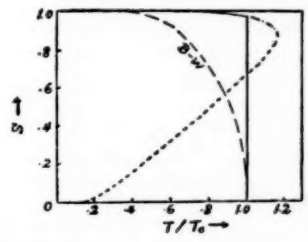

Quasi-chemical: stable — metastable — unstable

Bragg-Williams: B-W

FIG. 7. Long-distance order *vs.* temperature for CuAu.

[16] This was shown by A. H. Wilson using Bethe's method (Proc. Camb. Phil. Soc. **34**, 81, 1938).

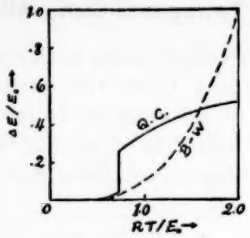

Q C: Quasi-chemical.
B-W: Bragg-Williams.

FIG. 8. Configurative energy *vs.* temperature for CuAu.

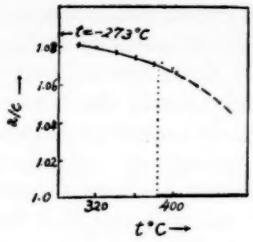

——— stable } calculated. Small dots, Gorsky's experi-
- - - - - - metastable } mental data.

FIG. 9. The ratio of lattice constants *vs.* temperature for CuAu.

$-E(S=1, T=0)$ is drawn against T (Fig. 8). We obtain the latent heat of the order-disorder transition

$$Q=0.228E_0.$$

For the purpose of comparison, the curves of Bragg-Williams theory are shown besides those of our curves in Figs. 7 and 8. According to the Bragg-Williams theory, the case considered here is only one of the superlattices of $\alpha\beta$-type and so the order-disorder transition should be continuous and no latent heat might be released during this transition. Even before the emergence of the Bragg-Williams theory, Gorsky had definitely proved that the disappearing of the tetragonal phase of CuAu occurs suddenly at a certain temperature. He also observed the metastable state and gave $T_c=385°C$. Table I gives a comparison between experimental data and

TABLE I.

	$T_c(\theta=\frac{1}{4})/T_c(\theta=\frac{1}{2})$	$Q(\theta=\frac{1}{4})/Q(\theta=\frac{1}{2})$
Experimental data*	1.01	**
Quasi-chemical method	1.13	1.03
Bragg-Williams method	0.825	0

* Z. W. Wilchinsky gave $T_c(\theta=\frac{1}{4})=388°C$ (J. App. Phys. **15**, 806 (1944).)
** No experimental value of $Q(\theta=\frac{1}{4})$ is available at the present time.

different theories. Gorsky's measurement[12] on the ratio of tetragonal lattices, a/c, is available for a trial on the theoretical $S_{eq}-T$ relation. At both the stable and metastable state S_{eq} is not much less than 1. For convenience, we take the approximative expansion:

$$(a/c)_{eq}=1.087-k_1(1-S_{eq}^2).$$

It is linear in S_{eq}^2 instead of S_{eq} itself; since we see that θ_1 and θ_2 are completely equivalent, an interchange between S and $-S$ leaves all the physical properties unchanged, and so they must be even functions of S_{eq}. By adjusting k_1 we draw Fig. 9. It shows the points of the experimental data lying close to the theoretical curve.

ACKNOWLEDGMENTS

I should like to express my sincere thanks to Professor E. A. Uehling for discussions and his kind interest in the work. My indebtedness also is due Professor J. S. Wang of Tsing Hua University of China, under whose guidance I approached the problem of the superstructure of alloys. I deeply appreciate the interesting discussion in a letter from Dr. C. N. Yang which has been digested in the argument of Conclusion (iii).

The Interpretation of the Vibrational Spectra of the C_6 Hydrocarbons 22-Dimethyl Butane, 22-Dimethyl-3-Butene, and 22-Dimethyl-3-Butyne*

N. SHEPPARD**
Spectroscopy Laboratory, Department of Physics, The Pennsylvania State College, State College, Pennsylvania
(Received October 14, 1948)

Assignments have been made for the observed infra-red and Raman frequencies of the molecules 22-dimethyl butane, 22-dimethyl-3-butene, and 22-dimethyl-3-butyne. By using the previously assigned characteristic frequency regions associated with the ethyl, vinyl, and C≡CH groups, it has been shown that the tertiary butyl group in all these molecules has frequencies near 1250, 1210(2), 1025(2), 880, and 700 cm^{-1}, in the range 1350–600 cm^{-1}. The assignment of these frequencies to skeletal C–C stretching and to methyl wagging modes is discussed.

INTRODUCTION

In a recent communication[1] an analysis was made of the infra-red and Raman spectra of some hydrocarbons containing the ethyl, vinyl, and C≡CH groups. It was shown that the various hydrogenic deformation modes of these three groupings all have fairly characteristic frequencies, i.e., occur in well defined and reasonably narrow regions of the spectra. It is clear that an extension of our knowledge of such frequencies will considerably simplify the interpretation of the spectra of polyatomic hydrocarbons. In the present paper the three molecules are considered in which a tertiary butyl group is attached in turn to each of the above structural units. In this manner it is hoped to obtain, by difference, similar characteristic frequency regions for the tertiary butyl group. Partial analyses of characteristic frequencies of the tertiary butyl group have already been published,[2–4] and these will be used as a guide in obtaining the complete assignments.

This series of molecules has the additional advantage that because of the trigonal symmetry of the tertiary butyl group, only one spectroscopically distinguishable rotational isomer will be obtained by skeletal rotation about the central C–C linkage. Hence, no preliminary low temperature study of these spectra is necessary before a vibrational analysis can be made, in contrast to the case of the normal paraffins.[5–7]

I. THE EXPERIMENTAL DATA

The infra-red spectrum of 22-dimethyl butane has been published by Avery and Ellis,[8] and as part of the *Catalog of Infra-Red Spectrograms* of the American Petroleum Institute Research Project 44.[9] The spectrum of 22-dimethyl-3-butene (33-dimethyl-1-butene) is also available from the latter compilation,[10] but no infra-red spectrum of 22-dimethyl-3-butyne (33-dimethyl-1-butyne) seems to be available.

The Raman spectra of 22-dimethyl butane and 22-dimethyl-3-butene have been obtained by Fenske *et al.*[11] (spectra Nos. 6 and 83) in their compilation of the Raman spectra of hydrocarbons, and that of 22-dimethyl-3-butyne has been published by Cleveland and Murray,[12] Rosenbaum, Grosse, and Jacobson.[13] Bazhulin,[14] has also obtained the Raman spectrum of 22-dimethyl butane. A schematic assignment for 22-dimethyl butane has been given by Kilpatrick and Pitzer,[15] and a partial analysis of the spectrum of 22-dimethyl-3-butyne has been made by the authors of the Raman spectrum.[12]

The observed frequencies, taken from the above sources, are given in Table I, and are followed by bracketed values for the relative intensities and, in the case of the Raman data, by the qualitative polarizations rounded off to a single significant figure. The table is set out so that corresponding regions of the spectra are opposite each other. No frequencies greater than 3350 cm^{-1} are included,

* This Research was carried out on Contract N6onr-269, Task V, of the Office of Naval Research.
** At the Department of Colloid Science, Cambridge University, Cambridge, England.
[1] N. Sheppard, J. Chem. Phys. **17**, 74 (1949).
[2] G. B. B. M. Sutherland and D. M. Simpson, J. Chem. Phys. **15**, 153 (1947): also the joint report by the Oxford and Cambridge infra-red laboratories, Institute of Petroleum Report XI (February, 1946).
[3] N. Sheppard, J. Chem. Phys. **16**, 690 (1948).
[4] R. S. Rasmussen, J. Chem. Phys. **16**, 712 (1948).
[5] G. J. Szasz, N. Sheppard, and D. H. Rank, J. Chem. Phys. **16**, 704 (1948).
[6] D. H. Rank, N. Sheppard, and G. J. Szasz, J. Chem. Phys. **16**, 698 (1948).
[7] N. Sheppard and G. J. Szasz, J. Chem. Phys. **17**, 86 (1949).
[8] W. H. Avery and C. F. Ellis, J. Chem. Phys. **10**, 10 (1942).
[9] Spectrograms Nos. 655 and 670, contributed by the U. S. Naval Research Laboratory, Washington, D. C.
[10] Spectrogram No. 199 contributed by the Shell Development Company, Emeryville, California, and Nos. 586 and 587 contributed by the U. S. Naval Research Laboratory, Washington, D. C.
[11] Fenske, Braun, Wiegand, Quiggle, McCormick, and Rank, Ind. Eng. Chem. Anal. Ed. **19**, 1700 (1947).
[12] F. F. Cleveland and M. J. Murray, J. Chem. Phys. **11**, 450 (1943).
[13] E. J. Rosenbaum, A. V. Grosse, and H. F. Jacobson, J. Am. Chem. Soc. **61**, 689 (1939).
[14] P. A. Bazhulin, Bull. Acad. Sci. U.R.S.S., Classe Sci. Chim. 198 (1943).
[15] J. E. Kilpatrick and K. S. Pitzer, J. Am. Chem. Soc. **68**, 1066 (1946).

TABLE I. The observed Raman and infra-red frequencies of 22-dimethyl butane, 22-dimethyl-3-butene, and 22-dimethyl-3-butyne.

22-dimethyl butane		22-dimethyl-3-butene		22-dimethyl-3-butyne
Raman[a,b]	Infra-red[c,d]	Raman[a]	Infra-red[e]	Raman[f]
				3307 (1)
			3090 (w)	
2967 (6)	2960 (v.s.)		2960 (s)	2968 (50) 0.8
2942 (6)				2923 (35) 0.2
2906 (10)				2905 (20) p
2890 (3)			2880 (m)	2887 (10) p
2871 (5)				2865 (9) p
2856 (2)				
				2105 (32) 0.4
		1648 (9) 0.1	1645 (s)	
1467 (5) 0.8	1468 (s)		1481 (s)	
1448 (5) 0.8		1456 (5) 0.7	1466 (s)	1453 (9) dp.
		1424 (4) 0.4	1420 (m)	
	1395 (w)	1390 (2) 0.4	1387 (m)	1390 (v.w.)
	1381 (m)			
	1366 (s)		1364 (s)	
1313 (0.5) 0.9	1307 (w)	1311 (6) 0.3		
1258 (1) 0.8	1252 (m)	1272 (2) 0.6	1271 (m)	1247 (1)
1221 (2) 0.8	1217 (s)	1209 (5) 0.7	1209 (s)	1205 (8) dp.
1080 (0.5)	1074 (s)	1067 (0.9)	1068 (m)	
1021 (1) 0.7	1018 (s)	1026 (1)	1027 (m)	1029 (1)
995 (0.5)	996 (m)	999 (2)	1000 (s)	
	986 (m)			
929 (2) 0.8	929 (m)	922 (6) 0.7		931 (6) dp.
			912 (v.s.)	
873 (1) 0.9	870 (w)	879 (3) 0.3	881 (m)	885 (4) p.
			821 (w)	
	782 (s)			
				722 (3)
714 (7) 0.1	711 (w)	715 (13) 0.1	715 (w)	690 (16) 0.1
	663 (v.w.)		683 (s)	633 (5)
			620 (w)	
484 (0.5)	486 (w)			
411 (0.5)		519 (2) 0.3	523 (w)	544 (2)
361 (1) 0.5				389 (2)
344 (1) 0.8		353 (4) 0.6		359 (3)
260 (0.5)		304 (4) 0.9		
194 (0.5)				183 (100) 0.90

(v.s.) very strong; (s) strong; (m) medium; (w) weak; (v.w.) very weak; (p) polarized; dp. (depolarized).

[a] See reference 11.
[b] See reference 13.
[c] See reference 8.
[d] See reference 9.
[e] See reference 10.
[f] See reference 12.

nor are any in the region 2800−1500 cm^{-1} except for the obvious C≡C and C=C stretching frequencies. It is well known that these regions are otherwise free of fundamentals. The weak frequencies at 659 and 612 cm^{-1} in the 22-dimethyl butane Raman spectrum, and at 657 and 615 cm^{-1} in the 22-dimethyl-3-butene spectrum, as given by Fenske *et al.*,[11] have not been included in the table as they are probably caused by double and triple excitation of the very strong 714- and 715-cm^{-1} lines by the five structure satellites of the 4358A Hg exciting line.[16] In the case of 22-dimethyl butane, these frequencies were not observed in the Raman spectrum of Rosenbaum, Grosse, and Jacobson.[13]

II. THE ASSIGNMENT OF FUNDAMENTALS

The most interesting region of the spectrum for our present purpose is that between 1350 and 600 cm^{-1}, as this will contain most of the CH deformation modes and all of the C−C skeletal stretching modes. Our assignments for these three molecules in this region are summarized in Table II, which is subdivided into the modes of vibration of different molecular groups so that closely related frequencies in the different molecules can be compared. The third and fourth columns of this table give the characteristic regions already known to be associated with certain of the modes, and the fifth column gives the appropriate references.[1,3,4,7,17] The frequencies above 1350 cm^{-1} can all be assigned with the help of well established rules, and those below 600 cm^{-1} are almost certainly all skeletal deformation or methyl torsional modes.

The probable symmetry of the 22-dimethyl-3-butyne molecule is C_{3v}, and hence the fundamentals can be divided into the three symmetry classes A_1, A_2, E. The first and last of these classes correspond to fundamentals with infra-red and Raman activity, whereas the A_2 modes are forbidden in both absorption and scattering. The degeneracies indicated in brackets after the description of the vibrations of the tertiary butyl group in Table II are strictly applicable to the 22-dimethyl-3-butyne molecule, and are apparently in practice also obeyed for the corresponding vibrations of the other less symmetrical molecules. The maximum symmetry that either of the other molecules could possess would be a single plane of symmetry, and hence all the fundamentals are allowed in the infra-red and Raman spectra. The detailed interpretation of the spectra will now be discussed according to the three regions distinguished above.

(a). The Region 3350–1350 cm^{-1}

The assignment of frequencies in this region to the normal modes of vibration of hydrocarbon groups is now a well established procedure. The types of fundamental that occur in this frequency range are the CH stretching fundamentals between 3350 and 2800 cm^{-1},[18] C≡C stretching modes near 2100 cm^{-1},[19] C=C stretching modes between 1700 and 1600 cm^{-1},[19] CH_3 asymmetrical and symmetrical deformation modes near 1450 and 1375 cm^{-1},[19] and the CH_2 bending modes of saturated and unsaturated groups near 1450[19] and 1420[17] cm^{-1}, respectively. Because of overlapping in the regions 3000–2800 cm^{-1} and 1470–1440 cm^{-1}, semi-schematic assignments only are possible within these frequency ranges. Our assignments for these three molecules in this region of the spectrum are given below without further comment.

22-Dimethyl-3-Butyne

CH_3 symmetrical stretching, 2887(2), 2865; CH_3 asymmetrical stretching, 2968(4), 2923(2); ≡CH

[16] D. H. Rank and J. S. McCartney, J. Opt. Soc. Am. **38**, 279 (1948).

[17] N. Sheppard and G. B. B. M. Sutherland, Proc. Roy. Soc. (London), in press.

[18] J. J. Fox and A. E. Martin, Proc. Roy. Soc. (London) **A175**, 208 (1940).

[19] G. Herzberg, *Infra-Red and Raman Spectra of Polyatomic Molecules* (D. Van Nostrand Company, Inc. New York, 1945), p. 195 and discussions of individual molecules.

TABLE II. The assignment of the fundamental frequencies in the spectral region 1350–600 cm^{-1} for the molecules 22-dimethyl butane, 22-dimethyl-3-butene, and 22-dimethyl-3-butyne.

Group	Description of vibration	Frequency range in cm^{-1}	Strong in:	Reference	22-dimethyl butane	22-dimethyl-3-butene	22-dimethyl-3-butyne
Tertiary	C–C stretching (1)				1258	1271	1247
	C–C stretching (2)	1250–1200*	i.r. and R	3*	1217	1209	1205
	C–C stretching (1)	750–690	R	3	714	715	690
Butyl	CH_3 wagging (2)	?			1018	1026	1029
	CH_3 wagging (2)	930–910*	R	3*	929	922	931
	CH_3 wagging (1)	?			870	879	885
	CH_3 wagging (1)	?			(950)	(950)	(950)
CCH	CH wagging (2)	650–600	i.r. and R		—	—	633
Vinyl	CH_2 rocking (in-plane)	1170–1090		1		1067	
	CH CH-bending (in-plane)	1320–1280	R	17, 1		1311	
	CH_2 wagging (out-of-plane)	920–900	i.r.	17, 1	—	912	—
	CH_2 twisting (out-of-plane)	680–600		1		683	
	CH CH-wagging (out-of-plane)	1010–980	i.r.	17, 1		1000	
Ethyl	C–C stretching	1100–880		7	996		
	CH_2 wagging	1340–1290	R	3, 4	1313		
	CH_2 twisting	1300–1240		3, 4	(1250)		
	CH_2 rocking	760–720	i.r.	3, 4	782	—	—
	CH_3 wagging (in-plane)	1150–1000		1	1074		
	CH_3 wagging (out-of-plane)	960–900		1	986		

* But see later discussion of results.
(R-Raman, i.r.-infra-red).

stretching, 3307; C≡C stretching, 2105; CH_3 symmetrical deformation, *1365*(2), 1390; CH_3 asymmetrical deformation, 1453(6).

22-Dimethyl-3-Butene

CH_3 symmetrical stretching, 2880(3); CH_3 asymmetrical stretching, 2960(6); $=CH_2$ symmetrical stretching, *3000;* $=CH_2$ asymmetrical stretching, 3090; =CH stretching, *3000;* C=C stretching, 1645; CH_3 symmetrical deformation 1364(2), 1387; CH_3 asymmetrical deformation, 1481(2), 1466(2), 1456(2); $=CH_2$ bending, 1424 cm^{-1}.

22-Dimethyl Butane

CH_3 symmetrical stretching, 2871(3), 2890 cm^{-1}; CH_3 asymmetrical stretching, 2967(4), 2942(4); CH_2 symmetrical stretching, 2856; CH_2 asymmetrical stretching, 2942; CH_3 symmetrical deformation, 1366(2), 1381, 1395; CH_3 asymmetrical deformation, 1468(4), 1448(4); CH_2 bending, 1448 cm^{-1}.

The frequencies are followed in brackets by the assigned degeneracies, and those not experimentally observed are printed in italics. In the case of the symmetrical 22-dimethyl-3-butyne molecule, some of the degeneracies are due to symmetry considerations, and two of the frequencies (one asymmetrical CH_3 stretching, and one CH_3 asymmetrical deformation mode) are forbidden in the Raman and infra-red spectra. These have not been distinguished separately above.

(b). The Region 1350–1600 cm^{-1}

Our assignments in this region are given in Table II and will be discussed below, molecule by molecule, starting with the symmetrical 22-dimethyl-3-butyne.

22-Dimethyl-3-Butyne

Although there does not appear to be an infra-red spectrum available for this compound, there are enough lines in the Raman spectrum for assignment to all the expected fundamentals in this region. The line at 633 cm^{-1} is clearly the expected deformation mode of the CH linkage attached to the triple bond, and the frequencies at 1247, 1205, 931, and 690 cm^{-1} correspond to characteristic frequencies previously found in the spectra of molecules containing the tertiary butyl group.[3] Of the remaining three frequencies, those at 1029 cm^{-1} and 885 cm^{-1} are chosen as the two remaining fundamentals because of their persistence in the spectra of the other two hydrocarbons. The remaining line at 722 cm^{-1} is probably the summation frequency 544+183=727 cm^{-1}. Of these six frequencies which are associated with the tertiary butyl group, *viz.*, 1247, 1205, 1029, 931, 885, and 690 cm^{-1}, the lowest one can be assigned with little doubt to the breathing frequency of the C_5 skeletal unit.[3] Of the others, those at 1247, 1205, and 931 cm^{-1} have previously been assigned to the remaining two C–C stretching modes and a methyl wagging mode, respectively, on the bases of studies of characteristic frequencies.[2,3]

Sutherland and Simpson[2] in particular showed that the 1247 and 1205-cm^{-1} modes could be explained as C−C stretching modes with the assumption of a reasonable value of the C−C stretching force constant. If this is correct the remaining two frequencies at 1029 and 885 cm^{-1} are the remaining methyl wagging modes, the latter being the symmetrical one on the basis of the polarization data. This assignment scheme is shown in Table II, and will be discussed in more detail below. The remaining A_2 type methyl wagging mode is forbidden in both the infra-red and Raman spectra, and has been given a schematic value of 950 cm^{-1} as being the center of the range of observed methyl wagging modes. It is possible, however, that it may have a value near 1200 cm^{-1} (see later discussion of results).

22-Dimethyl-3-Butene

If the assumption is made that the set of frequencies found for the vibrations of the tertiary butyl group in the case of 22-dimethyl-3-butyne will be reproduced fairly accurately in the spectrum of this compound, the frequencies at 1272, 1209, 1026, 922, 879, and 714 cm^{-1} can tentatively be assigned to these modes. This leaves frequencies at 1311, 1067, 999, 912, 821, 683 and 620 cm^{-1} to be assigned to the five CH deformation modes of the vinyl group that should occur in this region. As can be seen in Table II, such an assignment can easily be made with the previously established correlation rules. The 1067 cm^{-1} $=CH_2$ rocking frequency is slightly outside the expected region, but the correlation rule in this case is less well established than most of the others.[1] The weak 821 and 620-cm^{-1} frequencies are left unaccounted for. It is possible that the 821-cm^{-1} frequency is the remaining methyl wagging mode that was forbidden in the spectrum of 22-dimethyl-3-butyne, but as no corresponding frequency is found in the spectrum of 22-dimethyl butane, it seems more likely that it is to be assigned to the combination band 519+304=823 cm^{-1}. The weak 620-cm^{-1} infra-red frequency is presumed to be a skeletal bending mode and will be discussed in the next section.

22-Dimethyl Butane

Having elucidated the spectra of the previous two compounds, the assignment of the 22-dimethyl butane spectrum in this region is a fairly straightforward matter, as shown in Table II. The weak infra-red absorption at 664 cm^{-1} is tentatively assigned to the combination level 411+260=671 cm^{-1}.

(c). The Region below 600 cm^{-1}

The assignments in this region will necessarily be less complete because of the lack of infra-red data, but, even so, fairly complete assignments can be made for the skeletal bending modes. In general, the methyl torsion modes do not seem to be spectroscopically observable, undoubtedly because of the fact that to a first approximation the rotation of a single symmetrical $-CH_3$ group about its trigonal axis gives rise to no change in either dipole moment (infra-red) or polarizability (Raman spectrum).

22-Dimethyl-3-Butyne

This molecule would be expected to have four different skeletal bending modes in this region, three of them being of symmetry class E and one of class A_1. We make the assignment 544(2), 389(2), 359(1), 183(2). The Raman line at 183 cm^{-1} can probably be associated with the bending of the C≡C−C group as a low frequency at about this position seems to occur in the spectra of several acetylene derivatives.[20] If this is correct, the remaining five frequencies are mainly associated with bending modes of the C_5 skeletal unit, and the distribution of frequencies is in fair agreement with that of the analogous frequencies of neopentane, *viz.*, 414(3), 335(2).[3]

22-Dimethyl-3-Butene

Because of the lack of symmetry in this molecule, there should be six different skeletal bending modes in this region, and one skeletal torsional mode. Although only four frequencies have been noted in this region, *viz.*, 620, 519, 353, and 304 cm^{-1}, examination of the original Raman spectrum suggests that the frequency at 304 cm^{-1} may be double, and that there may also be a weak line at 400 cm^{-1}. We therefore assign the spectrum as follows: 620, 519, 400, 353, 304(2) cm^{-1}. The skeletal torsional mode does not appear to be observable in the spectrum.

22-Dimethyl Butane

In this case, we assign the following value to the skeletal bending modes: 484, 411, *400*, 361, 344, 260 cm^{-1}. We have replaced the 276-cm^{-1} line in the assignment of Kilpatrick and Pitzer[15] by the schematic frequency of 400 cm^{-1}, because the 276-cm^{-1} line does not appear to be observable in the recent Raman spectrum of Fenske *et al.*[11] Also, on the assumption that the mode associated mainly

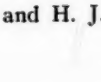

with the bending of the lone C C unit corresponds to one of the frequencies between 300 and 400 cm^{-1}, the schematic value of 400 cm^{-1} makes

[20] F. F. Cleveland, M. J. Murray, and H. J. Taufen, J. Chem. Phys. **10**, 172 (1942).

the average value of the remaining bending modes of the C_5 unit nearer to that found with neopentane.[3] The frequency at 194 cm^{-1} may be the skeletal torsion or one of the methyl torsional modes.

Although skeletal bending modes would be expected to have much less characteristic frequencies than the stretching modes, there is a frequency between 350 and 365 cm^{-1} in all these three compounds which is probably the symmetrical bending mode of the tertiary butyl group. A frequency near this value has previously been assigned as a characteristic frequency of this group.[3]

III. DISCUSSION OF RESULTS

Although the assignments for the fundamentals of the tertiary butyl group in the region 1350–600 cm^{-1} seem fairly straightforward, an interesting point has arisen with respect to their division between C–C stretching and methyl wagging modes. Our assignments were based on the results of calculations of Sutherland and Simpson,[2] who concluded that the frequencies near 1250 and 1200 cm^{-1} in branched hydrocarbons were probably C–C stretching modes. However, Rasmussen,[4] on the basis of similar calculations with a rather lower C–C stretching constant, has concluded that in neopentane the triply degenerate frequency at 1252 cm^{-1} is a methyl wagging mode and that the corresponding C–C skeletal mode is the 925-cm^{-1} Raman line in this compound. This carries corresponding implications for the spectra of doubly branched paraffins, and if this latter view were correct, the assignment given for 22-dimethyl-3-butyne would probably have to be changed to C–C stretching (1), 885; C–C stretching (2), 931; CH_3 wagging (2), 1205; CH_3 wagging (1), 1247 cm^{-1}, with corresponding changes for the other compounds. Also, the non-observed methyl wagging mode should probably then be assigned a value of *ca.* 1200 cm^{-1} rather than 950 cm^{-1}. On the other hand, evidence against this formulation comes from the observation that the frequency near 1200 cm^{-1} in all doubly branched paraffins seems to be relatively independent of the pattern of methyl substitution around the quaternary carbon atom, whereas the 925-cm^{-1} frequency is more sensitive to such changes.[3] This would seem to be surprising if the 1200-cm^{-1} frequency is a methyl wagging mode. Secondly, independent calculations by Ahonen, which have recently been shown to be in good general agreement with the observed C–C stretching modes of straight chain paraffins,[7] also predict frequencies at 1270 cm^{-1} and 847 cm^{-1} for infra-red active skeletal modes of the branched paraffin ditertiary butyl (i.e., 2233 tetramethyl butane). There are, in fact, strong lines in the infra-red spectrum of this substance,[21] at 1180 cm^{-1} and 800 cm^{-1}. Clearly fair agreement between theory and experiment would be achieved in this case if Ahonen's original C–C force constant were lowered somewhat, as was found to be necessary for the normal paraffins.[7]

However, it must be concluded that none of these points of evidence are completely satisfactory, and it is true that normal coordinate calculations in the past have not been very successful in predicting the frequencies of new structural groups, particularly when the force constants are in some doubt. Probably the best way to settle this problem would be to obtain the spectrum of a completely deuterated branched hydrocarbon such as neopentane. It should be a fairly straightforward matter to decide from such a spectrum which of the two neopentane frequencies had shifted most, and hence which was essentially the methyl wagging mode. Similar considerations apply also to the 1172 and 965-cm^{-1} frequencies of isobutane, and to the spectra of the corresponding singly branched paraffins.[2–4]

The assignment of 22-dimethyl butane spectrum differs in several respects from the schematic one of Kilpatrick and Pitzer.[15] The new values of the fundamentals were used to compute the gaseous specific heat of this compound at 342 and 449°K for comparison with the experimental data of Waddington and Douslin.[22] Using the Kilpatrick and Pitzer value of 4375 cal. $mole^{-1}$ for the barrier restricting rotation of the methyl groups, the calculated specific heats (assuming values of either *ca.* 1200 or *ca.* 950 cm^{-1} for the non-observed methyl wagging mode) were both too high by several tenths of a calorie, although the slope of the calculated curve was in fair agreement with experiment. However, in view of the satisfactory nature of the numerical spectroscopic assignments above 600 cm^{-1}, and because the magnitude of the specific heat values depends to some extent on the low frequencies (one at least of which is doubtful in magnitude) and on the simplified treatment of the restricted rotation of the four methyl groups, a more exact treatment was not attempted.

It can be seen that the assignments given above afford a very satisfactory explanation of all the strong features in both the Raman and infra-red spectra of these large molecules and at the same time give a very consistent set of fundamentals for the tertiary butyl group. It is important that this method of analysis by group frequencies can give reasonable interpretations to what has often been

[21] American Petroleum Institute, Research Project 44. Infra-Red Spectrogram No. 444, contributed by the Shell Development Company, Emeryville, California.

[22] G. Waddington and D. R. Douslin, J. Am. Chem. Soc. **69**, 2275 (1947).

considered the impossibly complex spectra region between 1350 and 600 cm^{-1} in polyatomic molecules. It is certain that a similar method of attack on the spectra of other series of structurally related molecules can yield valuable results, although it should be borne in mind that the very symmetrical tertiary butyl group may be exceptional in this respect. We would like to emphasize at this point that very considerable aid in making the assignments came from the results of previous empirical determinations of characteristic group frequencies[2-4] and that these two methods of approach (empirical correlations on series of large molecules, and detailed analyses of a few structurally related molecules) probably together constitute the best approach to the understanding of polyatomic spectra.

THE JOURNAL OF CHEMICAL PHYSICS VOLUME 17, NUMBER 5 MAY, 1949

Substituted Borazole Spectra: Gain and Loss of Aromatic Character

C. W. RECTOR, G. W. SCHAEFFER,* AND J. R. PLATT
Departments of Physics and Chemistry, University of Chicago, Chicago, Illinois
(Received October 4, 1948)

The far ultraviolet spectra of N-trimethyl, B-trimethyl, and B-trichloroborazole in *n*-heptane solution are compared with previous spectra of borazole and of the organic analogs, benzene and mesitylene. By N-substitution the negative charge on the boron atoms of the borazole ring is increased, increasing the double-bond character and the spectral resemblance to a benzene derivative. By B-substitution, the opposite effect is produced, increasing the spectral resemblance to a saturated compound. The physical and chemical properties of these borazoles show corresponding behavior.

INTRODUCTION

THE absorption spectra of *n*-heptane solutions of three trisubstituted borazoles have been obtained and examined in the region 2300–1790A. The compounds were: N-trimethylborazole, B-trimethylborazole and B-trichloroborazole. This study is a continuation of previous work on the borazole spectrum from this laboratory.[1,2]

Borazole and the boron-nitrogen compounds studied here have a striking resemblance to the corresponding isosteric and isoelectronic aromatic carbon compounds, benzene, mesitylene and 1,3,5-trichlorobenzene. This similarity is apparent in the comparison of the physical properties of the analogous boron-nitrogen and organic compounds given in Table I. This comparison suggests that the borazole ring possesses the Kekulé structure (II). However, the two analogous series of compounds do not exhibit the same close similarity in their chemical properties. For example, the borazoles add Lewis acids to the ring nitrogens and Lewis bases to the ring borons; they are easily hydrolyzed by dilute acids; and hydrogen halides, alcohols and similar reagents add to the ring, the negative addendum going to the boron atom of the ring, to give derivatives structurally similar to cyclohexane. These properties can be most conveniently interpreted by assuming a triborine-triamine structure (I).

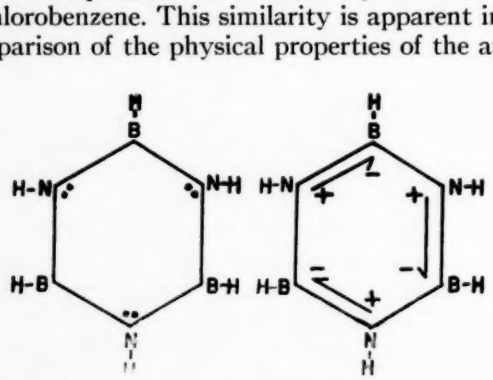

Structure I Structure II (two forms)

The importance of the Kekulé structures may be seen from the following considerations. The single tricovalent B−N bond distance is, correcting for trigonal conjugation,[3] 1.48A, as compared with a B,N distance of 1.45A in boron nitride, 1.44A in borazole, and a B=N distance of 1.30A, as calculated from the single bond distance assuming Pauling's factor of 0.86.[4] (The notation X, Y is used here to denote a general bond between X and Y.) These data are compared with the corresponding data for the analogous carbon compounds in Table II. The analogy is of course not perfect because the B−N single bond distance is for tri-

* Now at the Department of Chemistry, St. Louis University, St. Louis, Missouri.

[1] J. R. Platt, H. B. Klevens, and G. W. Schaeffer, J. Chem. Phys. **15**, 598 (1947).

[2] L. E. Jacobs, J. R. Platt, and G. W. Schaeffer, J. Chem. Phys. **16**, 115 (1948).

[3] H. I. Schlesinger and G. W. Schaeffer, "Hydrides and Borohydrides of Light Elements," PR XXIX, Contract Number N6ori-20, Dec. 31, 1947.

[4] L. Pauling, *The Nature of the Chemical Bond* (Cornell University Press, Ithaca, New York, 1945), 2nd edition.

TABLE I. Comparison of the physical properties of borazole and tri-substituted borazoles with their organic analogs.

Compound	Formula	Mol. wt.	b.p. °C	m.p. °C	$\Delta H_{vap.}$ kcal.	Trouton's constant	Vapor pressure °C	Vapor pressure mm	Solubilities water	alk.	ether	hydrocarbon
Borazole[a]	$B_3N_3H_6$	80.5	53	−58	7.0	21.4	0	85	insol.	sol.	sol.	sol.
Benzene	C_6H_6	78	80	+6	7.4	21.1	0	26.5	insol.	sol.	sol.	sol.
N-Trimethylborazole[b, d]	$B_3N_3H_3(CH_3)_3$	122.6	132	−9	9.4	23	20	9	insol.	sol.	sol.	sol.
B-Trimethylborazole[b, e]	$B_3N_3H_3(CH_3)_3$	122.6	127	32	10.1	25	20	5	insol.	sol.	sol.	sol.
Mesitylene	$C_6H_3(CH_3)_3$	120.2	165	−53	10.0	23	20	2	insol.	sol.	s. sol.	sol.
B-Trichloroborazole[c]	$B_3N_3H_3Cl_3$	183.9	~210 d. above 100	84	—	—	93.5	27.2	d.	—	—	sol.
Trichlorobenzene	$C_6H_3Cl_3$	181.5	208	63.5	—	—	—	—	insol.	sl. sol.	s. sol.	sol.

[a] E. Wiberg and A. Bolz, Ber. **73**, 209 (1940).
[b] E. Wiberg, K. Hertwig and A. Bolz, Z. Anorg. Chem., **256**, 177 (1948).
[c] C. A. Brown, private communication, May 23, 1948.
[d] H. I. Schlesinger, D. M. Ritter, and A. B. Burg, J. Am. Chem. Soc. **60**, 1297 (1938).
[e] H. I. Schlesinger, L. Horvitz, and A. B. Burg, J. Am. Chem. Soc. **58**, 409 (1936).

covalent boron while the C−C single bond distance is for quadricovalent carbon, and the B,N end points are hypothetical. But it seems to be as good an analogy as the difference in the atoms allows.

Penney[5] has attempted to correlate bond distances with bond character by defining the "bond order" of a bond in such a way that it assumes the values 1 and 2 for pure single and double bonds, respectively, and is a linear function of the bond energy for bonds of intermediate type. By calculating or defining the bond orders of the C,C bond in ethane, graphite, benzene, ethylene and acetylene as 1.00, 1.45, 1.62, 2.00 and 3.00, respectively, and knowing the experimental bond distances, 1.54, 1.42, 1.39, 1.33 and 1.20A, respectively, Penney was able to draw a smooth curve relating the bond order and bond distance. The curve is duplicated in Fig. 1 along with a B,N curve obtained by using the B−N and B=N distances for the end points and retaining the shape of the C,C curve. From this plot, the B,N bond order in borazole is about 1.15 or, in other words, has roughly 15 percent double bond character.

As already pointed out, the characteristic chemical behavior of borazole is that of an aminoborine which indicates that the contribution of structure (I) is important. Nevertheless, the contributions of (II) are also quite important as suggested by the comparison in Table I and in Fig. 1, and as verified by the spectra as discussed below.

APPARATUS AND TECHNIQUE

The apparatus and techniques used have in large part been described earlier.[1, 6]

[5] W. G. Penney, Proc. Roy. Soc. (London) **A158**, 306 (1937).
[6] J. R. Platt, I. Rusoff, and H. B. Klevens, J. Chem. Phys. **11**, 535 (1943); H. B. Klevens and J. R. Platt, J. Am. Chem. Soc. **69**, 3055 (1947).

The spectra were taken with a Cario-Schmidt-Ott vacuum fluorite spectrograph. The source employed was an Urey-type hydrogen discharge. The absorption cell was composed of two artificial sapphire windows, each of thickness about 3 mm, one attached to the source and the other to the spectrograph, and separated by a 0.13-mm copper spacer. The *n*-heptane solution was allowed to drip through the cell, filling the space between the windows by virtue of its surface tension.

Ilford *Q* spectroscopic plates ($4\times\frac{3}{4}''$) were used. They give more reproducible results and are more convenient to use than any other plates so far tried. Four exposures were taken on each plate, two one-minute exposures of the solution plus a one-quarter minute and a one half-minute solvent exposure for intensity calibration. The calibration was corrected for reciprocity failure.

The plates were photometered with a Leeds and Northrup microphotometer equipped with a Speedomax recorder. Extinction values were then computed from the traces. The positions of all detectable absorption peaks were also determined visually from the plates by use of a Lucite wave-length scale calibrated by a mercury arc. This was done because in some cases maxima were not indicated on the densitometer traces, yet could be detected visually, probably because of the St. John effect. When the maxima were clearly indicated the posi-

TABLE II. Boron-nitrogen and carbon-carbon bond distances (A).

Boron-nitrogen compound		Organic analogy	
B−N single bond	1.48	C−C single bond	1.54
Boron nitride	1.45	Graphite	1.42
Borazole	1.44	Benzene	1.39
B=N double bond	1.30	C=C double bond	1.34

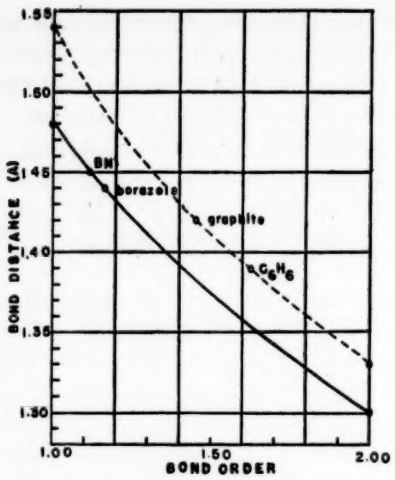

FIG. 1. Bond order and bond distance.

tions obtained from the traces differed at most by 5A from the positions obtained visually from the plates. Empirical curves were used to correct for the effect of scattered light, which becomes appreciable below 1900A. Earlier studies[7,8] indicate that the probable error in the intensity measurements is 10–15 percent.

Because the B-trichloroborazole is particularly sensitive to moisture in the air, hydrolyzing very rapidly, the solutions were handled under a blanket of dry nitrogen during the running of the spectrograph. In the case of the other compounds, only trivial hydrolysis occurred if all operations were performed rapidly.

The lower limit on the wave-length obtainable, about 1720A, was imposed by the solvent, *n*-heptane. This limit is reached only if the heptane is shaken for twenty-four hours with concentrated sulfuric acid to remove traces of absorbing unsaturated impurities.

PREPARATION OF THE MATERIALS AND SOLUTIONS

n-Heptane

In order to insure strictly anhydrous conditions, to prevent the hydrolysis of the boron compounds, the *n*-heptane, which was obtained from the Westvaco Chlorine Products Corp. (b.p., 98.42; m.p., −90.63; n_D^{20}, 1.38766) was refluxed over sodium hydride for several hours. It was then distilled onto sodium hydride contained in a receiver provided with a standard taper for attachment to the high vacuum apparatus. After the distillation was complete, the receiver was then attached to the vacuum apparatus and the heptane distilled in vacuum into a storage flask, separated from the rest of the system by a mercury float valve. The material was stored in this flask until needed.

N-trimethylborazole

The compound was prepared by the reaction of lithium borohydride with monomethylamine hydrochloride in diethyl ether solution;[9]

$$3LiBH_4+3CH_3NH_3Cl \rightarrow 3LiCl + 9H_2+B_3N_3H_3(CH_3)_3$$

and purified by repeated fractional condensations at −45° in vacuum. The heptane solution was prepared as follows. A sample of N-trimethylborazole of approximately the desired amount, as judged by its liquid volume, was distilled into a previously weighed tube attached to the vacuum system. The tube was closed and separated from the vacuum system, weighed and then reattached. The borazole compound was then distilled in vacuum directly into the sample tube. Somewhat more than the necessary amount of heptane was transferred from the storage flask to a small calibrated measuring tube, and then the desired volume was distilled from the measuring tube onto the borazole in the sample tube. The sample tube containing the solution was sealed under vacuum from the apparatus and opened just before use. The solution so obtained was 0.54 molar.

B-trimethylborazole

This compound was prepared by the pyrolysis of ammonia-trimethyl boron[10,11] in a sealed tube at 300° and purified by fractional condensation at −78° in the high vacuum apparatus. The final product melted between 27° and 31.5° (literature,[3,12] 31.5°) and had a vapor pressure of 11 mm at 28° (literature,[3] 9 mm). The heptane solution, 0.201 molar, was prepared in the manner described above.

B-trichloroborazole

Approximately one gram of this compound, in a sealed tube under vacuum, was obtained through the courtesy of Mr. Charles A. Brown and Dr. S. H. Bauer of Cornell University. The purity of the sample by analysis for boron, chlorine, and nitrogen was better than 99.5 percent.[12] A 0.48 molar solution was prepared in the manner previously described.

DESCRIPTION OF SPECTRA

The absorption spectra are shown in Fig. 2, together with the spectra of borazole[1] and the

[7] J. R. Platt and H. B. Klevens, Chem. Rev. **41**, 301 (1947).

[8] H. B. Klevens and J. R. Platt, "Geometry and spectra of substituted anilines" J. Am. Chem. Soc. (in press).

[9] E. R. Anderson, thesis, University of Chicago, August 1948. The details of this preparation will be given in a forthcoming publication from this laboratory.

[10] H. I. Schlesinger, L. Horvitz, and A. B. Burg, J. Am. Chem. Soc. **58**, 409 (1936).

[11] R. E. Moore, thesis, University of Chicago, June 1948.

[12] Private communication, Charles A. Brown, Cornell University, Ithaca, New York, May 3, 1948.

carbon analogs, benzene[6] and mesitylene.[13] The main features of these spectra are summarized in Table III.

Benzene has three electronic bands at 2550A, 2100A and 1840A. The first two, $^1A_{1g}-{}^1B_{2u}$ and $^1A_{1g}-{}^1B_{1u}$, are forbidden and the last one, $^1A_{1g}-{}^1E_{1u}$, allowed. These are believed to have exact analogs in the spectrum of borazole and its derivatives.[14,15] The bands of each compound have therefore been grouped in Table III with the benzene bands to which they seem to correspond.[2,15] To keep their relationships clear, the bands will all be called by the benzene names in the following discussion, even though their proper group theoretical designations are different.[15]

The molar extinction, ϵ, given in the table is defined by the equation,

$$\epsilon=(1/ct)\cdot\log(I_0/I),$$

I_0 being the initial intensity, I the final intensity, c the concentration of the solution in mols per liter and t the cell thickness in centimeters.

The oscillator strengths for the three transitions were computed from the integrated areas under the curves by the equation

$$f=4.32\times10^{-9}\int\epsilon_\nu d\nu$$

where ϵ_ν is the molar extinction and ν is measured in cm^{-1}.

The data for the $^1A_{1g}-{}^1B_{2u}$ transition of benzene and mesitylene were computed from the A. P. I. ultraviolet curves.[16]

It is believed that the $^1A_{1g}-{}^1B_{1u}$ transition in borazole and the three substituted borazoles may be hidden by the strong $^1A_{1g}-{}^1E_{1u}$ allowed transition in all four compounds.

Only in the case of N-trimethylborazole was it possible to obtain any reliable figure for the oscillator strength of the $^1A_{1g}-{}^1E_{1u}$ type transition, for in the other borazoles this peak lies below the wave-length limit obtainable. The rough estimates given in Table III for this f-value in the other borazoles were obtained, however, by assuming that their peaks all lie near 1710A and are symmetrical. This wave-length, 1710A, is the location of the peak in borazole vapor as determined in this laboratory by Dr. W. C. Price (unpublished results).

Table III also gives the "total spread" of the upper singlet states in the borazoles for comparison with the benzenes. This spread is the interval in wave numbers between the onset of absorption of the $^1A_{1g}-{}^1B_{2u}$ transition band and the $^1A_{1g}-{}^1E_{1u}$ transition peak. In the case of borazole and B-trimethyl and B-trichloroborazole the $^1A_{1g}-{}^1E_{1u}$ peak was again assumed to be near 1710A.

DISCUSSION

The Kekulé structure (II) of the borazoles may be considered as derived from the triborine-triamine structure (I) by internal donor-acceptor bonding; that is, the free electron pair of the nitrogen (structure II) being accepted by the open sextet of the boron. Substituents on the borazole ring which stabilize the internal donor-acceptor bond would increase the relative contribution of (II) to the structure of the molecule. The positive inductive effect of the methyl groups attached to the nitrogen of the ring should increase the availability of the electron pair and consequently produce such a stabilization. An increased contribution of structure (II) should be reflected in an even closer resemblance between the substituted borazoles and their benzene analogs. If the methyl groups are substituted on boron the effect should be the opposite.

This inductive effect of the methyl group is well known in the case of simple donor-acceptor bonding exemplified in the case of the unhindered amine-borine addition compounds. As an example, the addition compound ammonia-trimethylboron is more dissociated into its components than methylamine-trimethylboron, presumably because of the positive inductive effect of the methyl group and the consequent greater availability of the electron pair of

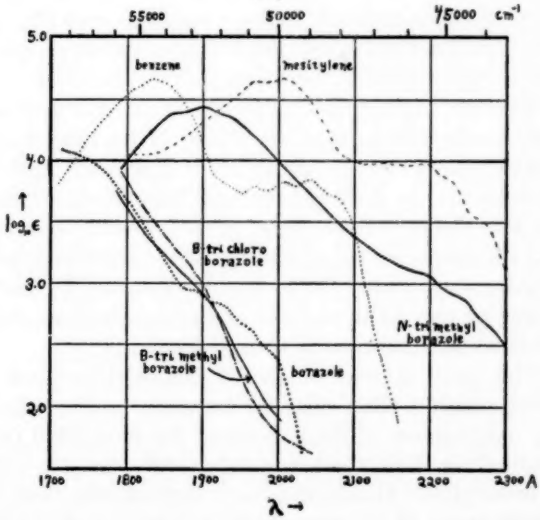

FIG. 2. Spectra of tri-substituted benzene and borazoles. (The B-trichloroborazole curve should be lowered 0.05 log unit. Data in tables have been corrected.)

[13] J. R. Platt and H. B. Klevens, "Further alkylbenzene spectra to 1750A" J. Chem. Phys. 16, 832 (1948).

[14] Footnote 12 of reference 1.

[15] C. C. J. Roothaan and R. S. Mulliken, J. Chem. Phys. 16, 118 (1948).

[16] American Petroleum Institute Research Project 44 at the National Bureau of Standards. Catalog of Ultraviolet Spectrograms: Serial No. 1, benzene, No. 142, mesitylene, contributed by the Texas Company, Beacon, New York; Serial No. 40, benzene, No. 164, mesitylene, contributed by the Shell Development Company, Emeryville, California.

TABLE III. Main features of spectra.

	Benzene	Mesitylene	Borazole	N-trimethyl-borazole	B-trimethyl-borazole	B-trichloro-borazole
			$^1A_{1g}-{}^1B_{2u}$ Forbidden transition			
Components	37250 38320 39220 40180 41070 42000	36750 37330 37670 38160 38640	50100 50950 51850 52750	43900 44600 45500	about 52400 (diffuse)	about 52600 cm^{-1} (diffuse)
ϵ_{max}	170	260	800	1200	~2000	~2000
f'	0.002	0.004	$\lesssim$0.009	$\lesssim$0.01	$\lesssim$0.02	$\lesssim$0.02
			$^1A_{1g}-{}^1B_{1u}$ Forbidden transition			
Components	48050 49000 49800 50900 51700 (?)	44000 44800 45700 46600	hidden near 54000 (?)	hidden near 46000 (?)	hidden near 54000 (?)	hidden near 54000 cm^{-1} (?)
ϵ_{max}	6900	9500	(?)	(?)	(?)	(?)
f'	0.10	0.12	(?)	(?)	(?)	(?)
			$^1A_{1g}-{}^1E_{1u}$ Allowed transition			
Components	53700 54500 55400	49800 50900	58400	51500 52600 53800	56800	56100 cm^{-1}
ϵ_{max}	46000	46000	13000	28000	6000	8000
Total osc. strength, f	0.79	0.89	~0.7 (?)	0.64	~0.7 (?)	~0.7 (?)
Total spread in cm^{-1}	17200	13500	8300	8700	5700	5300

the nitrogen. In the same way the addition compound, trimethylamine-borine is less dissociated into its components than is its methyl derivative, trimethylamine-methylborine. In this latter case, the inductive effect of the methyl group decreases the electron-pair acceptor ability of the boron.

The positive inductive effect of the methyl group is clearly demonstrated in the case of borazole by comparison of the spectrum of N-trimethylborazole with that of 1,3,5-trimethylbenzene and the spectrum of borazole with that of benzene (see Fig. 2). The N-trimethyl compound shows greater resemblance than the other borazoles to benzene and mesitylene in three ways: by the increased distinctness of the vibrational structure in its long wave-length bands, by its greater total spread, and by its red-shift. In borazole the long wave-length bands are less distinct than those of N-trimethylborazole and no structure at all can be seen in the B-substituted compounds. These bands presumably correspond to the 2600A bands of benzene whose sharp vibrational structure is so well known.[2,16]

The total spread of the N-trimethylborazole is more reliable than that of borazole and confirms our assignment of these bands,[2] for it is 2300 cm^{-1} larger than the spread from $^1A_{1g}-{}^1B_{1u}$ to $^1A_{1g}-{}^1E_{1u}$ in mesitylene. Hence it is very improbable that the 43900 band of N-trimethylborazole can be of the $^1A_{1g}-{}^1B_{1u}$ type.

From the benzene-mesitylene analogy, some red-shift would be produced in the borazole spectrum by methyl substitution even if there were no change in the ionic or double bond character. The N-trimethyl substitution evidently produces a substantial additional red-shift from this neutral ideal, i.e., it becomes almost aromatic; while the B-trimethyl produces a blue-shift and approaches a smooth saturated spectrum like cyclohexane[6] or, more properly, like the simple addition of borine and amine absorptions. [It might be worth while determining by x-ray or electron diffraction whether or not the N-valences tend, as they seem to do in some orthosubstituted anilines,[8] to become pyramidal with loss of double-bond character and produce a cyclohexane-like pucker in the borazole ring in B-substituted compounds.]

The total spread appears to be a useful measure of the electronic resemblance of the borazoles to benzene. It forms a quantitative index of the amount of double-bond character and resonance in the compounds. The ratio of the total spread of borazole to that of benzene is 0.49, that of N-trimethylborazole to mesitylene is 0.64 and that of B-trimethylborazole to mesitylene is 0.42. Qualitatively, this sequence is what might be expected. Possibly the spreads or their ratios might be used in estimating the bond order, B,N distance and other properties of such compounds. Obviously more theoretical and experimental work on these

properties is necessary before any such correlation can be established.

It is seen, then, that on the basis of both the spectrum and the expected inductive effects of the methyl substituents, the three compounds, B-trimethylborazole, borazole and N-trimethylborazole increase in "aromatic character" in the order given, that is, they behave more like and are structurally more similar to their aromatic analogs. This is indeed reflected in the chemical and physical properties of the compounds. A compound possessing a triborine-triamine structure (I) should, in common with other such substances, react with water and with hydrogen chloride; but a substance possessing the benzene-like structure (II) should, by analogy with the corresponding organic compounds, be inert towards these reagents. The reaction of the borazoles toward both water and hydrogen chloride decreases in the order trichloro, B-trimethyl, borazole and N-trimethyl, as expected.

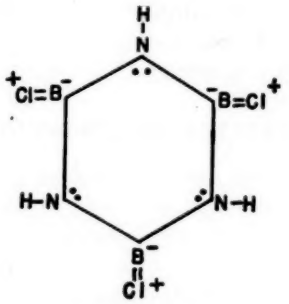

Structure III

The case of trichloroborazole requires special consideration. The inductive effect of the chlorine is negative, therefore the substitution of chlorine on boron should result in a stabilization of the internal donor-acceptor bond (cf. the great stability of amine-boron trihalide addition compounds). Thus it would be expected that the "aromatic character" of B-trichloroborazole be enhanced which, as may be seen from the data, is contrary to fact. However, the open sextet of the boron atom may be satisfied either by the electron pair of the adjacent nitrogen atoms (the Kekulé structure II) or by an electron pair of the chlorine, as illustrated by structure (III).

That the contribution of structure (III) more than compensates for the inductive effect is very reasonable in view of the analogous case of chlorobenzene. Structure (III) must be much more stable than the corresponding structure of chlorobenzene, yet even in chlorobenzene the inductive effect of the chlorine is masked by the contributions of structures containing double bonded chlorine, resulting in the ortho-para directing effect of the chlorine in electrophilic substitution.[18]

It is especially simple to relate all the spectroscopic and chemical effects of our substituents on borazole to their ortho-para directing effect on benzene. The connection may be seen as follows. A methyl- or chloro-substitution on a ring increases the relative reactivity of the ring at the ortho and para positions by increasing the relative charge density in the ring at these points. Hence a methyl or chloro N-substituted borazole will have relatively greater negative charge density at the B-positions. This means more ionic character, more of structure (II) and more double-bond character and resonance in the borazole ring. B-substitution evidently moves negative charge back to the N-positions producing less of structure (II), and the spectra and chemistry of the compound approach those of a saturated compound.

ACKNOWLEDGMENTS

We would like to express our appreciation to the University of Michigan for its gracious loan of the Cario-Schmidt-Ott fluorite vacuum spectrograph, to Mr. Charles A. Brown and Dr. S. H. Bauer for the sample of B-trichloroborazole, to Miss E. R. Anderson who prepared the N-trimethylborazole, to Mr. R. E. Moore who prepared the solutions and the sample of B-trimethylborazole, and to the Geology Department of the University of Chicago for the use of their Leeds and Northrup recording microphotometer.

This work was assisted by the Office of Naval Research under Task Order IX of Contract N6ori-20 with the University of Chicago.

[18] G. W. Wheland, *The Theory of Resonance* (John Wiley & Sons, Inc., New York, 1944), p. 268.

Absorption Intensities of Ethylenes and Acetylenes in the Vacuum Ultraviolet*

J. R. PLATT, H. B. KLEVENS,** AND W. C. PRICE***
Departments of Physics and Chemistry, University of Chicago, Chicago, Illinois
(Received July 28, 1948)

The spectra of three octenes, cyclohexene and 2,3-dihydropyrane, and of octyne-1 and -2 were obtained in *n*-heptane solution to 1700A. Intensity measurements on ethylene vapor to 1550A enable the contribution of the Rydberg bands to be separated from that of the continuum. The *f*-values in ethylene and the octenes are about 0.30, agreeing with Mulliken and Rieke's theoretical prediction within the experimental uncertainty of about 20 percent. The *f*-values of the octynes are about the same, but those of cyclohexene and dihydropyrane are about 0.20.

INTRODUCTION

THE spectra of octene-1, octene-2-*cis* and -*trans*, of cyclohexene and of 2,3-dihydropyrane were measured in *n*-heptane solution in an 0.13 mm cell to 1700A in order to discover the effects of substitution on the intensity of the double bond absorption peak near 1800A. These spectra are compared with preliminary intensity measurements on the corresponding peak in ethylene vapor near 1600A. Spectra of two substituted acetylenes, octyne-1 and octyne-2, were also obtained in *n*-heptane solution to 1700A.

Many previous studies have been made on the absorption of various substituted ethylenes in the vapor phase, but without intensity measurements. A complete bibliography was given in an earlier article.[1] Absolute intensity measurements on octene-3 and some other olefinic compounds in *n*-heptane solution were reported in two earlier papers,[2] but the *cis-trans* composition of the octene was unknown, and the other olefin spectra were altered by fatty acid absorption. Therefore we wished to get absolute intensity measurements and locate the absorption maxima in more primitive octenes and in a simple cyclic olefin.

A bibliography of previous work on acetylene vapor in the vacuum ultraviolet was also given in the earlier paper.[1] The spectrum of methylacetylene has since been obtained.[3] No intensity measurements on acetylenes in solution below 2000A have been reported heretofore.

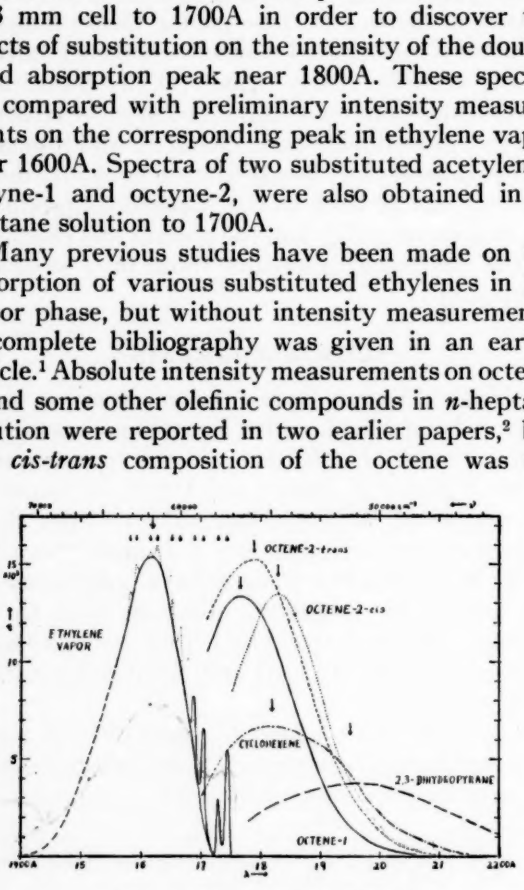

FIG. 1. Absorption of olefins.

APPARATUS AND TECHNIQUES

The apparatus and techniques for the solution studies are the same as those described earlier.[2,4] The uncertainty in the intensity measurements is about ±10 percent.

The ethylene vapor plates were taken in an attempt to see whether absolute intensity measurements could be made on vapors using the same hydrogen arc source and the same plate calibration technique that we used for liquids. Ethylene has both narrow bands and a broad continuous absorption. Fortunately, the first strong narrow bands lie in the hydrogen continuum where their width and central intensity can be accurately measured (see Fig. 1); but below 1650A, where measurements must be made using the strong but randomly spaced hydrogen emission lines, the absorption is essentially continuous.[5]

In taking the plates, a few mm pressure of the vapor was placed in a small gas pipette and the vapor was then released from the pipette into the spectrograph. The relative volumes of the pipette and spectrograph were known and the pressure in the spectrograph (about 20 microns) could be computed from the perfect gas law. The light path in the apparatus was 34 cm.

At first there was difficulty in obtaining repro-

* This work was financed in part by the Office of Naval Research under T.O. IX of Contract N6ori-20 with the University of Chicago.
** Present Address: Division of Agricultural Biochemistry, University of Minnesota, St. Paul, Minnesota.
*** Present Address: Imperial Chemical Industries (Billingham Division), England.
[1] J. R. Platt and H. B. Klevens, Rev. Mod. Phys. **16**, 182, (1944).
[2] J. R. Platt, I. Rusoff, and H. B. Klevens, J. Chem. Phys. **11**, 535 (1943); I. Rusoff, J. R. Platt, H. B. Klevens, and G. O. Burr, J. Am. Chem. Soc. **67**, 673 (1945).
[3] W. C. Price and A. D. Walsh, Trans. Faraday Soc. **41**, 381 (1945).
[4] J. R. Platt, H. B. Klevens, and G. W. Schaeffer, J. Chem. Phys. **15**, 598 (1947).
[5] W. C. Price, Phys. Rev. **47**, 444 (1935); W. C. Price and W. T. Tutte, Proc. Roy. Soc. (London) **A174**, 207 (1940).

ducibility, apparently because of the absorption of the vapor by stopcock greases and vacuum wax. Differences between extinction values from different plates were as great as 50 percent. Later work showed that the absorption of diene vapors is reproducible with mean deviations of about 10 percent if Silicone stopcock grease is used,[6] and this procedure was followed in obtaining the curves given here. With our present pumping system, additional errors may arise from traces of residual oxygen in the spectrograph as we approach the strong oxygen peak at 1450A. Increased variations which we observed below 1550A are probably from this cause.

The difficulties with photo-decomposition of static vapors reported by earlier workers were not troublesome, probably because in our spectrograph only about 2 percent of the vapor is in front of the spectrograph slit, exposed to the direct light of the arc.

Corrections were made for the scattered background light in the spectrograph by taking one exposure through the ethylene vapor, two exposures for intensity calibration with the spectrograph pumped out and a final exposure with air in the spectrograph so that no wave-lengths below 1850A are present. In the last exposure, all the light which appears to be below 1850A must be scattered light of longer wave-lengths and its contributions can be measured at the same positions as those at which the ethylene vapor absorption is measured. Corrections for scattered light were also made in the solution studies by a similar method. These corrections become appreciable only below about 1800A where the continuum from the hydrogen arc is relatively weak.

SOURCE AND PURITY OF COMPOUNDS

Commercial tank ethylene was used for the ethylene vapor studies, for its absorption in this region is very intense and traces of impurities would not change the extinction values by more than the experimental error. The octene-1 and octene-2-*cis* and -*trans* were kindly supplied by Dr. W. Nudenberg. Their physical properties were:

Octene-1,	b.p. 120–121°C;	$n_D^{20}=1.4089$
Octene-2-*cis*,	b.p. 125–125.5°C;	$n_D^{20}=1.4146$
Octene-2-*trans*,	b.p. 124–124.5°C;	$n_D^{20}=1.4132$.

The cyclohexene was obtained from Eastman Kodak Company and was distilled twice through a Podbielniak column with 50 effective plates, using the center cut from each distillation. It has a boiling point of 83.0°C, $n_D^{20}=1.4452$.

The dihydropyrane was obtained from Dr. R. F. Nystrom and was fractionated and the center cut taken, with boiling point of 85°C, $n_D^{20}=1.4391$. After redistillation through the Podbielniak, an earlier sample of dihydropyrane had turned brown after standing a short while, so the later sample was run immediately after being put through the column and having its refractive index checked.

Octyne-1 and -2 were obtained from Dr. J. B. Jerome. Their properties were:

Octyne-1, b.p. 126.0°C, $n_D^{20}=1.4163$
Octyne-2, b.p. 138°C, $n_D^{20}=1.4761$.

TABLE I. Main features of spectra.

Compound		λmax.	νmax.	εmax.	width cm^{-1}	f-value
ethylene						
$N\rightarrow V$		1,625	61,500	15,000	5,200	.34 ±.15
Rydberg		1,743	57,360	5,500	~230	
		1,729	57,840	3,000	~230	.03 ±.01
		—				
		—				
octene-1		1,770	56,400	13,000	(5,200)	.29 ±.08
octene-2-*trans*		1,790	55,900	15,000	(5,200)	.34 ±.08
octene-2-*cis*		1,830	54,600	13,000	5,200	.29 ±.08
cyclohexene		1,820	54,900	6,600	8,100	.23 ±.05
2,3-dihydropyrane		1,950	51,280	3,800	9,600	.18 ±.04
octyne-1	A	—	—	—	—	—
	B	1,850?	54,000	2,200	(3,600)	.04 ±.02
	C	2,225	45,000	120	(4,800)	.003 ±.002
octyne-2	A	1,775	56,300	10,000	(5,800)	.22 ±.08
	B	1,960?	51,000	~2,000	(2,900)	.04 ±.02
	C	2,225	45,000	160	(4,800)	.003 ±.002

SPECTRA

The spectra of the olefins are shown in Fig. 1 and some main features of the spectra are summarized in Table I.

The strong allowed electronic transition in ethylene has been designated as the $N\rightarrow V$ transition by Mulliken and Rieke.[7] This continuum has its maximum in ethylene at about 1625A as shown in Fig. 1. The curve above 1550A represents the average of the two best plates. The measurements become unreliable below about 1550A where the prism and window materials and traces of oxygen in the spectrograph begin to absorb appreciably. Below this point, the curve can be estimated with the help of Price's reproductions[4] which indicate that the intensity must go nearly to zero at 1400A. This half-width of the $N\rightarrow V$ continuum is then about 5200 cm^{-1}, which is close to the half-width of the more accurately measured octene-2-*cis* peak at longer wave-lengths. The ϵ-value, or oscillator strength, of the ethylene in Table I was obtained from the area under the curve by the usual procedure. It must be regarded as uncertain to ±50 percent. An attempt will be made to improve this value using new techniques.

Superimposed on the $N\rightarrow V$ continuum is a doublet series of narrow line-like bands which are

[6] Lois E. Jacobs and J. R. Platt, J. Chem. Phys. **16**, 1137 (1948).

[7] See the bibliography in reference 1, especially R. S. Mulliken and C. A. Rieke, "Reports on Progress in Physics," Phys. Soc. (London) **8**, 231 1941; and R. S. Mulliken, Rev. Mod. Phys. **14**, 265 (1942).

believed to involve the first electronic state of a Rydberg series.[5,7] Previously it had not been known how strong the centers of these bands were, so that no estimate could be made of their oscillator strength relative to that of the continuum; it was feared they might be too narrow for accurate intensity measurements. Densitometer traces on the present vapor plates showed that the lines are quite broad, about 6A half-width, and so the intensity measurements are straightforward. Price found five doublets forming a vibrational series with the spacing of the C=C stretching frequency. Only two of the doublets could be measured accurately in our hydrogen continuum. The peak absorptions of the first pair are given in Table I. The second pair has about 0.8 the intensity of the first, if measured using the continuous absorption underneath as a base line. The second member of each doublet has about 0.6 the intensity of the first member. The other three doublets could not be clearly seen in the hydrogen many-line spectrum, but have been sketched in on the curve in Fig. 1 in the way suggested by Price's reproductions. Probably the total *f*-value of the group of five is three or four times the *f*-value of the first doublet, or about 0.03.

(It is possible, of course, that this figure is too low because of the presence of unresolved fine structure which will produce an apparent departure from the Lambert-Beer law. With the slits used, the spectrograph will resolve $\frac{1}{4}$A or about 10 cm^{-1} at these wave-lengths, which is too coarse for detecting the widest rotational structure in ethylene. On the other hand, the narrow bands are quite symmetrical and show no visible evidence of heads or of branch structure. This suggests that the component lines may be naturally broadened so as to wipe out such features, in which case the procedure used will give correct *f*-values.)

The octene-1 curve is shifted about 5000 cm^{-1} to the red from the ethylene vapor curve as the combined result of substitution and of solution. It is about 1100 cm^{-1} to the red of the propylene vapor curve maximum as given by Price and Tutte.[5] The peaks of octene-2-*cis* and of cyclohexene (which must have approximately a *cis* configuration) are at substantially longer wave-lengths than the octene-2-*trans* peak. The increased intensity in the octene-2-*trans* may account for the fact that its molar refractivity is higher than that of the *cis* in spite of its shorter wave-length peak. Its absorption to the red of 2100A is also higher than that of *cis*.[8] This *cis-trans* difference of about 1200 cm^{-1} in peak position is larger than that given by Price and Tutte[6] for the vapors. They find the cyclohexene vapor peak is only about 800 cm^{-1} to the red of the butene-2-*trans*. The order of the *cis-trans* peaks here agrees with the order of the ionization potentials found by Walsh[9] in *cis*- and *trans*-dichloroethylenes—which were 9.66 and 9.96 electron volts, respectively. However the sequence of his strong 1900A bands in these compounds was reversed from ours, possibly as a result of some interaction in the excited state between the two chlorines.

The octene-3 studied earlier[2] must have been about 70 percent *cis* judging by its curve shape and peak position. The present peak values are higher, partly because of the corrections applied here for scattering at the short wave-lengths.

The long wave-length tail on the octene spectra is much more pronounced than in ethylene and is quite probably due to the contributions of the first Rydberg states. Such long wave-length tails, or step-outs, in the vapors of substituted ethylenes have been discussed at some length in the literature.[1] Their effect on the "transmission limits" of these octenes has been examined in a recent paper,[8] which gives microphotometer traces showing the differences in absorption from 2050 to 2500A.

The peak intensity of cyclohexene is certainly significantly lower than that of the octenes. We examined the idea that this might be due to a twist of the double bond out of its planar configuration in order to adjust the angles in the rest of the molecule to more favorable values. Inspection of a Fisher-Hirschfelder atom model confirms the likelihood of a twist of this kind. A computation using the usual bond distances shows that distortions of at least three or four degrees in all C—C—C angles would be necessary if no twist is allowed about the double bond. No doubt some of this distortion will be relieved by a few degrees of twist, the exact amount depending on the relative force constants for angle bending and for twisting. (This treatment leaves out of account the hydrogen repulsions used by Pitzer to explain the non-planarity and thermodynamic properties of cyclopentane and cyclohexene in a recent preliminary note.[10] Such repulsions might either favor or suppress the twist, depending in a detailed way on the exact model chosen.) Lister[11] concluded from thermochemical evidence that the angle of twist was zero. If the intensity followed a cosine-square law with angle of twist about the double bond, such as we found for the bands of some orthosubstituted dimethyl anilines,[12] the ratio of the cyclohexene *f*-number to that of the octenes would indicate an effective angle of twist (averaged over thermal motions) of about 30°. This is so far from Lister's prediction that we must conclude either that the change of intensity

[8] H. B. Klevens and J. R. Platt, J. Am. Chem. Soc. **69**, 3055 (1947).

[9] A. D. Walsh, Trans. Faraday Soc. **41**, 35 (1945).

[10] K. S. Pitzer, Science **101**, 672 (1945).

[11] Lister, J. Am. Chem. Soc. **63**, 143 (1941).

[12] H. B. Klevens and J. R. Platt, J. Am. Chem. Soc. **71** (1949), in press.

is very much faster than the cosine-square law, which seems unlikely, or that the loss of intensity is largely due to some other cause.

If twist is present it should not only decrease the intensity but should also produce red shifts. Mulliken and Roothaan[13] predicted strong red shifts with increasing angle of twist in ethylene. This will account qualitatively for the broadening of the cyclohexene spectrum with almost unchanged position of the peak, if we assume that under thermal motions, some molecules are almost untwisted and given an octene-2-*cis* spectrum while others are twisted various amounts and give progressive red shifts, though with progressive loss of intensity. Quantitatively, the red shift on the long-wave edge of the peak of about 1000 cm^{-1} in going from octene-2-*cis* to cyclohexene would correspond to something like 8° angle of twist, judging from the theoretical estimates of Mulliken and Roothaan on ethylene. Of course the long wave-length tail on cyclohexene may equally well be due to displacement of the Rydberg bands in this molecule. At 2100A the cyclohexene absorption is about ten times that of octene-2-*cis*. The general decrease of intensity in cyclohexene accounts in part for its low molar refractivity relative to that of the noncyclic hexenes.

The 2,3-dihydropyrane is the same molecule as cyclohexene, except that a CH_2 group next to the double bond is replaced by an oxygen. Manipulation with a model suggests that the twist in this case should be less than that of the cyclohexene. The shift to long wave-lengths and the additional reduction of intensity must then be the result of the oxygen substitution, and resonance of the lone pair oxygen electrons with π electrons of the double bond. A similar shift occurs in vinyl chloride vapor whose peak is near 1830A as compared with 1730A for propylene vapor.[9]

The acetylene spectra are given in Fig. 2. The intensities are plotted on a log scale so as to show the relation of the bands found here to the bands of acetylene vapor itself. What appear to be corresponding bands are marked by the same letters, *A*, *B*, *C*, on the vapor and solution curves. The shaded vapor curve is estimated from data on appearance pressures and path lengths as reported in earlier acetylene vapor studies;[1] the values are uncertain by a factor of at least three. Nevertheless, there is clearly a red shift of some 5000 cm^{-1}

[13] See reference 5, also R. S. Mulliken, Rev. Mod. Phys. **14**, 265 (1942); R. S. Mulliken and C. C. J. Roothaan, Chem. Rev. 41, 219 (1947); also further unpublished calculations.

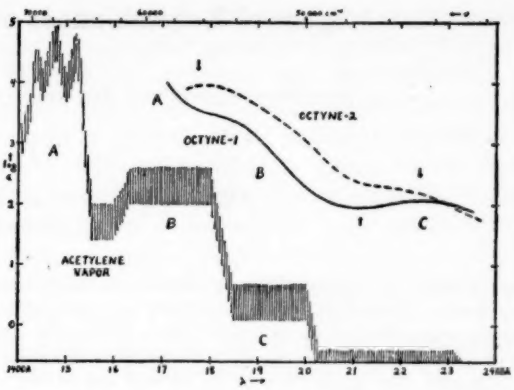

FIG. 2. Absorption of acetylenes.

in going from the simple vapor to the substituted compound in solution, just as was found with the ethylenes. Price and Walsh[3] found some 2000 cm^{-1} red shift in going from acetylene vapor to methylacetylene vapor.

The spectrum of octyne-1 does not go over any clear maximum before reaching 1700A but that of octyne-2 seems to do so. Very probably this maximum corresponds to the strong absorption in acetylene vapor at 1500A. The peak intensity seems to be less in the solution, but this may be because of the broadening effect of the solvent, since the vapor maxima are rather sharp. Since the measurements do not extend very far down over the peak on the short wave-length side, this uncertainty in the *f*-value is larger than the uncertainty in the intensity measurements; but the value appears to be about 0.27, not much different from that of ethylene.

The peaks or step-outs in the octynes near 2200A seem to be more intense than the 1900A bands in the vapor by a factor of 10. In this region, the absorption is weak enough to be much affected by impurities, but the two solution curves agree quite well with each other, and the uncertainty in the vapor estimates is of course large.

The red shift of 2500 cm^{-1} in going from octyne-1 to octyne-2 is almost twice as large as for the corresponding change in the ethylenes. It is associated with an increase in refractive index.

ACKNOWLEDGMENTS

We are grateful to Howard Carter, Dorothy Iker Lossy, Lois Jacobs, and Marvin Miller for technical assistance. We are indebted to the University of Michigan for the loan of the vacuum spectrograph used in this work.

THE JOURNAL OF CHEMICAL PHYSICS VOLUME 17, NUMBER 5 MAY, 1949

Spectral Resemblances of Cata-Condensed Hydrocarbons

H. B. KLEVENS
Division of Agricultural Biochemistry, University of Minnesota, St. Paul, Minnesota

AND

J. R. PLATT
Department of Physics, University of Chicago, Chicago, Illinois

(Received November 1, 1948)

The spectra of naphthalene, anthracene, naphthacene, phenanthrene, 1,2-benzanthrene, chrysene, and acenaphthene in *n*-heptane solution are extended to 1700A. Electronic energy levels of 17 such cata-condensed hydrocarbons are collected and compared. The lowest five or six excited states shift in a regular way with changes of molecular length and shape. Intensities and vibrational structures of corresponding bands are remarkably alike in the different compounds. The total oscillator strength is almost proportional to the number of π-electrons, but the proportionality constant differs from that in polyenes. With new identifications, the positions of energy levels in naphthalene, anthracene, and azulene agree remarkably well with previous LCAO molecular orbital calculations.

The lowest singlet state is of one type in benzene, naphthalene, and most non-linear systems; of another type in anthracene and the higher linear polyacenes because of a cross-over. This clears up some controversial questions, such as the relations among the spectra of naphthalene, anthracene, and phenanthrene.

I. PREVIOUS WORK

THE spectra of condensed ring systems have been investigated in the quartz ultraviolet[1,2] and Jones[3] has identified conjugation and steric effects, fine-structure changes and red shifts in the spectra resulting from different substitutions. The polarization of certain bands was used by Lewis and co-workers[4,5] and by Scheibe[6,7] in interpreting the effect of substitutions on the spectra of triphenylmethyl ions and dyes. The polarization was assumed to be along mutually perpendicular axes in the main plane of the molecule. In a long, narrow molecule, the longitudinal frequency would be lower than the transverse, just as in the analogous classical vibrations of a flat plate. Mulliken,[8] using LCAO (linear-combination-of-atomic-orbitals) molecular orbitals, showed theoretically that the longest wave-length transition in polyenes and similar compounds must be polarized approximately along the long axis, and shorter wave-length transitions will be polarized, some along the long axis and some along a transverse axis; and he explained intensity changes in *cis-trans*- isomerism. Zechmeister[9] applied these ideas to the changes in spectra accompanying isomerism in carotenoids.

Jones,[10] in a comprehensive review, favored extending the conclusions of Lewis and co-workers to the condensed ring systems. He showed that the first band of anthracene was probably transversely polarized, the second longitudinally. Coulson,[11] applying the LCAO method to the polyacenes or linear polycyclics, confirmed Jones' assignment. The longest wave-length absorption bands (26,000 cm^{-1} in anthracene) are from a transition of symmetry $A_{1g}-B_{2u}$, polarized across the width of the molecule. Coulson assigns the second band to a transition $A_{1g}-B_{1u}$, polarized along the length of the molecule. His intensity predictions were not so successful. Recently, Wheland and Mann[12] in calculating the expected dipole moments for azulene and fulvene, have shown that results based on Coulson's simplifying assumptions are in poor agreement with the experimental dipole moments of these molecules or with the results of more refined calculations. However, dipole moments, like intensities, are more sensitive to the accuracy of the wave-functions than energy levels. We shall show below that Coulson's LCAO computations made including overlap integrals, on the height of the states of polyacenes, and other similar calculations on azulene, an isomer of naphthalene,[13] give quite good agreement with the height of levels determined from the spectra (Fig. 4).

Sponer[14] has compared the HLSP method and the molecular orbital method of calculating levels, and has made calculations for the non-linear condensed ring systems, phenanthrene, 3,4-benzophenanthrene, 1,2-benzanthracene, chrysene, pyrene, and triphenylene, similar to those of Förster[15] on the

[1] See R. N. Jones, Chem. Rev. **32**, 1 (1943) for recent review.
[2] E. Clar, *Aromatische Kohlenwasserstoffe* (Verlag. Julius Springer, Berlin, 1941).
[3] R. N. Jones, J. Am. Chem. Soc. **67**, 2127 (1945).
[4] G. N. Lewis and J. Bigeleisen, J. Am. Chem. Soc. **65**, 520, 2102, 2107 (1943).
[5] G. N. Lewis and M. Calvin, Chem. Rev. **25**, 273 (1939).
[6] G. Scheibe, Kolloid Zeits. **82**, 1 (1938).
[7] G. Scheibe, Zeits. f. angew. Chem. **42**, 631 (1939).
[8] R. S. Mulliken, J. Chem. Phys. **7**, 364 (1939).
[9] L. Zechmeister, Chem. Rev. **34**, 207 (1944).
[10] R. N. Jones, Chem. Rev. **41**, 353 (1947).
[11] C. A. Coulson, Proc. Phys. Soc. **60**, 257 (1948).
[12] G. W. Wheland and D. E. Mann, J. Chem. Phys. **17**, 264 (1949).
[13] D. E. Mann, J. R. Platt, and H. B. Klevens, J. Chem. Phys. **17**, 481 (1949).
[14] H. Sponer and G. Nordheim, "Theoretical Studies on the Electronic Levels of Polynuclear Hydrocarbons," ONR Contract N6ori-107, T.O.1, Annual Report, June 1, 1948.
[15] Th. Förster, Zeits. f. physik. Chemie **B41**, 287 (1938).

lowest electronic singlet levels of the polyacenes. Förster and Sponer both took into account only the unexcited valence-bond structures.

Daudel and Pullman[16] and others of their school have modified the valence-bond method to what they term the "molecular diagram" method and applied it to anthracene and naphthacene by inclusion of polyexcited structures in their calculations.

Craig[17] has made new calculations of the long wave-length absorption bands in aromatic molecules, similar to those of Sklar[18] and Förster,[19] and has discussed assignments and polarizations.

There has been some confusion of assignments and of interpretations by different authors, and ignorance of weak bands and of higher levels. The spectra given here and the systematic correlation of energy levels shown in Figs. 4–7 may help to clear up some of these difficulties. To describe the regularities found here, a new system of naming the levels of many aromatics is proposed. This scheme is based on the free-electron metallic model used by Pauling,[20] Lonsdale,[21] Schmidt,[22] Bayliss,[23] Kuhn,[24, 24a] and others to interpret the diamagnetism and electronic spectra of various conjugated systems. It enables us to give the same names to corresponding states in different molecules. These names will be used in the present paper. Description of the properties each name connotes and justification of its assignment to a particular observed sequence of states in the different compounds will be found in the following paper (hereafter called II).[25]

A comparison is made in Table I of the names used in this system and those used in previous papers to describe the states and bands of individual molecules. The polarizations listed are those inferred from the free-electron model.

II. SPECTRA

The spectra of a series of condensed ring compounds, naphthalene, anthracene, naphthacene,

TABLE I. Correspondence between names of states used by different authors.

Jones (Names of bands)		Coulson				Symmetry species				Polarization*	
Anthracene	1,2-benzanthracene	Naphthalene		Anthracene		Benzene	Naphthalene, anthracene	Proposed		Anthracene	Phenanthrene
		N		N		$^1A_{1g}$	$^1A_{1g}$	$-+f^4$	^1A		
		P_2R_2		Q_2S_2		E_{1u}	B_{2u}	$--f^3g$	B_a	trans. strong	trans. allowed
$A-B$	$A-D$	S_1R_2	V_4	R_2S_2		E_{1u}	B_{1u}		B_b	long. strong	long. allowed
	$J-K$	P_2Q_2	V_2	Q_2P_3	V_2	B_{2u}	B_{1u}		L_b	long.	trans. very weak
$C-H$	$F-I'$	S_1Q_2	V_1	R_2P_3	V_1	B_{1u}	B_{2u}		L_a	trans.	long. very weak
		Q_1R_2		P_2S_2				$--e^2f^4g$	C_a	forb.	long. strong
		R_1R_2		S_1S_2					C_b	forb.	trans. strong
		Q_1Q_2	V_5	P_2P_3	V_5		A_{1g}		K_b	forb.	long. very weak
		R_1Q_2	V_3	S_1P_3	V_3		B_{3g}		K_a	forb.	trans. very weak
		P_1Q_2		Q_1P_3				$--d^3e^4f^4g$	J_b	long.	trans. very weak
				R_1P_3	V_4		B_{2u}		J_a	trans.	long. very weak

* trans: transverse is equivalent to along the short axis; long: longitudinal is equivalent to along the long axis; forb: forbidden.

[16] For references to this work, see: P. Daudel and R. Daudel, J. Chem. Phys. **16**, 639 (1948).
[17] D. P. Craig, Nature **158**, 235 (1946).
[18] A. L. Sklar, J. Chem. Phys. **5**, 669 (1937).
[19] Th. Förster, Zeits. f. Elektrochemie **45**, 548 (1939).
[20] L. Pauling, J. Chem. Phys. **4**, 673 (1936).
[21] K. Lonsdale, Proc. Roy. Soc. (London) **159A**, 149 (1937).
[22] O. Schmidt, Zeits. f. physik. Chemie **39B**, 59 (1938); **42B**, 83 (1939); **44B**, 185, 194 (1939); **47B**, 1 (1940).
[23] N. S. Bayliss, J. Chem. Phys. **16**, 287 (1948).
[24] H. Kuhn, J. Chem. Phys. **16**, 840 (1948); Helv. Chim. Acta **31**, 1441 (1948).
[24a] W. Kuhn, Helv. Chim. Acta **31**, 1780 (1948).
[25] J. R. Platt, J. Chem. Phys. **17**, 484 (1949).

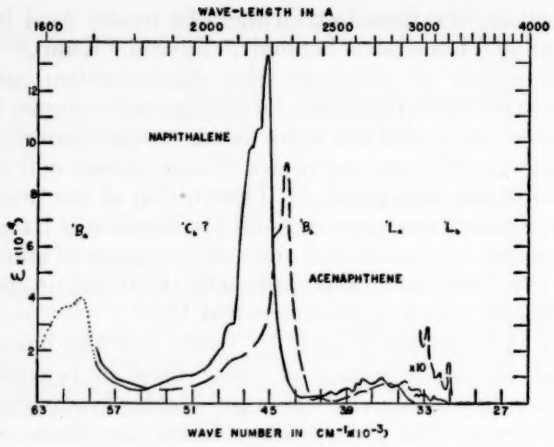

FIG. 1. Spectra of naphthalene and acenaphthene.

phenanthrene, 1,2-benzanthracene, chrysene and acenaphthene, were measured in *n*-heptane solution in an 0.13-mm lithium fluoride cell in the region 1700–2500A. These are all cata-condensed hydrocarbons, general formula $C_{4n+2}H_{2n+4}$, in which no carbon atom is shared by more than two rings. The significance of this in simplifying interpretation of the spectra will be discussed in II. The spectrograph used was a Cario-Schmitt-Ott vacuum fluorite instrument on loan from the University of Michigan. The experimental techniques used were similar to those described previously.[26,27] All the compounds, with the exception of naphthacene, were kindly given to us by Dr. R. N. Jones and had been purified for his studies by chromatographic adsorption. The naphthalene, anthracene, and phenanthrene were the most highly purified. Possible impurities in the other compounds range up to about 1 percent. The naphthacene (tetracene) was obtained from Dr. C. F. H. Allen and had been purified by repeated crystallization from benzene solution in a nitrogen atmosphere. It was kept in a nitrogen atmosphere while its spectrum was being run. Naphthacene dissolved and run in the presence of air showed strong new bands, which probably represent decomposition products. The intensity measurements are believed to be accurate to our usual figure of about ±10 percent, except for naphthacene. Its low solubility caused difficulty in weighing, and the uncertainty in its curve may be ±50 percent.

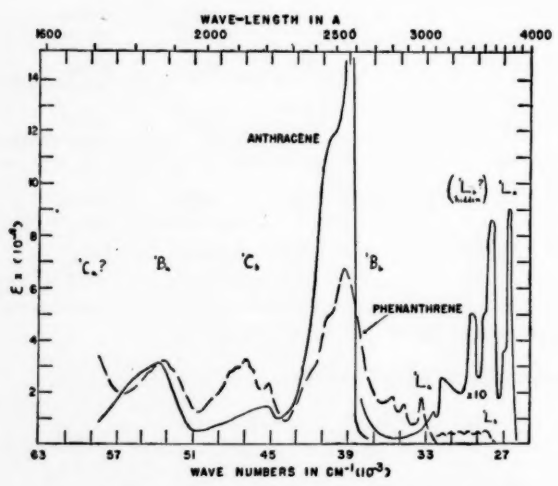

FIG. 2. Spectra of anthracene and phenanthrene.

The spectra are shown in Figs. 1–3 and some main features, such as location of main bands and components, ϵ_{max}, and oscillator strength, f, are summarized in Table II. The curves at longer wavelengths have been taken from various sources. In all cases, the curves in the overlap region, 2250–2500A, were in agreement within experimental accuracy. The naphthalene and anthracene long wave spectra are from Mayneord and Roe;[28] phenanthrene, 1,2-benzanthracene, chrysene, and acenaphthene from Jones.[10,29] The 3,4-benzanthracene data in Figs. 4–6 are from Mayneord and Roe;[30] triphenylene and the 5-ring data from Clar;[2] and the phosphorescent triplet levels are from Kasha.[31] The curve of naphthalene above 58,000 cm^{-1} is from visual estimates on an unpublished vapor spectrum plate taken by Dr. W. C. Price in this laboratory. The azulene data (Fig. 4) are from Mann, Platt, and Klevens.[13]

In Figs. 4–6, the excited electronic energy levels from these cata-condensed ring spectra are plotted for comparison with each other. The vibrational structure has been omitted for clearness.

Naphthalene-Acenaphthene

Acenaphthene is essentially a disubstituted naphthalene and has a spectrum similar to naphthalene (Fig. 1) except for about 1800 cm^{-1} red shift. The ^1C_b transition seems to be weaker or has shifted its relative position in the acenaphthene. [Since the ground state is always the same, we may designate a band after its upper state alone.] If this peak in naphthalene is the forbidden transition it is assumed to be in II, it should be somewhat more allowed in acenaphthene, though the effect of alkyl substitution on forbidden band intensities is often surprisingly small, as the benzene 2600A bands have shown.

Anthracene-Phenanthrene

The spectrum of anthracene in Fig. 2 looks much like the spectrum of naphthalene except for a red

[26] J. R. Platt and H. B. Klevens, Chem. Rev. **41**, 301 (1947).
[27] H. B. Klevens and J. R. Platt, J. Am. Chem. Soc. **69**, 3055 (1947).
[28] W. V. Mayneord and E. M. F. Roe, Proc. Roy. Soc. (London) **152A**, 299 (1935).
[29] R. N. Jones, J. Am. Chem. Soc. **67**, 2127 (1945).
[30] W. V. Mayneord and E. M. F. Roe, Proc. Roy. Soc. (London) **158A**, 634 (1937).
[31] M. Kasha, Chem. Rev. **41**, 401 (1947).

shift of about 5500 cm^{-1}. Also the very weak and sharp longest wave-length bands, ^1L_b, in naphthalene have disappeared. The red shift is probably due to a reduction of ionization potential by about the same amount.[31a] The location of the strongest, or ^1B_b, peaks in the other compounds will probably be correlated with ionization potential in the same way.

In phenanthrene the strong bands have about the same positions as in anthracene, but large differences in intensity. We believe ^1B_b becomes weaker because of the reduction of effective length; ^1C_b becomes stronger and allowed because of the loss of central symmetry, and should be polarized along the phenanthrene symmetry axis. Total f-values up to the limit of measurements seem to decrease as much as 0.5 in going from linear to non-linear isomers. In phenanthrene, this apparent loss may be partly due to the presence of an unobserved band of ^1C_a type at shorter wave-lengths.

The weak ^1L_b transition reappears in phenanthrene at longest wave-lengths, about 28,000 cm^{-1}; while ^1L_a has shifted from 26,000 cm^{-1} in anthracene to 33,000 cm^{-1} in phenanthrene. It seems a reasonable supposition that a band of ^1L_b type, like those in benzene and naphthalene (Fig. 4), is also present in anthracene at about 28,000 cm^{-1}, as extrapolation from benzene and naphthalene would indicate; but that it is hidden in anthracene by the stronger ^1L_a band, and becomes revealed at nearly the same location in phenanthrene when the ^1L_a band moves upward. This possibility was suggested by Sponer.[14] Further extrapolation of ^1L_b in polyacenes leads to another hidden band in naphthacene, but predicts a band near 23,000 cm^{-1} in pentacene, well above the ^1L_a. A weak band with sharp structure of the ^1L_b type is indeed found in Clar's pentacene curve[2] (Fig. 4), at just this place. It is still present at about the same place in very bent 5-ring systems (Fig. 7) when ^1L_a has again moved above it. The obvious conclusion is that bands of these two types, ^1L_a and ^1L_b, occur at the longest wave-lengths in every catacondensed system; but that in the polyacenes the curves of their position as a function of length cross between naphthalene and anthracene.

The ^3L_a state also moves upward 7000 cm^{-1} in phenanthrene. This motion parallels that of ^1L_a but not of ^1L_b and is a major reason for believing the phosphorescent state is of L_a type. The singlet-triplet separation should be roughly constant with changing molecular size or at least should vary in a regular way. From Fig. 4 it is seen that the phosphorescent state is 19,000 cm^{-1} below ^1L_a in benzene, 14,000 cm^{-1} in naphthalene, and 12,000 cm^{-1} in the longer systems. It has no such regular relation to ^1L_b; so again must be ^3L_a. The symmetry species of

[31a] W. C. Price, Chem. Rev. 41, 257 (1947).

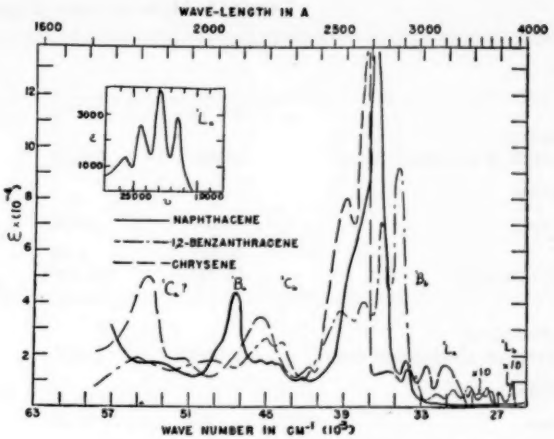

FIG. 3. Spectra of 4-ring aromatics.

the phosphorescent state in benzene, which has been in doubt, is correspondingly strongly indicated to be $^3B_{1u}$ according to these arguments. (See II.)

Kasha[31] tabulated the fluorescent-phosphorescent level separation in many compounds, and found strange variations in this separation, which he expected to be the singlet-triplet interval and therefore roughly constant. The explanation of his variations is seen in Fig. 4. The fluorescent level is the lowest singlet; but it is sometimes ^1L_a, the same type as the triplet, as in anthracene; and other times it is ^1L_b, as in phenanthrene, and gives an abnormally small fluorescent phosphorescent interval.*

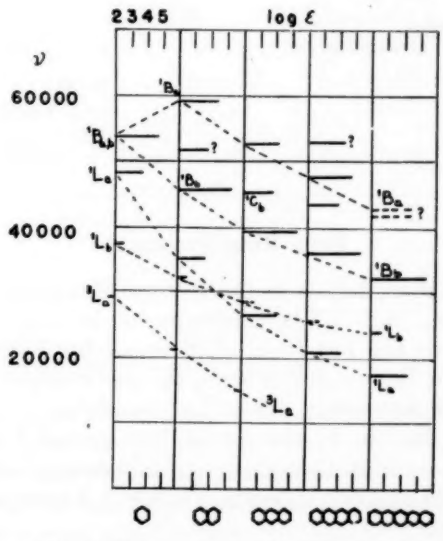

FIG. 4. Energy levels of polyacenes.†

† *Note on Figs. 4–7.* Lowest vibrational level shown. Remaining structure of each electronic band omitted for clearness. Length of horizontal lines indicates logϵ_{max} of transition from ground state on scale at top of figures. Lines for triplets drawn to left to indicate logϵ_{max} is less than 2. See note at end for additional triplet states.

* After the text of the present paper was prepared, M. Kasha and R. V. Nauman kindly let us see a prepublication copy of their manuscript "The Metastability of the Lowest

TABLE II. Main features of spectra of *cata*-condensed hydrocarbons.

	$^1A-{}^1L_b$	$^1A-{}^1L_a$	$^1A-{}^1B_b$	$^1A-{}^1C_b$	$^1A-{}^1B_a$	$^1A-{}^1C_a$	Total f-value
Benzene							
onset of absorption cm^{-1}	38000	48050					
peak			54500				
ϵ_{max}	220	6900	4600				
f	0.002	0.10	0.69				0.79
(to cut-off)	(45300)	(51200)	(59000)				
Naphthalene							
onset of absorption cm^{-1}	32000	34600					
peak			45400	52500?	~59800		
ϵ_{max}	280	9300	133000	10000	~30000		
f	0.002	0.18?	1.70	0.20	~0.6?		~2.8
(to cut-off)	(34000)	(42500)	(49500)	(55000)	(63000)		
Acenaphthene							
onset of absorption cm^{-1}	29800	33100			52700		
peak			43800				
ϵ_{max}	2800	7100	93000		~35000		
f	0.012	0.14	1.08		0.28		1.51
(to cut-off)	(33100)	(41500)	(52700)		(59500)		
Anthracene							
onset of absorption cm^{-1}		26400					
peak			39000	45300	53700		
ϵ_{max}		9000	180000	14500	32000		
f		0.10	2.28	0.28	0.65		3.31
(to cut-off)		(35000)	(44400)	(50800)	(59300)		
Naphthacene						unknown transition 55500	
onset of absorption cm^{-1}		21100		43500			
peak			36700		47400	53400	
ϵ_{max}		12500	180000	17000	44000	16000	40000
f		0.08	1.85	0.28	0.45	0.27	0.68	3.53
(to cut-off)		(29200)	(43000)	(46000)	(50500)	(54800)	(59500)	

Four-Ring Systems

The strong bands in the spectra of naphthacene, chrysene, and 1,2-benzanthracene in Fig. 3 are shifted to the red from anthracene by 2000–4000 cm^{-1}, the largest shifts being for the straight molecule, naphthacene. The ^1L_b transition is again masked by ^1L_a in the linear, but revealed in the bent, molecules. Generally, ^1L_a moves upward with increased number of bends. Thus in 1,2-benzanthracene it is shifted 8500 cm^{-1} to the blue, in 3,4-benzphenanthrene 9500 cm^{-1}, in chrysene 10,500 cm^{-1} and in triphenylene 14,000 cm^{-1} from its position in naphthacene.

Behavior of Bands

We may comment on some general trends observed with particular types of bands in moving from compound to compound.

^1L_b

The ^1L_b state moves the slowest with increasing chain length. It is little affected in position or intensity by rearrangements and substitutions within any family of compounds of the same number of π-electrons. The stability of location of this band in benzene with various substitutions has been repeatedly remarked in the literature. The greatest

Excited Singlet Level of Naphthalene," in which they prove Sponer's suggestion (see reference 14), which we have used here, that the long wave absorption of naphthalene consists of two electronic transitions. It is especially interesting that they report that the fluorescent state has similar properties—a long lifetime, near 10^{-6} second, and a motion upwards in low temperature rigid glass systems—in naphthalene, phenanthrene, and chrysene, where we have called the lowest singlet state ^1L_b; but that it has opposite properties—a short lifetime and a motion downwards in the glass—in anthracene, where this state is ^1L_a.

TABLE II.—*Continued.*

	$^1A-{}^1L_b$	$^1A-{}^1L_a$	$^1A-{}^1B_b$	$^1A-{}^1C_b$	$^1A-{}^1B_a$	$^1A-{}^1C_a$	Total *f*-value
Pentacene							
onset of absorption cm^{-1}		17100					
peak	24000		32300				
ϵ_{max}	600	12000	300000				
f		0.08	2.2				
(to cut-off)		(23600)	(40000)				2.28
Phenanthrene							
onset of absorption cm^{-1}	28300	33000				56400	
peak			39400	47100	53400		
ϵ_{max}	350	16000	65500	33000	31000		
f	0.003	0.18	1.09	0.60	0.59	0.29	
(to cut-off)	(32300)	(36300)	(44000)	(50800)	(56400)	(59500)	2.75
Chrysene							
onset of absorption cm^{-1}	27500	30200					
peak			37200	45600	51300	54300	
ϵ_{max}	650	16000	150000	34500	18500	50000	
f	0.005	0.36	1.29	0.69	0.22	0.76	
(to cut-off)	(29500)	(36700)	(41300)	(49300)	(52600)	(61000)	3.32
1,2-benzanthracene							
onset of absorption cm^{-1}	25800	27300					
peak			34800	45100	49300	54900	
ϵ_{max}	1000	8500	113000	33000	21000	23000	
f	0.003	0.13	1.67	0.53	0.42	0.54	
(to cut-off)	(27000)	(33600)	(42200)	(47300)	(52600)	(61000)	3.29
3,4-benzphenanthrene							
onset of absorption cm^{-1}	26700	30300					
peak			35600	45600			
ϵ_{max}	400	12000	85000	55000			
f	0.0056	0.12	1.57	1.38			
(to cut-off)	(28900)	(34000)	(42000)	(51000)			3.08
Triphenylene							
onset of absorption cm^{-1}	29200	33200					
peak			38900				
ϵ_{max}	900	20000	150000				
f	0.012	0.22	2.26				
(to cut-off)	(32300)	(36500)	(45000)				2.49

shift of ^1L_b in the levels of Figs. 4 to 6 is a red shift of 17,000 cm^{-1} found in going from the normal ring system naphthalene to its abnormal isomer, azulene, which has one 5-carbon and one 7-carbon ring; the shift accounts for the blue color of azulene. But azulene is quite a special case.

The arguments in II indicate a polarization for ^1L_b longitudinal in the polyacenes, but parallel to the symmetry axis in phenanthrene.

^1L_a

This band moves to the red the fastest with increasing length, and its interval from ^1B_b increases at the same time. The interval decreases by more than 50 percent for the first bend in the molecule, but changes little with further bending.

Jones[10] showed that the intensity of the ^1L_a band in polyacenes was increased by substitutions which increased the molecular width, and concluded that this band must be transversely polarized. This is supported by Coulson's calculations[11] and by the arguments of II. In phenanthrene it should be polarized perpendicular to the symmetry axis.

Since the position of the ^1L_a band is sensitive to bending of the molecule, and since the strong carcinogens are bent, we examined whether the ^1L_a

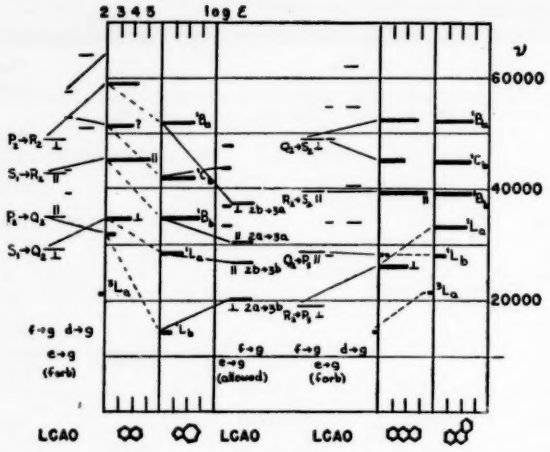

FIG. 5. Energy levels of naphthalene and azulene, anthracene and phenanthrene, with LCAO-predictions of centers-of-gravity of singlets and triplets.†

position was better correlated with carcinogenic potency of alkyl-substituted 1,2-benzanthracenes than the position of the ^1B_b band used by Jones for such a correlation.[32] We found that the wave-length of the peak ^1L_a vibration, which is given by Jones, does change nearly twice as fast with potency as the wave-length of the ^1B_b peak. But the exceptions to his correlation which Jones found remain exceptions to the ^1L_a correlation. They still remain exceptions when differences between the two bands are used for the correlation. The location of particular peaks of ^1L_a, including the first, is not so unambiguous as the location of ^1B_b.

^1B_b

The ^1B_b band increases in intensity almost linearly with increase in length, like the corresponding strong transition in the polyenes. This band must then be longitudinally polarized. Jones' work[10] confirms this. Coulson concluded this was the lowest longitudinal transition in anthracene and applied his calculations to it; but as we have seen above, the hidden ^1L_b band, if it is longitudinally polarized in polyacenes, as we suppose, must be the lowest of this type; and ^1B_b must be the second longitudinal band.

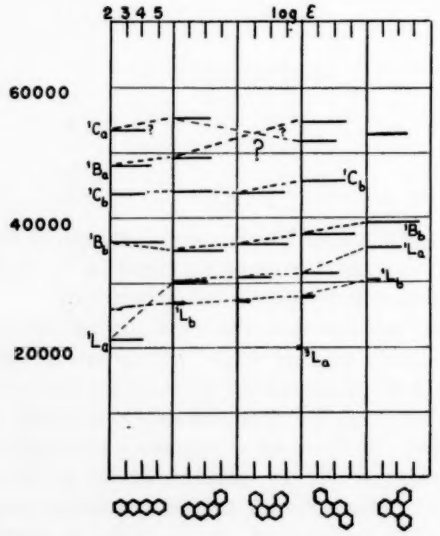

FIG. 6. Energy levels of 4-ring aromatics.†

[32] R. N. Jones, J. Am. Chem. Soc. **62**, 148 (1940).

^1C_b

The ^1C_b band which appears weakly in the polyacenes may be forbidden in them, according to II. It always increases in strength with destruction of central symmetry of the conjugated system. However, according to this argument, one would expect it to be stronger than it seems to be in acenaphthene, and weaker than it appears in chrysene, which is centrally symmetric again. Some of the discrepancy might be due to experimental error; or possibly the ^1C_b band has shifted in acenaphthene, or it may be misidentified in chrysene.

^1B_a

The ^1B_a band has almost constant intensity in polyacenes, and is taken to be due to an allowed transition polarized transverse to the long axis of the molecule. The intensity increases in some bent systems, presumably because the molecule is wider and the effective transverse dipole length has increased.

The ^1B_a and ^1B_b states should form a degenerate pair in benzene if they have the properties postulated in II and if they have been correctly identified in the spectra. Only one band is observed. The same should be true in any molecule with D_{3h} symmetry or higher. Triphenylene is such a molecule. A band has been observed in its spectrum at about 1900A[33] but this may be a ^1C band.

III. INDIVIDUALITY OF LEVELS

The preceding discussion has imputed distinct properties to levels of a given type, which they retain from compound to compound and which make possible unambiguous identification according to type. That states in compounds so diverse as benzene and benzanthracene should have so much in common seems to be a novel idea. To date, theory has offered no prediction of such a result, and indeed has sometimes denied the likelihood of it. We should therefore state this doctrine of types explicitly and summarize the evidence for it.

1. *Levels of a given type have unambiguous identifying characteristics*, which do not change from compound to compound. The most useful characteristics

[33] H. Mohler and J. Sorge, Helv. Chim. Acta **22**, 229 (1939).

are intensity and vibrational sharpness of the transition from the ground state to the level in question.

The intensities of the ^1L_b, ^1L_a, and ^1B_b bands are shown in Fig. 8 for all the cata-condensed systems of four rings or less. *There is no mixing or confusion of properties.* The ^1B_b bands vary in oscillator strength by a factor of two; but they are separated by a factor of ten from the ^1L_a oscillator strengths. In these compounds and among the longer wave-length bands there are no bands with oscillator strengths between these two groups. Similarly the ^1L_a bands vary in strength by a factor of four; but are two orders of magnitude stronger than ^1L_b, and there are no bands of intermediate strength. The ^1L_b strengths vary over a factor of ten, but there is no ambiguity as to type. The variability of intensities, increasing with increasing molecular size, shows that these rules are only first approximations; with seven- or eight-ring systems, the ranges of variability will begin to overlap as shown by the trends in Fig. 8, and doubtful assignments may occur. As might be expected, the variability produced by mixing affects the relative intensity of the weak bands more than that of the strong ones.

The case is the same with vibrational structure.

The ^1L_b bands have sharp vibrational structure, with individual vibrational peaks about 300 cm^{-1} in half-width. There are 5 or 6 visible peaks when not overlapped, the strongest one commonly the first or third.

The ^1L_a bands have more diffuse vibrational structure, with peaks about 500 cm^{-1} in half-width, but still with distinct maxima and minima. There are usually 5 or 6 visible peaks, the first, second or third the strongest. It is most remarkable that these same ^1L_b, ^1L_a distinctions are found in benzene[26] whose high symmetry is usually supposed to make it a special case.

The ^1B_b band is the strongest in each spectrum. The vibrational structure is still more diffuse so that often no clear minima can be seen, but only step-outs. After naphthalene, the first peak is narrow and much the strongest, and only two or three others can be seen.

The second strongest band is ^1B_a. It is broad and almost symmetrical and shows little structure.

These rules become less accurate for the larger and more unsymmetrical systems.

2. *Levels of a given type move in a systematic way* from compound to compound. Except for the $^1L_a-{}^1L_b$ crossover near anthracene, and the $^1C_b-{}^1B_a$ crossover which seems to occur near pentacene, the levels preserve their sequence in each compound. They all lie on smooth curves as a function of length, except for ^1L_a in bent systems. They generally lie near the same energy in isomers. Except for ^1L_a and except for the special case of azulene, levels of a given type in isomers all lie in a region only about 4000 cm^{-1} wide.

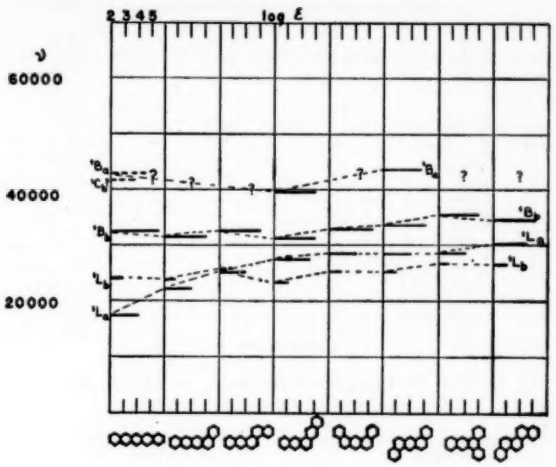

FIG. 7. Energy levels of 5-ring aromatics.†

The ^1L_a position is variable, but in a regular way. It moves upward with increased bending of the molecule. The $^1L_a-{}^3L_a$ separation changes smoothly with length, and is not changed in bent isomers even when both levels move far.

3. (a) *Each type, as determined from appearance and intensity alone, occurs once and only once in each compound.*

(b) *The number of lower levels remains constant* from compound to compound up to any particular upper level to which the spectra have been carried. There are a few reasonable exceptions, where degeneracies occur, or where a weak band is expected to be overlapped by a stronger and its upper state cannot be located accurately.

These rules should pretty well remove fears which have been expressed in the past that these spectra

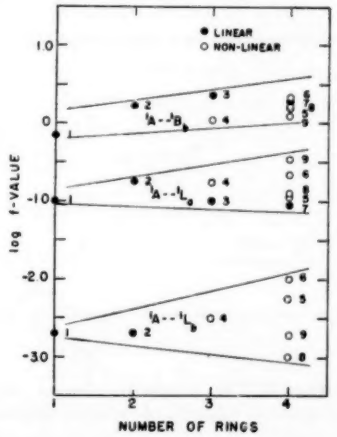

FIG. 8. Constancy of intensities in different band types.

Compounds:
1. benzene
2. naphthalene
3. anthracene
4. phenanthrene
5. 3,4-benzphenanthrene
6. triphenylene
7. naphthacene
8. 1,2-benzanthracene
9. chrysene

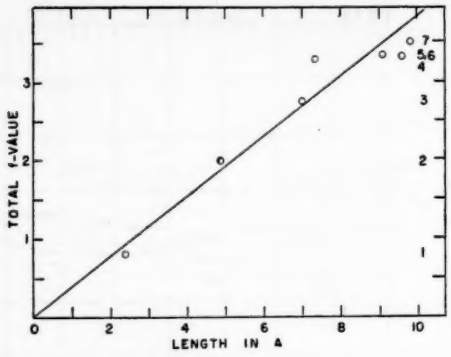

FIG. 9. Integrated intensity to 1700A as function of molecular length.

Compounds:
1. benzene
2. naphthalene
3. phenanthrene
4. anthracene
5. chrysene
6. 1,2-benzanthracene
7. tetracene

might never be understood because of their complexity, the breadth of the peaks and bands, and the numerous weak transitions which might be hidden by stronger transitions and never located. When the vibrational structure is ignored, only 4 to 6 electronic bands are found, as far as the spectra have been carried. Though they are broad, they are usually well separated. The three or four other singlet bands which might lie in this region are expected to be weak and therefore hidden, but their positions can be estimated from LCAO theory as seen below.

IV. OTHER REGULARITIES

Some other regularities discovered in the data are shown in Figs. 9 and 10 and in Table III. Figure 9 shows that the total oscillator strength, f, summed over all the bands up to the highest limits so far reached, is closely proportional to the greatest length of the conjugated system. Reasons are given

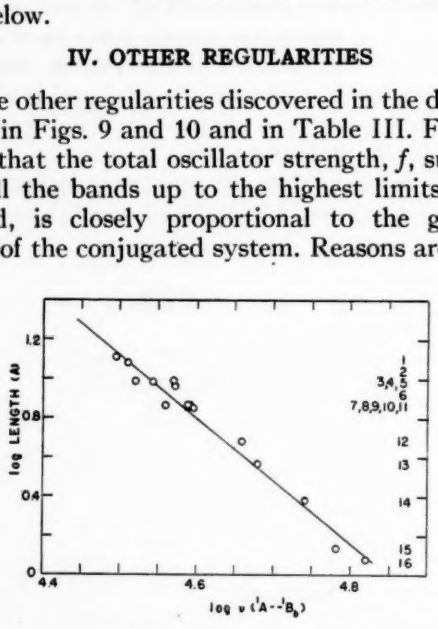

FIG. 10. Location of ^1B_b bands in chains, ring-chains and condensed rings as a function of greatest molecular length.

Compounds:
1. decapentaene
2. pentacene
3. octatetraene
4. 1,2-benzanthracene
5. tetracene
6. chrysene
7. 3,4-benzanthracene
8. anthracene
9. hexatriene
10. phenanthrene
11. triphenylene
12. naphthalene
13. butadiene
14. benzene
15. ethylene
16. acetylene

in II for believing that very little additional oscillator strength in π-electron transitions will lie at shorter wave-lengths. The molecular lengths were determined from scale drawings, using hexagonal rings, with 1.40A as the C−C distance. Some shorter "effective length" would be more suitable for the comparison, but it would not be so simple to determine its proper value in bent systems.

That total f is proportional to length in these compounds is not greatly different from saying that it is proportional to number of rings, or, what is the same thing, proportional to number of π-electrons. The mean contribution to f per π-electron is tabulated in Table III. It is seen to be nearly constant, between 0.19 and 0.23, for two-, three-, and four-ring systems. The benzene value is low. In polyene chains, the f-value per unit length is about $\frac{1}{4}$ that in condensed rings. The f-value per π-electron is between 0.11 and 0.14, which is about $\frac{1}{2}$ of its value in rings. The value for ethylene is higher, but is uncertain by ± 50 percent. Systems containing both rings and chains seem to have intermediate values of the contribution per π-electron, in proportion to the relative lengths of the chain and ring sections. The data in Table III is obtained in part from spectra reported here and from some unpublished data[34] except for the symmetric cyanine data which has been calculated from spectra reported by Brooker.[35] The spectra of the chains and ring-chains need to be extended to shorter wave-lengths before making a final comparison of the intensity contributions per π-electron.

The linear relation between the height and f-value of the first strong peak, $N-V_1$ (in our notation, $^1A-{}^1B_b$), in polyenes and the molecular length was found by Hausser, Smakula and co-workers,[36–38] and is in agreement with theoretical calculations of Mulliken.[39,40] Coulson[11] expected the longitudinal transitions in polyacenes, our $^1A-{}^1L_b$ and $^1A-{}^1B_b$, to have intensities proportional to the length. This result is approximately confirmed experimentally for $^1A-{}^1B_b$. Since these strong transitions in the straight polyenes and polyacenes have most of the oscillator strength, the total strength summed over all bands will also vary in much the same way with length. This result should then apply also to bent systems, for the strength which the strongest transition loses in these cases is gained by others, so that the total remains about constant. Actually, the total f-value is more accurately linear with length than

[34] Unpublished work of the authors.
[35] L. G. Brooker, Rev. Mod. Phys. **14**, 275 (1942).
[36] K. W. Hausser, Zeits. f. tech. Physik **15**, 10 (1934).
[37] A. Smakula, Zeits. f. angew. Chemie **47**, 657 (1934).
[38] K. W. Hausser, R. Kuhn and others, Zeits. f. physik. Chemie **29B**, 364 (1935).
[39] R. S. Mulliken, J. Chem. Phys. **7**, 364, 570 (1939).
[40] R. S. Mulliken and C. A. Rieke, Rep. Prog. Phys. **8**, 231 (1941).

the f-value of the $^1A-{}^1B_b$ transition alone even for the straight polyacenes. The longitudinal $^1A-{}^1L_b$ transition intensity seems to show no special dependence on length, but in the longer molecules our observation of it is restricted to bent systems, where interaction may alter intensities in an irregular way.

Figure 10 shows the dependence of the frequency of the first strong allowed longitudinal transition, $^1A-{}^1B_b$, on the greatest length of the conjugated system. Both polyenes and ring systems are included. The frequency is seen to vary approximately as the inverse 0.3 power of the length. The correspondence principle would indicate that this frequency should be a function of the length alone, but varying as the inverse first power, as in a macroscopic dipole antenna. The LCAO molecular orbital theory of polyenes also predicts too fast a variation,[39] as do the free-electron theories.[23,25] Kuhn[24] has suggested that introduction of a suitable periodic potential in the latter theories will improve the agreement. It would be extremely interesting to have spectra of "metallic" molecules in the little known range of lengths between 50A and a few microns, to see whether this kind of transition goes over asymptotically into the classical dipole frequency, and if so, what the law of dependence of frequency on length will be in this range.

V. NEW ASSIGNMENTS: COMPARISON WITH LCAO THEORY

For polyacenes, Coulson[11] computed the location of the centers of gravity of the lowest transverse singlet and triplet, which he called $N-V_1$, and of the lowest longitudinal pair, which he called $N-V_2$. (A comparison of Coulson's notation with that used here is given in Table I.) He included overlap integrals in his LCAO computations. Since our lowest longitudinal assignment, which we call $^1A-{}^1L_b$, differs from his, which would be our $^1A-{}^1B_b$, a new comparison between observation and prediction needs to be made. The results are shown in Fig. 11, and in Table IV. The $(N-V_2)/(N-V_1)$ energy ratio agrees with the computed ratio within 7 percent, where on Coulson's assignment, which involved unjustified assumptions about the location of the triplet states, the agreement was within 15 percent. The change of the $N-V_1$ band with length also agrees better with his calculation, by the present assignment.

The computed and observed centers of gravity of these two pairs of states are shown in Fig. 11, under the assumption that the factor β, the LCAO bond integral (Coulson's γ), is 23,000 cm^{-1}. Actually, since his prediction of the ratios of the centers is better than the absolute prediction with constant β, we can use the observed centers to determine the best value of β, or $\beta_{\text{spect.}}$, for each molecule. The results are in the sixth column of Table IV; β increases regularly from benzene to pentacene. With this increasing β, i.e., with essentially two empirically determined parameters, the nine centers can be predicted with a maximum deviation of less than 1000 cm^{-1} which is little larger than the variation of band locations from one solvent to another.

Similar computations on azulene[13] give about as good results. The $\beta_{\text{spect.}}$ must now be decreased about 20 percent from its value in naphthalene. The polarizations of the low states must be interchanged, in order to agree with the computed energies. This result is also predicted by the free-electron model.

For the upper states in these molecules the triplets are not known and the center-of-gravity calculations must be compared with the singlets, as shown in Fig. 5. They fit these about as well as they fit the low singlets. The centers are below the singlets, as they should be if the triplets are low; and the deviations for each type of state are about equal and in the same direction for all the compounds, including azulene. The ^1C_b transition has been tentatively

TABLE III.[a]

Compound	Number of π electrons	Total f	$\frac{f}{\pi \text{ electrons}}$
C=C	2	.30	.15
C=C—C=C	4	.55	.14
C=C—C=C—C=C	6	(~0.7)	.11
C=C—C=C—C=C—C=C	8	(~0.9)	.11
Vitamin A	10	1.05+	.11
Carotene	22	2.5–2.7	.12
Fulvene	6	(~1.2)	.20
Benzene	6	0.79	.13
Styrene	8	(~1.7)	.21
Naphthalene	10	2.1–2.8	.22
Diphenyl	12	2.36+	.20
Anthracene	14	3.3	.23
Phenanthrene	14	2.8	.20
Tetracene	18	3.5	.20
1,2-Benzanthracene	18	3.3	.19
Chrysene	18	3.3	.19
Symmetric cyanine	6	1.2*	.20
Symmetric cyanine	8	1.2*	.15
Symmetric cyanine	10	1.6*	.16
Symmetric cyanine	12	1.9*	.15

[a] These data will be discussed and correlated with physical properties in a forthcoming publication.
* Calculated from experimental data of Brooker (see reference 35).

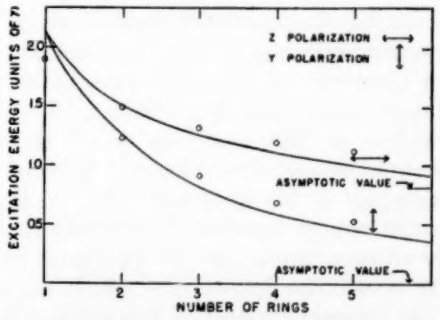

FIG. 11. Observed and predicted centers of gravity of lowest transverse and lowest longitudinal singlet-triplet pairs in polyacenes. $\beta = 23{,}000$ cm^{-1}.

TABLE IV. Computed and observed energies for lowest states.

	Type	In β units	Computed With $\beta=23{,}000$	With best β	Best $\beta_{spect.}$	Observed (solution) States	c. of grav.
			Benzene				
Trans. Long.	$^1A_{1g}-{}^1E_{1u}$	2.13[c]	49,000	(43,000)	20,200	^1L_a 48,000[a]; ^3L_a 29,300[d]; ^1L_b 38,200; ^3L_b 43,800$_{est.}$[b]; ^1B 53,000[a]; ^3B 39,500$_{est.}$[b]	43,000[b]
			Naphthalene				
Trans.	$N\rightarrow V_1$	1.267	29,000	28,200	22,300	^1L_a 35,000; ^3L_a 21,300[d]; ^1L_b 32,200; ^3L_b (36,200)$_{est.}$[b]	28,200
Long.	$N\rightarrow V_2$	1.532	35,000	34,200			34,200
			Anthracene				
Trans.	$N\rightarrow V_1$	0.836	19,000	20,200	24,100	^1L_a 26,700; ^3L_a 14,700[d]; ^1L_b (28,000)$_{est.}$; ^3L_b (32,000)$_{est.}$[b]	20,700
Long.	$N\rightarrow V_2$	1.261	29,000	30,500			30,000
			Naphthacene				
Trans.	$N\rightarrow V_1$	0.600[c]	14,000	14,900	24,800	^1L_a 21,000; ^3L_a (10,000)$_{est.}$[d]; ^1L_b (25,500)$_{est.}$; ^3L_b (29,500)$_{est.}$[b]	15,500
Long.	$N\rightarrow V_2$	1.135[c]	26,000	28,200			27,500
			Pentacene				
Trans.	$N\rightarrow V_1$	0.443[c]	10,000	11,400	25,700	^1L_a 17,300; ^3L_a 6,300$_{est.}$[d]; ^1L_b 24,000; ^3L_b (28,000)$_{est.}$[b]	11,800
Long.	$N\rightarrow V_2$	1.035[c]	24,000	26,600			26,000
			Azulene				
Trans.	$2a-3b$	0.871[f]	20,000	16,100	18,500	^1L_b 14,400; ^3L_b (18,400)$_{est.}$[e]; ^1L_a 28,300; ^3L_a (14,600)$_{est.}$[e]	16,400
Long.	$2b-3b$	1.171[f]	27,000	21,700			21,500

[a] Reference 26.
[b] C. C. J. Roothaan and R. S. Mulliken, J. Chem. Phys. **16**, 118 (1948), estimated the triplet states and the center of gravity in benzene. They estimated ^3L_b was about 5000 cm^{-1} above ^1L_b in benzene. We take this interval as decreasing to about 4000 cm^{-1} in longer molecules, since the $^3L_a-{}^1L_a$ separation decreases from 19,000 to about 13,000 cm^{-1}. We have reduced their center of gravity 1500 cm^{-1} to correspond to solution measurements.
[c] Estimated from Coulson's Fig. 4 and tables.
[d] Reference 31; naphthacene and pentacene $^3L_a-{}^1L_a$ separation assumed about 11,000 cm^{-1}.
[e] Assuming singlet-triplet separations in azulene the same as in naphthalene.
[f] Reference 13.

identified as the third forbidden transition of LCAO theory and the good agreement between calculated and observed positions for it is also shown in Fig. 5.

Coulson also made intensity predictions on the two lowest bands. His comparison of theory and experiment for the transverse band is not altered by the present assignments; but his intensity predictions for the longitudinal band are several hundred times larger than those observed in $^1A-{}^1L_b$. This would suffice to throw serious doubt on the new assignments, except that electron interaction has been neglected in his treatment. Such a treatment of benzene would lead to a fourfold degenerate strongly allowed transition for the lowest frequency band. It is electron interaction which partially removes the degeneracy and makes the two lowest of the resulting bands forbidden. In view of the strong resemblances found in the present paper between the longest-wave-length bands in benzene and the polyacenes, perhaps the same sort of thing will happen in the latter when electron interaction is introduced. The free-electron model leads to a simple treatment of this interaction and predicts this general weakness for the low frequency bands.

This work was assisted by the Office of Naval Research Contract N6ori-20, T.O. IX, with the University of Chicago. We are very grateful to Dorothy Iker Lossy and to Howard Carter for assistance in the determination of these spectra.

Note added in proof:—Recently, the free-electron model has been applied by W. T. Simpson [J. Chem. Phys. **16**, 1124 (1948)] to polyenes and to benzene, following unpublished results of K. S. Pitzer. Also the model has now been used by F. O. Rice and E. Teller in their book *The Structure of Matter* [(John Wiley & Sons, Inc., New York, 1949), pp. 107–11] to give a qualitative description of the ground

states of condensed-ring systems like that given here and in II. Kuhn's paper (reference 24) is announced as the first of a series applying the model to polyenes, cyanine dyes, and porphyrin bodies.

Additional triplet (^3L_a ?) states have now been located in some of the compounds of Figs. 1–7 by D. M. McClure [Ph.D. thesis, University of California, 1948: (also J. Chem. Phys., in press)] acenaphthene, 20,800 cm^{-1}; triphenylene, 23,800 cm^{-1}; 1,2-benzanthracene, 16,500 cm^{-1}; dibenzanthracene, 18,300 cm^{-1}. These new states have the usual 14,000–11,000 cm^{-1} separation from the ^1L_a states in these compounds as expected from the regularities found above.

Some of the 1,2-benzanthracene levels of Fig. 6 are in error. The two high states should have been omitted and the ^1L_a state should be lowered about 2000 cm^{-1}.

M. Kasha has called my attention to a calculation of the lowest excited levels of the naphthalene molecule by A. S. Davydov [J. Exper. Theor. Phys. (U.S.S.R.) **17**, 1106 (1947), translated by M. Kasha, Department of Chemistry, University of California]. The results appear to be identical with Coulson's LCAO results on naphthalene, though the identification with the observed bands is slightly different, and the triplets have been ignored in making the comparison with experiment.

THE JOURNAL OF CHEMICAL PHYSICS VOLUME 17, NUMBER 5 MAY, 1949

Spectral Resemblances in Azulene and Naphthalene

D. E. MANN* AND J. R. PLATT
Departments of Physics and Chemistry, University of Chicago, Chicago, Illinois

AND

H. B. KLEVENS
Department of Agricultural Biochemistry, University of Minnesota, St. Paul, Minnesota

(Received October 4, 1948)

The spectrum of the odd-ring compound azulene, $C_{10}H_8$, from 1730A to 7000A, is compared with that of its regular isomer naphthalene from 1600A to 3500A. The 5 band systems found in azulene seem to correspond, with respect to vibrational structure, intensity, and sequence to the 5 found in naphthalene, except that the former are all shifted to lower frequencies. The lowest band is shifted the most, about 17,000 cm^{-1}, and its absorption gives azulene its blue color. This band has quite different properties from those of the lowest band in the blue compound pentacene. The observed energy levels are compared with LCAO predictions of the lowest states in naphthalene (Coulson) and azulene. The qualitative agreement is good.

THE purpose of this note is to present some new data for the spectrum of azulene, and to draw attention to some resemblances between this spectrum and the spectra of naphthalene and other polyacenes. The spectrum of azulene from 2200 to 3700A was reported by Heilbronner and Wieland.[1] The visible spectrum has been reported several times by Plattner and his co-workers.[2–4] In this note the complete spectrum of azulene from 1730 to 7000A (58,000 to 14,000 cm^{-1}) is given (Fig. 1).

Theoretical studies of the azulene problem have been made by Sklar,[5] who computed the energy states by the Heitler-London-Slater-Pauling (HLSP) method; by Coulson and Longuet-Higgins,[6] who computed mobile bond order, free valence, and electron density; and by Wheland and Mann,[7]

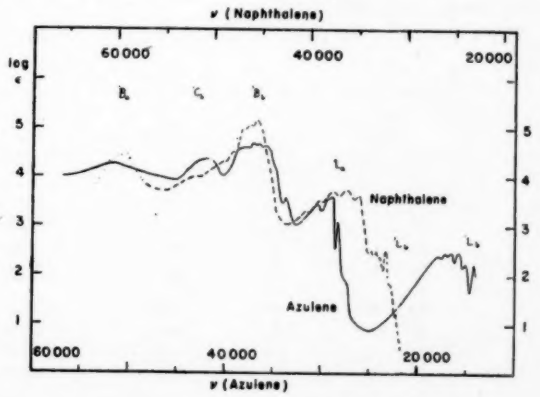

FIG. 1. Spectra of azulene and naphthalene.

* Du Pont Predoctoral Fellow during 1946–1948. Present address: School of Chemistry, University of Minnesota, Minneapolis 14, Minnesota.

[1] E. Heilbronner and K. Wieland, Helv. Chim. Acta **30**, 947 (1947).

[2] B. Susz, A. S. St. Pfau, and P. A. Plattner, *ibid.* **20**, 469 (1937).

[3] P. A. Plattner, *ibid.* **24**, 290/E (1941).

[4] P. A. Plattner and E. Heilbronner, *ibid.* **30**, 910 (1947).

[5] A. L. Sklar, J. Chem. Phys. **5**, 669 (1937).

[6] C. A. Coulson and H. C. Longuet-Higgins, La Revue Scientifique **15**, 929 (1947).

[7] G. W. Wheland and D. E. Mann, J. Chem. Phys. **17**, 264 (1949).

TABLE I. Main features of spectra.

	^1A—^1L_b	^1A—^1L_a	^1A—^1B_b	^1A—^1C_b	^1A—^1B_a
Onset of Absorption (cm^{-1})	31300	35000	4300	—	58000
Peaks of Component Bands (cm^{-1})	31300 31600 31900 32350 32750 32900 33200 33550	35000 36300 37800 38200 39000 40300	45250 46000 48000 48900	53000?	59700 60900
Maximum Molar Extinction ($E_{max.}$)	370	9500	133000	10000	~40000?
Oscillator Strength, f (to cut-off)	0.18 (34000)	1.68 (42500)	0.21 (51000)	~0.8? (55000)	(61000)
			Azulene		
Onset of Absorption (cm^{-1})	14400	25000	32700	40300	45000
Peaks of Component Bands (cm^{-1})	14400 15200 15900 16700 17300 17900 18600 19400 20100 20900	27500 28300 28800 29300 30500	33800 35700 36600 37100 38000	42300	51800
Maximum Molar Extinction ($E_{max.}$)	300	4000	47000	22000	18000
Oscillator Strength (f) (to cut-off)	0.009 (25000)	0.08 (32700)	1.10 (40300)	0.38 (45000)	0.65 (58000)

who computed the dipole moment by the linear-combination-of-atomic orbitals (LCAO) molecular orbital method for comparison with their measured values.

In the present work, azulene was prepared by the method of Plattner and Wyss.[8] The portion of the spectrum between 2340 and 7000A was obtained by the measurement of *n*-heptane solutions of azulene with a Beckman Model DU Quartz Spectrophotometer. Our results are in essential agreement with those of the Swiss workers.[1-4] The portion of the spectrum below 2340A was obtained by the use of techniques described previously.[9] The data for naphthalene above 58,000 cm^{-1} are estimated from unpublished vapor spectra taken by Dr. W. C. Price in this laboratory. The data for the long wave polyacene spectra are from Clar,[10] and for the shorter wave-lengths are from Klevens and Platt.[11]

TABLE II. Predicted levels in azulene.

Configuration*	One-electron Jump (see Fig. 3)	Name*	Polarization	Excitation Energy (in units of β)
$..f^3g$	$2a$—$3b$	L_b	trans	0.8713
	$2b$—$3b$	L_a	long	1.1709
	$2a$—$3a$	B_b	long	1.3307
	$2b$—$3a$	B_a	trans	1.6303
$..e^3f^4g$	$1a$—$3b$	K_b	trans	1.4574
	$1b$—$3b$	K_a	long	1.6138
	$1a$—$3a$	C_b	long	1.9169
	$1b$—$3a$	C_a	trans	2.0733

* See reference 12.

DISCUSSION

In Fig. 1 the spectrum of azulene is compared with that of naphthalene, the spectrum of the latter having been shifted about 9000 cm^{-1} to lower frequencies for easier comparison. There appear to be five distinct band systems in the azulene spectrum. These are labeled ^1B_a, ^1C_b, ^1B_b, ^1L_a, and ^1L_b. These labels are derived from a scheme of systematic nomenclature for condensed hydrocarbons which is described elsewhere.[12] It is seen that these bands resemble the similarly labeled bands in the naphthalene spectrum with respect to (a) intensity, (b) vibrational structure, and (c) position and separation, except for the lowest frequency band, ^1L_b. In peak intensity, the two sets of bands agree within a factor of about two. (See Table I summarizing the main features of the spectra.) In integrated intensity over the important ^1B_b band and over the whole spectrum, the agreement is still better. In position, on Fig. 1, the agreement is within about 2000 cm^{-1} for corresponding bands in the two compounds except for the ^1L_b set. The essential difference between the two spectra is then the following. With respect to the higher states (the ^1B's and ^1C_b) two states have moved: the ground state, ^1A, has moved upward by about 9000 cm^{-1}; and the ^1L_b state has moved downward by about 8000 cm^{-1}. The blue color of azulene is due to the resulting 17,000 cm^{-1} shift of the ^1L_b band.

In Fig. 2 and Table I the known singlet electronic states of azulene are compared with those of the naphthalene-pentacene series.[11] In Fig. 2 the vibra-

TABLE III. Computed and observed energies for lowest states.

	Computed	Observed States	Observed Center of Gravity
	Naphthalene		
Lowest transverse (N—V_1)	1.267γ* $=28{,}200$ cm^{-1a}	^1L_a 35,000 cm^{-1} ^3L_a 21,300 cm^{-1}**	28,200
Lowest longitudinal (N—V_2)	1.532γ $=34{,}100^a$	^1L_b 32,300 ^3L_b (36,000)[e]	34,100
	Azulene		
Lowest transverse	$.871\beta = 19{,}400^a = 16{,}100^b$	^1L_b 14,400 ^3L_b (18,200?)[d]	16,300
Lowest longitudinal	$1.171\beta = 26{,}100^a = 21{,}600^b$	^1L_a 28,300 ^3L_a (14,600?)[d]	21,500

[a] $\beta = \gamma = 22{,}200$ cm^{-1}; [b] $\beta = 18{,}500$ cm^{-1}; [e] estimated from benzene (see references 12, 16); [d] singlet-triplet separation assumed to be the same as in naphthalene.

* See reference 14.

** M. Kasha, Chem. Rev. 41, 401 (1947).

[8] Joachim Wyss, *Synthesen Einfacher Azulene* (University of Zürich Press, Zürich, Switzerland, 1941), p. 27ff.

[9] J. R. Platt and H. B. Klevens, Chem. Rev. 41, 301 (1947).

[10] E. Clar, *Aromatische Kohlenwasserstoffe* (Springer-Verlag, Berlin, 1941).

[11] H. B. Klevens and J. R. Platt, "Spectra of cata-condensed hydrocarbons," J. Chem. Phys. 17, 470 (1949).

[12] J. R. Platt, "Classification of States of cata-condensed hydrocarbons," J. Chem. Phys. 17, 484 (1949).

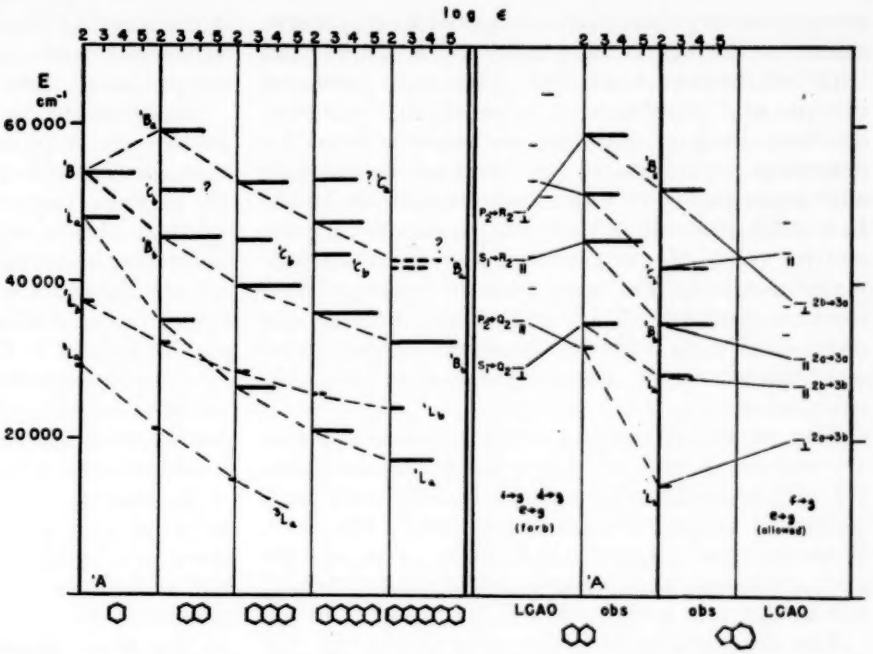

FIG. 2. Left: Energy levels of polyacenes. Observed values, see reference 11; Right: Comparison of energy levels of naphthalene and azulene. Observed values, and LCAO-predicted values of centers-of-gravity of singlets and triplets.

Note to Fig. 2.—In the observed spectra, only the lowest vibrational level is shown. Remaining structure of each electronic band omitted for clearness. Length of horizontal lines indicates $\log\epsilon_{max.}$ of transition from ground state on scale at top of figures. Lines for triplets drawn to left to indicate $\log\epsilon_{max.}$ is less than 2.

The symbols ^3L_a, ^1L_b, etc., are generic designations for states of similar properties in the different compounds (reference 12). The symbols $S_1 \rightarrow Q_2$, etc., to the left of the LCAO-predicted levels in naphthalene are from Coulson (see reference 13). The symbols $2a \rightarrow 3b$, etc., to the right of the LCAO-predicted levels in azulene are from the present paper (see Table II and Fig. 3). The symbols $f \rightarrow g$, etc., below the excited levels on the right half of the figure represent one-electron configuration changes, in the notation of reference 12. The $e \rightarrow g$ type of transitions are supposed to be parity-forbidden in naphthalene, but allowed in azulene.

tional structure is omitted for simplicity, and the lengths of the horizontal lines indicate $\log\epsilon_{max.}$ for absorption from the ground state. In the polyacene series (left half of Fig. 2), the ^1B_b—^1L_a separation increases with number of rings to a value of about 15,000 cm^{-1}. The ^1B_b—^1L_b separation decreases until in anthracene and naphthacene the ^1L_b band is concealed by the stronger ^1L_a, and reappears above it in pentacene. In the polyacene series, therefore, it is the ^1L_a band which is principally responsible for the visible color while in azulene (right half of Fig. 2) it is the ^1L_b band, some 20 times less intense, which is responsible.[13]

Coulson[14] has used LCAO molecular orbital theory, including overlap integrals, to compute the energy levels of naphthalene and other polyacenes. One of us (D.E.M.) has computed the energy levels of azulene by the same method (Figs. 2 and 3, and Table II). The reducible representation whose basis is the set of atomic orbitals on the carbon atoms in azulene has the irreducible components $6A_1$ and $4B_2$. The four lowest roots of the secular equation derived from the 6×6 symmetric (A_1) block are given in terms of y (where y is an abbreviation for $(\alpha-E')/\gamma_0$, α is the coulomb integral for a carbon atom in benzene, E' is the appropriate variational approximation to the correct eigenvalue, and γ_0 is the resonance or bond integral for benzene) on the left of Fig. 3; the three lowest roots of the 4×4 antisymmetric (B_2) block are given on the right side. The energy levels for azulene have been calculated from these roots, with the assumption that the overlap integral S has the rounded-off value 0.25, by the method of Wheland.[15] These results are given in Table II. The polarizations given in Table II are called transverse (or perpendicular) when the transition is between levels which belong to different symmetry classes, and longitudinal (or parallel) when the transition is between levels which belong to the

6th order (symmetric)			4th order (antisymmetric)	
			— 3a	+0.7376
3b	+0.4004	—		
Unfilled				
Filled				
			— 2a	−0.4772
2b	−0.8869	—		
			— 1a	−1.3556
1b	−1.6515	—		
0	−2.3103	—		

FIG. 3. Roots of secular equations for azulene.

[13] See G. W. Wheland, *The Theory of Resonance* (John Wiley and Sons, Inc., New York, 1944), pp. 159–160, for a bibliography, discussion, and criticism of theoretical studies on the long wave spectra of these and related compounds.

[14] C. A. Coulson, Proc. Phys. Soc. **60**, 257 (1948).

[15] G. W. Wheland, J. Am. Chem. Soc. **63**, 2026 (1941).

same symmetry class. Each computed level properly refers to the center of gravity of a singlet and triplet of the same kind. The energies are expressed in units of β (Coulson's γ), where β, the resonance or bond integral *corrected for overlap*, must be determined empirically. For accurate comparison with experiment, we must know the triplet levels. In naphthalene, one of these, ^3L_a, is known (Fig. 2), and the other, ^3L_b, can be estimated from the estimated singlet-triplet separation in benzene[16] and from the position of ^1L_b. In azulene, it seems not unreasonable to assume the same singlet-triplet separations as for the corresponding levels in naphthalene.

The computed values for the two lowest states are compared with the observed values in Table III. With $\beta = 22{,}200$ cm^{-1} in naphthalene, both centers of gravity are predicted within 100 cm^{-1}. With the same value of β in azulene, errors of 4500 cm^{-1} are found, but a lower value of β, 18,500 cm^{-1}, will fit the data within 200 cm^{-1}.

The comparison of the computations on the upper states is quite crude since only the upper singlets are known in either molecule. The computed centers of gravity are on Fig. 2, using a β of about 23,000 cm^{-1} for both molecules. (This figure is taken from reference 12, where this value of β was used in another comparison.) For each state, the deviations of computed levels from observed singlets are in the same direction and of about the same size in both molecules, if the assignments given are correct. The method of making these assignments is discussed in detail elsewhere.[12] This qualitative agreement tends to support them. No intensity computations were made here.

It should be noted that the values for β for azulene and naphthalene obtained from these spectroscopic considerations are not in agreement with the corresponding β's obtained from thermochemical (e.g., heats of combustion) measurements of resonance energies. For example, the β_{spect}'s for azulene, benzene, naphthalene, and anthracene are respectively 18,500 cm^{-1}, 20,600 cm^{-1}, 22,200 cm^{-1}, and 24,300 cm^{-1}. The corresponding β's, calculated from heat-of-combustion resonance energies,[15] are (10,000 cm^{-1}?), 13,400 cm^{-1}, 14,000 cm^{-1}, and 14,000 cm^{-1}. No explanation of these discrepancies is offered, and their investigation is desirable.

Here we have not compared the observed energy levels in azulene with the HLSP computations of Sklar.[5,13] Although his predicted frequencies for the lowest singlet-singlet transitions for a number of compounds agree well with the observed position of the first absorption bands, the spread in his excited electronic levels is much too large in azulene as well as in benzene and other molecules, and the sequence of his predicted levels is wrong, for example, in benzene. He attributes the unduly large spread to his neglect of ionic structures, which are known to be essential for describing excited states by the HLSP method.[13] The LCAO description which Mayer and Sklar applied later to benzene[17] is much more satisfactory in predicting excited states,[16] and a modification of the latter approach has been used here for that reason.

[16] C. C. J. Roothaan and R. S. Mulliken, J. Chem. Phys. **16**, 118 (1948).

[17] M. G. Mayer and A. L. Sklar, J. Chem. Phys. **6**, 645 (1938).

THE JOURNAL OF CHEMICAL PHYSICS VOLUME 17, NUMBER 5 MAY, 1949

Classification of Spectra of Cata-Condensed Hydrocarbons

JOHN R. PLATT
Physics Department, University of Chicago, Chicago, Illinois
(Received November 1, 1948)

The classification of π-orbitals in a cata-condensed aromatic system is like that of the orbitals of a free electron traveling in a one-dimensional loop of constant potential around the perimeter. To take into account electron interaction, certain quantities corresponding to angular momenta may be added or subtracted. Introduction of the cross-links in the molecule removes the degeneracy. The first excited configuration in such systems gives two low frequency singlet weak absorption bands and two higher singlet strong dipole absorption bands. Selection and polarization rules are given. The levels are identified from the spectra and some of their properties are determined. An explanation is given of the regularities found by Klevens and Platt. A systematic nomenclature is given. The results agree qualitatively with LCAO theory, can be applied easily to unsymmetrical molecules, and can possibly be extended to other types of ring systems.

I. THE FREE-ELECTRON MODEL

THE aromatic spectra which were extended into the vacuum ultraviolet in the preceding paper[1] (hereafter called I) show many empirical resemblances and regularities. In benzene, the LCAO (linear-combination-of-atomic-orbitals) mo-

[1] H. B. Klevens and J. R. Platt, J. Chem. Phys. **17**, 470 (1949).

lecular orbital theory satisfactorily explains the excited levels.[2,3] In the linear condensed-ring systems, or polyacenes, only the centers of gravity of singlet-triplet pairs have been calculated;[4] and intensity predictions are too large, especially for the low-frequency bands,[1] probably because electron interactions have not been included. The LCAO theory has not yet been applied to account for the regularities in the spectra of the unsymmetrical condensed ring systems. (Complete and up-to-date bibliographies of other theoretical and experimental work on aromatics will be found in I and in references 2, 4, 7, 12, 13, 16, 19, 20, 25, and 27.)

Another molecular orbital approach—the free-electron orbital method—will give less accurate but more rapid results, if simplifying assumptions are made. It can describe electron interactions in a simple way. Without introducing parameters to be determined empirically, it will give the approximate height of the excited states. It gives correct polarizations, accounts for the general weakness of the low frequency bands, and can easily be extended to unsymmetrical molecules. It explains the regularities observed in I, and leads to a useful new classification for the electronic states. Empirically similar bands in different compounds are given the same symbol, instead of different symbols as they are in theories which emphasize symmetry considerations.

The method assumes that the π-electrons of a planar conjugated system are free to move along the bonds throughout the system under a potential field which is, in first approximation, constant. This description was used to explain the diamagnetism of aromatic molecules by Pauling[5] and Lonsdale.[6] Schmidt[7] generalized it further by thinking of the conjugated system as simply a large flat box containing a Fermi gas of unsaturation electrons (π-electrons) in analogy to the two-dimensional metal model of graphite. He discussed excited states and spectra, but without any systematic correlation with the known levels. The idea of almost-free motion along the bonds has always lain in the background of molecular orbital discussion.[8–11] Lennard-Jones[9] coined the term "mobile electrons" to indicate this motion of the π-electrons throughout the whole molecule. Hückel[8] used complex molecular orbital eigenfunctions in treating benzene and related problems. These represent electron waves traveling around the benzene ring. He also used "orbital ring quantum numbers" describing angular momentum, as we shall do here, and showed how they add and subtract to give a "total ring quantum number" which characterizes the state of the system. However, the LCAO method with real coefficients has usually been regarded as the best starting point in molecular orbital theory. Bayliss[12] has recently returned to the idea of the Fermi gas in one dimension to explain the spectra of polyene chains. Kuhn[13] has announced that a modification will predict the strong allowed frequency in polyacenes; he makes no mention of the other transitions classified in the present paper.

In the present approach, it is assumed that the π-orbitals retain their main π-electron property, i.e., a node in the molecular plane. This quantization perpendicular to the plane of the molecule is assumed to be independent of the quantization in the plane. The closed-shell σ or single-bond electrons are assumed to be more tightly and locally bound than the π-electrons and cannot be treated by a free-electron approximation. They will not be further discussed here.

The cata-condensed ring systems, whose general formula is $C_{4n+2}H_{2n+4}$, include some of the most important aromatics and carcinogens. In them no carbon atom belongs to more than two rings and every carbon is on the periphery of the conjugated system. This makes possible a further simplification.

Postulate: *The classification of π-orbitals in cata-condensed systems is like that of the orbitals of a free electron traveling in a one-dimensional loop of constant potential around the perimeter.* The use of the perimeter is a convenience in visualization because of the importance of angular momentum in electron interactions and in selection rules. This postulate amounts to asserting that the wave equation for π-electrons is approximately separable in three coordinates, one along the perimeter, one perpendicular to the plane of the molecule, and one perpendicular to these two at the perimeter, and, further, that the main difference of the orbitals from each other is with respect to quantization in one of these coordinates only, i.e., along the perimeter.

To find the perimeter-free-electron orbitals and energies, the perimeter may first be distorted into a circle of the same length. The orbitals are those of a plane rotator. The energies are then

$$E = q^2h^2/2ml^2 = 1{,}210{,}000q^2/l^2,$$

where q is an integer, $0, 1, 2, \cdots$; h is Planck's constant; m is the mass of the electron, l is the

[2] C. C. J. Roothaan and R. S. Mulliken, J. Chem. Phys. **16**, 118 (1948).
[3] M. G. Mayer and A. L. Sklar, J. Chem. Phys. **6**, 645 (1938).
[4] C. A. Coulson, Proc. Phys. Soc. **60**, 257 (1948).
[5] L. Pauling, J. Chem. Phys. **4**, 673 (1936).
[6] K. Lonsdale, Proc. Roy. Soc. **159**, 149 (1937).
[7] O. Schmidt, Zeits. f. phys. Chem. **47B**, 1 (1940), and previous papers.
[8] E. Hückel, Zeits. f. physik. **70**, 204 (1931).
[9] J. E. Lennard-Jones, Proc. Roy. Soc. **158A**, 280 (1937).
[10] R. S. Mulliken, J. Chem. Phys. **7**, 369 (1939).
[11] C. A. Coulson and G. S. Rushbrooke, Proc. Camb. Phil. Soc. **36**, 193 (1940).
[12] N. S. Bayliss, J. Chem. Phys. **16**, 287 (1948).
[13] H. Kuhn, J. Chem. Phys. **16**, 840 (1948).

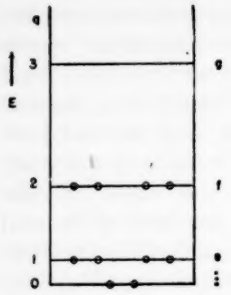

FIG. 1. One-electron states; and shells.

length of the perimeter (in angstroms), and E is the energy (in cm^{-1}) measured upward from the constant potential. The levels are quadratically spaced as shown in Fig. 1 and are all doubly degenerate except the lowest, since electrons that have a finite velocity may travel either clockwise or counterclockwise around the loop.

The orbital ring quantum number q, which measures angular momentum, determines the number of nodes of the wave function and the selection rules. It may be thought of as a vector perpendicular to the plane of the molecule. In the zig-zag perimeter, angular momentum is no longer a constant of the motion, because of the constraints, but linear momentum is. When the periodic potential due to the atoms is introduced, q no longer describes accurately any momentum. But it remains a good quantum number because it still determines the number of nodes around the perimeter.

In many-electron systems, the vector q's of the different electrons may be added and subtracted—algebraically and not vectorially, since they are restricted to one dimension—to give a total ring quantum number Q for the system.[14] This procedure gives a qualitative model for electron interactions similar to the vector model for representing these interactions in a diatomic molecule.

II. NAMES AND CHARACTERISTICS OF STATES

Shells, Configurations, and States

In cata-condensed systems of n rings, the $2(2n+1)$ carbons each bring one π-electron to the system. These will fill the successive shells as shown in Fig. 1. The highest filled shell will be for $q=n$, and we will designate the 4 electrons in this shell as f-electrons, those in the next lowest shell as e-electrons, and so on. The first empty shell will be the g-shell, with $q=n+1$, the next, the h-shell, and so on. Since the "optical" electrons are those in the last one or two filled shells, it will be convenient to have a notation which is the same for these top shells in molecules of the same general type even when the ring quantum numbers are different.

[14] I am indebted to Prof. Mulliken for suggesting the names, "orbital ring" and "total ring quantum number" for q and Q. Hückel (see reference 8) used the symbols, k and K, for these quantities.

In the states of interest, the total momentum number, Q, may take on the values, 0, 1, 2, ···. Such states we may designate by A, B, C, ···. We will see that it may also take on the values ···, $2n$, $2n+1$, $2n+2$, ···. These states we may designate ···, K, L, M, ···, the letters being kept the same regardless of the value of n.

In the perimeter-constant-potential approximation, all of the states are doubly degenerate except the A state since the total momentum may be in either direction. Introduction of the crosslinks and of the periodic potential due to the atoms along the perimeter removes the degeneracy except in some states of highly symmetric molecules such as benzene and triphenylene. Because of its removal, the states will be split. The two components may be given subscripts a and b, whose significance we will examine later.

The most important spectra will be electron-hole spectra, produced like those of the rare-gas atoms by the excitation of one electron from a filled shell to an empty one. Spectra produced by the excitation of two electrons will be weak, as in atoms, and will require higher excitation energies. The excited electron interacts with the remaining tenants of its former shell, or, more simply, with the hole it leaves behind.

Thus, when an electron goes from an f to a g orbital, the new system has states with the f and g ring quantum numbers added or subtracted, i.e., with $Q=(n+1)\pm n=1$ or $(2n+1)$. These are B and L states. Removing the degeneracy, they become B_a, B_b, L_a, L_b. The electron and hole spins may be antiparallel or parallel, giving two sets of excited states, singlets and triplets. This makes 8 types of states for this f^3g configuration. All singly excited configurations will have 8 states.* The Pauli principle makes the ground state singlet and single.

The lower configurations, and the states to which they give rise, are given in Table I.

The configurations have been grouped according to their arithmetic sum of momentum numbers, Σq.

TABLE I.

$\Delta\Sigma q$ (from ground state)	Configuration	States
3	$\left\{\begin{array}{l}\ldots\ldots f^3i\\ \ldots\ldots e^3f^4h\\ \ldots d^3e^4f^4g\end{array}\right.$	$^{1,3}D_{a,b}$ $^{1,3}N_{a,b}$ $^{1,3}D_{a,b}$ $^{1,3}L_{a,b}$ $^{1,3}D_{a,b}$ $^{1,3}J_{a,b}$
2	$\left\{\begin{array}{l}\ldots\ldots f^3h\\ \ldots e^3f^4g\end{array}\right.$	$^{1,3}C_{a,b}$ $^{1,3}M_{a,b}$ $^{1,3}C_{a,b}$ $^{1,3}K_{a,b}$
1	$\ldots\ldots f^3g$	$^{1,3}B_{a,b}$ $^{1,3}L_{a,b}$
0	$\ldots\ldots f^4$	^1A

* *Note added in proof:* This assumes that degenerate states are counted twice. There is also the obvious exception of excitation from $q=0$ states as in the e^3f^4g configuration of benzene.

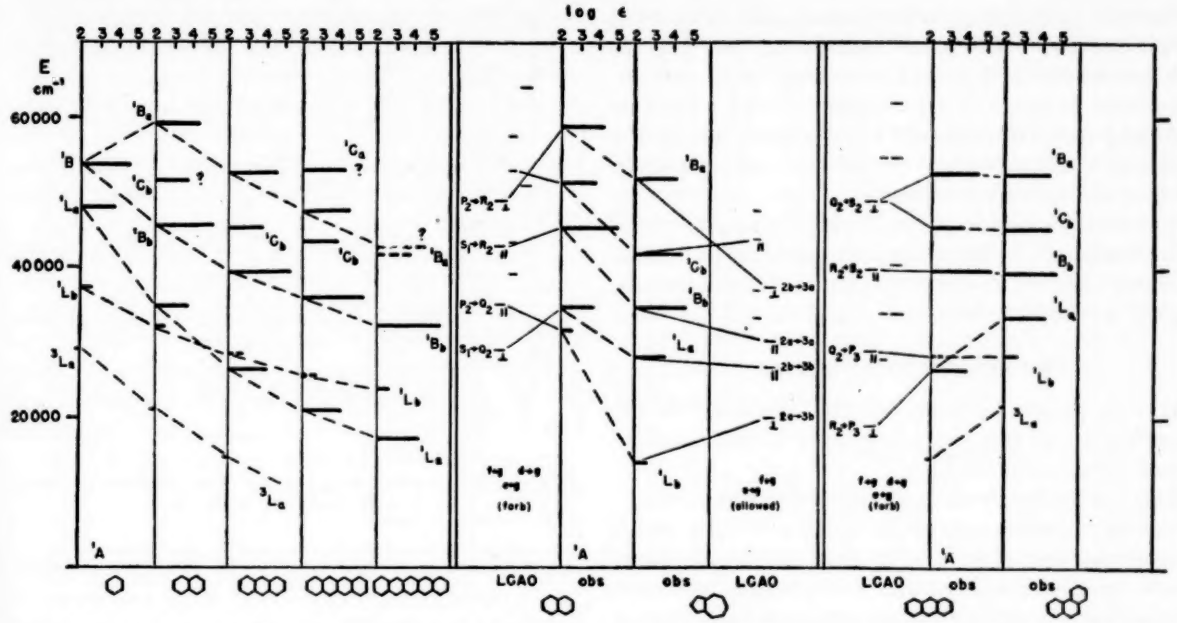

FIG. 2. Electronic energy levels of polyacenes and isomers. Comparison of LCAO center-of-gravity predictions with observed singlets in naphthalene, azulene, anthracene.

Note: Lowest vibrational level shown. Remaining structure of each electronic band omitted for clearness. Length of horizontal lines indicates $\log\epsilon_{max}$ of transition from ground state on scale at top of the figure. Lines for triplets drawn to left to indicate $\log\epsilon_{max}$ is less than 2.

In a large system with almost equally spaced one-electron states, the configuration energies will be grouped the same way. In smaller molecules with increasing spacing near the *f*-shell, the $e \rightarrow g$ absorption bands will lie at lower frequencies than the $f \rightarrow h$ bands. The first ultraviolet bands will therefore be of $f \rightarrow g$ type and the next of $e \rightarrow g$ type. Such groupings may be seen in the energy levels of Fig. 2. Higher bands become weak, and only the Rydberg series bands, which fall outside this π-electron classification, can be seen at very short wavelengths.

Empirically, the order of states of a given configuration is determined by the Hund rule, which holds for molecules as well as atoms.[15a] Triplets lie below singlets; and within the singlet group, or the triplet group, states of high Q lie below low Q states. Thus in the states in Fig. 2, which have been identified by this scheme as described below, one ^3L always lies below any ^1L; and the ^1L's always below the ^1B's.

Selection and Intensity Rules

The selection rules are as follows.

1. *Singlet-triplet strongly forbidden.* This is the familiar rule in light atoms and in molecules containing light atoms. Triplet states in aromatics are known only from phosphorescence and from absorption with very long paths.

2. ΔQ *must be odd in centrally symmetric systems.* This will be justified under Rule 3. $\Delta Q = 1$ is always allowed and strong—the dipole transition when the perimeter is a circle. The higher values of ΔQ would be forbidden multipole transitions if the perimeter were a circle. They would be allowed but weak, as in polyenes,[10,12] if it were a double straight line. They will therefore be generally weak, but their exact strength will depend on the molecular shape. Very high ΔQ values, near $2n$, will be practically forbidden, but may become stronger through vibrational interaction, like the forbidden bands in benzene.

Thus, in the observed spectra (see I), the $^1A - {}^1B$ transitions have oscillator strengths from 0.5 to 3.0. The $^1A - {}^1L_b$ transitions in benzene as well as in the other molecules have oscillator strengths near 0.002; and the $^1A - {}^1L_a$, near 0.1.

3. $\Delta\Sigma q$ *must be odd in centrally symmetric systems.* This is equivalent to Rule 2 in the molecules we are discussing. In centrally symmetric systems, the states may be divided into "even" and "odd," or "*g*" and "*u*," depending on whether the electronic wave function is symmetric or antisymmetric with respect to reflection in the center of symmetry. Even states have Σq even; odd states have Σq odd.

The proof of Rule 3 is therefore the same as the proof of the selection rule even↔odd, even←|→even, odd←|→odd; the procedure for this proof is like that indicated for diatomic molecules by Herzberg.[15b]

Vibrations destroy the symmetry, and in several

[15] G. Herzberg, *Molecular Spectra and Molecular Structure. I. Diatomic Molecules* (Prentice-Hall, New York, 1939), (a) p. 360, (b) pp. 136, 264.

symmetric polyacenes, what seem to be even-even transitions ($^1A - {}^1C_b$) have been found (see Fig. 2) with intensities 1/5 to 1/2 as strong as in the unsymmetric isomers. Large values of $\Delta\Sigma q$ become more and more improbable by the Franck-Condon principle, because they begin to involve large changes in electron velocity.

By correspondence-principle, $\Delta\Sigma q$ gives the order of the harmonic in the analogous classical flat metal oscillator. $\Delta\Sigma q = 1$ corresponds to the fundamentals, $\Delta\Sigma q = 2$ to the first harmonics, and so on.

The Polarization Diagram

At this point we examine the meaning of the subscripts a and b, which are related to the polarization of absorption bands.

If the perimeter were a circle, the states A, B, C, $\cdots$ would correspond to Σ, Δ, Π, $\cdots$ of a plane rotator configuration. A transition $A \rightarrow B$ corresponds to $\Sigma \rightarrow \Pi$, and so on. The possible polarizations of such a transition are the same as those of the corresponding one-electron transition, $\sigma \rightarrow \pi$. They are determined by the location of the nodes of a π-orbital.

This leads to a convenient diagram for determining polarization of absorption from the ground state. Draw the perimeter line. Indicate the atom positions, and mark where the line is cut by planes of symmetry. Expand the line to a circle. For the transition between the ground state and a state of momentum number Q, draw the nodes for a free-electron standing-wave orbital of momentum number $q = Q$. Since the orbitals are doubly degenerate, there will be two independent sets of these nodes. Each set will have $2Q$ nodal cuts across the perimeter. The nodes of one set will lie at antinodes of the other set. Where there is a symmetry axis, they are easy to construct. In one set the nodes will lie on the axis, in the other set the antinodes. We will call that set, a, which proves to have a nodal line cutting crosslinks (see Fig. 3) when the perimeter is returned to its normal shape; b, that set in which the crosslinks are uncut.

The polarizations of transitions from the ground state will be the same as if we located + and − point charges at alternate antinodes, shrank the perimeter back to its normal shape, and determined the direction of the resulting electric moment.

If we normalize the sum of all + charges to $+\frac{1}{4}$, and the sum of all − charges to $-\frac{1}{4}$, the size of the electric moment in this diagram will give a rough qualitative idea of the transition moment integral, or effective dipole length Z (Q in the usual notation). From this we can estimate the oscillator strength,[16]

$$f = 1.08 \times 10^{-5} \nu G Z^2 \text{ cm/A}^2$$

[16] R. S. Mulliken and C. A. Rieke, Rep. Prog. Phys. **VIII**, 231 (1941).

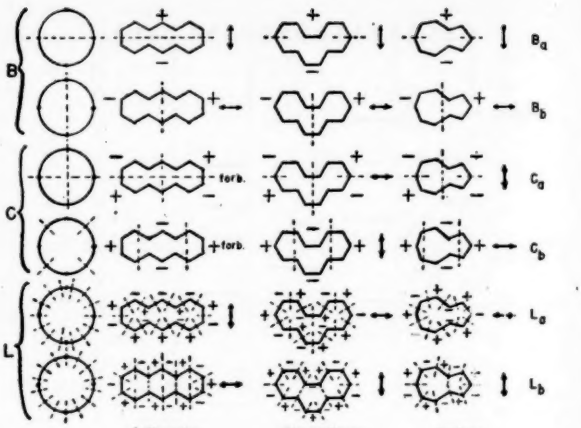

FIG. 3. Polarization diagrams for low absorption bands of representative molecules.

where ν is the frequency of the absorption band (in wave numbers); where G is 1 for a non-degenerate state, 2 for a doubly-degenerate state; and where Z is the dipole length (in A).

This method of estimating Z and f amounts to replacing ($\Psi_{gd}\Psi_{exc}$) in the transition moment integral

$$Z = \int \Psi_{gd}(\sum \mathbf{r}_i)\Psi_{exc} d\tau$$

by a real charge density, ρ, which has the same symmetry properties and which represents the corresponding transition in a one-electron system. A normalization of ρ to $+\frac{1}{2}$ and $-\frac{1}{2}$ would correspond to approximating the ψ's by two normalized, orthogonal point functions which each take the absolute value $1/(n)^{\frac{1}{2}}$ at n points in the molecule. However, since the effective charges are not so localized, but are distributed, the effective dipole lengths are shorter by about a factor of 2, and this can be taken into account by normalizing the ρ's to $+\frac{1}{4}$ and $-\frac{1}{4}$ as indicated above. Thus, for a long polyene chain transition with one node, we would have effective charges of $+\frac{1}{4}$ and $-\frac{1}{4}$ at each end of the chain, effective dipole length $\frac{1}{4}$ the chain length. Bayliss gives this dipole length from the transition moment integral as 0.21 times the chain length.[12] Similarly in benzene, the one-electron transition moment integral for an $f \rightarrow g$ transition in a circular ring is $\frac{1}{4}$ the diameter, and the polarization diagram using the rules above would give about the same value for the effective dipole length.

Perhaps it should be emphasized that such a polarization diagram is a device for visualization and not a classical model. It is not suited for accurate intensity predictions, since they require proper introduction of the total wave functions in the transition moment integral; but it will give polarizations correctly. Several of these diagrams are

shown in Fig. 3 for some important transitions in anthracene, phenanthrene, and azulene.

The two highly allowed $^1A-{}^1B$ transitions are always polarized along mutually perpendicular axes in the molecule. It is these two transitions which go over by the correspondence principle into the classical fundamental electrical oscillations of a flat metal plate, which were used as analogies by Lewis and Calvin.[17,18] Classically, ν would vary inversely with Z in the above formulas, and the intensity of each of these transitions would be proportional to the molecular diameter, suitably averaged, parallel to the transition axis.[10] Empirically, according to the assignment of Fig. 2, the longitudinal transition, $^1A-{}^1B_b$, lies at the longer wave-length, as does its classical counterpart.

The $^1A-{}^1C$ bands, as shown by Rule 2 and as confirmed in Fig. 3, will be forbidden in centrally symmetric systems. The polarization diagram for the $^1A-{}^1C_b$ band in long, non-centrally-symmetric systems will presumably be cut by roughly parallel nodal lines transverse to the length, as $^1A-{}^1B_b$ was, and as shown in Fig. 3. If the system has no center of symmetry, but has an axis of symmetry, as phenanthrene and azulene do, the transition, $^1A-{}^1C_b$, will then be allowed and will have a moment parallel to the symmetry axis. In all long bent systems, this moment will probably be roughly transverse to the long dimension, as in phenanthrene. The moment of $^1A-{}^1C_a$ will be perpendicular to the symmetry axis, if any, or roughly longitudinal in long bent systems.

The $^1A-{}^1L$ bands will have the following special property. In their polarization diagram, the number of nodes on the perimeter is $2Q=2(2n+1)$, which is just the number of carbons on the perimeter, so the nodal separation is just the mean carbon-carbon distance. In the diagram for $^1A-{}^1L_a$, every peripheral bond will be cut by a node and we must put the effective charges on the atoms. For $^1A-{}^1L_b$, the atoms are at nodes and the effective charges go on the bonds. It is seen from Fig. 3 that in these transitions the elementary dipoles are nearly canceled within each ring, regardless of gross molecular shape, so the total intensity will be very small. Other transitions of high ΔQ are weak for the same reason.

For hexagonal ring systems, when some bonds are just parallel or perpendicular to a symmetry axis, the $^1A-{}^1L_a$ moment will be parallel to these bonds, the $^1A-{}^1L_b$ moment perpendicular. In azulene, which has an odd number of carbons in each ring, the a and b naming is ambiguous by the rule given above, but we can continue to draw the effective charges at the atoms in $^1A-{}^1L_a$. As may be seen in Fig. 3, this interchanges the polarizations in the two L bands from their directions in the isomer, naphthalene (whose polarization diagrams are like those of anthracene).

In the classical macroscopic flat plate analogy, the intensity of these very high multipole $^1A-{}^1L$ transitions must approach zero, as they would correspond to the oscillations of a line of microscopic dipole charges around the edge of the plate. They should therefore not correspond to the Lewis and Calvin fundamental vibrations; Coulson[4] emphasized that this correspondence did not hold for the lowest frequency bands, which are the ones identified here with $^1A-{}^1L$.

Height of Levels

The average height of a configuration should be given by the energy of the one-electron jump from the ground configuration. It is easily shown that this would predict an average frequency of absorption almost inversely proportional to the perimeter length. Actually, the frequency of the strongest band varies about inversely as the 0.3–0.5 power of the length (see I). The same difficulty, that the predicted frequency varies too rapidly with length, is found in the free-electron theory of polyenes[12] and in the LCAO theory of polyenes[10] and of polyacenes.[4] Addition of the periodic potential in the free-electron model may improve the predictions.[13]

The arrangement of levels of a given configuration is given by the Hund rule, as noted above.

The particular advantage of the free-electron model is that it may be extended easily to unsymmetrical cata-condensed systems. For all systems of a given number of rings, the perimeter is the same, the number of crosslinks is the same and the area is the same. Therefore the location of the levels should be approximately the same in isomers. This is seen in the spectra of I for isomers having the usual 6-carbon rings. The levels of azulene, with a 5-carbon and a 7-carbon ring are systematically lower than those of its 6-carbon isomer, naphthalene.

Electron Density

The possible importance of high local charge density in determining reactivity and potency in carcinogenic hydrocarbons such as benzanthracene, dibenzanthracene, and their derivatives, has been emphasized by Schmidt,[6] and quantitative predictions of density variations have been made by Daudel and Pullman and others.[19] The free-electron model with suitable boundary conditions will give alternating charge densities in successive bonds near the end of a polyene chain, though Bayliss

[17] G. N. Lewis and M. Calvin, Chem. Rev. **25**, 273 (1939).
[18] G. N. Lewis and J. Bigeleisen, J. Am. Chem. Soc. **65**, 520, 2102, 2107 (1943).
[19] For bibliography, see P. Daudel and R. Daudel, J. Chem. Phys. **16**, 639 (1948).

did not point this out. However, the perimeter model gives uniform charge density for condensed systems, if they are unsubstituted. Introduction of crosslinks will produce local density variations of Schmidt's type. Substitution on the perimeter will introduce a perturbing potential, and cause mixing of the wave functions and further variation of charge density. In this way, the free-electron model could probably be extended to account for directing effects in benzene rings and for similar effects in the carcinogens.

It is unfortunate that the terminology proposed here uses two letters, A and B, in different senses from their use in group theory. But spectroscopy has taken its toll throughout the alphabet and there seems to be no other series of consecutive letters with fewer conflicts. Especially, it seemed wise to avoid the established angular momentum letters in either English or Greek, since the case here is so different. It is hoped that the different subscripts will help to avoid confusion with the group theory designations.

III. CORRELATION WITH SPECTRA

In I the levels of 17 cata-condensed systems were identified according to the scheme just outlined. Levels of a few important molecules are given again in Fig. 2. Justification of this system of naming must be in two parts: (a) justification of giving the same names at all to levels of different compounds; and (b) justification of the particular names chosen, since they now imply definite properties. Subsequently some general support from LCAO theory, and some ambiguous identifications, will be discussed.

(a) Empirical Identity of Levels in Different Compounds

The following general results are derived from I; details may be found there.

1. *Levels of a given type have unambiguous identifying characteristics*, which do not change from compound to compound. The most useful characteristics are intensity and vibrational sharpness of the transition from the ground state to the level in question. *There is almost no mixing or confusion of properties.*

2. *Levels of a given type move in a systematic way from compound to compound.* All lie on smooth and almost parallel curves as a function of length. They generally lie near the same energy in isomers.

3a. *Each empirical type occurs once and only once in each compound.*

3b. *The number of lower levels remains constant* from compound to compound up to any particular upper level as far as the spectra have been carried. There are a few reasonable exceptions where degeneracies occur or where a weak band is expected to be overlapped by a stronger band and its upper state cannot be located accurately.

Levels that resemble each other so much in different compounds must have some important properties in common. The same name should be given to all of them to indicate these properties. Actually, according to any present theories, including the free-electron method used for the interpretation here, we should expect more change than there is in the band characteristics, such as the "forbiddenness" of the ${}^1A - {}^1L_b$ bands, in going from benzene to the unsymmetrical 4-ring systems, and we should expect more mixing and loss of identity of band types than there is in the spectrum of any of these larger systems. Nevertheless, the empirical evidence for distinctness and preservation of identity of band types seems fairly convincing. We can proceed only by taking that evidence at face value in justifying the names and predicting the properties of the different types of states.

(b) Justification of Names

${}^1L_b$

There is a band in benzene at 39,000 cm^{-1}. LCAO theory shows the upper state is a singlet, probably of symmetry B_{2u},[3] though B_{1u} is not ruled out.[2] Assuming B_{2u} is correct, the polarization diagram must have nodal lines through the atoms. This kind of state we have named ${}^1L_b$. If anything like it exists in the larger molecules, it will also be ${}^1L_b$. There is just one similar band found in every aromatic molecule, except where it is expected to be hidden by a stronger one. It always has nearly the same intensity, $\log\epsilon \sim 2.5$, and the same kind of sharp vibrational structure running to about 6 bands, as in benzene. The upper states of these bands, when plotted against the number n of rings, lie on a smooth curve starting with the 39,000 cm^{-1} state of benzene. We therefore call them ${}^1L_b$, and hope that we have guessed correctly the common property.

${}^1L_a$

Similarly, by LCAO theory, the benzene 48,000 cm^{-1} state is ${}^1B_{1u}$,[3] though ${}^1B_{2u}$ is not ruled out.[2] Assuming the former, our diagram must have nodes between atoms. This state lies on a smooth curve with similar levels in the longer molecules. All transitions to these levels have 5 or 6 diffuse bands with $\log\epsilon \sim 3.8$. They are therefore ${}^1L_a$, according to this scheme. The scheme predicts transverse

polarization for ${}^1A-{}^1L_a$ in polyacenes (Fig. 3). This has been found in naphthalene and anthracene.[4,20] This correct prediction is an argument for the correctness of our assumption that ${}^1L_b$ has symmetry ${}^1B_{2u}$ in benzene and that ${}^1L_a$ has symmetry ${}^1B_{1u}$.

$${}^1B_b, {}^1B_a$$

These should be together in benzene and split in the other molecules studied in I. The benzene 55,000 cm^{-1} transition is the strongest in benzene. By LCAO it is allowed and of type ${}^1A_{1g}-{}^1E_{1u}$, which corresponds to our definition of ${}^1A-{}^1B$. It lies on a smooth curve with the strongest transitions in the longer compounds, when plotted against length. With increasing length, these bands have an increasingly sharp first peak followed by two or three weaker diffuse bands. The intensity of transitions on this curve increases with molecular length as expected. In naphthalene and anthracene these transitions are longitudinally polarized.[4,20] They are at the same wave-length as the strong bands of polyenes of the same molecular length (see I). Therefore they have all the properties expected of the longitudinal ${}^1A-{}^1B_b$ bands.

In each of the compounds except benzene another strong band lies higher. Its intensity does not increase much with molecular length. It can therefore be the transverse ${}^1A-{}^1B_a$, which should have this property.

$${}^1C_b, {}^1C_a$$

A band appears between the two ${}^1B$ bands in every compound but benzene. (A band which may be similar appears above the B band in unsymmetrical alkylbenzenes.) It is doubtful in naphthalene, but clear in anthracene, about as strong as ${}^1A-{}^1L_a$. Its intensity increases in the non-centrally symmetric isomers azulene and phenanthrene, becoming about as strong as ${}^1A-{}^1B_a$. Therefore it is possibly forbidden in centrally symmetric molecules. Among the low transitions, this behavior is expected of ${}^1A-{}^1C$ and ${}^1A-{}^1K$ bands. The intensity when it is strong is more like the dipole ${}^1A-{}^1B$ than the multipole ${}^1A-{}^1L$ so it is probably ${}^1A-{}^1C$. Since no similar band appears lower, but one appears higher in the 4-ring systems, the band between the two ${}^1B$ bands can be assigned to ${}^1A-{}^1C_b$ and the higher one to ${}^1A-{}^1C_a$. Presumably the ${}^1A-{}^1K$ bands lie lower but are weaker than ${}^1A-{}^1C$ (and also forbidden in centrally symmetric molecules), and are concealed by the strong ${}^1A-{}^1B_b$ bands or by ${}^1A-{}^1L_a$.

$${}^3L_a$$

The phosphorescent level has been assigned to ${}^3B_{1u}$ (our ${}^3L_a$) in benzene[3] but ${}^3B_{2u}({}^3L_b)$ has not been ruled out.[2] In the whole group of molecules, its separation from ${}^1L_a$ varies smoothly with length, from 19,000 cm^{-1} in benzene to 12,000 cm^{-1} in three- and four-ring systems, and is constant among isomers even when both levels move far. On the other hand, its separation from ${}^1L_b$ varies widely, especially among isomers (cf. anthracene-phenanthrene in Fig. 2). Since the singlet-triplet separation should be roughly constant, this phosphorescent level then must be of the same type as ${}^1L_a$, and so is called ${}^3L_a$. In turn, this is an argument for the assignment of ${}^3B_{1u}$ to the phosphorescent level in benzene, if we accept the reasoning above as establishing the ${}^1L_a$ level as ${}^1B_{1u}$ in benzene.[21]

(c) Identifications and LCAO Predictions

Coulson[4] calculated, by the LCAO method without neglect of overlap integrals, the center of gravity positions and the polarizations of singlet-triplet pairs in polyacenes. If the center of gravity of the lowest transverse pair of bands, as given by the present assignments, is close to his lowest predicted transverse center; and if the observed lowest longitudinal center is close to his predicted lowest longitudinal, then his calculations give a general support to these assignments. This is found to be the case, as was shown in I. Coulson's ignorance of the triplet states and of ${}^1L_b$ caused confusion in his original comparison with the data.

The upper triplets are unknown, so Coulson's calculations must there be compared with the singlets, and they show as good agreement as they do with the lower singlets. (See Fig. 2.) Thus his predicted total spread of the states corresponding to our $f\rightarrow g$ system is about 20,000 cm^{-1} in naphthalene, 30,000 cm^{-1} in anthracene where the total spread of the singlets, according to our identifications, is about 27,000 cm^{-1} in both cases. In his upper two singlet transitions, the longitudinal one should be at lower frequencies. This agrees with the present identifications of ${}^1B_b$ and ${}^1B_a$.

His predictions for the third forbidden transition of $e\rightarrow g$ type in naphthalene and anthracene also lie within about 5000 cm^{-1} of the level we have

[2] R. N. Jones, Chem. Rev. **41**, 353 (1947).

[21] H. Shull at the University of California has also shown from analysis of the phosphorescent band in benzene that it is made allowed by the same types of vibrations as those which would make the ${}^1A_{1g}-{}^1B_{1u}$ band allowed. (Private communication.) The two other independent pieces of evidence in the present paper which show its empirical relation to this singlet band are: (a) the almost constant separation of the phosphorescent band in benzene and the larger molecules from ${}^1A-{}^1L_a$, which we have concluded is probably ${}^1A_{1g}-{}^1B_{1u}$ in benzene; and (b) the good agreement between the center of gravity of this pair of bands in the different molecules and the LCAO calculations—any other pairing would destroy the agreement. Nevertheless, R. S. Mulliken points out that we cannot conclude with certainty that the phosphorescent state in benzene should be labelled ${}^3B_{1u}$ until the theoretical spectroscopic combining properties of corresponding singlet and triplet states have been established.

named correspondingly, ^1C_b. (See Table I.) The two lower forbidden transitions, our $^1A-{}^1K$ bands, should also be weaker according to the present arguments, and have not been found.

Mann's LCAO calculations on the azulene levels[22] also support the identifications, as shown in Fig. 2. The predicted centers of gravity deviate from the singlets in the same direction and about the same amount as the corresponding LCAO predictions deviate in naphthalene. A mistake in identification would have been revealed by large changes in these deviations.

Because of the reversal of polarizations from naphthalene to azulene, Mann's results also confirm the correctness of the nodal properties assumed here in the polarization diagrams for the L bands. In azulene, $^1A-{}^1L_b$ should be transverse, $^1A-{}^1L_a$ longitudinal, as indicated by the diagram in Fig. 3. These bands are identified at 14,000 cm^{-1} and 28,000 cm^{-1}, respectively, by the usual empirical resemblances. Now the LCAO calculation also gives the low singlet-triplet pair as transverse, the next pair as longitudinal. The separation of the pairs is great enough that the sequence of the singlet levels could not reasonably be interchanged from the LCAO-predicted sequence of the pairs, if we remember how accurate the LCAO energy predictions are in the polyacenes (I). Therefore, if the LCAO has predicted these polarizations correctly, then the properties assumed here for the L states also predict them correctly.

The failure of the LCAO predictions of intensities does not much weaken the importance of the good agreement on energies, because intensities are known to be generally much more sensitive to the accuracy of the wave functions than the energies are.

(d) Possible Misidentifications

There are three bands described in I in which there is some question about the identifications according to the present scheme.

The weak band called ^1C_b in naphthalene, and presumed to be forbidden, seems to be still weaker or has moved in acenaphthene, which is essentially an alkyl-substituted naphthalene. One would expect it to be somewhat stronger. On the other hand, the difference in strength is not much larger than the experimental error.

The band called $^1A-{}^1C_b$ in naphthacene, and presumed to be forbidden, becomes stronger in bent 4-ring systems, as it should. However, the band we have called $^1A-{}^1C_b$ is also stronger in chrysene. This molecule again has a center of symmetry, so that this band should again be forbidden. If there is not a mistake in identification, perhaps some interaction with allowed transitions nearby will account for the larger intensity.

On almost any theory, the ^1B state in triphenylene, which has D_{3h} symmetry, should be single and doubly degenerate. However, two strong bands have been found with about the usual $^1B_b-{}^1B_a$ separation, about 10,000 cm^{-1}. The higher band must be of some type other than ^1B_a, but it is not certain what.

These points deserve further study. It does not seem likely that they will invalidate the classification, since the latter is supported by nearly a hundred other identifications in which the band properties and their variations among isomers are correctly predicted.

IV. COMPARISON WITH THE LCAO METHOD: BENZENE

The free-electron method will also be justified by its close basic correspondence with LCAO method in the construction of orbitals and states, in cases where the latter method has been worked out. The comparison will be made for two such cases: benzene and anthracene.

In benzene, one free electron in the loop of perimeter $l=8.4$A would have energies

$$E=17{,}000q^2 \text{ cm}^{-1}.$$

No arbitrary constants are involved in this formula. These one-electron states are plotted in the left half of Fig. 4.

The quadratic spacing with interval ratios 1:3:5 agrees qualitatively with LCAO calculations which include overlap integrals. The latter give the interval ratios 1:4:5, as shown on the right in Fig. 4.[23] If the LCAO bond integral, $-\beta$, is set at 28,000 cm^{-1}, the energies agree within about 10 percent with the free-electron energies. However, a smaller value of β, about 20,000 cm^{-1}, fits the observed states better.[2]

The LCAO theory predicts only four one-electron states, with the top one single, where free-electron model predicts an infinity of higher states, all doubly degenerate. The difference is due to the restriction of LCAO to combinations of atomic p-orbitals. The additional free-electron states correspond to combinations of d- and f-orbitals and so on. The difference is unimportant in practice since the observed spectra involve only the lowest excited states.

On the free-electron model, the classification of the lower states in the six-π-electron benzene problem is as given in Table II.

Excitation of an electron from the f-shell to the g-shell leads to states with $Q=2-1$ and $Q=2+1$, according as the electron and hole q-vectors are

[22] D. Mann, J. R. Platt, and H. B. Klevens, J. Chem. Phys. 17, 481 (1949).

[23] C. C. J. Roothaan, private communication.

added or subtracted. These have angular momentum 1 (B-state) and 3 (L-state) and would correspond to Π- and Φ-states, in diatomic notation, with respect to the 6-fold axis. Because of the high symmetry the B-state is not split, but the L-state is so this configuration gives three singlet and three triplet states.

Four of these six excited states are known as shown in Fig. 2. The group-theory classification is fairly well established[2, 3] except for the triplet whose identity seemed to be established by the arguments of the last section. The position of the other levels has been estimated.[2] The forbidden $^1A - {}^1L$ bands are supposed to become somewhat allowed through vibrational interactions of the proper symmetry.

In the strong allowed transition, the polarization diagram method gives an effective dipole length, Z, about 1/4 of the greatest diameter, or 0.7A. This gives $f=0.59$. This is in fair agreement with the experimental value, 0.79 for the integrated $f \rightarrow g$ transition intensity.[24] Because of the crudeness of the method, only the relative intensity estimate as compared to anthracene (below) is of significance. The relative agreement is fairly good. The LCAO method predicts $f=2.35$.[16] When this is corrected by a standard empirical factor of 0.3, it is in fair agreement with the observed value.

The center of gravity of the levels of the f^3g system in benzene is estimated[2] from the spectrum to lie at about 44,000 cm^{-1} which may be compared with the free-electron prediction of 51,000 cm^{-1}.

V. COMPARISON WITH THE LCAO METHOD: ANTHRACENE

For anthracene, with one free electron on an ideal perimeter loop of length $l=19.6$A, the energies will be

$$E=3150q^2 \text{ cm}^{-1}.$$

Again this quadratic spacing agrees well qualitatively with the increasing spacing found in Coulson's LCAO calculations[4] (Fig. 5).

TABLE II.

Configuration	Free-electron states	Group theory notation
....	....	...
$\ldots f^3g$	$\begin{cases} {}^1B \quad {}^3B \\ {}^1L_a \quad {}^3L_a \\ {}^1L_b \quad {}^3L_b \end{cases}$	$\begin{matrix} {}^1E_{1u} & {}^3E_{1u} \\ {}^1B_{1u} & {}^3B_{1u} \\ {}^1B_{2u} & {}^3B_{2u} \end{matrix}$
$\ldots f^4$	^1A	$^1A_{1g}$

Coulson's orbitals are divided into two groups: without (P, Q) and with (R, S) a longitudinal nodal line; and each of these into two sub-groups: without (P, R) and with (Q, S) a transverse nodal line across the center of the molecule. The free-electron $q=0$ orbital with no nodes corresponds to his P_1. The free-electron degenerate $q=1$ with two nodes on the perimeter corresponds to his two non-degenerate orbitals, Q_1 with nodes at the sides, and R_1 with nodes at the ends of the perimeter. Similarly $q=2$ with 4 nodes on the perimeter corresponds to his P_2 and S_1; and so on. The number of nodes for corresponding levels is the same in the two systems, and the only difference is in the removal of the free-electron degeneracy. The surprising thing is not that the degeneracy is removed, but that the splits are not wider. Thus in naphthalene and anthracene, the LCAO levels are arranged in order of increasing free-electron q; and crossovers occur first in naphthacene. (Coulson's levels for anthracene are accidentally degenerate, as shown in Fig. 5.) By choosing Coulson's LCAO factor $\gamma=23{,}000$ cm^{-1}, the energy predictions of the two schemes agree as shown in Fig. 5. All but two of the 7 excited free-electron states lie between their split LCAO counterparts. The maximum separation of any free-electron state from the center of gravity of its split counterparts is 7000 cm^{-1}.

The lower states of anthracene would then have the correspondence in the two systems shown in Table III.

The identification of the observed states by this system in Fig. 2 differs from Coulson's identifica-

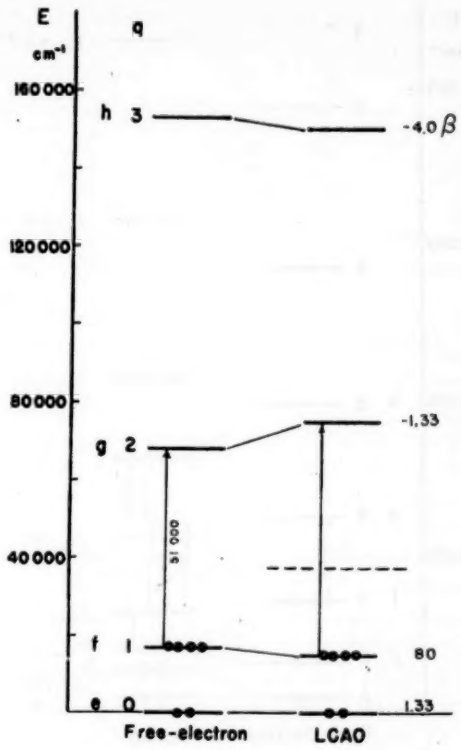

FIG. 4. Comparison of free-electron and LCAO states and shells: benzene.

[24] J. R. Platt and H. B. Klevens, Chem. Rev. 41. 301 (1948).

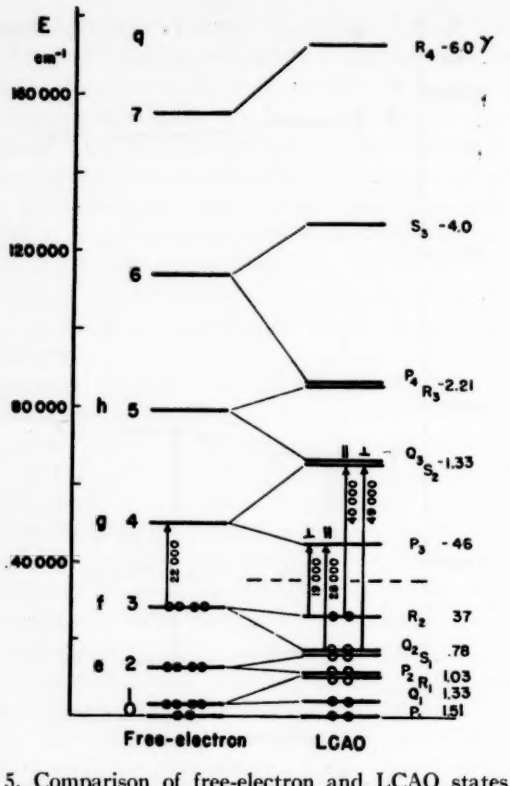

FIG. 5. Comparison of free-electron and LCAO states and shells: anthracene.

tion. Coulson knew only the two singlet bands 26,000 cm^{-1} (experimentally transverse) and 39,000 cm^{-1} (experimentally longitudinal), and naturally identified the latter with his longitudinal $N-V_2$. The identifications of Fig. 2, setting 39,000 cm^{-1} as his R_2-S_2 state and the hidden 28,000 cm^{-1} as V_2, are in much better agreement with his energy predictions, as was shown in I.

If this is correct, his intensity calculations on $N-V_1$ are about ten times too high, and those on $N-V_2$ are several hundred times too high.[1,4] Configurations involving his P_3 state actually make only weak transitions to ground. The qualitative success of the present model would imply that electron interactions, and the mixing of transverse R_2-P_3 with transverse Q_2-S_3, and of longitudinal Q_2-P_3 with longitudinal R_2-S_3, may have to be considered in order to get the correct intensities by LCAO theory.

The free-electron prediction of about 22,000 cm^{-1} for the center of gravity of the f^3g states (Fig. 5) is to be compared with its experimental location near 30,000 cm^{-1}. The frequencies predicted by either method become too low in long chains, as remarked above.

For intensities, the effective dipole lengths may be estimated from the polarization diagram, giving the values shown in Table IV. The $^1A-{}^1B_a$ transition is across the molecule and its dipole length is correspondingly near that of benzene, about 1/4 the width, or 0.7A. The $^1A-{}^1B_b$ transition is along the molecule and its dipole length is taken as 1/4 the chain length. The $^1A-{}^1L_a$ band has a polarization diagram with nodes between the atoms, as seen in Fig. 3. If we think of the end rings as having balanced charges, the remaining center dipole with 1/7 of the charge will give an effective transverse dipole length of about $\frac{1}{7}(\frac{1}{4}\cdot 2.8\text{A})$ or about 0.1A. The $^1A-{}^1L_b$ has a polarization diagram with nodes at the atoms, as seen in Fig. 3. This would give a zero moment if all the effective charges were equal and the rings were perfectly hexagonal, but will give a small longitudinal moment otherwise.

The known polarizations agree with these assignments, and the sequence of intensities is correctly predicted. More accurate calculations do not seem justified without introducing the periodic potential and connecting links, and the vibrations, especially in computing the multipole bands.

It is strange that the benzene $^1A-{}^1L$ transitions should have the same intensities as their counterparts in larger, and even in unsymmetrical, molecules. In the latter there are many mechanisms—variations in bond distance and electron density, the crosslinks, and so on—by which even multipole transitions should gain intensity and "become allowed," just as Coulson expected for the L bands. It is similarly strange that these benzene bands have much the same diffuseness or sharpness as in the larger molecules. It is usually supposed that $^1A-{}^1L_a$ is moderately strong and diffuse in benzene, and $^1A-{}^1L_b$ is weak and sharp, because the former is nearer the allowed transition and more perturbed, or possibly because of predissociation in the former. But $^1A-{}^1L_a$ gets far away from strong allowed transitions in the other molecules and remains moderately strong and diffuse, while $^1A-{}^1L_b$ comes between it and the strong allowed transitions in pentacene, yet remains weak and sharp. It seems improbable that predissociation would occur just

TABLE III. Anthracene: names of states and polarizations of absorption bands abbreviated.

Configuration	Free-electron states (Singlets and triplets)	Coulson notation (Singlets and triplets)	Symmetry species	Polarization of transition to ground
$\ldots d^3e^4f^4g$	D_a	Q_1-S_2	B_{2u}	trans
	D_b	R_1-S_2	B_{1u}	long
	J_b	Q_1-P_3	B_{1u}	long
	J_a	R_1-P_3 or V_4	B_{2u}	trans
$\ldots\ldots e^3f^4g$	C_a	P_2-S_2	B_{3g}	forb
	C_b	S_1-S_2	A_{1g}	forb
	K_b	P_2-P_3 or V_5	A_{1g}	forb
	K_a	S_1-P_3 or V_3	B_{3g}	forb
$\ldots\ldots f^3g$	B_a	Q_2-S_2	B_{2u}	trans
	B_b	R_2-S_2	B_{1u}	long
	L_b	Q_2-P_3 or V_2	B_{1u}	long
	L_a	R_2-P_3 or V_1	B_{2u}	trans
$\ldots\ldots f^4$	^1A	N	A_{1g}	—

at the ^1L_a level in all these molecules, especially since this level moves more widely than any other. Evidently there is more in common in corresponding bands than current theory will allow. This is useful for identification but puzzling.

Possibly all these sources of extra intensity in the larger molecules are negligible, like the ones used in the rough calculations of Table IV, which predicted too low L-band intensities. If this were so, the only important contribution to intensity in these bands would always be the result of vibrations, just as in benzene. Then, since vibration amplitudes and charge densities must be much the same in compounds with similar force constants and masses and π-electron densities, we would have an explanation of the constancy of the L-band properties.

In benzene and anthracene, we see that the free-electron model does not contradict the LCAO method in principle at any point. The only practical divergence is on predicted L-band intensities, but this may disappear when electron interaction is included in the LCAO treatment. No doubt by introducing the periodic potential and making vector-model-type estimates of the size of the electron interactions in the free-electron scheme, we could improve the quantitative predictions and determine the sequence and location of the excited states. This might mean a considerable increase in the ease and accuracy with which we can describe the spectra of unsymmetrical systems.

VI. SPECTRA OF OTHER TYPES OF MOLECULES

The free-electron model can be adapted to classifying other conjugated ring and ring-chain spectra. The kind of classifications required may vary with the type of topological connectedness of the conjugated system. In simple polyene chains, for example, the levels of the first excited configuration reduce to our ^1B_b and ^3B_b, with selection rules and intensities depending only on the bending of the chain and its dimensions.

For ring-chain systems and peri-condensed systems (in which some carbon atoms belong to three rings), study of the spectra[25,25] shows that in many cases the lowest bands still seem to be of B and L types. However, there is more mixing of characters, both vibrational and intensity, just as is expected in the larger cata-systems (Fig. 8 of I). Identification of types is correspondingly less certain in many of the spectra.

We can account for the existence in these molecules of L states and other states giving weak multipole absorption bands, by means of a theorem of Coulson and Rushbrooke.[10] This applies to systems containing rings with only an even number of carbon atoms. By LCAO theory with neglect of overlap, the theorem says that the occupied and unoccupied one-electron states may be classed in pairs with equal and opposite binding energy. Call the members of any pair, a and a'. If we translate this into the language of classical interacting oscillators, state a corresponds to a particular phase difference between adjacent oscillators. Call this difference $(\pi/2)-\alpha$. Then state a' corresponds to phase difference $(\pi/2)+\alpha$. Similarly, translating into free-electron terms, the phase difference in the Schrödinger wave between the two ends of a bond will be $(\pi/2)-\alpha$ in state a, and $(\pi/2)+\alpha$ in state a'.

When an electron jumps from state a to a', the electron and hole momenta in the two-dimensional network may be added or subtracted. This gives two kinds of states, with total momenta corresponding to a phase difference between adjacent carbons of either 2α or π. On the polarization diagram, an absorption band to the state with 2α has only a few nodal lines across the molecule, i.e., it is a dipole or a low "multipole." An absorption band diagram to the state π will have nodal lines either in the middle of every bond, in which case it is like $^1A-{}^1L_a$; or at the ends of bonds, in which case it is like $^1A-{}^1L_b$.

Thus it seems reasonable that the first few singlet bands of the more complicated systems can again be called $^1A-{}^1L_b$, ^1L_a, ^1B_b, ^1B_a. If mixing of characters is strong, a more exact treatment, or perhaps a different kind of approximation, will be required. Probably the first four distinctive bands in the spectrum of pyrene[25] are of these four types. In aniline and styrene there are also four prominent bands.[26] In diphenyl,[26] only three are seen, but the fourth weak one reappears in fluorene, which is a bent alkyl-substituted diphenyl so this weak band may simply be hidden in diphenyl itself.

I must express my especial debt to Herzfeld[27] for his emphasis on the importance of the nodes, and to Mulliken, Longuet-Higgins, and many other colleagues for helpful criticisms and discussion.

Note added in proof: Several very recent applications of the free-electron method are described in a footnote at the end of I.

TABLE IV. Estimated oscillator strengths in anthracene.

Transition	Polarization	Z	ν	f_{est} (free-elect)	f_{obs} (from I)
$^1A-{}^1B_a$	trans	.7A	54,000	0.30	0.65
$^1A-{}^1B_b$	long	1.8A	39,000	1.4	2.28
$^1A-{}^1L_a$	trans	.1A	26,000	.003	.10
$^1A-{}^1L_b$	long	.00A	(28,000)	.0000	(.002) (phenanthrene)

[25] E. Clar, *Aromatische Kohlenwasserstoffe* (Springer-Verlag, Berlin, 1941).
[26] H. B. Klevens and J. R. Platt, unpublished results.
[27] K. F. Herzfeld, Chem. Rev. **41**, 233 (1947).

Letters to the Editor

THIS section will accept reports of new work, provided these are terse and contain few figures, and especially few half-tone cuts. The Editorial Board will not hold itself responsible for opinions expressed by the correspondents. Contributions to this section should not exceed 600 words in length and must reach the office of the Managing Editor not later than the 15th of the month preceding that of the issue in which the letter is to appear. No proof will be sent to the authors. The usual publication charge ($4.00 per page) will be made and no reprints will be furnished free.

A Note on Low Frequency Dispersion in Ionic Crystals

T. B. GRIMLEY
University of Liverpool, formerly of H. H. Wills Physical Laboratory, University of Bristol, Bristol, England
March 1, 1949

IN a recent issue of this journal, Breckenridge[1] has reported a new region of anomalous electrical response in ionic crystals. The response occurs at low frequencies and the behavior of the dielectric constant and the loss angle is typical of a dipole reorientation process. It is the purpose of this note to discuss the mechanism of this polarization in terms of the various lattice defects which may be present in the crystals.

Consider first the alkali halides where the defects are known to be of the Schottky type. Then, since the vacant cation and anion sites bear effective negative and positive charges, respectively, the isolated single vacancies attract each other and a certain proportion of them will coagulate into neutral pairs. This process has been discussed at some length by Seitz[2] who has shown that, on quenching from near the melting point, a large number of defects may be frozen in as neutral pairs of vacancies. The existence of such neutral pairs will give rise to relaxation effects similar to those reported by Breckenridge. The activation energy for the dipole reorientation process is that associated with the motion of the cation vacancy between its six possible positions (Fig. 1). This activation energy must be less than that for the corresponding motion of the anion vacancy and considerably less than the activation energy for the motion of an isolated cation vacancy (~0.83 ev in KCl). Now experimental evidence from the darkening of KCl by x-rays indicates that the activation energy for the motion of the *anion* vacancy of a neutral pair is 0.5 ev or less,[2] while a direct calculation by Dienes[3] on the basis of Born's lattice theory has given a value of 0.38 ev. It appears therefore that with this mechanism of polarization, the activation energy derived from measurements of the dielectric relaxation time should certainly be less than 0.5 ev. The experimental result, however, is 0.78 ev, so that there is a large discrepancy to be faced. This seems to us to be a general feature of the result. The activation energies are altogether too high to enable us to place any confidence in the interpretation of the experimental results in terms of the existence in the lattice of neutral pairs of vacancies.

A second possible mechanism of the polarization arises, however, if there are divalent cation impurities present in the lattice. Vacant cation sites will combine with the oppositely charged impurities to form neutral centers, and again we shall have dispersion effects typical of a dipole reorientation process. With this type of polarizing center, it is not immediately apparent whether the divalent impurity or the vacant cation site will be the more mobile. In either case, however, it is evident that the activation energy will not be markedly different from that of the isolated cation vacancy. We believe therefore that the relaxation effects reported by Breckenridge are not characteristic of the pure material, but depend for their origin on the presence in the lattice of divalent cation impurities.

Turning now to the experimental results for AgCl, we must point out that, contrary to the statement made in the original paper, the discovery of two peaks in the loss angle *cannot* be explained on the hypothesis that Frenkel defects are present in this crystal. The association of an interstitial cation and a vacant cation site in close proximity is clearly unstable, the interstitial cation will be captured by the vacant cation site and the defect annihilated. Crystals containing only Frenkel defects cannot therefore give rise to the observed relaxation effects. The occurrence of two peaks in the case of AgCl must be due to the presence of two species of divalent cation impurity, and the agreement between the values of the activation energy found by this method (0.21 ev and 0.26 ev) and Koch and Wagner's[4] result for the motion of isolated cation vacancies (0.26 ev) is fortuitous.

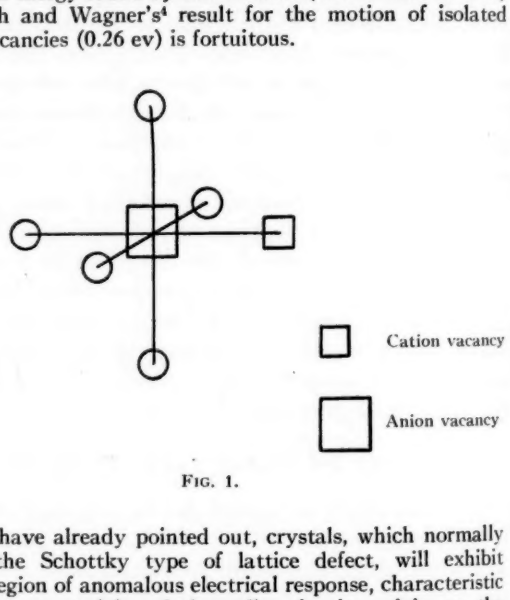

FIG. 1.

As we have already pointed out, crystals, which normally contain the Schottky type of lattice defect, will exhibit another region of anomalous electrical response, characteristic of the pure material and depending for its origin on the presence in the lattice of neutral pairs of vacancies. This region should be observable with the experimental techniques at present available, but we expect the activation energies for the dipole reorientation processes to be roughly half those so far reported. In this respect the behavior of the silver halides is of particular interest, for, as Mitchell[5] has recently pointed out, there is considerable evidence to suggest that the defects normally present in these crystals are actually of the Schottky type. It is to be expected therefore that this second region of anomalous dispersion will be present in these crystals also.

[1] R. G. Breckenridge, J. Chem. Phys. **16**, 959 (1948).
[2] F. Seitz, Rev. Mod. Phys. **18**, 384 (1946).
[3] G. J. Dienes, J. Chem. Phys. **16**, 620 (1948).
[4] E. Koch and C. Wagner, Zeits. f. physik. Chemie **B38**, 295 (1937).
[5] J. W. Mitchell, to be published in Phil. Mag., March 1949.

Micelles in Non-Aqueous Media

R. W. MATTOON* AND M. B. MATHEWS
Department of Chemistry, University of Chicago, Chicago, Illinois
March 25, 1949

SMALL-angle x-ray scattering and electrical transference experiments have been performed on pure di (2-ethylhexyl) sodium sulfosuccinate (Aerosol OT, mol. wt. 444) dissolved in *n*-dodecane; solubilized water has also been added.

TABLE I. Solutions studied.

Solution	Aerosol OT	n-$C_{12}H_{26}$	H_2O	Small-angle x-ray scattering intensity
#A	0 gram	100 grams	0 gram	none
#B	5	95	0	very weak
#C	15	85	0	weak
#D	15	85	1	↓
#E	15	85	2	↓
#F	15	85	5	medium
#G	15	85	20	↓
#H	15	85	26 (saturated)	strong
#I	25	75	0	medium
#J	25	70	5	↓
#K	25	65	10	↓
#L	25	60	15	strong

Ni-filtered Cu K_α x-rays were used in a vacuum camera, previously described,[1] with a flat film 15.0 cm from the solution at 25°C sealed in a rotating Pyrex capillary. All solutions were sealed in glass ampules, were mechanically shaken for equilibration, appeared water-clear, and were optically isotropic at rest.

For the exposures used, pure n-dodecane showed no appreciable scattering, whereas each of the remaining solutions showed scattering which steadily decreased in intensity with increasing scattering angle. The scattering distribution has been compared with the relation discussed by Guinier[2] and others for spheres in solution:

$$I/I_0 = A \exp(-Bk^2R^2); \quad k = 4\pi \sin\theta/\lambda.$$

A and B are constants. With no water present (# B, C, and I, Table I), the radius of the sphere R is about equal to the length of the OT molecule. As the amount of solubilized water is increased (# C−H and I−L), the micelle radius correspondingly increases and may be at least doubled by water addition (# H, L). Under identical experimental conditions the scattering intensity trends are indicated in Table I. Results from rigorous analysis of the films will be reported later.

The critical concentration for the formation of micelles in non-aqueous solvents has been briefly discussed by Arkin and Singleterry.[3] For OT in n-dodecane it is less than 5 weight percent since # B still shows some scattering.

Schulman and Riley[4] have used the term "hydrophilic oleomicelle" for a micelle containing solubilized oil and in a water-continuous phase and "oleophilic hydromicelle" for a micelle containing solubilized water and in an oil-continuous phase. They say their evidence supports the concept of a spherical shape for both types. The present work indicates a spherical shape for OT in n-dodecane. However, from other x-ray work[5] it was concluded that the hydrophilic oleomicelle was a small cylinder two molecular layers thick, partly because superimposed on the exponential scattering was an intermicelle band (I) whose long-spacing increased with dilution and another band (M) whose medium long-spacing was independent of concentration. One reason for the difference in x-ray scattering pattern from the two types of micelles may be that with the oleophilic hydromicelle the outwardly directed paraffin chains of the colloidal electrolyte merge continuously at the sphere surface with the paraffin chain media with no appreciable electron density change whereas with the hydrophilic oleomicelle (cylinder or sphere) there is an abrupt electron density change at the micelle exterior surface.

In a preliminary investigation, the velocity of migration of micelles in an electric field was estimated by direct observation of a moving boundary. The lower portion of a vertical tube was filled so as to cover one electrode with an OT solution to which was added water containing 0.1 percent methylene blue. A visible boundary was then formed by the addition of more solution (without dye) to cover the second electrode. The electric current was measured.

As a first approximation Stokes's law with the force from the electric field was assumed for isolated, charged, spherical particles of uniform radius in an insulating medium. The calculated radius was in agreement with the value from x-ray scattering. The apparent charge per particle was positive and less than unit electronic charge in absolute magnitude. The concentration was about 10^{18} particles per cubic centimeter.

Acknowledgment is made to Professor W. D. Harkins for the use of the x-ray camera.

* Present address: Reseach Laboratory, Procter and Gamble Company, Cincinnati 17, Ohio.

[1] W. D. Harkins, R. W. Mattoon, and M. L. Corrin, J. Am. Chem. Soc. **68**, 220 (1946).
[2] A. Guinier, Ann. de physique **12**, 161 (1939) and later papers.
[3] L. Arkin and C. R. Singleterry, J. Am. Chem. Soc. **70**, 3965 (1948).
[4] J. H. Schulman and D. P. Riley, J. Colloid Sci. **3**, 383 (1948).
[5] R. W. Mattoon, R. S. Stearns, and W. D. Harkins, J. Chem. Phys. **16**, 644 (1948).

Characteristics of 16.5-Minute Y^{94}*

LEON J. BROWN AND SEYMOUR KATCOFF**
Los Alamos Scientific Laboratory of the University of California, Los Alamos, New Mexico

March 21, 1949

DURING a search for short-lived yttrium fission products it was noted that the half-life of Y^{94} was shorter than the 20-min. value reported previously.[1] Therefore a redetermination of the half-life was undertaken.

The isotope was isolated from the fission products of uranium and plutonium. For most of the Y samples, the difficult chemical separation from rare earths was avoided by two methods. In one, advantage was taken of the large difference in range of the yttrium and rare earth fission recoil fragments.[2] By collimating a beam of plutonium fission recoils it was possible to collect on thin films only those whose range was greater than that of any of the rare earth fragments (mass > 139). In the second method uranyl nitrate solution was neutron irradiated for 3 minutes. Within the following 3.5 minutes, barium, yttrium, and rare earth activities were removed from the solution by precipitating $BaCrO_4$ twice and

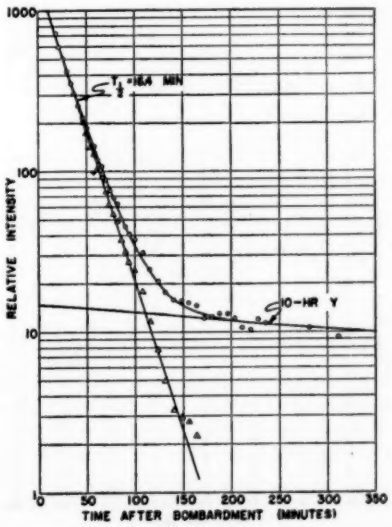

FIG. 1. Beta-decay curve.

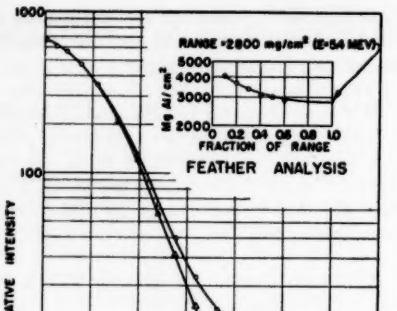

FIG. 2. Beta-absorption curve.

LaF_3 twice. Then after allowing 1.5 minutes for more Y^{94} to grow in from its 2-min. Sr parent, yttrium was isolated from the solution.

From eleven beta-decay curves (Fig. 1) and four gamma-decay curves the average value of the half-life was determined as 16.5±1.0 minutes. The decay curves showed two major components: 16.5-min. Y and 10-hr. Y. In most cases a very small amount of an intermediate component appeared also, probably 3.5-hr. Y. The latter introduced some uncertainty into the resolution of the decay curves. By irradiating for no more than 10 minutes and by doing the analyses within a few minutes after the irradiations, the amount of 3.5-hr. Y which grew from its 2.7-hr. Sr parent was kept very low. However, it could not be eliminated entirely. The decay curves published by Hahn and Strassmann[1] show the 3.5-hr. component in considerably higher relative intensity. This may be an indication of rare earth contamination since a 3.7-hr. La is known. The greater value of 20 minutes they report for the half-life of Y^{94} may have been caused by contamination with 19-min. La and other rare earth isotopes.

The γ-ray intensity seemed to decay with a slightly shorter half-life (15.5 min.) than the β-ray intensity (16.7 min.)

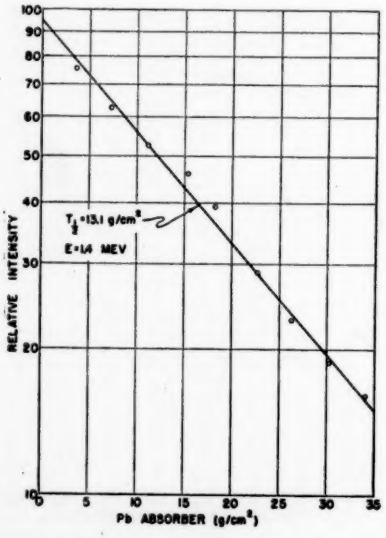

FIG. 3. Gamma-absorption curve.

Although the difference was within experimental error, the possibility of the existence of two Y isotopes with similar half-lives and radiations was considered. This appears improbable because the half-lives obtained were the same whether the samples were isolated directly from fission recoils or from the strontium parent(s). The assumption of two Y isotopes would imply that their half-lives are almost identical and/or that both have strontium parents of approximately equal half-lives. Either situation is unlikely.

The beta- and gamma-radiations were investigated by following the decay of several samples through a series of Al and Pb absorbers using a mica window (3 mg/cm²) Geiger-Mueller counter. From the resolved decay curves the absorption curves shown in Figs. 2 and 3 were constructed. The Feather analysis of the aluminum absorption curve indicates a range for the beta-rays of 2800 mg Al/cm², corresponding to a maximum energy of 5.4 Mev. The half-thickness in lead for the gamma-rays is 13.1 g/cm², corresponding to an energy of 1.4 Mev. The Y samples used for the γ-ray absorption curve were isolated directly from an irradiated uranyl nitrate solution. Standard rare earth separations were used only in this case. It was found that six potassium rare earth double sulfate precipitations were needed in order to remove rare earths sufficiently. Praseodymium and neodymium carriers were added as well as lanthanum.

* This document is based on work performed at Los Alamos Scientific Laboratory of the University of California under Government Contract W-7405-eng-36.

** Now at Brookhaven National Laboratory, Upton, Long Island, New York.

[1] O. Hahn and F. Strassmann, Zeits. f. Physik **121**, 729 (1943).
[2] Katcoff, Miskel, and Stanley, Report LA-659 (Feb. 1948).

The Absolute Configuration of *d*-Tartaric Acid

JÜRG WASER
The Rice Institute, Houston, Texas
March 11, 1949

IT is well known that the usual x-ray data alone do not permit a distinction between the two possible enantiomorphic structures of an optically active crystal. It seems to have escaped general notice, however, that in favorable cases such an assignment may be made if the face development of the crystal is taken into consideration.

The crystal structure of *d*-tartaric acid published recently by Beevers and Stern[1] makes possible an absolute determination of the structural configuration of the *d*-tartaric acid molecule. This is all the more important, as an assignment of absolute configuration to a molecule related to tartaric acid and therefore to a whole class of optically active molecules on the basis of a physical theory of optical activity,[2] seems to be open to criticism.[3]

Figure 1 represents a projection onto the (100) plane of the structure of *d*-tartaric acid as determined by Beevers and Stern.[1] The *a* axis is oriented towards the reader, the *b* axis to the right, and the *c* axis up (although the possibility is left open by Beevers and Stern[1] that the *b* axis might point to the left). The van der Waals radii of carbon and oxygen were chosen to be 1.4A and 1.6A, respectively, and the hydrogen atoms were omitted. The molecules drawn with heavy lines lie above the others to which they are related by twofold screw axes in the *b* direction. A molecule in the upper left shows in detail the relationship between the carbons and oxygens except for one concealed carboxyl oxygen. Figure 2 shows the habits of the monoclinic hemihedral crystals of dextro-rotatory (*d*+) and of levo-rotatory (*l*−) tartaric acid. The monoclinic angle between the faces (100) and (001) is 100° 17′ in either crystal. The orientation of the *b* axis is the same in the two figures.

The important distinguishing feature is seen to be the appearance of the right sphenoid (011) (faces (011) and (01$\bar{1}$)) on dextro-rotatory tartaric acid and of the corresponding left sphenoid on levo-rotatory tartaric acid. It is apparent that the structure of Fig. 1 corresponds to the face development of the dextro-rotatory tartaric acid crystal. A molecular arrangement as drawn would tend to develop the faces (011) and (01$\bar{1}$) whose traces are shown in Fig. 1. The rate of growth perpendicular to these faces would be low, due to the unfavorable orientation of the molecules. For instance, a molecule approaching from the right a completed layer bounded by the plane (011) (Fig. 1) would have to be oriented properly within a narrow margin to be able to form the one or two hydrogen bonds that will hold it in position. Furthermore, only this one, or these two, hydrogen bonds will keep the molecule from breaking loose again before further supporting molecules have been captured in its neighborhood by the surface. The resulting low rate of crystal growth normal to (011) will cause the face (011) to develop very prominently. The non-appearance of the faces (0$\bar{1}$1) and (0$\bar{1}\bar{1}$) is, on the other hand, due to rapid crystal growth normal to the corresponding planes. Let, for instance, a crystal be bounded by the layer of molecules to the right of the trace of (011) in Fig. 1 (this trace

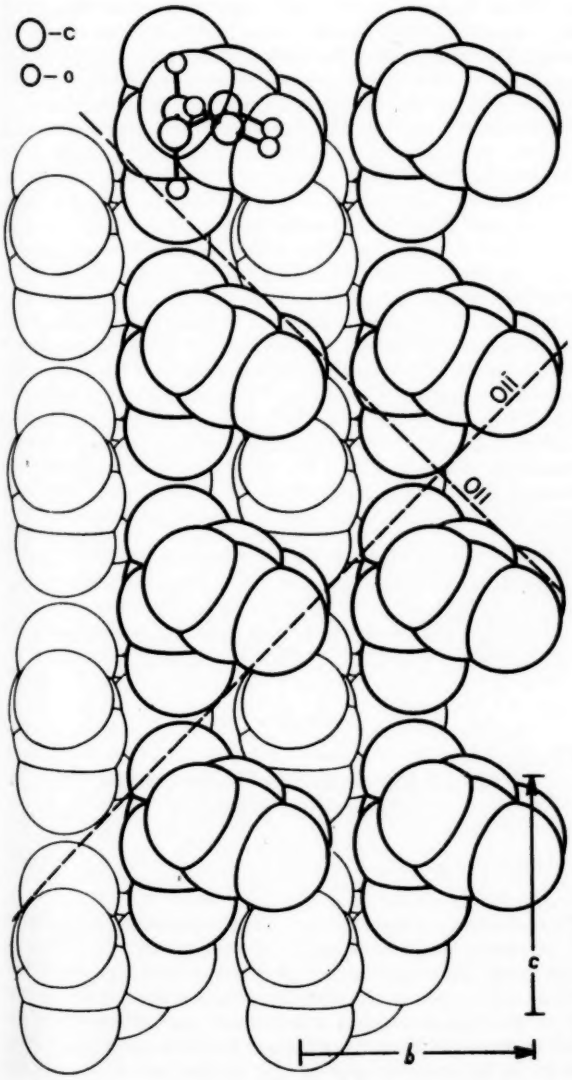

FIG. 1.

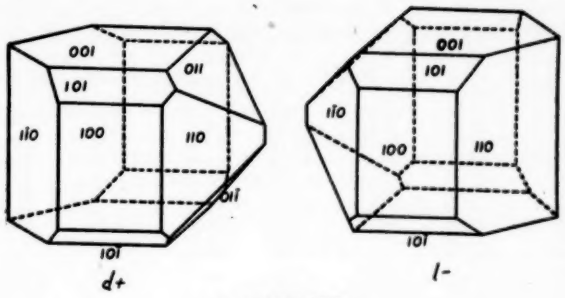

TARTARIC ACID

FIG. 2.

would thus actually correspond to the face (0$\bar{1}\bar{1}$)). A molecule approaching from the left would eventually be bonded to the surface by three or four hydrogen bonds and would be captured and swing into position from a much wider range or orientation than was the case for the (011) face. The face (1$\bar{1}$0), can also be visualized in Fig. 1. It intersects the figure plane parallel to the c axis, for instance along the left-hand margin of the figure, and slants down from the right to the left.

The absolute configuration of dextro-rotatory tartaric acid is therefore that given by the molecule in the upper left corner of Fig. 1 or, if represented by the projection formula,[4]

$$\begin{array}{l} {}^{1}\mathrm{COOH} \\ | \\ \mathrm{H}\text{—}{}^{2}\mathrm{C}\text{—}\mathrm{OH} \\ | \\ \mathrm{HO}\text{—}{}^{3}\mathrm{C}\text{—}\mathrm{H} \\ | \\ {}^{4}\mathrm{COOH}, \end{array}$$

by the provision that the hydroxyl groups and methylene hydrogens are to lie below the plane containing carbon atoms 2 and 3 and the carboxyl groups to lie above that plane. This is just the opposite configuration from the one assigned by E. Fischer[4] on a postulatory basis.

A determination of absolute configuration on the basis of the pyroelectric effect[5] would involve an assumption about the charge distribution in the molecule and require a knowledge of the position of the hydrogen atoms.

[1] C. A. Beevers and F. Stern, Nature **162**, 854 (1948).
[2] W. Kuhn, Zeits. f. physik. Chemie **B31**, 23 (1936); Naturwiss. **26**, 289 (1938); J. G. Kirkwood, J. Chem. Phys. **5**, 479 (1937); **7**, 139 (1939); Gorin, Walter, and Eyring, J. Chem. Phys. **6**, 824 (1938).
[3] E. Hückel, Zeits. f. Elektrochemie **50**, 13 (1944); W. Kuhn and R. Rometsch, Helv. Chim. acta **27**, 1346 (1944), p. 1363; R. Rometsch and W. Kuhn, *ibid.* **29**, 1483 (1946).
[4] See e.g., K. Freudenberg, *Stereochemie* (Leipzig und Wien, 1933), p. 662ff.
[5] See e.g., P. Groth, *Physikalische Krystallographie* (Leipzig, 1895), p. 353.

Thermodynamic Functions of CH_3SH and $(CH_3)_2S$

JOHN L. BINDER
Akron, Ohio
March 9, 1949

SOME time ago the writer had occasion to compute the thermodynamic functions of methyl mercaptan and dimethyl sulfide for use in equilibrium studies. In view of the present interest in sulfur compounds it seemed desirable to present the results of these calculations in an abbreviated form now for the use of others. A more complete discussion of the calculations will be published later.

The entropies, free energies, heat capacities, and heat contents were calculated for several temperatures by the usual statistical methods. The hindered rotation potentials,

TABLE I.

	CH_3SH					
$T°K$	S^0	$-(F^0-H_0^0)/T$	C_p^0	$(H^0-H_0^0)/T$	$H^0-H_0^0$	$\Delta Ff^0(S_{rh})$
298.16	60.86	51.16	12.12	9.70	2892	−989
300	60.94	51.23	12.15	9.71	2913	−971
400	64.67	54.10	14.11	10.57	4228	+208
500	68.08	56.60	15.96	11.48	5740	1641
600	71.13	58.76	17.62	12.37	7422	3228
700	73.96	60.73	19.08	13.23	9261	4952
800	76.59	62.55	20.38	14.04	11232	6778
900	79.06	64.25	21.53	14.81	13329	8703
1000	81.38	65.85	22.54	15.53	15530	10714
1100	83.58	67.37	23.43	16.21	17831	12800
1200	85.64	68.80	24.21	16.84	20208	14951
1300	87.60	70.17	24.89	17.43	22659	17174
1400	89.47	71.49	25.49	17.98	25172	19416
1500	91.25	72.75	26.00	18.50	27750	21783

TABLE II.

	CH_3SCH_3					
$T°K$	S^0	$-(F^0-H_0^0)/T$	C_p^0	$(H^0-H_0^0)/T$	$H^0-H_0^0$	$\Delta Ff^0(S_{rh})$
298.16	68.25	55.69	17.00	12.56	3745	+2096
300	68.36	55.77	17.15	12.59	3777	2160
400	73.75	59.64	20.25	14.11	5644	5899
500	78.55	62.92	23.27	15.63	7815	10029
600	82.99	65.90	26.07	17.09	10254	14361
700	87.19	68.66	28.56	18.53	12971	18860
800	91.15	71.23	30.76	19.92	15936	23493
900	94.91	73.69	32.68	21.22	19098	28218
1000	98.47	76.01	34.35	22.46	22460	33045
1100	101.84	78.23	35.82	23.61	25971	37941
1200	105.03	80.34	37.10	24.69	29628	42912
1300	108.02	82.33	38.22	25.69	33397	47976
1400	110.88	84.28	39.17	26.60	37240	53035
1500	113.61	86.13	40.01	27.48	41220	58213

1460 cals./mole. for CH_3SH and 1900 cals./mole. for $(CH_3)_2S$ were obtained from the measured entropies.[1,2]

The free energies of formation of the two compounds were computed by means of the free energy functions of the reactants and products after determining ΔH_0^0 for the reactions. ΔH_0^0 was found, in each case, from Karasch's[3] heat of combustion data and Kelley's[4] data on sulfur compounds along with the functions computed here. For CH_3SH, $\Delta H_0^0 = -17{,}172$ cals./mole and for $(CH_3)_2S$, $\Delta H_0^0 = -20{,}172$ cals./mole. The data for the thermodynamic functions are accurate to 0.01 or 0.02 unit but the results for the free energies of formation may differ by as much as perhaps 10 percent from those obtained using more accurate data for the heats of formation of methyl mercaptan and dimethyl sulfide now available.

A summary of the calculations is given in Tables I and II.

[1] Russell, Osborne, and Yost, J. Am. Chem. Soc. **64**, 165 (1942).
[2] Osborne, Doescher, and Yost, J. Am. Chem. Soc. **64**, 169 (1942).
[3] J. Research Nat. Bur. Stan. **2**, 359 (1929).
[4] *Thermodynamic Properties of Sulfur and Its Inorganic Compounds*, Bureau of Mines Bulletin 406 (Washington, 1937).

Evaporation of Polar Hydrocarbon Monolayers*

J. KARLE
U. S. Naval Research Laboratory, Washington, D. C.
March 21, 1949

MONOLAYERS of cerotic acid and *n*-octadecylamine were produced on soda glass from the melt of the pure compounds.[1,2] The rate of evaporation of these films in vacuum was studied by means of the rate of decrease of scattered electron intensity relative to that of the substrate. It was found that throughout the course of the evaporation the structure of the films did not change. For example, analysis of the diffraction patterns[3,4] from cerotic acid on soda glass showed that the angle of tilt of the molecules remained at $25\pm3°$ throughout the course of the evaporation. The molecules of *n*-octadecylamine did not vary from a vertical position by more than 5°. This implies that the films exist as patches on the surface with evaporation occurring mainly from the edges of the patches. If evaporation occurred from within the patches an increase in the angle of tilt should be expected as the evaporation proceeds. This result is of interest since Epstein has also found evidence for a patch-work structure by means of electron microscope studies.[5]

The main purpose of the evaporation experiments was to study the evaporation at various temperatures in order to evaluate the energy of activation and relate this energy to the binding energy of the molecules to each other and to the surface of attachment. It was found that when the relative amount of material evaporated was small, thereby maintaining the ratio of the number of molecules on the perimeter of a patch to those within a patch approximately constant, that the evaporation rate followed the rate equation for a first-order reaction. The specific reaction rate for a particular temperature can be found from the slope of a plot of the logarithm of the intensity of scattering *versus* the time. From the theory of reaction rates, the specific reaction rate, k, is given by

$$k = Ae^{-E/RT},$$

where E is the activation energy and A is the frequency factor which does not change very rapidly with temperature. The activation energy for the endothermic evaporation process may therefore be calculated from a determination of k at two different temperatures. The endothermic activation energy is composed of the activation energy for the exothermic process, usually a small part of the total energy, plus the energy of binding of the evaporating molecule. The energy of binding involves the energy of attachment of the polar group to the surface plus forces which may exist between the molecule and its neighbors. Application of this method to a film of cerotic acid on soda glass gave a value of 6 kcal. for the activation energy for evaporation. This value may be compared to a value of about 20 kcal., for the energy of binding of a molecule of cerotic acid within a film on Pt estimated from the work of Bigelow, Glass, and Zisman.[6] The difference is more than can be accounted for on the basis of the different energies of adsorption for a carboxyl group on glass and platinum. The value for a carboxyl group on Pt is estimated to be about 6 kcal.[6] We therefore have further evidence for evaporation taking place mainly on the perimeter of the patches since the activation energy is only a fraction of the binding energy for a molecule within the film and therefore only a fraction of the bonds has to be broken for evaporation to take place.

* Presented at the A.S.X.R.E.D. Meeting, Ste. Marguerite Station, Quebec, June 23, 1947.
[1] Bigelow, Pickett, and Zisman, J. Coll. Sci. **1**, 513 (1946).
[2] L. O. Brockway and J. Karle, J. Coll. Sci. **2**, 277 (1947).
[3] Jerome Karle, J. Chem. Phys. **14**, 297 (1946).
[4] J. Karle and L. O. Brockway, J. Chem. Phys. **15**, 213 (1947).
[5] H. T. Epstein, Bull. Am. Phys. Soc. **24**, (No. 3) 9 (1949).
[6] Bigelow, Glass, and Zisman, J. Coll. Sci. **2**, 563 (1947).

Note on the Selection Rules for Ions in Crystalline Surfaces

MARCEL W. NATHANS
Department of Chemistry, University of California, Berkeley, California
March 21, 1949

IN a theoretical investigation of the electronic energy states of ions in the interior and in the surface of a crystal it has been found that the number of distinct levels in the surface will be larger than in the interior, provided that in the interior all of the degeneracy has not already been removed. It has also been found that the absolute energies of corresponding states in the interior and in the surface are different. The entire treatment will be published shortly.

TABLE I.

$L=$	$4p$	$4p+1$	$4p+2$	$4p+3$
Γ_1	$p+1$	$p+1$	$p+1$	$p+1$
Γ_2	p	p	p	p
Γ_3	p	p	$p+1$	$p+1$
Γ_4	p	p	$p+1$	$p+1$
Γ_5	$2p$	$2p+1$	$2p+1$	$2p+2$

In general, if the z axis is chosen normal to the surface, any state whose degeneracy in the interior is due to the equivalence of the z and x (and/or y) axes, will be split in the surface. For example, in a hydrogen-like ion, the state $n=2$ is split into two states in a field of cubic symmetry, namely a $2-s$ state and a doubly degenerate $2-p$ state.[1] In the surface of a cubic crystal, where the z axis is no longer equivalent to the other axes, the p state undergoes a further splitting into a single level ($m=0$) and a degenerate level ($m=\pm 1$). It will be true in general that all levels belonging to states for which $m=0$ are single. Moreover, these states have the same symmetry properties in the surface, namely they are all totally symmetric with respect to all symmetry operations for the surface field. Therefore, it is possible that all these states mix; in that case, the matrix elements of the z component of the dipole moment between two states with different principal quantum number but with (apparently) the same azimuthal quantum number will not vanish and transitions with $\Delta l=0$ become possible, in particular $s-s$ transitions.

This can be generalized for the case of atoms and ions with any number of electrons by applying the group theoretical method developed by Bethe[1] to the energy levels of an ion in the surface. In the surface the highest possible symmetry is C_{nv}, where $n=2$, 3, 4, or 6. For all values of L and all integral values of J one can show that the totally symmetric representation is contained at least once in the $2L+1$-, $2J+1$-dimensional representation of the three-dimensional rotation-reflection group. The procedure is exactly the same as Bethe's. Because Bethe does not give the characters for the classes consisting of reflections, they will be given here. Since all planes of reflection pass through the z axis, which is considered normal to the surface, the effect of a reflection in one of these planes is merely the replacement of a right-handed coordinate system by a left-handed system. Therefore, $P_1^m(\cos\vartheta)e^{im\varphi}$ will go over into $P_1^m(\cos\vartheta)e^{-im\varphi}$, but $P_1^0(\cos\vartheta)$ will go over into itself. Therefore, the characters of the symmetry classes which consist of these reflections are all $+1$. Once these characters have been obtained it is simple to reduce the $2L+1$-, the $2J+1$-dimensional representations of the rotation-reflection group. If, for example, the symmetry of the crystal is cubic, the 100-plane has C_{4v}-symmetry. This group has five symmetry classes and eight elements. Therefore, there are four one-dimensional representations and one two-dimensional representation. Following Bethe[1] these shall be called Γ_1, Γ_2, Γ_3, Γ_4, and Γ_5. Γ_1 is the totally symmetric representation. In Table I the frequency of occurrence of these irreducible representations has been given. In this table, p may be any positive integer.

This result is remarkable in one respect. Although the C_{4v} and D_4 groups are isomorphic, the $2L+1$-dimensional representations reduce differently in the two groups.

Physically it is clear that all states which have axial symmetry about the z axis, i.e., states for which M_L or M_J are zero, and which do not depend on φ, are symmetric with respect to all operations of the groups C_{nv}. It follows that the matrix elements connecting these states will in general not vanish. Mixing of states with different L (or J) values will, therefore, be more pronounced for the surface than for the inside of a crystal. In this case, the matrix elements of the z components of the dipole moments between these states will in general not vanish. Consequently, a breakdown of the selection rules for L or J in the surface will take place to a considerably higher extent than in the inside of a crystal. In particular the transition $J=0\rightarrow 0$ may become allowed. A quantitative investigation of the change in the absolute transition probabilities has not yet been made.

The application of this to the absorption spectra of rare earth ions in crystals is evident. It reopens the question of the cause of the additional lines observed in reflection over that found in absorption, which was originally reported by Freed and Spedding.[2] The explanation proposed by Spedding and Baer[3] that the additional lines were due to a "filter effect" has been generally accepted. Unquestionably both effects play a role. At present, it is not possible to evaluate the relative importance of each.

[1] H. Bethe, Ann. d. Physik **3**, 133 (1929).
[2] S. Freed and F. H. Spedding, Phys. Rev. **39**, 212 (1930).
[3] F. H. Spedding and R. S. Baer, Phys. Rev. **39**, 948 (1932).

The Infra-Red and Raman Spectra of Chlorine Trifluoride*

E. A. JONES, T. F. PARKINSON, AND R. B. MURRAY**
K-25 Research Laboratories, Carbide and Carbon Chemicals Corporation, Oak Ridge, Tennessee
February 28, 1949

THE Raman spectrum of liquid chlorine trifluoride and the infra-red absorption spectrum of the gas in the 2 to 25 μ-region have been investigated. Material from two commercial sources was used. Purification by fractional distillation may not have been entirely successful, and it is possible that some of the infra-red bands currently listed may be due to impurities.

The infra-red data from 2 to 15 μ were obtained with a Perkin-Elmer Model 12B automatic recording spectrometer with NaCl optics. The 15 to 25 μ-region was mapped with a KBr prism in a similar spectrometer. Fluorothene[1] absorption cells with NaCl or KBr windows as described in another letter[2] were used in the infra-red investigation. A fluorothene Raman tube suitable for handling highly corrosive materials was developed for this work. Technical details on the use of fluorothene in infra-red and Raman spectroscopy are scheduled for publication in the near future.

The Raman spectrum of the liquid was obtained with a Lane Wells Spectrograph, Type 40-A, and Excitation Unit Type 60-A. Because of absorption of ClF_3 in the 4047A and 4358A regions, it was necessary to use Hg 5461A as the exciting line. Exposure times were of the order of several hours. Raman tubes were supported vertically in an unsilvered Dewar flask and were cooled by a stream of nitrogen which had passed through a coil immersed in liquid nitrogen. The sample was maintained at approximately -60°C. The filter used was an aqueous solution of neodymium nitrate contained in an outer jacket of the Dewar flask.

TABLE I. Infra-red and Raman frequencies in the ClF_3 spectrum.

Infra-red bands (gas) cm^{-1}	Raman lines (liquid) cm^{-1}
	321 v.w.
485 m.s.	424 v.w.
540 m.s.	
630 m.w.	502 v.s.
710 v.s.	514 v.s.
741 m.s.	
759 m.s.	753 m.s.
848 v.w.	
888 v.w.	
952 v.w.	
1028 v.w.	
1110 m.s.	
1235 m.s.	
1265 m.s.	

The results of both Raman and infra-red measurements are given in Table I. Intensities are specified as v.s., s., m.s., w., and v.w., representing very strong, strong, medium, weak, or very weak, respectively. The presence of five Raman frequencies is surprising since the expected pyramidal or planar models should have four and three Raman active frequencies, respectively. These considerations suggest either an unsymmetrical form or more probably association in the liquid state. Studies of ClF_3 in the gaseous phase are planned for the near future. A more complete account of the experimental details and an analysis of the results will be published later.

We wish to express appreciation to Professor A. H. Nielsen of the University of Tennessee, and Dr. J. S. Kirby-Smith of the K-25 Research Laboratories for assistance and direction in this investigation, and to the Department of Physics at the University of Tennessee for the use of the infra-red spectrometer which made possible the study of the 15 to 25 μ-region.

* This document is based on work performed for the AEC by Carbide and Carbon Chemicals Corporation, Oak Ridge, Tennessee.
** Now at the Ohio State University, Columbus, Ohio.
[1] Polytrifluorochloroethylene.
[2] P. J. H. Woltz and E. A. Jones, J. Chem. Phys. **17**, 502 (1949).

The Infra-Red and Raman Spectra of Carbonyl Fluoride*

PATRICIA J. H. WOLTZ AND E. A. JONES
K-25 Research Laboratories, Carbide and Carbon Chemicals Corporation, Oak Ridge, Tennessee
February 28, 1949

THIS letter is a preliminary report on the investigation of the infra-red and Raman spectra of carbonyl fluoride. The samples thus far studied were prepared in this laboratory and may contain some impurities. Further samples are being prepared, and investigation of possible impurity or decomposition product content is being made.

The infra-red spectrum of gaseous F_2CO was recorded on a Perkin-Elmer Model 12B infra-red spectrometer. A NaCl prism was used to scan the 2 to 15 μ-region. The measurements from 15 to 25 μ were made with a similar spectrometer having KBr optics. Considerable difficulty was encountered in handling the F_2CO because of its great instability. An absorption cell 10 cm long and 4 cm inside diameter was constructed of fluorothene[1] plastic and found satisfactory. Windows of NaCl and KBr were sealed to this cell with fluorothene-W. A transfer system for filling the cell was constructed of copper and fluorothene. Observations were made with a variety of gas pressures ranging from 2 mm for the most intense absorption to 760 mm for the weakest. A number of different slit widths was used for each band in order to get the optimum resolution. Sixteen absorption bands were observed, six of which were considerably more intense than the rest. These have been named the fundamentals, though definite assignment of the normal modes has not yet been made.

For the Raman spectrum measurements on liquid F_2CO, a specially designed Raman tube[2] of fluorothene was used to contain the sample. The F_2CO was maintained in the liquid state by blowing a stream of nitrogen, which had been passed through a coil immersed in liquid introgen, over the Raman tube. A Lane-Wells Spectrograph No. 40-A was employed for these measurements. The exciting radiation was the 4358A line of Hg filtered through a jacket containing DuPont Rhodamine 5 GDN Extra plus *p*-nitrotoluene in ethyl alcohol. The exposure times ranged up to three hours.

Table I lists the infra-red bands and Raman lines observed up to the present time. The molecule is taken to be planar, of the same type as H_2CO and Cl_2CO. This model has six fundamental modes, all of which are Raman and infra-red active. Those bands marked with an asterisk are believed to be the fundamental vibrations. An estimate of the intensities designated by v.s., s., m.s., w., v.w., meaning very strong, strong, moderately strong, weak, very weak, respectively, is also given in the table. With the exception of the band at 626 cm^{-1}, which appears to have doublet structure, the fundamental bands have well defined *P*, *Q*, and *R* branches. An attempt to make vibrational analysis of these data is in progress.

TABLE I. Infra-red and Raman frequencies in the spectrum of carbonyl fluoride.

Infra-red bands (gas) cm^{-1}		Raman lines (liquid) cm^{-1}
4120 v.w.	1941* v.s.	1944 v.w.
3882 w.		1909 m.
3696 v.w.		
3403 v.w.	1249* v.s.	1238 v.w.
3163 v.w.	965* s.	965 s.
2887 w.	775* s.	771 v.w.
2682 v.w.	626* m.s.	620 m.
2472 w.	584* m.s.	571 w.

We are indebted to the Physics Department at the University of Tennessee for the use of the infra-red spectrometer with KBr optics and to Mr. Wilbur Simon for the preparation of the samples used in this investigation. A detailed report on the preparation and handling of carbonyl fluoride will be published elsewhere. Grateful acknowledgment is made of the assistance and direction given by Professor A. H. Nielsen of the University of Tennessee and by Dr. J. S. Kirby-Smith of the K-25 Research Laboratories.

* This document is based on work performed for the AEC by Carbide and Carbon Chemicals Corporation, Oak Ridge, Tennessee.
[1] Polytrifluorochloroethylene.
[2] Jones, Parkinson, and Murray, J. Chem. Phys. **17**, 501 (1949).

The Exchange of Ag^+ Ions between Aqueous Solutions and Surfaces of Metallic Silver

C. C. COFFIN AND I. I. TINGLEY
Chemistry Department, Dalhousie University, Halifax, Nova Scotia, Canada
March 2, 1949

THE exchange of Ag^+ ions between solutions of silver nitrate and surfaces of metallic silver is being studied with a radioactive isotope (Ag^{110}, half-life 225 days). On the basis of measured areas, etched and polished surfaces of annealed silver foil exchange with 0.1*N* $AgNO_3$ solutions to depths of about 10 and 100 atomic layers, respectively. Inactive crystalline (etched) surfaces pick up their maximum activity from stirred oxygen-free active (40,000 counts per minute per ml) solutions in a matter of seconds; under the same conditions polished surfaces acquire about 90 percent of their final equilibrium activity in 24 hours. Polished surfaces made active in this way, and immersed in non-active solutions, lose about 25 percent of their activity at roughly the same rate as they had acquired it. No decrease in the remaining activity occurs during a week's stirring in the non-active solution. Under similar conditions, crystalline surfaces appear to retain their entire activity which, however, is so low (10–20 counts above background) that the experimental results are highly uncertain.

Etched surfaces of unannealed foil, or of annealed foil that has been cold-worked in various ways, show visually distinct patterns of crystalline and "non-crystalline" metal. The latter appears as light smooth streaks or patches (depending on how the specimen was cold-worked) on the uniformly dark gray crystalline metal. (The term non-crystalline is used here to designate the condition sometimes referred to as the Beilby

or polish layer, the vitreous, amorphous, or cold-worked state, etc.) Such "mixed" surfaces, although they may be largely crystalline, pick up activities commensurate with those acquired by highly polished surfaces (100–200 counts per min. per cm²), and give autoradiographs showing that this activity is largely confined to the crystalline areas. This means that crystalline silver, which by itself shows little tendency to exchange with ions in solution, receives a deposit of metal when it is mixed with non-crystalline silver. This must be the result of an electrolytic action in which ions enter the solution from the anodic worked areas and deposit from solution on the cathodic crystalline surface. However, many attempts to increase the activity take-up of an etched annealed foil by connecting it electrically with a polished foil in the same solution have been fruitless. It would seem that the potential differences involved are so small that they are effectively short-circuited by imperfections in the polish layer.

The fact that polished surfaces slowly acquire a partially removable activity and that considerable activity is picked up by the smooth anodic areas of a mixed surface suggests to the writers that two exchange mechanisms are involved. One of these, the electrochemical, discussed above, accounts for the greater part of the activity acquired by the crystalline areas of a mixed surface. The other, kinetic in nature, is responsible for the activity taken up by polished surfaces and the anodic non-crystalline areas of cold-worked specimens. The enhanced reactivity and solvent properties of metals brought about by polishing and cold-working are well known, and it is probable that such surfaces would take part in exchanges that are impossible for crystals. Preliminary experiments on the pre-treatment of surfaces in non-active solutions indicate that it is possible to separate these two effects. Other tracer experiments on corrosion of metals, the autoradiographic measurement of small potentials, and the phenomena of cold-working are in progress. Details are being published in the Canadian Journal of Research.

Financial assistance from the National Research Council of Canada is gratefully acknowledged.

Note on Steric Factors for Some Reactions Involving Free Radicals*

TERRELL L. HILL
Department of Chemistry, University of Rochester, Rochester, New York
March 21, 1949

FOR purposes of possible comparison with experimental results from this Laboratory to be reported later, we have calculated steric factors for several reactions involving free radicals, using the theory of absolute reaction rates of Eyring and others.

I. An approximate calculation for the reaction,

$$CH_3+CH_3COCH_3\rightarrow CH_4+CH_2COCH_3, \tag{1}$$

leads to $P=2\times10^{-4}$ (the accuracy is such that the possible range is about $6\times10^{-4}-6\times10^{-5}$). It is probably not worth while to give the details of the calculation, but we might indicate the general features. We write, in the usual notation,

$$k=\kappa(kT/h)(F^{\ddagger}/F_AF_B)\exp(-E_0/kT), \tag{2}$$
$$=f(T)\exp(-E_0/kT). \tag{3}$$

We define the experimental activation energy E_{exp} by

$$E_{exp}\equiv kT^2(d\ln k/dT) \tag{4a}$$
$$=E_0+kT^2(d\ln f/dT). \tag{4b}$$

The steric factor P is not a fundamental quantity in the theory of absolute reaction rates. However, one can obtain a value for P by comparing the collision theory expression

$$k=PZ\exp(-E/kT),\quad E=E_{exp}-\tfrac{1}{2}kT, \tag{5}$$

with Eq. (3), using Eq. (4b) for E_{exp}. This gives

$$P=\frac{f(T)e^{-\frac{1}{2}}}{Z\exp[-T(d\ln f/dT)]}. \tag{6}$$

Z is the collision number.

Thus P can be calculated, without knowing the activation energy (either E_0 or E), by an approximate treatment of the geometry, vibrational frequencies, moments of inertia, and internal rotations of the activated complex and the reactants. Because the individual factors in the vibrational partition functions are not much greater than unity, the calculation is fortunately not very sensitive to the vibrational assignment. We took $\kappa=\frac{1}{2}$ here because of the probability of the existence of a potential basin. Whether the mean molecular diameter in Z is taken from the estimated geometry of the activated complex or from an estimate of the kinetic theory, collision diameter turns out to make no appreciable difference in this case.

This type of calculation was suggested by the discussions of Glasstone, Laidler, and Eyring[1] (pp. 16–25) and Kistiakowsky and Ransom.[2]

II. Eyring, Gorin, and co-workers have given a treatment[3] of free radical and atomic association reactions (e.g., $CH_3+CH_3\rightarrow C_2H_6$) in which a crucial role is played by the rotational energy in determining the activated complex. In this treatment the activated complex turns out to correspond to relatively large interatomic or inter-radical distances. This allows, to a good approximation, considerable cancellation in and simplication of the expression for the absolute reaction rate. The rather general results for any reaction of this type is

$$k=\frac{\kappa 2^{11/6}\pi^{\frac{1}{2}}\Gamma(\frac{2}{3})\beta^{\frac{1}{2}}(kT)^{1/6}}{\sigma\mu^{\frac{1}{2}}}, \tag{7}$$

where σ is the symmetry number, and μ is the reduced mass of the activated complex considered as a diatomic molecule. The potential of intermolecular force is assumed to have the form $-\beta/r^6$, which should be adequate for the large values of r of interest here.

One way to test Eq. (7) is to deduce a steric factor for comparison with experiment. Using Eqs. (4a), (5), and (7), together with

$$Z=D^2/\sigma(8\pi kT/\mu)^{\frac{1}{2}}, \tag{8}$$

where D is the mean molecular diameter, one finds

$$P=\frac{\kappa\Gamma(\frac{2}{3})}{D^2}\left(\frac{2\beta}{ekT}\right)^{\frac{1}{2}}. \tag{9}$$

In comparing P from Eq. (9) with P deduced from experimental data, one should use the same value of D in both cases.[4]

For the association of two methyl radicals, we estimate[5] $\beta=1.475\times10^{-58}$ erg-cm,[6] and for the kinetic theory collision diameter,[6] $D=3.5$A (at 120°C). At 120°C, this gives, from Eq. (9), $P=1.39\kappa$.

As has been pointed out,[3] the neglected hindered rotation of the two methyl radicals in the activated complex, owing to their interaction, will reduce the above values of P by a factor of perhaps two or three.

In the expression $P=1.39\kappa$, it is quite possible that κ is much less than unity. If deactivation of the associated molecule by collision occurs in every case before redissociation, $\kappa=1$. A high foreign gas pressure and a long lifetime of the associated molecule tend to make $\kappa\rightarrow1$. There has already been some discussion (but no definite conclusions) using classical mechanics,[7,8] of the increase in lifetime to be expected as a result of the possibility of distributing the energy originally belonging to the reaction coordinate among the various vibrational modes. This effect might well lead to $\kappa\leqq1$ for sufficiently complicated cases (e.g., $C_2H_5+C_2H_5$), but of

course is not involved in the simplest cases (e.g., H+H). The case CH_3+CH_3 would appear to be of an intermediate nature.

The present model introduces another factor to be considered in the above connection. The (mean) activated state, in CH_3+CH_3, comes at[4] 5.90A. Ignoring the distribution of vibrational energy among other vibrational degrees of freedom, the lifetime of the associated molecule should be increased by virtue of this relatively large distance. We have calculated, using classical mechanics, the time necessary for two methyl radicals to go from $r=5.90$A to $r=r_0$ (see below) and back to $r=5.90$A for an average case. The location of the activated complex, $r=r^*$, depends on the value of $J(J+1)$. For the average case calculated, we have chosen that value of $J(J+1)$ which gives $r^{*2}=(5.90)^2$. The rotational energy U_R is then

$$U_R=[h^2J(J+1)/8\pi^2\mu r^2]. \tag{10}$$

For the interaction energy U_I we have used $U_I=-\beta/r^6$ for $r>4$A and a Morse curve (giving $r_e=1.54$A, $\nu_{C-C}=993$ cm^{-1} and $D_{C-C}=79.1$ kcal./mole) for $r<2.5$A. A smooth, arbitrary transition curve was used in the range $2.5\text{A}<r<4\text{A}$. The time for a classical particle of average energy $\frac{3}{2}kT$ (rotation plus vibration) and mass μ to go from $r=5.90$A to $r=r_0$ and back to $r=5.90$A in the potential field $U=U_R+U_I$ was then computed by numerical integration, where $U(r_0)=\frac{3}{2}kT$ ($r_0=1.20$A; also, the potential barrier at $r=5.90$A turns out to be 101 cal./mole). For 120°C, this time was found to be 5.4×10^{-13} sec. The corresponding time for a harmonic oscillator of frequency $\nu=993$ cm^{-1} is 0.34×10^{-13} sec., which is smaller by a factor of 16.

However, in the presence of acetone at 117.4 mm pressure,[6,9] the mean interval between collisions of such an associated molecule with acetone molecules is 6.75×10^{-10} sec. Hence, in the lifetime 5.4×10^{-13} sec., the probability of deactivation by collision (assuming every collision is effective) is 8.0×10^{-4}. This value can probably be considered a lower limit for κ (at this pressure and temperature), as the effect studied by Kimball[7] and Kassel[8] will of course tend to increase κ.

The author is indebted to Professor W. A. Noyes, Jr., for suggesting this problem and to Professor Noyes, Professor W. D. Walters, and Dr. L. M. Dorfman for helpful discussions.

* This work was carried out with the support of the ONR.

[1] Glasstone, Laidler, and Eyring, *Theory of Rate Processes* (McGraw-Hill Book Company, Inc., New York, 1941).
[2] Kistiakowsky and Ransom, J. Chem. Phys. **7**, 725 (1939).
[3] Summarized on pp. 127–133, 260–261 of reference 1.
[4] The mean square inter-radical distance in the activated complex, using k_J as a weighting function in computing the average, where k_J is the rate of the reaction for an activated complex with rotational quantum number J, turns out to be $2^{\frac{1}{2}}\Gamma(\frac{1}{4})(\beta/kT)^{\frac{1}{2}}/\Gamma(\frac{3}{4})$. Using this for D^2 in Eq. (9) gives $P=\kappa[\Gamma(\frac{1}{4})]^2/\Gamma(\frac{3}{4})e^4=0.49\kappa$ for any reaction of this type. For the combination of two methyl radicals at 120°C, and using the β mentioned, the root-mean-square inter-radical distance in the activated complex is 5.90A.
[5] T. L. Hill, J. Chem. Phys. **16**, 399 (1948).
[6] T. L. Hill, J. Chem. Phys. (to be submitted).
[7] G. E. Kimball, J. Chem. Phys. **5**, 310 (1937).
[8] L. S. Kassel, J. Chem. Phys. **5**, 922 (1937).
[9] Estimating kinetic theory collision diameters of 4.95A for acetone and 5.1A for a rather expanded ethane.

Symmetry Species of Overtones of Degenerate Vibrational Fundamentals

J. C. Decius*
Metcalf Research Laboratory, Brown University, Providence, Rhode Island
March 17, 1949

THE symmetry species of overtones of degenerate vibrational fundamentals have been derived by Tisza,[1] whose calculation of the characters of such levels involved essentially a recursion relation between the characters of successive overtones. It is the purpose of this note to describe several closed expressions for such characters; the expressions are limited to the cases of double and triple degeneracy of the fundamental.

By choosing polar normal coordinates, defined in terms of the "cartesian" normal coordinates, Q_a, Q_b, and Q_c, the (unnormalized) wave functions assume the following forms:

(i) Doubly degenerate case:

$$\psi_{vl}=\exp(-\gamma\rho^2/2)F_{v|l|}(\gamma^{\frac{1}{2}}\rho)\exp(il\phi). \tag{1}$$

(ii) Triply degenerate case:

$$\psi_{vlm}=\exp(-\gamma r^2/2)G_{vl}(\gamma^{\frac{1}{2}}r)P_l^{|m|}(\cos\theta)\exp(im\phi). \tag{2}$$

The polar coordinates, ρ and ϕ; r, θ, and ϕ, are defined by

$$\text{(i)}\quad Q_a=\rho\cos\phi \quad Q_b=\rho\sin\phi, \tag{3}$$

$$\text{(ii)}\quad Q_a=r\sin\theta\cos\phi \quad Q_b=r\sin\theta\sin\phi \quad Q_c=r\cos\theta. \tag{4}$$

The quantum numbers assume the following values: (i) $v=0, 1, 2\cdots$; $l=0, \pm2, \pm4, \cdots\pm v$ if v even, $l=\pm1, \pm3, \pm5\cdots\pm v$ if v odd; (ii) $v=0, 1, 2, \cdots$; $l=0, 2, 4, \cdots v$ if v even, $l=1, 3, 5, \cdots v$ if v odd; $m=0, \pm1, \pm2, \cdots\pm l$.

In order to determine the characters of overtones ($v=2, 3, \cdots$) it is necessary to determine from a character table two properties of the doubly or triply degenerate fundamental species corresponding to $v=1$. These are: (a) whether the (irreducible) representation matrix has a positive or negative determinant; (b) an angle, α_R, such that

$$\chi_R^{(1)}=2\cos\alpha_R \text{ (doubly degenerate case)}, \tag{5}$$

$$\chi_R^{(1)}=\pm1+2\cos\alpha_R \text{ (triply degenerate case)}. \tag{6}$$

In (5) and (6), $\chi_R^{(1)}$ is the character of a group operation, R, for a doubly or triply degenerate species which corresponds with the fundamental level ($v=1$) in question. It is unnecessary to solve (5) if the matrix has a negative determinant; the choice of signs in (6) corresponds precisely to positive or negative determinants.

The criteria for the signs of the determinant are:

(i) Doubly degenerate case:

The sign is negative if $\chi_R^{(1)}=0$ and $\chi_{R^2}^{(1)}=+2$; otherwise positive.

(ii) Triply degenerate case:

The sign is positive if $\chi_{R^2}^{(1)}=(\chi_R^{(1)})^2-2\chi_R^{(1)}$ when $\chi_R^{(1)}\neq0$, or if $\chi_{R^3}^{(1)}=+3$ when $\chi_R^{(1)}=0$; otherwise negative.

In the above expressions, $\chi_{R^n}^{(1)}$ means the character of the nth power of the group operation, R.

The following character formulas can then be shown to hold (R^+ mean a group operation whose matrix in the given irreducible representation has a positive determinant, R^- a negative determinant):

(i) Doubly degenerate case:

$$\chi_{R^+}^{(v)}=\frac{\sin(v+1)\alpha_{R^+}}{\sin\alpha_{R^+}}, \tag{7}$$

$$\chi_{R^-}^{(v)}=\begin{cases}0, & v \text{ odd}\\ 1, & v \text{ even}\end{cases}. \tag{8}$$

(ii) Triply degenerate case:

$$\chi_{R^+}^{(v)}=\frac{\{\sin[(v+1)\alpha_{R^+}/2]\}\{\sin[(v+2)\alpha_{R^+}/2]\}}{[\sin(\alpha_{R^+}/2)][\sin\alpha_{R^+}]}, \tag{9}$$

v odd $$\chi_{R^-}^{(v)}=\frac{\{\sin[(v+1)\alpha_{R^-}/2]\}\{\cos[(v+2)\alpha_{R^-}/2]\}}{[\cos(\alpha_{R^-}/2)][\sin\alpha_{R^-}]}, \tag{10}$$

v even $$\chi_{R^-}^{(v)}=\frac{\{\cos[(v+1)\alpha_{R^-}/2]\}\{\sin[(v+2)\alpha_{R^-}/2]\}}{[\cos(\alpha_{R^-}/2)][\sin\alpha_{R^-}]}. \tag{11}$$

It is also possible to give character formulas for the sublevels of a given v, which will be useful particularly in studying the splitting of degeneracies when anharmonic potential terms and vibration-rotation interaction energies are included in the general molecular problem. Thus, in the doubly degenerate case, it is possible to express $\chi_R^{(v)}$ in the form:

TABLE I. Symmetry species of the overtone $v=6$ of E_g in the Group D_{4h}.

D_{4h}	E	$2C_4$	C_4^2	$2C_2'$	$2C_2''$	σ_h	$2\sigma_v$	$2\sigma_d$	$2S_4$	i	Species
$\chi_R^{(v)}$, $v=1$	2	0	−2	0	0	−2	0	0	0	2	E_g
Determinant sign	+	+	+	−	−	+	−	−	+	+	
α_R	0	$\pi/2$				π			$\pi/2$	0	
$\chi_R^{(\lvert l\rvert)}$; $\lvert l\rvert=0$	1	1	1	1	1	1	1	1	1	1	A_{1g}
$\lvert l\rvert=2$	2	−2	2	0	0	2	0	0	−2	2	$B_{1g}+B_{2g}$
$\lvert l\rvert=4$	2	2	2	0	0	2	0	0	2	2	$A_{1g}+A_{2g}$
$\lvert l\rvert=6$	2	−2	2	0	0	2	0	0	−2	2	$B_{1g}+B_{2g}$
$\chi_R^{(v)}$, $v=6$	7	−1	7	1	1	7	1	1	−1	7	$2A_{1g}+A_{2g}+2B_{1g}+2B_{2g}$

TABLE II. Symmetry species of the overtone $v=7$ of F_2 in the group T_d.

T_d	E	$8C_3$	$3C_2$	$6\sigma_d$	$6S_4$	Species
$\chi_R^{(v)}$, $v=1$	3	0	−1	1	−1	F_2
Determinant sign	+	+	+	−	−	
α_R	0	$2\pi/3$	π	0	$\pi/2$	
$\chi_R^{(l)}$: $l=1$	3	0	−1	1	−1	F_2
$l=3$	7	1	−1	1	1	$A_1+F_1+F_2$
$l=5$	11	−1	−1	1	−1	$E+F_1+2F_2$
$l=7$	15	0	−1	1	1	$A_1+E+2F_1+2F_2$
$\chi_R^{(v)}$, $v=7$	36	0	−4	4	0	$2A_1+2E+4F_1+6F_2$

$$\chi_R^{(v)}=\sum_{|l|}\chi_R^{(|l|)} \tag{12}$$

in which the permitted values of $|l|$ are as described above, and

$$\left.\begin{aligned}\chi_{R^+}^{(|l|)}&=2\cos l\alpha_R\\ \chi_{R^-}^{(|l|)}&=0\end{aligned}\right\} l\neq 0, \tag{13}$$

$$\chi_{R^-}^{(|0|)}=1. \tag{14}$$

Similarly, for the triply degenerate case,

$$\chi_R^{(v)}=\sum_l \chi_R^{(l)}, \tag{15}$$

where

$$\chi_{R^+}^{(l)}=\frac{\sin[(2l+1)\alpha_{R^+}/2]}{\sin(\alpha_{R^+}/2)}, \tag{16}$$

$$\chi_{R^-}^{(l)}=\frac{\cos[(2l+1)\alpha_{R^-}/2]}{\cos(\alpha_{R^-}/2)}. \tag{17}$$

Examples of the application of these formulas are given in Tables I and II.

* This work was supported by the ONR under Contract N6 ori-88, Task Order No. 1.

[1] L. Tisza, Zeits. f. Physik **82**, 48 (1933).

Search for Short-Lived Y, ZR, and CB Fission Products*

SEYMOUR KATCOFF** AND LEON J. BROWN
Los Alamos Scientific Laboratory of the University of California, Los Alamos, New Mexico

March 21, 1949

TABLE II of "Nuclei Formed in Fission," issued by the Plutonium Project,[1] is noteworthy for the great number of gaps it contains where one would expect fission products to exist. In most cases, these missing nuclei have not been identified yet because of their short half-lives and the relatively long time required for their chemical isolation. It has recently been shown[2] that, in certain cases, the chemical procedures can be shortened by effecting some separation of the fission products from each other during the bombardment by utilizing their different recoil ranges in air. Collimated fission fragments from a thin Pu foil were allowed to pass through air at 140 mm pressure. By placing a few very thin zapon films at the appropriate distances from the Pu, selected fission fragments could be collected completely separated from fragments of very different masses and partially separated from fragments of neighboring mass numbers.

This procedure is most useful for the separation of yttrium from the rare earth activities, since the chemical separation is slow and difficult, and the range method permits a complete and automatic separation. Several runs were made using this technique plus the following chemical operations: one YF_3 precipitation, one $Sr(NO_3)_2$ scavenging precipitation from fuming nitric acid, another YF_3 precipitation, and a final yttrium oxalate precipitation. Counting was begun as soon as 10 minutes after a 5-minute irradiation. In no case was there a shorter-lived component than the previously reported 16.5-min. $Y^{(94)}$.[3] Therefore, any short-lived unidentified Y fission products, with an appreciable fission yield, must have a half-life shorter than 3 minutes.

In the case of zirconium, it was found that the range separation technique offered no advantages over the chemical separation from neutron-irradiated solutions of uranium or plutonium. In the first few runs, when the standard chemical procedure[4] was abbreviated slightly and the final precipitation of zirconium with cupferron was omitted, a new component with a 14-min. half-life appeared in the decay curves. This period was eliminated when four instead of three barium fluozirconate precipitations were performed and when the precipitation with cupferron was included. In the best two runs, counting was begun at 15 minutes after the end of 10-minute bombardments. The characteristic growth of 75-min. Cb from 17-hr. Zr was observed, but no short-lived activity was found. Thus, no zirconium isotopes with half-lives between 3 minutes and 17 hours result from fission in appreciable yield.

The experiments with columbium were performed both with and without the fission recoil apparatus. The chemical purifications consisted mainly of repeated Cb_2O_5 precipitations and Bi_2S_3 scavenging precipitations.[5] Small amounts of short period activities were observed when the purely chemical method was used, but the half-lives and yields varied from run to run, thus indicating that these were contaminations. In the two runs in which the recoil method was used, counting started at about 16 minutes after 3-minute irradiations. Very little activity was found. Thus, any new Cb fission products with an appreciable yield must have shorter half-lives than 4 minutes.

* This document is based on work performed at Los Alamos Scientific Laboratory of the University of California under Government Contract W-7405-eng-36.

** Now at Brookhaven National Laboratory, Upton, Long Island, New York.

[1] J. Am. Chem. Soc. **68**, 2411 (1946); J. C. Slater, Rev. Mod. Phys. **18**, 441 (1946).
[2] Katcoff, Miskel, and Stanley, Report La-659 (February, 1948).
[3] L. Brown and S. Katcoff, Report LADC-568.
[4] Hume, Ballou, and Glendenin, Report CN-2815 (June 30, 1945); D. N. Hume, Plutonium Project Record IX B, 8.8.4 (1946).
[5] L. E. Glendenin, Plutonium Project Record IX B, 8.9.1 (1946).

The Dissociation Energy of the First N−H Bond in Ammonia

M. SZWARC
Department of Chemistry, The University of Manchester, Manchester, England

January 5, 1949

TO determine experimentally the dissociation energy of the first N−H bond in ammonia we have used three different methods: the pyrolysis of NH_3, the pyrolysis of N_2H_4, and the pyrolysis of $C_6H_5\cdot CH_2\cdot NH_2$.

The first method would provide a direct way of attacking this problem. We hoped that at high enough temperatures it would be possible to observe the homogeneous, unimolecular decomposition of NH_3, according to Eq. (1)

$$NH_3 \rightarrow NH_2 + H, \quad (1)$$

followed by reaction (2)

$$NH_3 + H \rightarrow NH_2 + H_2. \quad (2)$$

To investigate this process we used the method described previously.[1] In agreement with earlier workers,[2] it was found that the decomposition of NH_3, even at temperatures as high as 1000°C, was a heterogeneous reaction, occurring on the walls of the silica vessel, and yielding N_2 and H_2 in the molar ratio of 1:3. This avenue of approach was therefore abandoned.

The second method, i.e., the pyrolysis of N_2H_4, gave indirectly the required result. As the weakest bond in hydrazine is the N−N bond, this bond therefore would be broken first during the thermal decomposition of N_2H_4. Thus the study of the pyrolysis of N_2H_4 should enable us to determine the dissociation energy of the N−N bond. Having this dissociation energy we are able to calculate the heat of formation of the NH_2 radical and finally the dissociation energy of the first N−H bond in ammonia.

The investigation of the thermal decomposition of hydrazine is complicated by the occurrence of wall reactions, first studied by H. S. Taylor and his collaborators.[3] To overcome this difficulty we applied the technique developed previously for the investigation of the pyrolysis of ethylbenzene.[4]

The vapors of anhydrous hydrazine were pyrolyzed in a great excess of toluene which was used as a carrier gas. The advantage of using toluene as a carrier gas was twofold. If N_2H_4 were decomposed into NH_2 radicals

$$N_2H_4 \rightarrow 2NH_2, \quad (3)$$

then these radicals would be quickly removed in the presence of excess of toluene by

$$C_6H_5 \cdot CH_3 + NH_2 \rightarrow C_6H_5 : CH_2 + NH_3 \quad (4)$$

and benzyl radicals produced by reaction (4) would eventually dimerize yielding dibenzyl. Thus the complications which could be caused by the occurrence of reactions between NH_2 radicals and undecomposed N_2H_4 are avoided. In addition the rate of formation of dibenzyl measures the rate of decomposition of N_2H_4 proceeding according to Eq. (3), as we have shown that the heterogeneous decomposition of hydrazine, which produces H_2, N_2, and NH_3, *does not* produce dibenzyl. We have, therefore, a method which makes it possible to discriminate between the heterogeneous decomposition of hydrazine and the decomposition proceeding according to reaction (3). It was found that reaction (3) accounts for about 2 percent of the total decomposition of hydrazine at 660°C, and for about 30 percent of the total decomposition at 780°C.

Variation of the partial pressure of hydrazine (by a factor of 14), of the time of contact (by a factor of 4), together with the investigation of the influence of packing the reaction vessel proved that reaction (3) is a homogeneous gas reaction of the first order. The plot of log of the rate constant of reaction (3) against $1/T$ is shown in Fig. 1. We found that the activation energy is 60±3 kcal./mole and the frequency factor is 4.10^{12} sec.$^{-1}$, the latter value is of the same order as expected on theoretical grounds[5] for a unimolecular reaction, and this is taken as a good evidence that (3) is indeed a unimolecular process.

Assuming that the recombination of NH_2 radicals does not involve an activation energy—see however, W. Heitler and G. Rumer, Zeits. f. Physik **68**, 12 (1931)—we interpret the observed activation energy of (3) as being equal to the dissociation energy of the N−N bond in hydrazine. Thus we

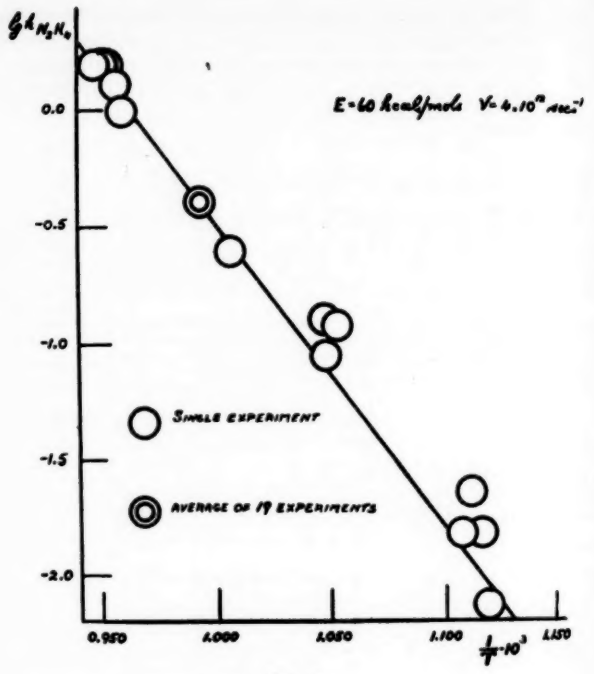

FIG. 1.

reach the following values: $D(NH_2-NH_2) = 60 \pm 3$ kcal./mole, heat of formation of the NH_2 radical 41 kcal./mole (accepting the heat of formation of gaseous, anhydrous hydrazine as 22 kcal./mole), and $D(NH_2-H) = 104 \pm 2$ kcal./mole. Knowing the heat of formation of the CH_3 radical as 31 kcal./mole, and taking the heat of formation of gaseous $CH_3 \cdot NH_2$ as −9 kcal./mole (Thomsen[7]), or −5 kcal./mole (Muller[8]) we calculate the $D(CH_3-NH_2)$ as 77 kcal./mole and 81 kcal./mole, respectively.

The third method, i.e., the pyrolysis of benzylamine, supports the above results. There is no doubt that the weakest bond in benzylamine is the C−N bond, and hence the first step in the pyrolysis of this compound should be represented by

$$C_6H_5 \cdot CH_2 \cdot NH_2 \rightarrow C_6H_5 \cdot CH_2 + NH_2. \quad (5)$$

We again used for this investigation the technique in which toluene is the carrier gas. As before the NH_2 radicals were removed by reaction (4), and in agreement with this reaction scheme, we found the ratio of dibenzyl produced to NH_3 collected to be 1:1. The rate determining step was reaction (5), and it was shown, varying by a factor of 4, both the partial pressure of benzylamine and the time of contact, and investigating the influence of packing the reaction vessel, that this process also was a homogeneous, first order gas reaction. The plot of $\log k$ against $1/T$ is shown in Fig. 2. The activation energy is 59±4 kcal./mole, and the frequency factor is 6.10^{12} sec.$^{-1}$, the latter being a strong evidence for unimolecular character of reaction (5). Assuming, as usually, zero activation energy for the recombination process, we reach the conclusion that $D(C_6H_5 \cdot CH_2-NH_2)$ is 59±4 kcal./mole.

The heat of formation of benzyl radical is known from the value of the dissociation energy of the C−H bond in toluene[9] as 37.5 kcal./mole. Unfortunately, modern data on the heat of combustion and the heat of vaporization of benzylamine are not available. Using for the former the value reported by Petit,[10] and for the latter 11 kcal./mole (by analogy with other amines), we calculated the heat of formation of the NH_2 radical as 35.5±4 kcal./mole, neglecting the uncertainty involved in the heat of formation of benzylamine. The agreement with our previous value seems to be satisfactory.

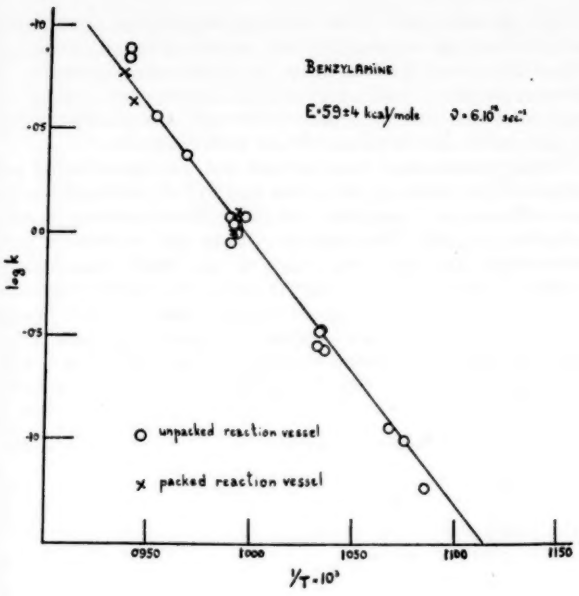

FIG. 2.

Finally it should be noted that the proposed value of 104 kcal./mole for the dissociation energy of the first N−H bond in ammonia strongly favors the value of 225 kcal./mole for the dissociation energy of N_2 as deduced by Gaydon.[11]

A full account of this work is in process of publication.

[1] M. Szwarc, J. Chem. Phys. **17**, 284 (1949).
[2] C. N. Hinshelwood and R. E. Burk, J. Chem. Soc. **1105** (1925).
[3] J. C. Elgin and H. S. Taylor, J. Am. Chem. Soc. **51**, 2059 (1929). P J. Askey, *ibid.* **52**, 970 (1930).
[4] M. Szwarc, J. Chem. Phys. **17**, 505 (1949).
[5] M. Polanyi and E. Wigner. Zeits. f. physik. Chemie **A139**, 439 (1928). Glasstone, Laidler, and Eyring, *The Theory of Rate Processes* (McGraw-Hill Book Company, Inc., New York, 1941).
[6] Hughes, Corruccini, and Gilbert, J. Am. Chem. Soc. **61**, 2639 (1939).
[7] Thomsen, Zeits. f. physik. Chemie **52**, 343 (1905).
[8] Muller, Ann. Chim. Phys. (8) **20**, 116 (1910).
[9] M. Szwarc, J. Chem. Phys. **16**, 128 (1948).
[10] Petit, Ann. Chim. Phys. (6) **18**, 149 (1889).
[11] A. G. Gaydon, Nature **153**, 407 (1944).

Thermodynamic Transition from Adsorption to Solution

TERRELL L. HILL
Department of Chemistry, University of Rochester, Rochester, New York
March 11, 1949

WE confine ourselves for brevity to systems in which a perfect gas A is in equilibrium with a condensed phase containing A and B. The problem will be discussed in more detail and generality (with A and B both mixtures, for example) at a later time. The phase $A+B$ might be, for example, H_2+Pd, H_2O+NaCl, N_2+graphite, etc. In particular, cases of the type H_2O+protein, or C_6H_6+rubber are of interest. Thus, at low benzene gas pressures, we have benzene sorbed on rubber (with swelling). At higher benzene pressures, the $A+B$ phase goes over into a solution of rubber in benzene. It is important to be able to give a single thermodynamic treatment which follows this transition. Now this can of course be done,[1] in the first instance, using the standard methods of solution thermodynamics, the extension to the adsorption case presenting no formal difficulty. We present here a second way of handling the problem which has the property (useful in some cases) of reducing to the treatment already given[2] for an adsorbate on an inert adsorbent in this special case.

Suppose we have two identical samples of B (for example, if a solid, with the same state of subdivision, etc.), N_B molecules in each, at P and T. We add N_A molecules of A to one sample to form the phase $A+B$ at P and T. Using solution thermodynamics for this phase, we write

$$dE = TdS - PdV + \mu_A dN_A + \mu_B dN_B. \tag{1}$$

and arrive at well-known results such as

$$\left(\frac{\partial \ln p_A}{\partial T}\right)_{N_A/N_B} = \frac{H_G - \bar{H}_A}{p_A T(v_G - v_A)} \tag{2}$$

(G=gas, $H = H/N$, etc.), where

$$\bar{H}_A = (\partial H/\partial N_A)_{P,T,N_B}, \tag{3}$$

etc. $H_G - \bar{H}_A$ is the isosteric heat, q_{st}, in adsorption terminology. In Eq. (1) (and (4)) it is understood that dN_B refers to addition of B in the same state as the original samples of pure B (thus the "area" is not an additional independent variable and need not be introduced into the discussion).

In the second method, we combine Eq. (1) with

$$dE_{0B} = TdS_{0B} - PdV_{0B} + \mu_{0B} dN_B, \tag{4}$$

which refers to the second original sample of pure B, to obtain

$$dE_s = TdS_s - PdV_s - \Phi dN_B + \mu_A dN_A, \tag{5}$$

where $E_s \equiv E - E_{0B}$, etc., and $\Phi \equiv \mu_{0B} - \mu_B$. Using the identical procedures of reference 2, one can then write, for example,

$$\begin{aligned} F_s &\equiv \mu_A N_A = E_s - TS_s + PV_s + \Phi N_B \\ H_s &\equiv F_s + TS_s = E_s + PV_s + \Phi N_B, \end{aligned} \tag{6}$$

$$\Phi = \int_0^{p_A} \frac{N_A}{N_B}\left(\frac{kT}{p_A} - v_s\right) dp_A \quad (T \text{ constant}), \tag{7}$$

$$\bar{H}_A = H_s - \frac{TN_B}{N_A}\left(\frac{\partial \Phi}{\partial T}\right)_{N_A/N_B,P}, \tag{8}$$

$$v_A = v_s + \frac{N_B}{N_A}\left(\frac{\partial \Phi}{\partial P}\right)_{N_A/N_B,T}, \tag{9}$$

$$\left(\frac{\partial \ln p_A}{\partial T}\right)_{\Phi} = \frac{H_G - H_s}{p_A T(v_G - v_s)}, \tag{10}$$

$$\mu_A = \left(\frac{\partial F}{\partial N_A}\right)_{P,T,N_B} = \left(\frac{\partial F_s}{\partial N_A}\right)_{P,T,\Phi} = H_s - TS_s = \bar{H}_A - TS_A, \tag{11}$$

where $H_s = H_s/N_A$, etc. In brief, these equations (i) illustrate the fact that the results of reference 2 carry over to this much more general case without formal change, and (ii) give relations between partial molar quantities as ordinarily defined (e.g., $\bar{H}_A$) and related differential quantities defined in terms of the functions H_s, F_s, etc.

[1] See, for example, A. S. Coolidge, J. Am. Chem. Soc. **48**, 1795 (1926).
[2] T. L. Hill, J. Chem. Phys. **17**, 503 (1949).

Osmosis in Electrical Fields of Various Frequencies

Z. LÁSZLÓ
Budapest, Hungary
March 28, 1949

IN a previous publication[1] the following phenomenon and the means for studying it were reported.

A parallelepiped glass tank was separated into two compartments by a glass plate, into which a Jena glass filter "*G*3" of 16×16-mm dimensions was molded (see Fig. 1). In both

FIG. 1. Experimental arrangement.

compartments one gilt square electrode was placed on the same height as the glass filter; the electrode of the first compartment being near to the diaphragm, that of the other farther away. These electrodes were cooled by water to prevent the rise of temperature of the liquids above room temperature. The liquids were continually stirred by a rotating stirrer. The voltage on the condensers was supplied by a transformer from the main line, its value measured by a Braun-electrometer.

In course of our measurements the first compartment was filled with a liquid without permanent dipole moment (mostly benzene) the second however with liquids of a dipole moment (nitrobenzene, pyridine, acetone, and various alcohols). If each compartment was filled to a certain level, conforming to the hydrostatic equilibrium of those liquids, the height difference tended gradually to disappear, owing to intermixing of the liquids. If the liquids were initially on the same height, then the hydrostatic equilibrium was first established, afterwards the level difference begins to vanish.

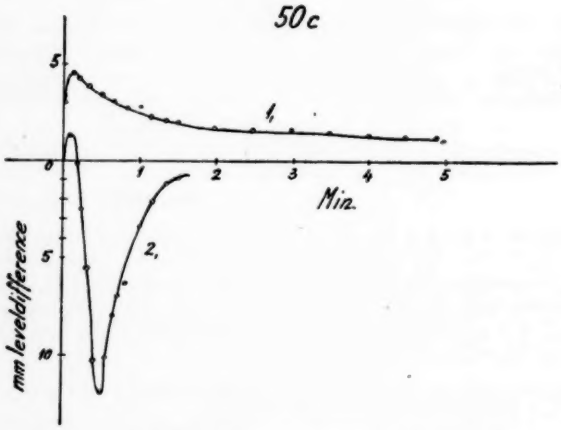

FIG. 2. Osmosis in system benzene-nitrobenzene in function of time without electric field (1) and with a.c. 3500 v, 50 cycles (2).

After these plausible observations the experiments were repeated by simultaneously applying to the electrodes an alternating voltage in the magnitude of some kilovolts, 50 cycles. Under the influence of the alternating electric field, the phenomenon of the ambipolar osmosis underwent substantial variations. Figure 2 describes the time-dependence of the osmosis in the system benzene-nitrobenzene, Fig. 3, in the system benzene-pyridine. The level differences are set as ordinates *versus* the time as abscissa, the level difference having been taken with a positive sign, when the benzene has mounted higher, with the negative sign, when the dipole is liquid.

This present paper deals with the dependence of this phenomenon on the frequency of the applied alternating voltage. This voltage was supplied by an audiofrequency generator, a 20-watt amplifier, and a high voltage transformer. The above apparatus was able to supply 4000 volts alternating voltage of sine-wave form between 50 and 1000 cycles.

The measurements were carried out first on benzene and acetone. Due to the approximate equality of the densities, the level differences arising from difference in the hydrostatic pressures is negligible. The influence of the electric field is only observable when the intermixing of the liquids has reached a definite point. By applying 50 cycles the acetone begins to rise first at a specified concentration. Then a rapid change sets in, the benzene goes higher, and lastly, because of the already greatly progressed intermixing, the difference gradually vanishes (Fig. 4). The dashed line signifies the time variation of voltage on that and following figures. The voltage was not constant during measurement, as the lesser insulating liquid flowed across the filter, thereby increasing the load and reducing the tension.

FIG. 3. Osmosis in system benzene-pyridine in function of time without electric field (1) and with a.c. 3500 v, 50 cycles (2).

Measurements were performed at 3500 volts by 150, 300, 500, and 1000 cycles (Figs. 5–8). As can be seen from the figures, the elevation of the acetone is diminishing by higher frequencies, contrary to the benzene, which mounts higher as the frequency is greater. The osmosis at 1000 cycles is quite opposite to the osmosis at 50 cycles. The influence of the field is beginning to be felt at approximately the same concentration, and it is not the acetone which tends to rise, but the benzene.

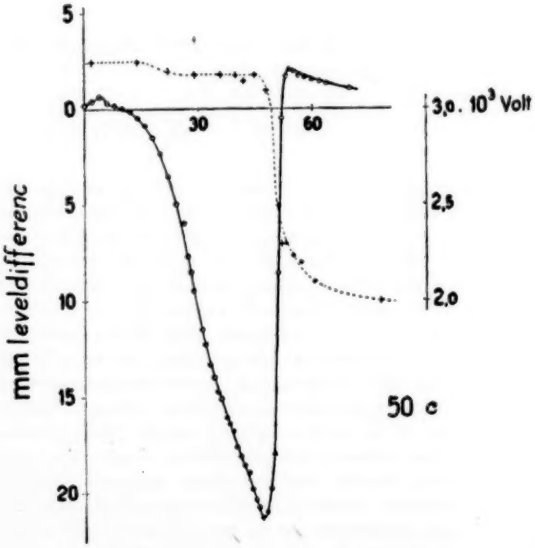

FIG. 4. Osmosis in system benzene-acetone in function of time with a.c. 3500 v, 50 cycles.

By comparing the results at 50 and 1000 cycles, it is to be seen that there exists a definite time interval, in which the two selected frequencies correspond to the elevation of the one and other liquid. This latter surmise can be verified also experimentally, when the audiofrequency generator is set once to 50, then again to 1000, then back to 50 cycles, the repetition of which procedure is accompanied by subsequent variations in heights, until that concentration is reached at which the benzene mounts higher at both frequencies.

The osmosis in the system benzene-nitrobenzene is not subjected to such essential changes by applying 50 or 1000 cycles. The elevation of the nitrobenzene at 1000 cycles is less than 50 cycles of the same voltage.

The temperature difference of this phenomenon was also subject of study. The experiments were performed on room temperature and at a temperature, near to the boiling points of the used liquids. The influence of the temperature was found to be immaterial.

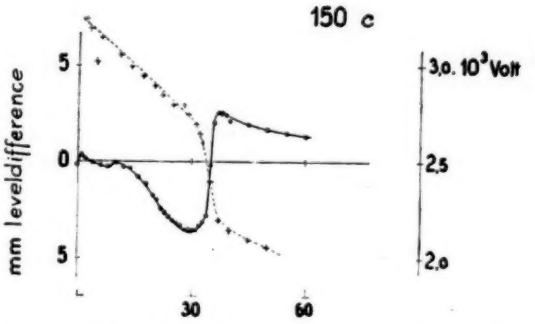

FIG. 5. Osmosis in system benzene-acetone in function of time with a.c. 3500 v, 150 cycles.

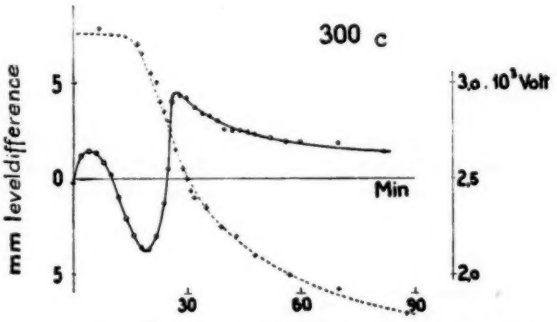

FIG. 6. Osmosis in system benzene-acetone in function of time with a.c. 3500 v, 300 cycles.

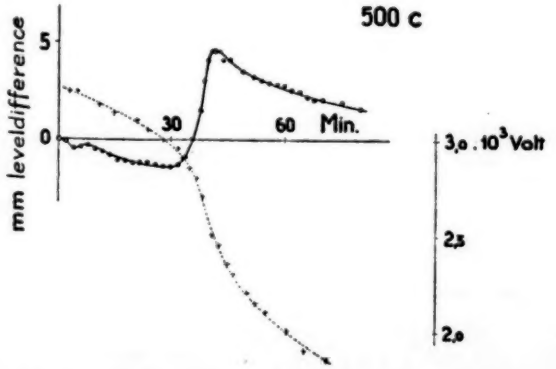

FIG. 7. Osmosis in system benzene-acetone in function of time with a.c. 3500 v, 500 cycles.

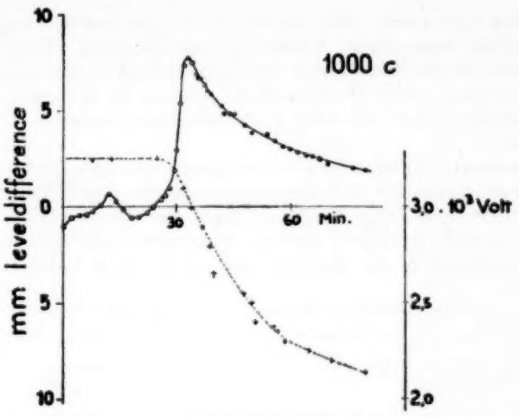

FIG. 8. Osmosis in system benzene-acetone in function of time with a.c. 3500 v, 1000 cycles.

The above described phenomena are not to be explained by electro-osmotic effects. Their most probable explanation must be sought for in the domain of ponderomotoric forces and molecular associations.

[1] Acta Physica Hungarica (1949).

Viscosity of Deuterium Oxide and Water from 5° to 125°C*

R. C. HARDY AND R. L. COTTINGTON
National Bureau of Standards, Washington, D. C.
March 28, 1949

MEASUREMENTS of the viscosity of deuterium oxide and of water were made over the temperature range 5° to 125°. This work was undertaken to provide accurate data over a wider temperature range than covered by previous work by other investigators.[1] The deuterium oxide was obtained from the AEC and was of 99.5-mol percent purity with respect to deuterium content. Viscosity values for 100-mol percent deuterium oxide were obtained by linear extrapolation and are given in Table I. The sample contained 0.9-mol percent oxygen 18. No corrections of the viscosity data were made for this abnormality of the material.

TABLE I. Viscosity of deuterium oxide* and water.

Temperature °C	Absolute viscosity, centipoises: ordinary water	Absolute viscosity, centipoises: deuterium oxide	Relative viscosity: Relative to water at 20°C: ordinary water	Relative viscosity: Relative to water at 20°C: deuterium oxide	Relative viscosity: Relative to water at *t*° deuterium oxide
5	1.5230	1.9878	1.5154	1.9779	1.3052
20	1.0050[a]	1.2514	1.0000	1.2452	1.2452
40	0.6551	0.7872	0.6518	0.7833	1.2017
60	0.4679	0.5513	0.4656	0.5485	1.1782
80	0.3558	0.4141	0.3541	0.4120	1.1637
90	0.3158	0.3658	0.3142	0.3640	1.1583
95	0.2985	0.3454	0.2970	0.3437	1.1570
100	0.2830	0.3265	0.2816	0.3250	1.1538
110	0.2557	0.2941	0.2544	0.2927	1.1504
120	0.2328	0.2669	0.2316	0.2656	1.1467
125	0.2227	0.2551	0.2216	0.2538	1.1456

* Viscosity values for D_2O were obtained by linear extrapolation of measurements on material of 99.5-mol percent purity with respect to D content. This material contained 0.9-mol percent O^{18}. No corrections were made for this abnormally high concentration of O^{18}.
[a] Assigned value used as basis for calibration of instruments.

A Bingham variable pressure viscometer calibrated with water at 20° was used in the temperature range 5° to 95°. An Ostwald type viscometer of special design was used for measurements in the range 90° to 125°. This viscometer was cali-

brated with water using the viscosity data obtained with the Bingham instrument. Values for the absolute viscosity of water and deuterium oxide shown in Table I are estimated to be accurate within 0.1 percent in relation to the value 1.005 centipoise which was used as the absolute viscosity of water at 20°.

Incidental to the viscosity measurements with the Ostwald type instrument it was necessary to determine the density of the deuterium oxide sample in the range 90° to 125°. Values for the density of 100 percent deuterium oxide obtained by extrapolation of the observed data are given in Table II.

TABLE II. Density of deuterium oxide.*

Temperature °C	Deuterium oxide A* g/cm³	B* g/cm³
90	1.0716	1.0708
100	1.0638	1.0630
110	1.0554	1.0547
120	1.0466	1.0459
125	1.0421	1.0414

* Density values obtained by linear extrapolation of measurements on material of 99.5-mol percent purity with respect to D content. This material contained 0.9-mol percent of O^{18}. Values in Column A have not been corrected for abnormal concentration of O^{18}. Column B contains values for D_2O with normal (0.2-mol percent) concentration of O^{18}.

The work is described more fully in a paper soon to be published in the Journal of Research of the National Bureau of Standards.

* This work was supported by the AEC.

[1] G. N. Lewis and R. T. McDonald, J. Am. Chem. Soc. **55**, 4730 (1933); H. S. Taylor and P. W. Selwood, J. Am. Chem. Soc. **56**, 998 (1934); W. N. Baker and V. K. LaMer, J. Chem. Phys. **3**, 406 (1935); G. Jones and H. J. Fornwalt, J. Chem. Phys. **4**, 30 (1936).

Overlap Integrals and Chemical Binding*

R. S. MULLIKEN, C. A. RIEKE,** D. ORLOFF, AND H. ORLOFF
Departments of Physics and Mathematics, University of Chicago, Chicago, Illinois

March 28, 1949

THE overlap integral S ($S=\int \chi_a^* \chi_b d\tau$) for the AO's (atomic orbitals) χ_a and χ_b of two atoms which form a bond is a quantity of recognized importance in the theory of chemical binding. Although the literature contains formulas and numerical values for several cases, a more systematic and comprehensive study seemed desirable. Accordingly, we have made computations for detailed numerical tables on all the most important AO pairs involving ns, $np\sigma$, and $np\pi$ AO's, using simple AO's of the Zener-Slater type. The S values are recorded in 20 master tables against two parameters p and t, where $p=\frac{1}{2}(\mu_a+\mu_b)R/a_0$, R being the interatomic distance, and $t=(\mu_a-\mu_b)/(\mu_a+\mu_b)$; μ is Z/n^*, where Z and n^* are Slater's effective nuclear charge and principal quantum number for the atom and AO in question. The tables cover wide ranges of p and t values, at fairly small intervals to permit interpolation. Five similar tables and two graphs are also given for $1s$, 2σ and 2σ, 2σ overlap integrals for various $s-p\sigma$ hybrid AO's. Although the master tables are for Slater AO's, simple linear combinations of the tabulated integrals can be used to obtain S values for AO-pairs including any desired types of ns, $np\sigma$, or $np\pi$ AO's (orthogonalized AO's, hybrid AO's of all kinds, self-consistent-field AO's); also for molecular group orbitals.

S values for selected atom pairs have also been tabulated with interesting results. The integral S seems to be the most natural quantitative measure of overlap in applying the well-known "criterion of maximum overlapping," proposed by Slater and by Pauling in 1931 as an index of bond strength. However, Pauling has used a different index, namely a number proportional to the magnitude of the bond orbital in the direction of the bond.[1] In agreement with Pauling's index, the present computations give much larger S values for s, $p\sigma$ hybrid bonds than for pure s or pure $p\sigma$ bonds. In sharp contrast to Pauling's index, however, S is larger for s than for $p\sigma$ bonds, except at large R values as in F_2.[2] Also, S is somewhat less for tetrahedral AO's than for AO's with more s character, contrary to the results with Pauling's index. In partial disagreement with Pauling, $p\pi$ AO's give larger overlap than $p\sigma$ AO's at triple-bond distances, although the order is reversed at larger R values. The foregoing results are illustrated for two-quantum homopolar bonds by the following computed S values.[3] (Similar results are obtained for σ-bonds in diatomic hydrides.)

S for:	$2s$	$2di$	$2tr$	$2te$	$2p\sigma$	$2p\pi$
C_2H_2 (1.20A)	0.51	**0.87**	0.81	0.76	0.29	0.34
C_2H_4 (1.34A)	0.44	0.82	**0.78**	0.73	0.32	**0.27**
C_2H_6 (1.54A)	0.34	0.70	0.68	**0.65**	0.33	0.19
F_2 (1.44A)	0.12	0.29	0.29	0.29	**0.18**	0.04

Notes: (a) di = digonal, tr = trigonal, te = tetrahedral. (b) Bold-face is used for S values believed to correspond most closely to actual bond AO's.

The computed S values are interesting and suggestive also in other ways which space forbids enumerating here. The master formulas and tables will be submitted for publication shortly, with discussion in a second paper somewhat later. In conclusion, our thanks are due Mr. Tracy J. Kinyon for his indispensable work on the numerical computations.

* This work was assisted by the ONR under Task Order IX of Contract N6ori-20 with the University of Chicago.

** Present address: Physics Department, Purdue University, Lafayette, Indiana.

[1] Computations in support of this criterion are given by Pauling and Sherman, J. Am. Chem. Soc. **59**, 1450 (1937).

[2] A. McColl of University College, London, England (private communication, 1948) has independently noted this same point, in connection with computations on S values for $p\pi$, s, $p\sigma$, and s, $p\sigma$-hybrid bonds.

[3] The results for the hydrocarbons were presented at a symposium some time ago, but only an abstract has hitherto been published: R. S. Mulliken and C. A. Rieke, Rev. Mod. Phys. **14**, 259 (1942).